The role of cytohesins in the regulation of immune responses

Anastasia Solomatina

ORCID ID:
0000-0002-7939-6401

from Moscow, Russia

Submitted in total fulfilment of the requirements of the joint degree of

Doctor of Philosophy (PhD)

of

The Medical Faculty

The Rheinische Friedrich-Wilhelms-University Bonn

and

Department of Microbiology and Immunology

The University of Melbourne

Bonn/Melbourne, 2020

Performed and approved by the Medical Faculty of The Rheinische Friedrich-Wilhelms-University Bonn and The University of Melbourne

1. Supervisor: Prof. Dr. Natalio Garbi

2. Supervisor (shared): Prof. Dr. Waldemar Kolanus

Prof. Dr. Elizabeth Hartland

Month and year of the original thesis submission: September 2019

Month and year of the oral examination: January 2020

Institute in Bonn: Life & Medical Sciences Institute (LIMES)

Director: Prof. Dr. Waldemar Kolanus

Whatever you meant to do, do it now!
The conditions are always im*possible*.

-Doris Lessing

Table of Content

Index of Abbreviations

2-DG	2-deoxy-D-glucose
AIM	absent-in-melanoma
Akt	protein kinase B
AM	alveolar macrophages
ALRs	absent-in-melanoma (AIM)-like receptors
AP-1	activator protein-1
APC	antigen-presenting cells
Arf	adenosine diphosphate ribosylation factor
ATP	adenosine triphosphate
BAL	bronchoalveolar lavage
BCR	B cell receptor
BlaM	β-lactamase
BSA	bovine serum albumin
CCR2	C-C chemokine receptor type 2
CCR7	C-C chemokine receptor type 7
cDCs	conventional DCs
CD	clusters of differentiation
CTLA-4	cytotoxic T lymphocyte antigen-4
CTLs	cytotoxic effector cells
CX3CR	C-X-3-C motif chemokine receptor 1
DAG	diacylglycerol
DAMPs	damage-associated molecular patterns
DCs	dendritic cells
DNA	deoxyribonucleic acid
Dot	defect-in-organelle-trafficking
EHEC	enterohaemorrhagic *Escherichia coli*
EPEC	enteropathogenic Escherichia coli
ER	endoplasmic reticulum
ERK	extracellular signal-regulated protein kinase
FBS	fetal bovine serum
FOXP3	forkhead box P3
GAPs	GTPase-activating proteins
GATA3	GATA-binding protein 3
GDP	guanosine diphosphate
GEFs	guanine nucleotide exchange factors
GTP	guanosine triphosphate
GTPases	molecular guanosine triphosphatases
HA	hemagglutinin
iBMDM	immortalized bone marrow-derived macrophages
ICAM-1	intracellular adhesion molecule-1

Icm	intracellular multiplication
iDCs	immature DCs
IFN	interferon
IgA	immunoglobulin
IKK	IκB kinase
IL	interleukin
IP_3	inositol triphosphate
IpgD	inositol phosphate phosphatase
ITAMs	immunoreceptor tyrosine-based activation motifs
KO	knockout
L.pn$^+$	*Legionella pneumophila* positive
Lck	lymphocyte-specific protein tyrosine kinase
LCV	*Legionella*-containing vacuole
LFA-1	lymphocyte function-associated antigen-1
Ly6	lymphocyte antigen 6
Mac-1	macrophage antigen-1
MAP	mitogen-activated protein
MCs	monocyte derived cells
MDCK	Madin-Darby Canine Kidney
MHC	major histocompatibility complex
MHCII	MHC class II
MPEC	memory precursor effector cell
MyD88	myeloid differentiation primary response gene-88
NA	neuraminidase
NADH	Nicotinamide adenine dinucleotide
NADPH	Nicotinamide adenine dinucleotide phosphate
NFAT	nuclear factor of activated T cells
NFκB	nuclear factor κB
NFκB	nuclear factor kappa-light-chain-enhancer of activated B-cells
NKs	natural killer cells
NLRs	NOD-like receptors
NOD	nucleotide-binding and oligomerization domain
NP	nucleoprotein
NP366	$NP_{366-374}$
NS2	non-structural protein 2
p.i.	post-infection
PA	PA polymerase
PA224	$PA_{224-233}$
PB	polybasic
PB1	polymerase basic protein 1
pBMDM	primary bone marrow-derived macrophages
PD-1	programmed cell death protein 1
PDK1	phosphoinositide-dependent kinase-1
PH	pleckstrin homology

PI3K	phosphoinositide 3-kinase
PIP_2	phosphatidylinositol-4,5-bisphosphate
PIP_3	phosphatidylinositol 3,4,5-trisphosphate
PKC	protein kinase C
PLC	phospholipase C
PLD	phospholipase D
PMA	phorbol 12-myristate 13-acetate
pMHC	peptide loaded MHC
PRRs	pattern-recognition receptors
RalF	recruitment of Arf1 to *Legionella* phagosome
RIG-I	retinoic acid inducible gene-I
RLRs	retinoic acid inducible gene-I (RIG-I)-like receptors
RNA	ribonucleic acid
RORγT	the retinoic acid receptor-related orphan receptor gamma-T
ROS	reactive oxygen species
SidM	substrate of the Dot/Icm secretion system
siRNA	small interfering RNA
SLEC	short-lived effector cell
STAT	signal transducer and activator of transcription
T4SS	type IV secretion system
Tbet	T-box transcription factor
TCA	tricarboxylic acid
TCA	tetracarboxylic acid cycle
TCM	central memory T cell
TCR	T cell receptor
TEM	effector memory T cell
TGF-β	transforming growth factor beta
TGN	trans-Golgi network
Th	helper T cells
TLR	Toll-like receptors
TNF	tumor necrosis factor
TPG	Isopropyl β-d-1-thiogalactopyranoside
TRAM	TRIF-related adaptor molecule
Tregs	regulatory T cells
TRIF	TIR-domain-containing adapter-inducing interferon-β
VCAM-1	vascular cell adhesion molecule-1
WRC	WAVE regulatory complex
WT	wildtype
ZAP-70	zeta-chain-associated protein kinase 70

List of tables

List of figures

Abstract

Cytohesins are guanine nucleotide exchange factors for adenosine diphosphate ribosylation factor (Arf) proteins and promote the switch of Arfs to the active GTP-bound form. Cytohesins have been shown in different *in vitro* settings to affect cell motility, cell adhesion and chemotaxis of various leukocytes, which are fundamental processes necessary for efficient innate and adaptive immune responses. Furthermore, due to their engagement in phagocytic processes, cytohesins are also targeted by different pathogens during bacterial invasion to evade the immune responses and to exert their full pathogenicity. However, all the evidence for the regulation of immunity by cytohesins has derived from *in vitro* studies. The primary impact(s) of different cytohesins on the regulation and coordination of the immune responses in the control of infection *in vivo* has not been elucidated.

The aim of this PhD thesis was to investigate the *in vivo* function of cytohesin-1, cytohesin-2 and cytohesin-3 in the complex immune responses and in pathogenesis by using acute infection with the respiratory pathogens *Legionella pneumophila* and influenza A virus in knockout mice. *L. pneumophila* is a Gram-negative bacteria and the causative agent for Legionnaires' Disease, and influenza A virus causes ”flu”, which occurs in seasonal and pandemic outbreaks.

These studies revealed that cytohesin-1 promotes T cell responses in both bacterial and viral respiratory infections. Moreover, in influenza A infection, cytohesin-1 deficiency hampered development of cognate T cells and their response to cognate antigens. Cytohesin-1 was demonstrated experimentally to be involved in the initial activation phase of naïve T cells and was required for optimal metabolic switching of T cells following activation. Lack of cytohesin-1 impaired the differentiation of distinct helper T cells, but also different memory and effector cell types.

Myeloid-specific deletion of cytohesin-2 transiently impaired cDC recruitment in the course of bacterial infection highlighting a potential intrinsic role in cDC biology. However, this did not have major effects on the overall phenotype of *L. pneumophila* or influenza A infection.

Interestingly, cytohesin-3 had an opposing role on T cells compared to cytohesin-1 and suppressed T cell immune responses in both *L. pneumophila* and influenza A infection. Increased infiltration of several different T cell subpopulations to the site of infection and increased acquisition of antigen-specific responses was observed in cytohesin-3 deficient mice. Furthermore, cytohesin-3 deficient T cells were more reactive to cognate stimulation leading to enhanced cellular immune responses. Additionally, recovery from *L. pneumophila* infection was delayed in cytohesin-3 deficient mice, suggesting that cytohesin-3 is important for preventing overactivation of T cells and any resulting inflammatory disease.

In conclusion, this PhD thesis provided for the first time a broad *in vivo* examination of the role(s) of different cytohesins in the immune responses to pulmonary infections. Although minor roles were found for cytohesins in regulating innate immune responses, the primary role(s) of cytohesin-1 and cytohesin-3 appear to lie in the regulation of T cells. Cytohesin-1 promotes T cell responses potentially by providing the optimal (signalling) threshold and by supporting the bioenergetic adaptation following T cell activation, while cytohesin-3 may suppress T cell responses by acting as an immune checkpoint.

Declaration

This is to certify that:

(i) This thesis comprises only my original work towards the PhD except where indicated in the Preface,

(ii) Due acknowledgement has been made in the text to all other material used,

(iii) This thesis is less than 100,000 words in length, exclusive of tables, maps, bibliographies, and appendices.

Anastasia Solomatina

Preface

Contribution of others to this work:

Influenza experiments in Chapter 4 were performed by Dr. Paul Whitney in collaboration with Sammy Bedoui laboratory, the University of Melbourne. Analysis and interpretation of these data was performed by Anastasia Solomatina.

.

1. Literature review

The immune system is a host defence system, comprising an interactive network of molecular and cellular factors, which protects the organism against infection and disease. Infectious diseases are caused by microorganisms such as bacteria, viruses, fungi and parasites which can invade the host by different routes including via the skin, respiratory passages and intestinal tract. The task of the immune system is to recognize these pathogens or their toxins and to eliminate them. The immune system is subdivided into two branches termed the innate and the adaptive immune system. The two parts vary in the speed and specificity of responses. Innate immunity is evolutionarily older and provides an immediate and antigen-independent response. Therefore, it is usually seen as the first line of defence. Adaptive immunity is a component of the immune system of higher animals and is acquired over time. Adaptive immune response acts in an antigen-specific manner and provides a more focused and powerful response to a pathogen. Following the first response to a specific pathogen, adaptive immunity develops an immunological memory which plays an essential role upon a secondary infection by the same pathogen. In order to perform their functions both immune branches use humoral and cell-mediated immunity.

1.1 Innate immune system

The innate immune defence comprises different elements including physical, chemical and microbiological barriers, as well as soluble factors such as complement proteins, defensins and cytokines, and innate immune cells.

1.1.1 Pattern-recognition receptors

There are five different classes of pattern-recognition receptors (PRRs) found in Mammalia: retinoic acid inducible gene-I (RIG-I)-like receptors (RLRs); C-type lectins; absent-in-melanoma (AIM)-like receptors (ALRs); Toll-like receptors

(TLR); and nucleotide-binding and oligomerization domain (NOD)-like receptors (NLRs). TLRs and C-type lectins are associated with the plasma membrane, while the NLRs, RLRs and ALRs are located intracellularly. C-type lectins recognize microbial glycans (1), RLRs detect viral RNA (2) and ALRs are cytosolic DNA sensors (3). The recognition of specific microbial patterns by PRRs initiates signalling pathways and the transcription of genes, driving a targeted proinflammatory immune response.

Toll-like receptors

The TLR family represent one major PRR class which is expressed by different types of cells. There are 10 TLRs found in humans and 12 in mice (4). Each TLR recognizes specific patterns of microbial products, allowing a targeted innate immune response according to the invading pathogen. Therefore, TLRs sensing characteristic lipids, carbohydrates and proteins of the microbial cell surface are expressed on the host cell surface, while TLRs recognizing nucleic acids of pathogens are located within endosomal membranes (5). Recognition of microbial components by TLRs leads to two signalling pathways. The first pathway involves signal transduction via the intracellular adapter protein called myeloid differentiation primary response gene-88 (MyD88), which initiates the activation of nuclear factor κB (NFκB) and the expression of inflammatory cytokines (4, 6). The second pathway is only utilized by the TLR3, and uses Toll receptor-associated activator of interferon (TRIF) and TRIF-related adaptor molecule (TRAM). The signal cascade initiated by TRIF and TRAM results in the expression of type I interferons (7).

NOD-like receptors

In humans there are 22 proteins of the NLR family, which mediate different functions including inflammasome formation, signalling transduction, transcription activation and autophagy (8). Two well-described receptors are NOD1 and NOD2. NOD1 recognizes components of the peptidoglycan component found in Gram-negative bacteria, while NOD2 senses muramyl dipeptide from both Gram-posi-

tive and Gram-negative bacteria (9, 10). Stimulation of NOD proteins induces the NFκB signalling pathway and drives the proinflammatory cytokine response.

Following recognition of pathogen-associated patterns a subgroup of NLRs forms a multimeric protein complex termed inflammasome, which leads to the activation of caspase-1 (11). In turn, caspase-1 causes the maturation and secretion of pro-inflammatory cytokine interleukin (IL)-1β and IL-18, and induces the inflammatory cell death called pyroptosis (11). Two well-studied components are NLR-family apoptosis inhibitory protein (NAIP) and NLR family CARD domain-containing protein 4 (NLRC4). Together they form the NAIP-NLRC4 inflammasome upon recognition of bacterial flagellin and the bacterial type III secretion system (12, 13). Given to this function, NAIP-NLRC4 inflammasome has been associated with the susceptibility to some bacterial infections (14, 15).

1.1.2 Neutrophils

Neutrophils are the most abundant myeloid cell type circulating in the blood and are an essential component of the innate immune system. Neutrophils are short-lived (~2 days) and are constantly produced within the bone marrow. Although the bone marrow releases neutrophils into circulation daily, it also harbors a large reserve of neutrophils that will exit the bone marrow following infection or inflammatory insult (16). Neutrophils then migrate quickly to the site of inflammation and enter the infected tissue in large numbers, where they exert effector functions. Neutrophils have different cell surface receptors recognizing microbial material, as well as complement receptors that bind to opsonized pathogens (17). These receptors facilitate phagocytosis, which results in the degradation of the pathogen via granular components containing many proteolytic and antimicrobial substances (18, 19). To restrict bacterial growth, neutrophils reduce molecular oxygen to superoxide radicals and reactive oxygen species (ROS), and release these toxic metabolites in a process called respiratory burst (20, 21). Neutrophils die within a few hours after entering the site of infection, forming a creamy exudate called pus.

1.1.3 Monocytes

Monocytes are an important cell type of the innate immune system, fulfilling a role in inflammation and in the homeostasis of tissue macrophages and dendritic cells (DCs) (22, 23). Monocytes originate in the bone marrow and are released into the blood circulation where they patrol the environment. Based on their functional properties and the expression of chemokine receptors, monocytes can be subdivided into two major subsets. The high expression of lymphocyte antigen-6 C (Ly6C) in mice defines the 'classical' or 'inflammatory' monocyte subset, whereas low expression of Ly6C is linked to 'non-classical' monocytes (24, 25). Inflammatory monocytes circulating in the blood migrate into tissues in a C-C chemokine receptor type 2 (CCR2)-dependent fashion upon infection or inflammation, where they undergo terminal differentiation and mediate proinflammatory responses (24). Differentiated monocytes overlap in function and morphology with tissue-resident macrophages and conventional DCs, and are consequently referred to as monocyte derived cells (MCs) (26-28). MCs phagocyte microorganisms and cell debris. They drive the proinflammatory cytokine response to activate other leukocytes following infection (29, 30). The function of nonclassical monocytes lies in the homeostasis. They replenish the pool of tissue macrophages and DCs under basal and inflammatory conditions (30-32).

1.1.4 Macrophages and dendritic cells

Macrophages are mononuclear phagocytes that specialize in the digestion of microbial invaders, apoptotic cells and foreign matter. Macrophages are large and irregularly shaped, and display many vacuoles within the cytoplasm which contain engulfed material. In contrast to neutrophils, macrophages are long-lived cells and are resident in tissues. Consequently, they are the first phagocyte to encounter an invading pathogen in infected tissue, which leads to the secretion of soluble mediators to recruit other leukocytes to the site of infection. Apart from their function in the host defence, they are important in wound healing and immune regulation (33). Some of their specific functions are described in more detail in section

1.5.2.2. Additionally, macrophages function as antigen-presenting cells (APC) in the activation of T cells (34, 35).

DCs are professional APCs and have a branched dendritic morphology. DC precursors exit the bone marrow and reside within body tissue in an immature state termed immature DCs (iDCs). Although they share common functions with macrophages, their key task is to link innate and adaptive immunity. In response to activation by infection or insult, DCs undergo phenotypical and functional maturation (36). In this process, DCs sense invaders through the PRRs, engulf the pathogen and process antigens to peptides which are presented on the major histocompatibility complex (MHC). Following maturation, DCs upregulate the expression of MHC class II (MHCII) molecules, co-stimulatory receptors and chemokine receptors, such as C-C chemokine receptor type 7 (CCR7) (36-40). In order to alert the adaptive immune system following pathogen invasion or insult, DCs will leave the infected tissue, cross the endothelium of lymphatic vessels and migrate to the T cell zones in secondary lymphoid organs (41). Here, the presentation of antigens to cognate T cells by mature DCs triggers antigen-specific immune responses (42, 43).

1.2 Adaptive immune system

The hallmark of adaptive immunity is its recognition for specific antigens. In contrast to receptors of innate immune cells, which recognize a broad spectrum of damage-associated molecular and pathogen-associated molecular patterns, the B cell receptor (BCR) and T cell receptor (TCR) are highly antigen-specific. These receptors achieve specificity to a wide array of molecules by undergoing random “rearrangements” in the encoding gene in each cell during development, leading to the production of billions of receptor variants (44). Because this can result in malfunctional receptors and self-functional lymphocytes, T and B cells undergo positive and negative selection in the primary lymphoid organs, which eliminates the cells carrying these variants (45). The recognition of the specific antigen of an infecting pathogen by its cognate BCR or TCR, results in the activation of the

lymphocytes bearing this receptor. Consequently, this lymphocyte will then proliferate and differentiate into effector cells to provide a targeted immune response. B cells provide the adaptive humoral immunity, which is mediated by antibodies produced by plasma cells. The T cell pool contains different subpopulations, therefore the cellular immune response of activated T cells is more diverse (44).

1.2.1 T cells

T cell precursors derive from the bone marrow and travel to the thymus where they develop to mature T cells. T cell development within the thymus includes the gene arrangements and the formation of α:β and γ:δ T cell receptors. T cells with α:β TCR are called conventional T cells and represent the majority of T lymphocytes (46, 47). They can be further subdivided by the expression of CD4 or CD8 cell surface proteins, into CD4+ and CD8+ T cells respectively. After maturation, T cells leave the thymus and circulate as naïve T cells through the blood and lymphoid tissue until they encounter their cognate antigen.

1.2.2 CD4+ T cells

CD4+ T cells are also termed helper T cells (Th) because of their function to provide help in the immune activity of other innate and adaptive immune cells. In order to give a targeted and efficient immune response in the course of infection, helper T cells differentiate into distinct effector cells following activation. The lineage-specific differentiation depends on various factors including cytokine milieu of the microenvironment, antigen concentration, strength of interaction between T cell and APC, and costimulatory molecules.

Th1 cells

In the presence of IL-12 and IFNγ, CD4+ T cells differentiate towards Th1 cells (48). IL-12 is secreted by different myeloid cells after their activation via PRRs (49, 50). In turn, IL-12 stimulates the production of IFNγ by natural killer cells (NKs) and other T cells. IFNγ activates the signal transducer and activator of tran-

scription 1 (STAT1) protein. This in turn triggers the activation of the T-box transcription factor (T-bet), which is the key regulator in the Th1 differentiation (51). T-bet not only induces the differentiation to Th1 cell type, but also suppresses the polarization of opposing cell lineages such as Th2 cell type (52, 53). Th1 effector cells develop in response to intracellular pathogens. They mainly secrete IFNγ and IL-2 cytokines, which increases the bactericidal activity of macrophages, induces B cell antibody class switch and drives the production of opsonizing antibodies.

Th2 cells

Development of Th2 cell lineages depends on the presence of IL-4 and IL-2 cytokines. IL-4 induces STAT6 which is one of the essential transcription factors in Th2 differentiation. STAT6 upregulates the expression of GATA-binding protein 3 (GATA3) (54-56). GATA3 enhances Th2 cell type cytokine production and selective polarization towards Th2 subtype, and also suppresses Th1 differentiation (54). Th2 cells are required in the defence to extracellular parasites. However, Th2 immunity has also been linked to the development of asthma and other allergic diseases (57, 58). Th2 cells secrete a range of cytokines including IL-5, IL-9, IL-13, IL-10, IL-25, with IL-4 being the key cytokine. Th2 cells mainly facilitate B cell differentiation and the production of neutralizing antibodies.

Th17 cells

The commitment of CD4+ T cells to become Th17 effector cells depends on different cytokines such as IL-6, IL-21, IL-23 and transforming growth factor beta (TGF-β), and the transcription factor called RAR-related orphan receptor gamma-T (RORγT) (59). Th17 cells arise in response to extracellular bacteria and fungi. Their function has also been associated with the generation of autoimmune disease (59, 60). The main cytokines released by Th17 cells include IL-17A, IL-17F, IL-21, and IL-22. IL-17 induces the production of proinflammatory cytokines, such as IL-6, IL-1, TNFα, as well as proinflammatory chemokines supporting the migration of inflammatory cells to sites of inflammation (61).

Tregs

Regulatory T cells (Tregs) play a major role in the regulation and suppression of immune responses and are important in the maintenance of immunological tolerance to self- and nonself-antigens. The differentiation of Tregs relies on the expression of forkhead box P3 (FOXP3) protein. A critical cytokine in the development of induced Treg is TGF-β (62, 63). Tregs are essential in the negative regulation of immune responses after the successful clearance of the invaded pathogen, which prevents immunopathology (63-65). The cytokines released by Tregs are IL-10, TGF-β and IL-35 (63-65).

1.2.3 CD8+ T cells

Following activation naïve CD8+ T cells become cytotoxic effector cells (CTLs). Usually, this activation requires strong co-stimulatory activity, which is provided by DCs, the most potent APC type. In an event where APCs provide suboptimal co-stimulation, activated CD4+ T cells can assist in the activation of CD8+ T cells (66). In this case, CD4+ T cell must recognize its antigen on the same APC, bind to it and secrete cytokines to either stimulate the APC and/or CD8+ T cell (66). Following activation, CD8+ T cells synthesize IL-2 and its high-affinity receptor, which together drive the proliferation and differentiation of CD8+ T cells. The function of CTLs lies in killing infected or cancerous cells. In order to do so, CTLs target infected cells presenting their specific antigen on MHCI complex and perform their cytotoxic activity. The cytolytic activity of CTLs is mediated by two distinct pathways and requires direct cell-cell contact (67). One pathway involves the Fas ligand, which is expressed on the surface of CTLs. The binding of Fas ligand to the Fas receptor on the target cell triggers apoptosis through the classical caspase cascade in the target cell (68). The second pathway involves the release of cytotoxic proteins such as perforin and granzymes into the intercellular space. The uptake of this cytotoxic material by the target cell causes apoptosis in a caspase-dependent and -independent manner (69).

1.2.4 T cell activation

Activation of T cells is initiated by the recognition of the cognate antigen, presented on the MHC molecule by the TCR. MHCI molecules are expressed by almost all cell types, while MHCII is expressed by professional APCs including DCs, macrophages and monocytes. CD8 molecules support the binding of TCR to the peptide loaded MHC (pMHC) I, and CD4 molecules are important in the binding of TCR to pMHCII (70). The ligation of the TCR to its cognate antigen-MHC, initiates an intracellular signalling cascade downstream of the TCR receptor (**Figure 1.1**). This signal is essential to activate naïve T cells but requires an additional second co-stimulatory signal for full T cell activation. The second co-stimulatory signal is provided by another cell-surface protein expressed on T cells, namely CD28. The ligation of CD28 to its agonist B7.1 (CD80) or B7.2 (CD86) on the cell surface of professional APCs, with the simultaneous engagement of TCR to the pMHC complex, generates an intracellular signal sufficient to completely activate naïve T cells. The contact region of the association of TCR and co-receptors on the T cell to their agonists on the APC, is called immunological synapse or short immune synapse. Within this immune synapse, the specific receptors on the T cell and the APC cluster together, with cell-adhesion molecules forming a tight bond around this region (71, 72).

1.2.4.1 Signalling pathways initiated by the TCR complex and co-receptors

The stimulation of the TCR complex leads to a signal transduction through the cytoplasmatic region of CD3 proteins, to the interior of the T cell. CD3 proteins are components of the TCR complex and harbor immunoreceptor tyrosine-based activation motifs (ITAMs) in their cytoplasmatic domain, which can engage with cytoplasmatic protein tyrosine kinases such as Fyn (73, 74). Following receptor clustering these kinases are activated and phosphorylate tyrosine residues in the ITAMs, leading to the recruitment of other signal molecules and enzymes binding to the phosphorylated residues, resulting in their activation (74). Subsequently, this initiates and amplifies other intracellular signalling pathways resulting in the alteration of gene expression.

An essential signal molecule in this signalling cascade is zeta-chain-associated protein kinase 70 (ZAP-70) (75). ZAP-70 binds to the phosphorylated ζ chain of the TCR complex, that is further phosphorylated by the lymphocyte-specific protein tyrosine kinase (Lck) associated with the cytoplasmatic tails of CD4 and CD8 molecules (76). Activated ZAP-70 triggers three major signalling pathways which are present in many other cell types.

In a series of events, ZAP-70 leads to the activation of phospholipase C-γ (PLCγ), which in turn cleaves the phospholipid phosphatidylinositol-4,5-bisphosphate (PIP_2) to membrane lipid diacylglycerol (DAG) and the second messenger inositol triphosphate (IP_3) (77).

Activation of transcription factor NFAT

Production of IP_3 mediates the increase of intracellular calcium (Ca^{2+}) cations (78). These Ca^{2+} cations bound to calcium-sensitive proteins including calmodulin, induce a conformational change (79). In this form, calmodulin interacts with other proteins such as phosphatase calcineurin. Calcineurin initiates the release of the nuclear factor of activated T cells (NFAT) (80).

Activation of transcription factor AP-1

The generation of DAG activates two signalling pathways involving protein kinase C-θ (PKCθ) and guanine nucleotide exchange factor RasGRP (81). DAG-initiated activation of RasGRP facilitates the activation of Ras and the mitogen-activated protein (MAP) kinase signalling cascade (82, 83). In subsequent steps of this signalling pathway, the extracellular signal-regulated protein kinase-1 (ERK-1) and -2 (ERK-2) are activated (84). The ERK signalling pathway activates the transcription of Fos which together with Jun, are components of the transcription factor activator protein-1 (AP-1) (85).

Activation of transcription factor NFκB

The signalling pathway of PKCθ targets the IκB kinase (IKK), which in turn phosphorylates the IκB (86, 87). IκB restrains the nuclear factor kappa-light-chain-enhancer of activated B-cells (NFκB) in its inactive form in the cytoplasm. How-

ever, the phosphorylation of IκB results in its ubiquitination, leading to the release of NFκB and translocation into the nucleus (88).

The combined effects of the transcription factors NFAT, AP-1 and NFκB activate the transcription of genes that direct and drive T cell proliferation and development of effector functions. The gene encoding IL-2 is among these genes. IL-2 is an important mediator to drive proliferation and differentiation of T cells.

CD28-mediated signalling

Co-stimulatory signalling initiates the phosphoinositide 3-kinase (PI3K) - protein kinase B (PKB, also called Akt) signalling pathway, which is a central signalling cascade regulating cell cycle, cell proliferation, cell survival and metabolism (89). Following ligation of CD28 to its ligand, the intracellular domain region with a specific YXXXM sequence is phosphorylated. Subsequently, PI3K is recruited to these phosphorylated sites of CD28 (90). PI3K catalyses the membrane lipid PIP_2 to phosphatidylinositol 3,4,5-trisphosphate (PIP_3). PIP_3 is an essential second messenger in many cellular processes and arises in response to different growth factors. PIP_3 facilitates the recruitment of various proteins to the side of the plasma membrane. These proteins harbor a specific region called pleckstrin homology (PH) domain, which allows the binding to phosphatidylinositol lipids such as PIP_3 (91). In this way, two serine kinases namely phosphoinositide-dependent kinase-1 (PDK1) and Akt are recruited to the plasma membrane, which results in the phosphorylation of Akt and its efficient activation (89).

In addition to the PI3K-Akt signalling pathway, CD28 stimulation can support the TCR signalling through the activation of Ras. As described previously, activation of Ras induces the MAP kinase signalling cascade resulting in the activation of AP-1.

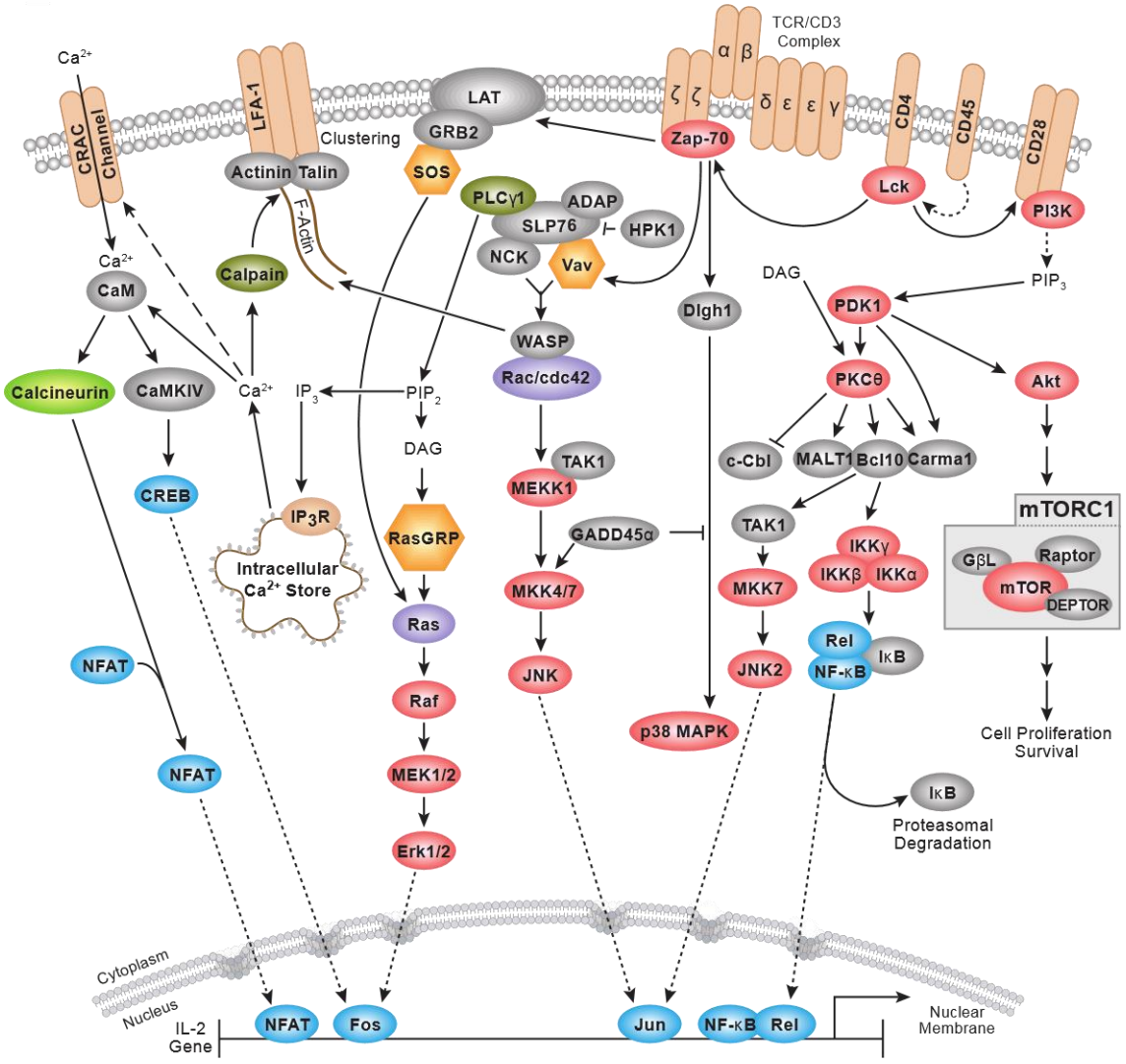

Figure 1.1: Overview of the central signalling cascades downstream of T cell receptor and co-stimulatory receptors involved in T cell activation. The activation of signalling pathways such as NFAT, Fos, Jun and NFκB leads to the expression IL-2 which drives T cell proliferation and differentiation. Illustration reproduced courtesy of Cell Signaling Technology, Inc. (www.cellsignal.com).

1.2.5 T cell anergy and peripheral tolerance

T cell anergy describes an unresponsive state of T cells where cells are intrinsically functionally inactivated following antigen encounter (92, 93). The purpose of this is thought to be the inactivation of T cells that recognize self-antigens but were not eliminated during the selection process within the thymus, and have matured and entered the peripheral circulation. The lack of co-stimulatory activating signals when these cells recognize self-antigen usually does not result in the activation of the T cells and actually causes anergy, which is characterized by the inability to produce IL-2, proliferate and differentiate (94). These co-stimulatory signals include the receptor B7, which is expressed on APCs (94, 95). Thus, T cell anergy provides peripheral tolerance to protect the body from developing autoimmune diseases (96). Peripheral tolerance can also be induced by inhibitory receptors. The immune system has evolved several immune checkpoints and distinct regulatory pathways to limit and to counteract T cell activation. Two prominent receptors expressed on activated T cells are cytotoxic T lymphocyte antigen-4 (CTLA-4) and programmed cell death protein 1 (PD-1) (97, 98). CTLA-4 binds to B7 receptors and PD-1 to PD-1 ligand (PD-L1) which are both expressed on the cell surface of APCs. Ligation of these two receptors initiates signalling pathways that suppress T cell activation, cell proliferation and effector functions. The function of these receptors has a significant role in controlling T cell responses following chronic inflammation and infection, and is associated with T cell exhaustion. Therefore, CTLA-4 and PD-1 are targeted in cancer immunotherapy and chronic viral infections in order to boost T cell immune responses (99-101).

1.2.6 Immunometabolism of T cells

To provide a sufficient and fast immune response immune cells are conditioned to react with cellular reprogramming to inflammatory and antigenic signals. This cellular transformation has specific bioenergetic and biosynthetic requirements which are met by dynamic changes in the cell metabolism. The emerging field of immunometabolism elucidates key metabolic pathways such as glycolysis, fatty

acid and mitochondrial respiration, and their dynamic regulation upon immunological challenges. Glycolytic metabolic pathway involves the uptake of extracellular glucose and its subsequent intracellular processing to pyruvate in the cytosol. Glycolysis is not the most efficient metabolic pathway to generate cellular energy in form of ATP, resulting only in two molecules of ATP per unit of glucose. However, glycolysis has other two key functions: on the one hand it provides the reduction of NAD+ to NADH, which is required as cofactor for diverse enzymes and to sustain biosynthesis during anabolic growth, on the other hand the enzymatic breakdown of glucose supplies the cell with biosynthetic intermediates which are necessary for the synthesis of ribose for nucleotides, amino acids and fatty acids. In this way, glycolysis plays an important role in the metabolism of rapidly proliferating cells. The fate of generated pyruvate can lead to the reduction to lactate in order to recycle NADH to NAD+ or it can enter the citric acid cycle (also called tricarboxylic acid, termed TCA) which takes places in the mitochondria. The TCA cycle not only oxidizes glucose-derived pyruvate but also incorporates other nutrients like fatty acids and glutamine. The TCA cycle has two essential roles in providing precursors for amino acid and lipid biosynthesis and in producing energy-rich components such as three NADH, one FADH2, and one GTP per cycle. The generated NADH can then be further used in the mitochondrial electron transport chain to yield efficiently ATP during oxidative phosphorylation. The TCA cycle is believed to be used in most quiescent or non-proliferative cells, while oxidative phosphorylation is acquired by cells that require high energy and longevity.

In the context of T cell biology, the dynamic modulation of metabolic processes such as glycolysis, fatty acid and mitochondrial metabolism have been determined to be critical factors in shaping T cell responses. Naïve T cells are quiescent and more in an inactive metabolic state. Upon antigen encounter and T cell activation, naïve CD4+ and CD8+ T cells become highly proliferative and differentiate to distinct effector cells. In order to meet these emerging bioenergetic and biosynthetic needs during T cell activation, the metabolism shifts to an active state. This process also includes expression of transporter for extracellular nutri-

ents such as Glucose transporter 1 (Glut1) leading to an enhanced uptake of glucose (102). In activated T cells the imported glucose is processed to pyruvate and further to lactate rather than being oxidated in mitochondrial respiration to produce ATP. This metabolic phenomenon of aerobic glycolysis or so called 'Warburg Effect' is necessary to ensure rapid proliferation providing the cell with biosynthetic intermediates generated during glycolysis and is more favoured rather than diversion to oxidative phosphorylation increasing ATP production in activated T cells. However, even though activated T cells are highly glycolytic, mitochondrial respiration is increased after TCR-mediated stimulus and play an essential role in T cell activation and the acquisition of effector functions (103). Interestingly, different T cell subtypes display divergent metabolic profiles. In contrast to effector T cells, memory T cells do not have energetic requirements as they do not have high proliferation rate and do not secrete large amounts of cytokines, consequently their metabolic properties resemble more the catabolic metabolism of naïve T cells (104). However, a feature of memory CD4+ and CD8+ T cells is their increased mitochondrial mass and their higher spare respiratory in comparison to naïve T cells (105) allowing them a faster metabolic shift during a re-encounter with specific antigens. Furthermore, Tregs also resemble the metabolic profile of naïve T cells being less glycolytic and relying more on oxidative phosphorylation (106, 107). Interestingly, differences in the lipid metabolism is observed among different T cell subtypes. In Tregs the metabolic pathway is more shifted to fatty acid oxidation, while effector T cells of the Th17 lineage rely on *de novo* fatty acid synthesis during differentiation and maintenance (106, 108).

Taken together, T cell metabolism is a key element in controlling T cell development and function, and in shaping the T cell immune responses. Understanding of how metabolic processes can shape T cell immune responses can be used as tool to drive T cell responses in a specific direction. Nutrient shortage and dysfunction in metabolic pathways not only lead in T cells to insufficient immune responses and but also can influence the outcome of the disease.

1.3 Leukocyte migration and integrins

The motility of leukocytes between blood and tissues is a fundamental process in all aspects of immune response. In response to tissue damage or infection, effector immune cells are required to migrate to sites of inflammation, eventually cross the venular walls, and enter the interstitium. This transendothelial migration is part of a process called leukocyte extravasation. The attraction of effector cells to the site of inflammation can be initiated by the presence of pathogen-associated molecular patterns, or released pro-inflammatory cytokines and chemokines (109). Transendothelial migration is a temporally controlled cascade of events mediated by complementary pairs of adhesion molecules and can be subdivided in four general steps (110). The first event is a weak and transient adhesive interaction between circulating leukocytes and endothelial cells of postcapillary venular walls, which slows down leukocytes. This is usually facilitated by adhesion molecules called selectins and vascular addressins (111). In this reversible attachment, leukocytes detach and attach from these bounds, resulting in a rolling movement along the vascular walls. A firm adhesion and leukocyte arrest which represents the second step is mediated by adhesion molecule family integrins to vascular cell adhesion molecule-1 (VCAM-1) and intracellular adhesion molecule-1 (ICAM-1) (112). The third step is called diapedesis, leukocytes squeeze through the endothelial cell barrier reaching the basement membrane (113). The last step involves the directed movement of leukocytes towards a chemokine gradient to the centre of the infection site.

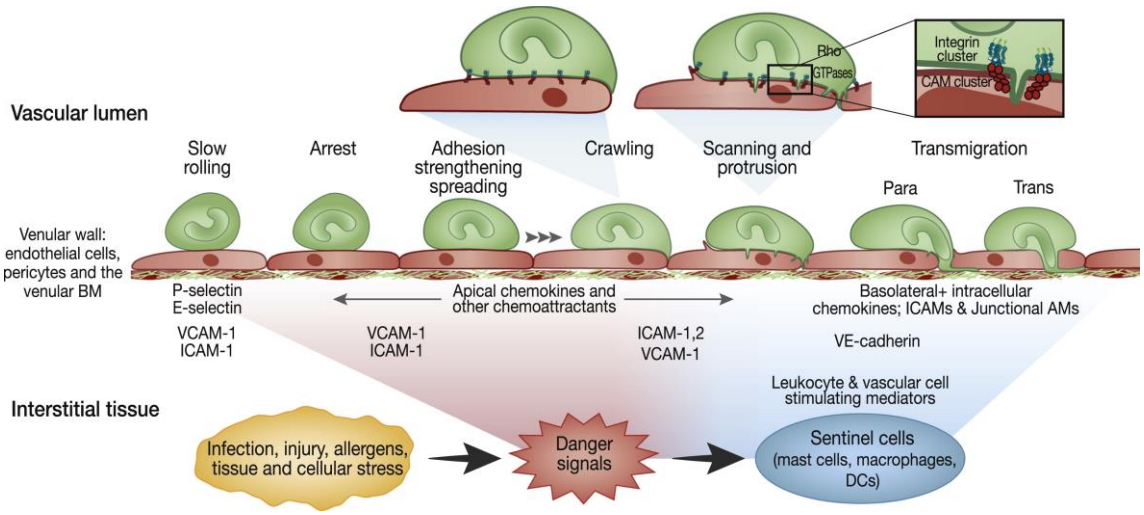

Figure 1.2: Leukocyte-vessel wall interactions. Overview of the sequential events in the transendothelial migration and the adhesion molecules involved. Image adapted from Nourshargh *et al*. (110).

1.3.1 Integrins

Integrins present an essential transmembrane protein family which facilitate cell-cell and cell-extracellular matrix contact and adhesion. Therefore, they play a fundamental role in tissue integrity and cell migration. Integrins are heterodimeric proteins consisting of two noncovalently associated type I transmembrane glycoproteins, the α and the β subunits (114). In mammals there are 18 α and 8 β subunits found, which can make up to 24 integrin proteins in different combinations. The β_2 subunit is exclusively expressed in leukocytes and forms with different α subunits different integrin proteins including the lymphocyte function-associated antigen-1 (LFA-1, $\alpha_L\beta_2$), macrophage antigen-1 (Mac-1, $\alpha_M\beta_2$) and very late antigen-4 (integrin VLA-4, $\alpha_4\beta_1$), which are essential for the intact functioning of immune cells (114).

Because integrins are mechanical transmembrane linkers connecting extracellular events to the cytoskeleton, their signalling is bidirectional and is often referred as “inside-out” and “outside-in” signalling. The affinity and avidity of ligand binding is mediated by the conformational changes and clustering of integrins. Integrins

have three major conformational states, which are classified as low affinity, high affinity and ligand occupied (115, 116). Under basal conditions circulating leukocytes maintain their integrins in a non-active, low affinity state. The binding of different receptors to their agonists (e.g. chemokines or cytokines) triggers intracellular events leading to conformational change to integrins' active form (inside-out signalling) (117). Ligation of integrin to its extracellular ligand induces integrin clustering leading to the formation of highly organized intracellular complexes including signalling molecules that eventually result in the activation of downstream signalling (outside-in signalling). Subsequently, these signalling events mediate cell spreading and migration, and enhance signalling pathways leading to cell proliferation and survival (117).

1.4 Arf-GTPases exchange factors of the cytohesin family

1.4.1 Arf-GTPases

Adenosine diphosphate ribosylation factor (Arf) proteins are small molecular guanosine triphosphatases (GTPases) of the Ras superfamily. Arf proteins play a pivotal role in fundamental cellular processes involving vesicular trafficking, organelle organization and actin remodelling (118). In Mammalia there are six members of the Arf protein family found which are numbered Arf1 to Arf6. They are further subdivided in three classes based on their sequence homology. The class I consists of Arf1, Arf2 and Arf3. These proteins are highly conserved in all eukaryotes and are involved in recruiting proteins of the secretory pathways to the trans-Golgi network (TGN) (119). Arf4 and Arf5 represent class II, which arose evolutionary later during animal cell evolution (120). The functions of Arf4 and Arf5 are not well understood but some evidence suggests a role in the early Golgi transport and in recruiting coat components to trans-Golgi membranes (120, 121). Arf6 is the only member of class III and acts on the site of the plasma membrane (122). The function of Arf6 lies in the regulation of endosomal-membrane traffic and actin reorganization (118). Arf6 can activate phospholipase D (PLD),

which subsequently initiates processes at the plasma membrane such as ruffling, phagocytosis and cell motility (118, 122-124).

Because of their important cellular functions, Arf proteins need a tight regulation. In response to intracellular changes and signalling, Arf GTPases can switch between active guanosine triphosphate (GTP)-bound and inactive guanosine diphosphate (GDP)-bound confirmations (125). This cycle of GTP binding and hydrolysis is tightly regulated by guanine nucleotide exchange factors (GEFs) and GTPase-activating proteins (GAPs) (**Figure 1.3**) (125, 126). GEFs mediate the exchange of GDP to GTP. The binding of GTP leads to a conformational change of Arf proteins and allows the interaction with target proteins. Due to the low intrinsic GTPase activity, GTP hydrolysis is triggered by GAPs (126). There are six Arf-specific GEF and eleven GAP protein subfamilies which coordinate the Arf activity (127, 128).

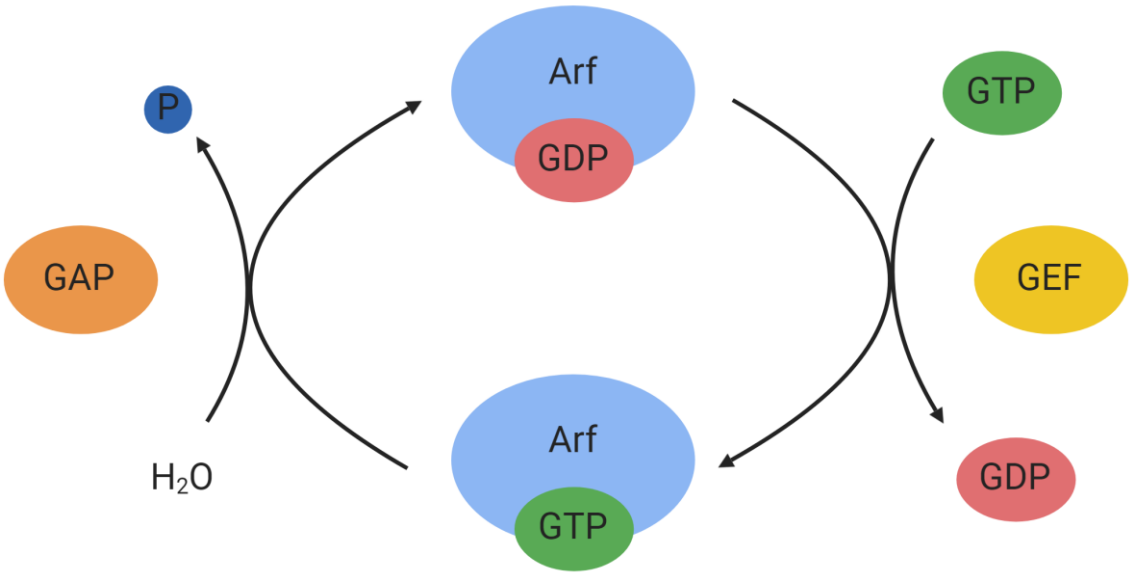

Figure 1.3: Regulation of GDP/GTP exchange in Arf proteins by guanine nucleotide exchange factors (GEFs) and GTPase-activating proteins (GAPs).

1.4.2 Structure and regulation of cytohesins

One important Brefeldin-A insensitive subfamily of Arf-GEFs are cytohesin proteins. In comparison to other GEF subfamilies, cytohesins are small in size (~ 47 kDa) and have only four family members; cytohesin-1 (*Cyth1*) (129), cytohesin-2 (*Cyth2* or ARF nucleotide-binding site opener, short ARNO) (130), cytohesin-3 (*Cyth3* or General receptor of phosphoinositides 1, short Grp-1 and *Steppke* in *Drosophila*) (131) and the less well studied cytohesin-4 (*Cyth4*) (132).

All four proteins share similar protein domain structure that contains a N-terminal coiled-coil domain, a central Sec7 domain and a C-terminal PH domain, which is followed by a short polybasic (PB) region (**Figure 1.4**). The coiled-coil domain is required for protein-protein interactions and dimerization (133). The Sec7 domain harbors highly conserved regions and is essential for cytohesins' GEF activity (131). A Sec7 specific inhibitor termed SecinH3 can block this activity for all cytohesins, and has been utilized as a tool for dissecting the biological function of cytohesins in recent years (134). The PH domain is associated with the binding of cytohesin to inositol phospholipids and therefore, its recruitment to the plasma membrane (135, 136). The membrane association of cytohesin proteins can be regulated by PI3K, which converts PIP_2 to PIP_3 (137). Depending on the alternative splice variants for either two or three glycine residues in the inositol-binding site of cytohesin proteins, cytohesins show selective affinities for PIP_2 or PIP_3 binding (138, 139). The triglycine isoform shows low affinity for PIP_3. So far, it is not completely understood, how these splice variants are regulated, however evidences suggest that Arf- and Arf-like proteins can promote the association of cytohesin to the plasma membrane by binding to its PH domain, irrespectively their diglycine or triglycine isoforms (140, 141). Moreover, the C-terminal PB region, which contains positively charged amino acids, stabilizes the membrane association and the interaction of the PH domain to PIP_3 (142).

Interestingly, cytohesin-1 and cytohesin-2, which are highly similar in protein organization, have phosphorylation sites at the C-terminal polybasic region, that can be phosphorylated by the protein kinase C (PKC) (143). Cytohesin-1 bears

one threonine- (threonine 395) and two serine- (serine 393 and serine 394) phosphorylation sites, while cytohesin-2 contains only one serine (serine 392) phosphorylation site (143, 144). The phosphorylation of cytohesin-1 and cytohesin-2 influences the association to the plasma membrane. Notably, cytohesin-3 does not harbor any phosphorylation sites at the C-terminus, which indicates differences among the cytohesins in their regulation and recruitment to membranes and consequently, their cellular distribution. Furthermore, cytohesins display different expression profiles. Cytohesin-1 and cytohesin-4 are mainly expressed in immune cells, whereas cytohesin-2 and cytohesin-3 are ubiquitously expressed. These differences may influence their distinct functional properties in the cell and explain distinct differences among the members despite their similar structural organization and high sequence homology (70-90% among cytohesins).

Cytohesins also differ in their preferences of Arfs. Cytohesin-1 catalyses Arf1, Arf3 and Arf6, whereas cytohesin-2 and cytohesin-3 exchange GDP to GTP for Arf1 and Arf6 (130, 132, 145, 146). In contrast, cytohesin-4 is a GEF for Arf1 and Arf5 (132).

In addition to their role as regulators of GTPases, cytohesins show a variety of other cellular functions, which some are discussed below. A feature of the cytohesins is their ability to interact with different transmembrane proteins. Through these interactions they can transmit extra- or intracellular signals and in this way, participate in diverse cellular signalling pathways. Two prominent transmembrane proteins which interact with cytohesins are integrins and the insulin-receptor. Both transmembrane receptors fulfil essential roles in tissue integrity, cell motility, growth, development and metabolic homeostasis.

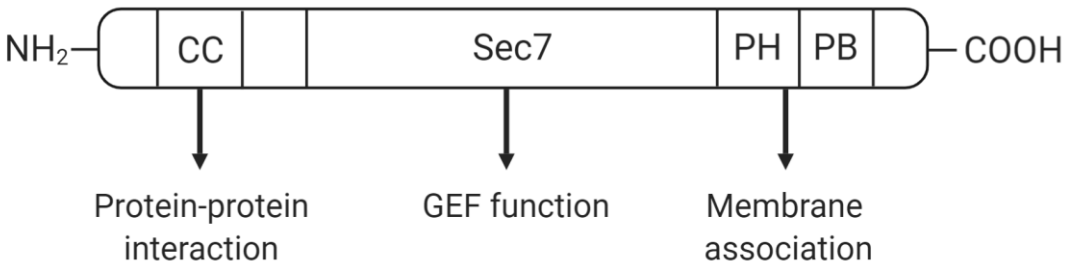

Figure 1.4: Structural domains of the cytohesin proteins.

1.4.3 Cytohesins in development and metabolism

Over the past years more evidence has emerged identifying some members of the cytohesin protein family to have significant function in development and metabolism. Cytohesin-2 appears to be essential in the development of mice as full knockout of cytohesin-2 is neonatal lethal in mice (Jux, B., unpublished). Although the mechanisms behind is not quite understood, studying distinct tissue-specific cytohesin-2 knockout mice suggests that the impaired mouse development must originate from an accumulated effect of different organs (Jux, B., unpublished).

A prominent role of cytohesin-3 in the metabolism and development has been elucidated by diverse studies for vertebrates as well as invertebrates. In *Drosophila* the complete deletion of *Steppke* is early embryonic lethal, while transheterozygous deletion of *Steppke* leads to a decreased body size and weight in larvae, pupae and adults (147). Here, *Steppke* acts upstream of PI3K (147). Lack of *Steppke* results in a defective insulin signalling leading to a reduced phosphorylation Akt (**Figure 1.5**) (147).

Subsequent studies analysed cytohesin-3's role in the insulin-receptor signalling in Mammalia. Mice fed with SecinH3 containing chow develop hepatic insulin resistance, leading to elevated expression of genes involved in gluconeogenesis, and decreased expression of genes involved glycolysis in an insulin-dependent

manner compared to mice not on a SecinH3 diet (148). Cytohesin-3 deficient mice show upon age or under high fat diet a reduced body weight gain, as well as decreased blood glucose levels in comparison to wildtype littermates (149). This corresponds to a lower weight of body fat and reduced glycogen levels. Deletion of cytohesin-3 leads in adipose tissue to a reduced activation of Akt and ERK signalling pathways after insulin injection (149). These observations support the idea that lack of cytohesin-3 results in an impaired signalling downstream of the insulin-receptor and strengthen the concept of cytohesin-3 to be required for intact insulin-receptor signalling and lipogenesis.

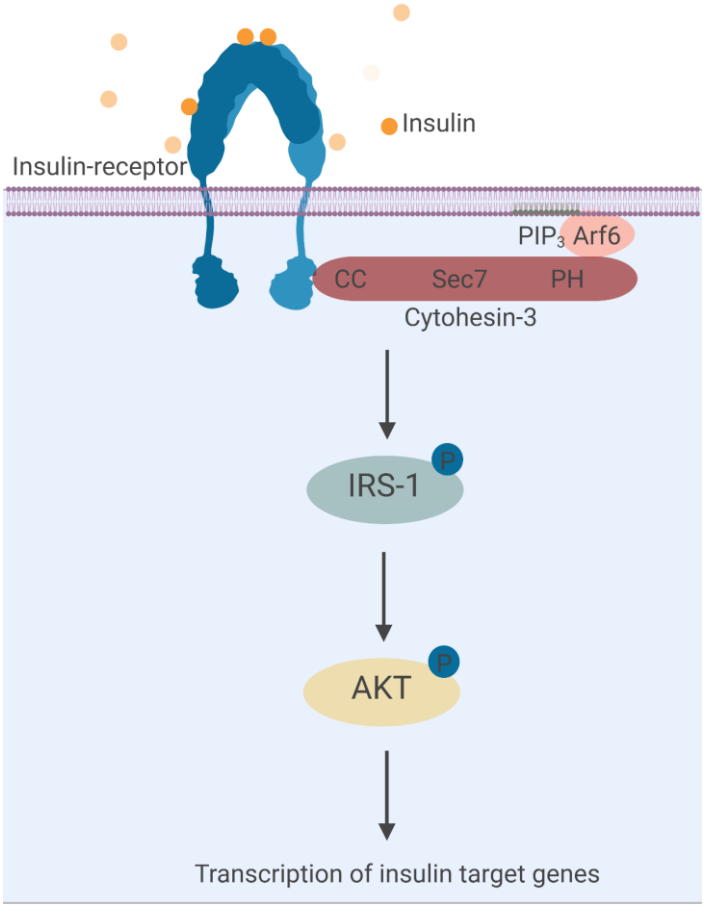

Figure 1.5. Involvement of cytohesin-3 in the insulin-receptor signalling. Upon insulin stimulus, translocation of cytohesin-3 to the plasma membrane is required for the phosphorylation of insulin-receptor substrate 1 (IRS-1) which leads in further cascade to the phosphorylation of Akt, followed by the transcription of insulin target genes.

1.4.4 Cytohesins in the regulation of integrins, cell motility and adhesion

Other important functions of cytohesins involve distinct intracellular signalling pathways associated with cell motility, cell adhesion, chemotaxis and rearrangement of the cytoskeleton in leukocytes and non-immune cells (129, 150-152). Cytohesin-1 was first described to interact with the cytosolic β2 chain of LFA-1 (129). In this study, overexpression of cytohesin-1 or its Sec7 domain led to increased binding of Jurkat T cells to ICAM-1. Further studies also determined a role for cytohesin-3 in LFA-1/ICAM-1 mediated adhesion (153).

Even though, the exact mechanistic role of cytohesins in integrin biology is not completely understood, the current findings suggest that the function of cytohesin does not follow a unidirectional pathway, but is rather multifaceted. Some aspects are explained below.

Inside-out/Outside-in signalling

In response to extracellular events, cytohesins participate in integrin inside-out signalling as well as outside-in signalling. One example for cytohesin-1-mediated inside-out signalling has been demonstrated by work of our laboratory (154). Here, cytohesin-1 acts upstream of Ras homolog gene family member A (RhoA) to induce chemokine-dependent conformational changes of β2 chain of integrin in mature DCs and consequently, modulates the integrin-dependent adhesion and migratory behaviour (155). Furthermore, ligation of integrins initiates downstream signalling which involves cytohesins and Arf proteins, and drives the cytoskeletal rearrangements (150, 151, 156-158).

Differential regulation of β1 and β2 integrins

Notably, the interactions between integrins and cytohesins have differential effects on the adhesive properties of integrins depending on the integrin and the adhesion matrix involved.

In activated polymorphonuclear neutrophils (PMNs), siRNA mediated abrogation of cytohesin-1 leads to increased Mac-1 mediated cell adhesion to immobilized fibrinogen (159), which suggests a negative regulation of Mac-1 activation and

Mac-1 dependent adhesion by cytohesin-1. In contrast, LFA-1 mediated cell adhesion of PMNs to human umbilical vein endothelial cells (HUVEC) is decreased when cytohesin-1 is abrogated (160) implying that cytohesin-1 positively regulates LFA-1 adhesion. Interestingly, adhesion of activated PMNs to fibronectin, which is predominantly facilitated by β1 integrins is decreased when cytohesin-1 is overexpressed, leading to the conclusion that cytohesin-1 negatively regulates β1 integrin mediated adhesion (160).

These observations illustrate the complex specificity and differential functions of cytohesins in cell motility. It shows a selective regulation of distinct β2 integrins such as LFA-1 and Mac-1 by cytohesin-1. Furthermore, it displays cytohesins' opposing effects on β1 and β2 integrins. Mac-1 and LFA-1 fulfil different functions in endothelial transmigration: LFA-1 mediates slow cell rolling and cell arrest while Mac-1 facilitates a crawling motion (161). β1 integrins interact with fibronectin, which is likely to be found in the interstitial space. A sequential activation of different integrins during cell migration is essential for controlled and directed cell movement. The given observations favour the concept of cytohesin as a candidate for mediating fine-tuning of the sequential activation of various integrins, coordinating the crosstalk between various integrins as well as the adapter proteins that connect the cytoplasmic domain of integrins to the actin cytoskeleton.

Reciprocal regulation by different cytohesins

In addition to the functional specificity of cytohesins in integrin regulation, different members of the cytohesin family show divergent effects on cell migration. Knockdown of cytohesin-2 in Madin-Darby Canine Kidney (MDCK) cells leads to a reduced cell migration whereas cytohesin-3 silencing results in an increased cell migration (162).

Selective coordination of podosome formation

Furthermore, recent evidence by our group and others, discovered cytohesin-2 to be important in podosome formation (163). Podosomes are actin-rich structures which localize on the outer surface of the plasma membrane and are important in cell motility and invasion (164-166). Cytohesin-2 exerts selective coor-

dination of podosome formation depending on the extracellular matrix (Namislo, A., unpublished). Deletion of cytohesin-2 in iDCs results in an increased podosome formation on gelatine-rich surface and a decrease in podosome formation on fibronectin matrix (Namislo, A., unpublished).

Taken together, cytohesins play a prominent role in the regulation of integrins, and in this way, modulate precise processes involved in cell migration. However, the exact underlying molecular and cell biological mechanisms are not well understood yet.

1.4.5 Cytohesins in T cell activation

A role of cytohesins in T cell activation has also been suggested by different studies. As mentioned previously, cytohesins are involved in LFA-1-mediated signalling. Perez *et al.* demonstrated that the threshold for T cell activation was lowered in T cells when LFA-1 stimulation was absent (167). The group revealed that extracellular stimulation of LFA-1 resulted in the phosphorylation of the cytosolic β2 integrin chain which in turn led to a signalling cascade involving ERK and cytohesin-1. Blocking the function of cytohesin-1 affected IL-2 production and Th1 differentiation (167). Furthermore, cytohesin-3's function was linked to T cell anergy. Comparative analysis of gene expression in anergic and responsive murine T cells showed an increased expression of cytohesin-3 in T cell anergy (168). In addition, work by our laboratory demonstrated in an *in vitro* peripheral tolerance model that cytohesin-3 expression was increased in attenuated CD8+ T cells. Induced expression of cytohesin-3 depended on PD-1 co-stimulation (Tolksdorf, F., PhD thesis, Paul, B., PhD thesis). The given observations suggest a regulatory function of cytohesins in T cell biology.

1.4.6 Cytohesins are utilized by pathogens

Since cytohesins appear to play a significant role in cell biology, they are also targeted by various pathogens. *Salmonella* actively utilizes cytohesins to promote bacterial internalization into the host cell (169). Efficient *Salmonella* invasion requires membrane ruffling and host cell macropinocytosis which is mediated by the WAVE regulatory complex (WRC) and Arf proteins (170). In this process, cytohesin-2 acts as a mediator for WRC and Arf1 recruitment, and their activation. Upon infection, *Salmonella* injects effector proteins such as SopB, a phosphoinositide phosphatase, into the host cell that recruits cytohesin-2 to the invasion site at the host cell plasma membrane. This in turn modulates the underlying actin polymerization and consequently, facilitates bacterial ingestion (169).

The link between cytohesin-2 and pathogen invasion was also established for *Shigella flexneri* infection (171). Cytohesin-2 is recruited by the *Shigella* virulence factor, inositol phosphate phosphatase (IpgD), to the bacterial entry site at the host plasma membrane, where it functions upstream of Arf6 creating a positive feedback loop supporting *Shigella* invasion into the host cell.

Interestingly, mechanistic modulation of cytohesin-2 in a counteracting fashion towards pathogen phagocytosis has been described for enteropathogenic (EPEC) and enterohaemorrhagic *Escherichia coli* (EHEC) (172). To remain extracellular and to evade engulfment by macrophages, EPEC and EHEC interfere in the actin remodelling processes controlled by the WRC, by injecting effector proteins into the phagocytes via the type 3 secretion system (T3SS). One of the effector proteins EspG binds to Arf6 which sterically hinders the association of Arf6 with cytohesin-2 and in turn, its translocation to the plasma membrane. This then antagonizes cytohesin-2-regulated signalling to WRC.

All the discussed functional observations are largely based on *in vitro* studies and little is known about the pathogenic and immunologic relevance of cytohesins during mammalian infection. This project aims to determine the immunological role(s) of cytohesins during *in vivo* infection with respiratory pathogens including *L. pneumophila* and influenza A virus.

1.5 *Legionella pneumophila* and Legionnaires' disease

L. pneumophila is a flagellated Gram-negative bacillus and the causative agent of an acute pneumonia known as Legionnaires' disease (173, 174). Naturally *L. pneumophila* is found in freshwater and soil-environments where it can form complex biofilms, or within unicellular protozoa such as *Acanthamoebae* and *Naegleria,* which serve as replicative niche (175-177). Contamination of water-bearing structures including cooling towers and water fountains can facilitate bacterial transmission of *L. pneumophila* to humans. Inhalation of *L. pneumophila* contaminated aerosols can then lead to pulmonary infection in immune compromised and elderly people.

To cause infection, *L. pneumophila* is internalized by alveolar macrophages (AM) in the lung, which fail to kill the bacteria. Engulfed *L. pneumophila* utilizes a type IV secretion system (T4SS) termed defect-in-organelle-trafficking/intracellular-multiplication (Dot/Icm) to translocate more than 300 effector proteins into the host cell (178-181) (**Figure 1.6**). These effector proteins interfere with host cell structure and function in order to evade the cell intrinsic immune response, and to form a replicative vacuole termed *Legionella*-containing vacuole (LCV) (182, 183). The LCV interacts transiently with mitochondria, and forces the recruitment of host derived smooth vesicles, ribosome-studded membrane fragments and multiple endoplasmic reticulum (ER)-associated proteins to the LCV (184). One prominent Dot/Icm effector protein in this complex process is the recruitment of Arf1 to *Legionella* phagosome (RalF). RalF harbors a Sec7 homology domain and can act as GEF for Arf1 (185). By hijacking Arf1 to the vacuolar membrane, RalF modulates vesicle trafficking, in particular the ER-to-Golgi traffic. In similar fashion, the small GTPase Rab1 is recruited to the site of LCV by multiple Dot/Icm effectors, including substrate of the Dot/Icm secretion system (SidM) (**Figure 1.7**) (186). A hallmark of *Legionella* effector proteins is their overlapping and redundant functionality in myriad processes. However, the Dot/Icm secretion system is essential for bacterial replication in macrophages and amoebae (182, 184). At the end of the infection cycle, when *Legionella* replication is completed and host

cell nutrients are exhausted, *Legionella* initiates host cell lysis and subsequently, infects neighbouring cells (**Figure 1.6**) (187).

Healthy individuals usually remain asymptomatic when infected with *L. pneumophila* and do not develop Legionnaires' disease. However, *Legionella* infection is a significant public health problem with infection risk highest in immune compromised people such as elderly adults, smokers, and patients on immunosuppressive therapies (182, 188).

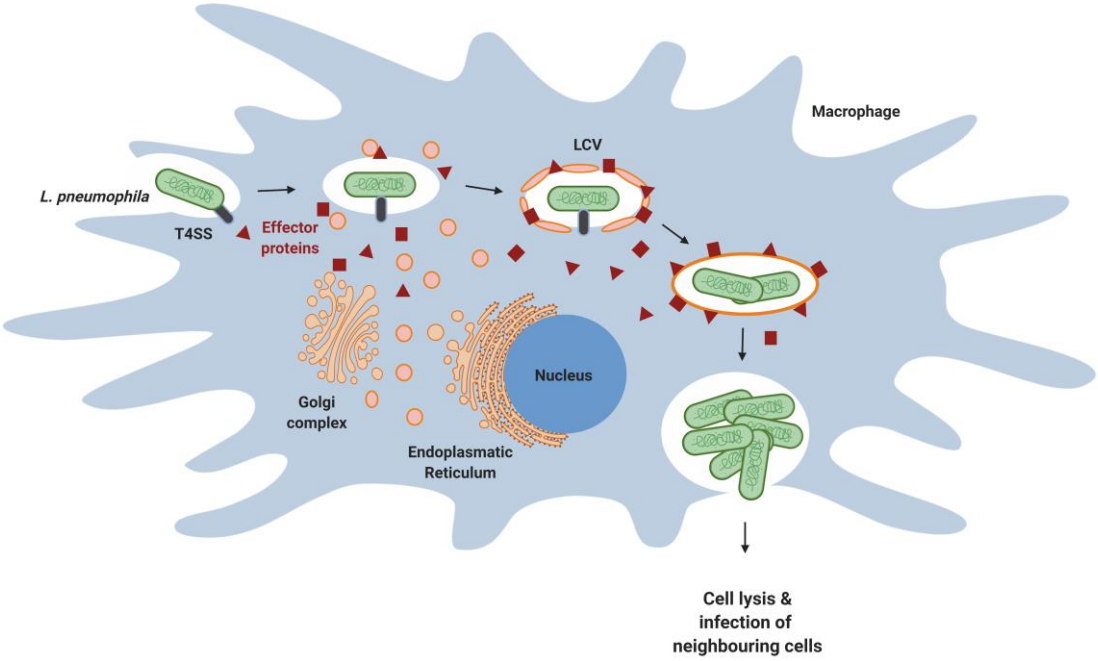

Figure 1.6: Infection cycle of *L. pneumophila* in macrophages. *L. pneumophila* is internalized by macrophages. *L. pneumophila* utilizes the type IV secretion system (T4SS) to inject effector proteins into the host cell. These effector proteins hijack host proteins and ER-derived vesicles to establish the *Legionella*-containing vacuole (LCV). Following replication and at the end of the infection cycle, *L. pneumophila* lyses host cell and infects neighbouring cells.

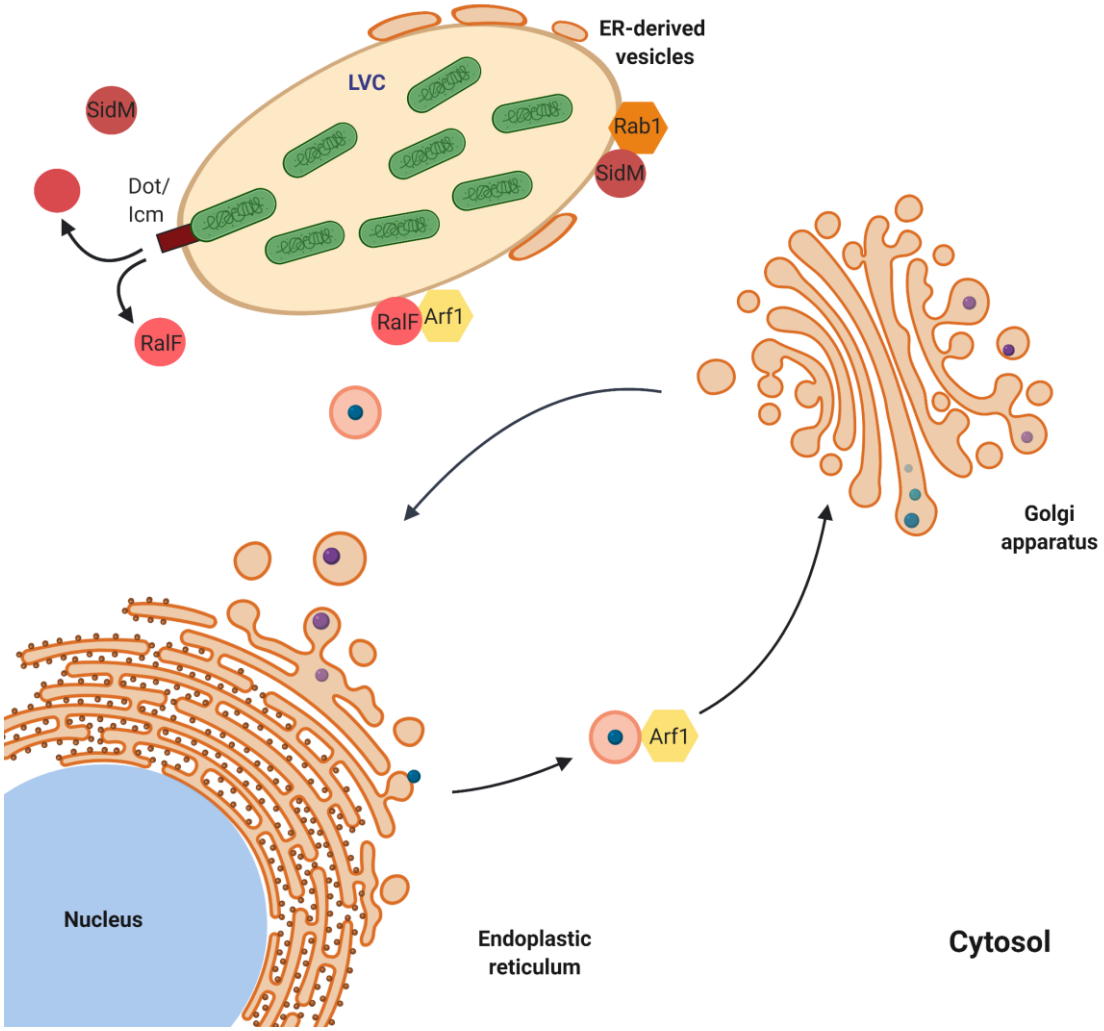

Figure 1.7: Biogenesis of *Legionella*-containing vacuole. *L. pneumophila* injects different effectors including SidM and RalF into the cytosol of the host cell through the Dot/Icm secretion system (T4SS). To recruit vesicles from the host cell secretory pathway to the vacuole, host proteins Arf1 and Rab1 are hijacked by *L. pneumophila* effectors and translocated to the vacuole.

1.5.1 Animal mouse model of Legionnaires' Disease

To study *Legionella* pathogenicity, different small mammalian models including guinea pigs and mice have been developed, that have provided a better understanding of the host-pathogen interaction and the immune response to *Legionella* infection. However, most of the inbred mouse strains infected with *L. pneumophila*, clear the pathogen from the lung within a week of infection without developing

pneumonia (189-191). One exception is the A/J mouse strain, which is permissive for *Legionella* infection. The infection progresses to an acute pneumonia, showing similar characteristics to human disease such as acute bronchopneumonia with consolidation of alveolar spaces and epithelial necrosis, as well as strong population of neutrophils and eosinophils in the alveolar septa (190, 192).

Further investigation of the susceptibility of A/J mice to *Legionella* infection revealed polymorphisms in the *Lgn1* genetic locus on chromosome 13 encoding *Naip5* (182, 193-195). In wildtype C57BL/6 mice, *Legionella*-derived flagellin is sensed by NAIP5 leading to formation of the NLCR4 inflammasome, which in turn results in the cleavage and activation of caspase-1, IL-1β and IL-18, and pyroptosis (196-198). In A/J mouse strain this response is weakened leading to more severe disease. This knowledge has led to the use of aflagellated *L. pneumophila* mutants in C57BL/6 mice, to bypass stimulation of the NLRC4 inflammasome and TLR5 signalling, allowing greater bacterial replication in the lung (199-201).

1.5.2 Immune responses to *L. pneumophila* in mice

The immune response to *L. pneumophila* involves a series of molecular and cellular events that lead to a robust pro-inflammatory response produced by a cooperative network of tissue-resident and inflammatory phagocytes (202). The infection can generally be controlled within 5 – 7 days by a rapid innate immune response, however sterile clearance usually requires adaptive immunity (203-205).

1.5.2.1 Recognition of *L. pneumophila* by PRRs

Studying the innate immune responses to *L. pneumophila* infection has revealed that TLR-MyD88 signalling pathway is an essential component in the clearance of *L. pneumophila* in infected macrophages (206). Mice deficient in MyD88 are incapable of eliminating *L. pneumophila*, which leads to bacterial dissemination followed by death (207, 208). Additionally, the production and secretion of pro-inflammatory cytokines and chemokines, as well as leukocyte recruitment, depends on MyD88 signalling (207, 209). The recognition of *L. pneumophila* by murine macrophages requires all of TLR2, TLR5 and TLR9 (199, 210-212). TLR2

recognizes bacterial lipopeptides and the 19 kDa highly conserved peptidoglycan-associated lipoprotein in peritoneal macrophages, which induces the production of cytokines such as IL-6 and TNF. TLR5 senses the flagellin which results in the activation of NFκB and the production of IL-6 and TNF (213, 214). TLR9 recognizes CpG motifs and leads to the production of TNF and IL-12 (212, 215, 216). Interestingly, studying different TLR knockout mice during *L. pneumophila* infection has revealed that only TLR2 deficiency had an impact on bacterial clearance in the lung. However, none of the single or multiple TLR knockouts displayed the same phenotype as MyD88 knockout mice, indicating that other MyD88 pathways may be involved in the clearance of *L. pneumophila* (217-219).

Besides TLRs, cytosolic NLRs play a role in bacterial sensing. NOD1 and NOD2 can be stimulated through the recognition of bacterial peptidoglycans in the cytosol. Their stimulation results in the recruitment of NFκB, which depends on RIPK2 and MAPK signalling (220, 221). Both NLR proteins contribute to neutrophil recruitment and the restriction of intracellular replication (222).

1.5.2.2 Cell recruitment and cellular interactions during *L. pneumophila* infection

Immune cell recruitment and cellular responses to infection play an essential role in the clearance of *L. pneumophila* (207). The lung harbors a number of tissue-resident phagocytes including macrophages and cDCs which present the first immune defence barrier for microorganisms that enter the airways (32).

Lung-tissue-resident macrophages comprise alveolar (AM), interstitial, and bronchial macrophages. 90% of these macrophages are AM which are located at the epithelia of the alveolar space (32, 223). The function of AM lies in inflammatory or tolerogenic responses. They engulf foreign particles and microbes, and mediate pro-inflammatory responses. Further, they remove apoptotic cells and sustain tissue homeostasis (224). In addition to that, they display immunomodulatory properties, regulating the inflammatory responses of alveolar epithelial cells, DCs and T cells (223). Upon infection, AM increase their oxidative burst and the production of pro-inflammatory cytokines and chemokines, such as IL-1α/β, IL-6,

TNF, and CXCL2 (223, 225-227). As AM represent the replicative niche for *L. pneumophila* infection, macrophage-like cell lines have been used extensively to investigate LCV biogenesis (181, 182, 184). After ingestion, *L. pneumophila* counteracts fusion of the LCV with lysosomes and blocks autophagy (228-233). In addition, *L. pneumophila* inhibits protein translation leading to reduced cytokine production, although infected AM can partially overcome this inhibition and release IL-1α and IL-1β to initiate the paracrine production of TNF by proximal non-infected macrophages (234-237). AM can interfere with *L. pneumophila* replication through cell death by apoptosis and pyroptosis (238-243). Due to cell death and cell lysis mediated by *Legionella pneumophila* the number of AM decreases in the early phase of infection, however, the population is replenished in the course of bacterial clearance (244).

Following *L. pneumophila* infection cDCs, neutrophils and inflammatory monocytes infiltrate the lung in the first days of infection (244). cDCs show two populations in the lung. The first one, expressing CD103, is found on the basolateral face of the epithelia in the alveolar space and the second subtype, expressing CD11b, is located deeper in the lung parenchyma (32, 223, 245-247). Upon *L. pneumophila* infection, cDCs are recruited to the lung but, in contrast to AM, are not efficiently infected by *L. pneumophila.* Engulfed *L. pneumophila* also does not efficiently translocate effector proteins into cDCs (248). *In vitro,* DCs may control *L. pneumophila* replication either through pyroptosis mediated by caspase-1-Naip5/NLRC4 or through Bax/Bim-dependent apoptosis (249). However, the major contribution of cDCs likely lies in priming the T cell response.

In response to *L. pneumophila* infection, neutrophils rapidly populate the lungs of mice and represent one of the dominant cell types in the innate response to *L. pneumophila* (244). The amount of neutrophils negatively correlates with bacterial load in the lung (250), and mice depleted of neutrophils cannot efficiently restrict pulmonary *L. pneumophila* infection (251-253). After infiltration, neutrophils phagocyte *L. pneumophila* and become the largest cell population staining

positive for *L. pneumophila* in the early stages of infection in mice (244). Interestingly and similar to AM, translocation of *L. pneumophila* effector proteins has been observed in neutrophils (248). However, in comparison to AM, neutrophils restrict *L. pneumophila* replication (244, 248). The bactericidal activity of neutrophils requires ROS produced by the NADPH oxidase complex (254). Neutrophils also produce TNF, IL-17A and IL-1α, which affects the secretion of IFNγ by bystander cells (248, 251, 255).

MCs are major contributors to the clearance of *L. pneumophila* infection. MCs engulf bacteria and show similar levels of *L. pneumophila*–positive staining as neutrophils (244). Apart from their bactericidal activity, MCs are a crucial source of TNF during *L. pneumophila* infection and they stimulate lung-infiltrated lymphoid cells to produce IFNγ, including NK cells and T cells, which in turn stimulates the bactericidal activity of MCs (244).

NK cells and T cells are recruited in the early acute phase upon *L. pneumophila* infection and represent the main source of IFNγ (Brown, A.S., PhD thesis). Work of our group identified that T cells, which enter the lung in the early acute phase of infection, to be not *L. pneumophila*-specific and to participate in the IFNγ response in a non-cognate manner (244). However, in the late stage of *L. pneumophila* infection, Th1 and Th17 cells are primed at the mediastinal LNs and migrate to the site of infection, where they mediate IFNγ and IL-17 responses (256).

B cells also migrate to the site of infection and memory B cells can still be found 7-10 days after infection in the lung. B cells mediate humoral responses against *L. pneumophila* including IgG and IgA responses (257).

1.6 Influenza

Influenza, also often referred as ‘flu’, is an acute respiratory disease which is primarily caused by influenza A and B virus (258). Influenza outbreaks occur in seasonal and pandemic fashion (259). The common symptoms of seasonal influenza include high fever, sore throat, runny nose, headache, muscle pain, coughing and feeling tired. However, the symptoms can vary from mild to more severe leading in some cases to complications and lethal pneumonia (260, 261). Yearly, influenza virus infection leads to 3–5 million cases of severe illness worldwide (258). Elderly, immunocompromised individuals, as well as pregnant women and young children represent high-risk groups (259, 262, 263). Human transmission of influenza usually happens through contact and droplets from sneezing or coughing of infected person (264). Usually, infected immunocompetent humans recover from the common flu within one week (259).

Influenza represents a big health care burden and because of its potential morbidity and mortality in human, it has been a focus of intense research in the past. Over the last years different animal models have been established to elucidate the pathogenesis of influenza viruses and to study adaptive immune responses in viral infections.

1.6.1 Adaptive immune responses to influenza in mice

Mice infected with murine-adapted influenza virus strain develop a lower respiratory infection, which clinically manifests as a primary viral pneumonia accompanied with laboured breathing and severe pulmonary histopathology (265-267).

The adaptive immune response to influenza virus in mammals compromises both humoral and cellular elements. Infection by influenza virus initiates the production of virus specific antibodies by B cells. Antibodies targeting the viral hemagglutinin (HA) and neuraminidase (NA) proteins have been shown to provide protective and sterilizing immunity (268-270). Furthermore, non-neutralizing antibodies secreted by B cells facilitate viral elimination and support specific antibody-depend-

ent cell-mediated cytotoxicity. This process initiates cell lysis of infected cells by NK cells (271, 272).

Adaptive cellular immune response to influenza infection is mediated by influenza-specific T cells (273). Th1 cells produce IL-2 and IFNγ which stimulates CTL responses. Th2 cells secrete cytokines including IL-4, IL-5 and IL-13 and facilitate the activation and differentiation of B cells (274-276). CTLs restrict the viral propagation by lysing the infected cells in a perforin-, and granzyme-manner (277-279). Additionally, CTL-secreted TNF restricts viral replication and increases the lytic activity (280). The expression of FasL is enhanced and induces the apoptosis of infected cells (278). Depending on the infection conditions, effector CTLs can be detected in the murine infected lungs by day 7 and CTL numbers peak around day 9 or 10 day post infection (281). After the infection, effector T cells shrink to a pool of influenza-specific memory T cells which remains within lung tissue (273). These long-lived memory T cells play a significant role in the protection against secondary infection and heterosubtypic immunity (281, 282).

1.7 Aims of this PhD thesis

Although cytohesins regulate many processes that are critical for immune cell function, and have already been demonstrated to modulate immune cells in certain limited circumstances, most of these observations are derived from *in vitro* studies, which cannot adequately reflect the physiological and immunological complexity of an animal or human. The full impact(s) of cytohesins in the regulation of the immune responses and the control of infection has not been elucidated yet.

Therefore, the overall aim of this PhD study was to define the role of cytohesins in the immune response to respiratory infections. A key aspect of this PhD study was to characterize the immune responses to *Legionella pneumophila* in cytohesin deficient mice and to investigate whether immune processes including cell recruitment and phagocytosis, are altered in the absence of different cytohesins. Further experiments including the use of the influenza A virus infection model should examined the function of cytohesins in the T cell mediated immune responses in more detail. The results of this PhD study contribute to a deeper understanding of how individual cytohesins regulate innate and adaptive immune responses to infections.

2. Material and methods

2.1 General reagents

2.1.1 Flow cytometry reagents

2.1.1.1 Directly conjugated monoclonal antibodies

Antigen	Clone	Conjugate	Company	Reference
CD11b	M1/70	BV711	BioLegend	101242
CD11c	HL3	PE-CF594	BD Biosciences	562454
CD127	A7R34	PE-Cy7	BioLegend	135013
CD19	B4	BV605	BioLegend	115539
CD3ε	145-2C11	PerCP-Cy5.5	BioLegend	100328
CD3ε	17A2	BV785	BioLegend	100231
CD3ε	17A2	BV510	BioLegend	100233
CD4	RM4-5	eFluor® 450	eBioscience	48-0042-82
CD4	RM4-5	FITC	BioLegend	100505
CD4	RM4-5	PerCP-Cy5.5	BioLegend	100538
CD44	IM7	Alexa Fluor® 700	BioLegend	103026
CD44	IM7	BUV394	BD Biosciences	740215
CD45	30-F11	V500/BV510	BD Biosciences	561487
CD45	30-F11	PE-Cy7	eBioscience	25-0451-82
CD45.2	104	PE	Biolegend	109808
CD62L	MEL-14	FITC	BD Biosciences	553150
CD62L	MEL-14	BV605	BD Biosciences	563252
CD64	X54-5/7.1	Alexa Fluor® 647	BD Biosciences	558539
CD8α	53-6.7	BV711	BD Biosciences	563046
CD8α	53-6.7	Pacific Blue®	BioLegend	100728
FcεRI	MAR-1	PE-Cy7	eBioscience	25-5898-82
GATA3	L50-823	PE	BD Biosciences	560074
IFNγ	XMG1.2	PE-Cy7	eBioscience	25-7311-82
IL-4	11B11	APC	eBioscience	17-7041-82

KLRG1	2F1	BV711	BD Biosciences	564014
Ly6C	AL-21	BV605	BD Biosciences	563011
Ly6G	1A8	PerCP-Cy5.5	BD Biosciences	560602
MHCII	M5/114.15.2	Alexa Fluor® 700	BioLegend	107622
NK1.1	PK136	APC	BD Pharmingen	550627
NKp46	29A1.4	Biotinylated	eBioscience	13-3351-82
Siglec F	E50-2440	BV421	BD Biosciences	562681
Siglec F	E50-2440	PE	BD Biosciences	552126
Tbet	4B10	eFluor® 660	eBioscience	50-5825-82
TCRβ	H57-597	APC-eFluor® 780	eBioscience	47-5961
TCRβ	H57-597	BV510	BD Biosciences	563221

2.1.1.2 Unconjugated monoclonal antibodies

Antigen	Clone	Company	Reference
CD16/32	93	eBioscience	16-0161
CD28	37.51	BioLegend	102101
CD3ε	145-2C11	BioLegend	100301
IFNγ	R4-6A2	BioLegend	505706
IL-4	11B11	BioLegend	504122

2.1.1.3 Directly conjugated polyclonal antibodies

Antigen	Clone	Conjugate	Company	Reference
Legionella	Polyclonal	FITC	ViroStat	6053

2.1.1.4 Secondary staining reagents

Molecule	Conjugate	Company	Reference
Streptavidin	PE-CF594	BD Horizon	562284

2.1.1.5 Tetramers

Antigen	Conjugate	Source
PA_{224}	PE	kindly provided by Andrew Brooks and Jie Lin
NP_{366}	APC	kindly provided by Andrew Brooks and Jie Lin

2.1.1.6 Viability dyes

Dye	Company	Reference
Fixable Viability Dye eFluor™ 780	eBioscience	65-0865-14
Fixable Viability Dye eFluor™ 506	eBioscience	65-0866-14
LIVE/DEAD™ Fixable Near-IR Dye	ThermoFisher	L10119
Propidium Iodide	ThermoFisher	P1304MP

2.1.1.7 Cytometric bead array

CBA Flex Set	Compnay	Reference
IFN-γ Flex Set (Bead A4)	BD Biosciences	558296
IL-10 Flex Set (Bead C4)	BD Biosciences	558300
IL-12p70 Flex Set (Bead D7)	BD Biosciences	558303
IL-17A Flex Set (Bead C5)	BD Biosciences	560283
IL-1α Flex Set (Bead E4)	BD Biosciences	560157
IL-6 Flex Set (Bead C4)	BD Biosciences	558301
MCP-1 Flex Set (Bead B7)	BD Biosciences	558342
TNF Flex Set (Bead C8)	BD Biosciences	558299

2.1.1.8 Other flow cytometry reagents

FACS buffer was made of 1X PBS with (w/v) 0.1% BSA (Carl Roth/Sigma Aldrich) and 2 mM EDTA (Sigma Aldrich). For permeabilization and fixation prior intracellular staining, Foxp3 Transcription Factor Staining Buffer Set (eBioscience; 00-5523-00) and Cytofix/Cytoperm™ kit (BD Biosciences; 554714) were used. For

other all cell fixation PFA (Carl Roth) or methanol-free PFA (ThermoFisher; 28908) was applied.

2.1.2 *In vitro* cell culture reagents

2.1.2.1 Stimulation reagents

Reagents	Final concentration	Company	Reference
$PA_{224-233}$	1 µg/mL	GenScript®	RP19991
$NP_{366-374}$	1 µg/mL	GenScript®	RP19991
$PB1_{703-711}$	1 µg/mL	GenScript®	N/A
$NS2_{114-121}$	1 µg/mL	GenScript®	N/A
CD28 (37.51)	1 µg/mL	BioLegend	102101
CD3ε (145-2C11)	5 µg/mL	BioLegend	100301
2-Deoxy-D-glucose	100 mM	Sigma Aldrich	D8375
Glucose	10 mM	Agilent Technologies	103577-100
Oligomycin	1 µM	Sigma Aldrich	75351

For PMA and Ionomycin stimulation Cell Stimulation Cocktail was used from eBioscience (00-4970-03). BrefeldinA was purchased from Sigma Aldrich (final concentration 5 ng/mL). Cytokines for *in vitro* differentiation of helper T cells were purchased from PeproTech®.

2.1.2.2 Red blood lysis and tissue digestion buffer

Reagent	Concentration	Company	Reference
RPMI 1640		PAN™ Biotech	P04-16500
FBS (heat inactivated)	3%	PAN™ Biotech	P30-1302
DNAse I	1 mg/mL	Worthington Biochemical Corporation	N/A
Collagenase III	1 mg/mL	Worthington Biochemical Corporation	LS004182

Erythrocyte lysis was performed in a red blood lysis (RBL) buffer made of 10 mM Tris hydrochloride solution (pH 7.5) and 8.3 g/L ammonium chloride (Roth).

2.1.3 Media

2.1.3.1 Bacterial culture media

Buffered charcoal yeast extract (BCYE) agar was used for *L. pneumophila* cultivation (283). For antibiotic selection, BCYE were supplemented with 50 µg/mL streptomycin or chloramphenicol accordingly if the *Legionella* strain required selection. All media was prepared by the Media Preparation Unit, the Department of Microbiology and Immunology, the University of Melbourne.

2.1.4 Cell culture media

2.1.4.1 BMDM medium

Reagent	Concentration	Company	Reference
DMEM		PAN™ Biotech	P04-03550
FBS (heat inactivated)	20%	PAN™ Biotech	P30-1302
SecinH3 (in DMSO)	10 µM	abcam	ab145048

2.1.4.2 T cell medium

Reagent	Concentration	Company	Reference
RPMI 1640		PAN™ Biotech	P04-16500
FBS (heat inactivated)	20%	PAN™ Biotech	P30-1302
β-Mercaptoethanol	500 µM	Gibco®	31350-010
Penicillin	100 µg/mL	PAN™ Biotech	P06-07100
Streptomycin	100 µg/mL	PAN™ Biotech	P06-07100
L-Glutamine	2 mM	PAA Laboratories	M11-004
Sodium pyruvate solution	1 mM	PAA	S11-003

2.1.4.3 Seahorse T cell medium

Reagent	Concentration	Company	Reference
Seahorse XF RPMI		Agilent Technologies	10336-100
L-Glutamine	2 mM	PAA	M11-004
Sodium pyruvate solution	1 mM	PAA	S11-003
Glucose solution*	10 mM	Agilent Technologies	103577-100

*Addition of glucose solution in the medium was excluded in experiments where glucose was used as stimulant.

2.2 Bacteria

2.2.1 *Legionella* strains

No.	Strain	Characteristics
1.	*L. pneumophila ΔflaA*	in-frame deletion of *flaA*
2.	*L. pneumophila ΔdotΔflaA*	in-frame deletion of *dotA* and *flaA*
3.	*L. pneumophila ΔflaA* pXDC61	1. with vector expressing β-lactamase
4.	*L. pneumophila ΔflaA* pXDC61 RalF-BlaM	1. vector expressing β-lactamase/RalF fusion protein
5.	*L. pneumophila ΔdotΔflaA* pXDC61 RalF-BlaM	2. vector expressing β-lactamase/RalF fusion protein

The genetically modified *L. pneumophila* (130b) strain used here was originally a clinical isolate from USA (Serogroup 1; ATCC BAA-74). *L. pneumophila* was grown on BCYE plates for 3-4 days. Strains numbered 3-5 required the culture on BCYE agar containing chloramphenicol and 0.1 M Isopropyl β-D-1-thiogalactopyranoside (ITPG).

2.3 Animals and animal procedure

2.3.1 Mice strains

Mouse line	Source
Cyth1$^{-/-}$	Junji Yamauchi, Tomohiro Torii
Cyth2$^{fl/fl}$	European Mouse Mutant Archive
Cyth3$^{-/-}$	KOMP Repository (UC Davis, USA).
LysM/Cre	provided by Irmgard Försters
C57BL/6JArc	Animal Resources Centre

2.3.2 Genotyping

To extract DNA for genotyping, murine ear tags and tail tips were lysed in 200 µL of sodium hydroxide solution (50 mM) at 95°C for 20 min. Subsequently, 75 µL of 1 M Tris hydrochloride solution (pH 8) was added and samples were centrifuged for 4°C for 4 min. 1-2 µL of supernatant was taken for genotyping PCR. PCR reaction were performed with OneTaq® DNA Polymerase (New England Bio-Labs).

PCR for *Cyth1* mice

Primer name	Sequence (5'-3')
mCyth1_wt for	CCA CTA CTC CCA GCC GTT TTA T
mCyth1_wt rev	GTT CGA GTG CAT GCT TTG CC
mCyth1_neo for	AAC CAA ATT AAG GGC CAG CTC A

Thermocycler program:

Step	Temp.	Time	Cycles
Initial Denaturation	94°C	30sec	
Denaturation	94°C	30 sec	
Annealing	64°C	30 sec	x30
Elongation	68°C	1 min	

68°C	10 min
4°C	∞

WT band: ~520bp KO band: ~400bp

PCR for *Cyth2*$^{fl/fl}$ mice

Primer name	**Sequence (5'-3')**
Pscd2 WT1 screen for:	CAGAAATGCCAGGGCTTTCTCAGC
Pscd2 WT1 screen rev	GCATAGGTTTCAGGGCTGGAAACAC

Thermocycler program:

Step	**Temp.**	**Time**	**Cycles**
Initial Denaturation	95°C	3 min	
Denaturation	95°C	45 sec	x35
Annealing	64.5°C	45 sec	
Elongation	72°C	1 min	
	72°C	1 min	
	4°C	∞	

WT band: 531bp floxed band: 687bp

PCR for *LysM/Cre* mice

Primer name	**Sequence (5'-3')**
Cre8	CCC AGA AAT GCC AGA TTA CG
MLys1	CTT GGG CTG CCA GAA TTT CTC
MLys2	TTA CAG TCG GCC AGG CTG AC

Step	Temp.	Time	Cycles
Initial Denaturation	95°C	3 min	
Denaturation	95°C	30 sec	x34
Annealing	62°C	30 sec	
Elongation	72°C	1 min	
	72°C	1 min	
	4°C	∞	

WT band: ~350bp Cre band: ~700/1700bp

PCR for *Cyth3*$^{-/-}$ mice

Primer name	Sequence (5'-3')
TG-380	CAC ATG GGA CAC ACA ATC GC
TG-381	AAT AGG AAC TTC GGT TCC GGC
TG-387	ACA GAC TTC GCT GTG GTG AG

Step	Temp.	Time	Cycles
Initial Denaturation	95°C	3 min	
Denaturation	95°C	45 sec	x35
Annealing	60°C	45 sec	
Elongation	72°C	1 min	
	72°C	1 min	
	4°C	∞	

WT band: 500 bp KO band: 257bp

2.3.3 Animal handling and procedure

2.3.3.1 Intravenous injection

To *in vivo* label vasculature associated leukocytes intravenous injections were required. Mice were placed under a heat lamp to promote vasodilation. During the injection procedure, mice were restrained with a restraining device and the tail was disinfected with (80% v/v) ethanol. Intravenous injections of 300 µL of CD45.2 antibody (3 µg/injection) diluted in PBS was performed through the lateral tail veins using 29 G needles. PBS alone was injected into negative controls.

2.3.3.2 Intranasal inoculation

For intranasal inoculation mice were placed into a sealed induction chamber and mice were anaesthetised under controlled isoflurane induction. Under anaesthesia mice were held loosely by skin at the scruff of the neck and 50 µL of inoculum was administered by pipetting dropwise directly on the nares as the mice were breathing. Each droplet was administrated sequentially while ensuring mice had inhaled each droplet prior to the next being administered.

2.3.3.3 Tissue harvest

Mice were euthanised via controlled exposure to CO_2 in appropriated installed containers. After killing, mice were fixed in supine position and skin sterilised with 80% ethanol. Skin was removed and mice were dissected. Using scissors and forceps, tissues including lungs, inguinal and axillary lymph nodes, and spleens were collected in conical tubes filled with sterile PBS. Tissues within the conical tubes were kept on ice until processed.

2.3.3.4 Bronchoalveolar lavage

Mice were killed as described in 2.3.3.3. Skin was disinfected with 80% ethanol prior removal. Muscle tissue from the throat was removed to expose the trachea and incisions were made into the upper trachea. A 20 G catheter (Sureflo® I.V.) was inserted into the lungs through the trachea. The lungs were flushed once

with 1 mL chilled PBS and returned volume of the liquid was collected into a 1.5 mL microfuge tube. Cells were pelleted and used for further analysis. The supernatant was used for cytokine analysis as described in 2.6.1.6.

2.4 Methods

2.5 *In vitro* experiments

2.5.1 *L. pneumophila* replication assay in SecinH3 treated BMDMs

pBMDMs or iBMDMs were seeded with 1.5 x 10^5 cells per well in 24-well tissue culture plate (Corning) using culture medium supplemented with SecinH3 or DMSO alone (vehicle control) one day before infection. The next day (18 h post seeding) cell medium was replaced with fresh medium supplemented with SecinH3 or DMSO one hour before infection. Cells were then infected with *L. pneumophila 130b ΔflaA* diluted in the same medium at a multiplicity of infection (MOI) of 1. Plates were centrifuged at 1000 rpm for 5 min at room temperature (RT) to synchronise infection, then cells were incubated for 2 h at 37°C with 5% CO2 before medium was replaced with fresh medium containing 100 µg/ml gentamicin to kill extracellular bacteria. After 1 h of gentamicin treatment, cells were washed 3 times with pre-warmed PBS to remove gentamicin, and 500 µL of fresh cell medium supplemented with SecinH3 or DMSO was added to the cells. Cells were incubated at 37°C with 5% CO2 till further procedure. For the 3 h post infection (p.i.) time point (directly after gentamicin treatment) cells were washed with PBS and lysed with 200 µL of 0.05% (w/v) digitonin (Sigma Aldrich) diluted in PBS for 5 min before adding 800 µL PBS. Cells were harvested and 100 µL of cell solution were plated onto BCYE agar plates. For time points 24 h and 48 h p.i. cell medium was collected from the wells and cells were lysed with 200 µL 0.05% (w/v) digitonin solution for 5 mins before adding 300 µL PBS. Cells were harvested and combined with the collected medium in a 1.5 mL microfuge tube. Lysates were serially diluted 10-fold, then 100 µL of the cell/medium dilutions were plated onto BCYE agar plates and incubated for 3 days at 37°C. *L. pneumophila* colonies were then counted to determine the colony-forming units (CFU).

2.5.1.1 Isolation of CD4+ T cells from spleen and lymph nodes

For single cell solution, murine spleen or inguinal and axillary lymph nodes were placed on 40-µm cell strainer (Greiner bio-one) containing 3 mL PBS in 60 × 15 mm petri dishes. Using the plunger of a 6-ml syringe, tissue was disrupted against the bottom of the strainer into the petri dish in circular motions. The strainer was then rinsed with 2 mL PBS to wash off remaining cells. The single cell solution was collected from the petri dish and transferred into a new 50 mL conical tube and washed with 20 mL PBS. Cells were centrifuged for 8 min at 300 x g at 4°C. Next, erythrocyte lysis was performed for splenocytes. Therefore, cells were re-suspended in 2 mL RBL buffer and left for 2 mins at RT before adding 18 mL PBS. Cells were centrifuged for 8 mins at 300 x g at 4°C and washed again with 20 mL PBS. For T cell enrichment AutoMACS® Pro Separator (Miltenyi Biotec) was used. Negative isolation of total CD4+ T cells or only naïve CD4+ T cells was performed accordingly to the manufacturer's instruction using isolation kits (Miltenyi Biotec; 130-104-454 or 130-104-453). The purity of the enriched CD4+ T cell populations was checked via flow cytometry.

2.5.2 Differentiation of naïve T cells to Th1 and Th2 cell type

2.5.2.1 Cell proliferation dye

Cell proliferation dye was used to determine whether T cells proliferated efficiently under the polarizing conditions. Naïve CD4+ T cells were washed with PBS to remove any serum (8 min, 300 x g, 4°C). Next, cell suspension was adjusted to 1 x 10^7 leukocytes/ml in PBS (minimum volume 5 ml). Cells were resuspended at 2X the desired final concentration in PBS (pre-warmed to RT). CFSE dye solution (1 µM, eBioscience) was prepared in the same volume of sterile PBS. Dye solution was added to the cells and cells were vortexed. Samples were incubated for 10 min at RT in the dark. Labelling was stopped by adding 4-5 volumes of full T cell medium and incubated on ice for further 5 min. Cells were washed 2x with complete medium before further use.

2.5.2.2 *In vitro* differentiation

Round bottom wells of 96 well tissue culture plates were coated with α-CD3ε (1 µg/mL) and α-CD28 (5 µg/mL) antibodies at 4°C overnight. Next day, wells were washed 3x with PBS and 5 x 10^4 naïve CD4+ T cells were seeded in a volume of 100 µL into wells. 100 µL of T cell media supplemented with polarizing cytokines and reagents for Th0, Th1 or Th2 differentiation were added to the cells. Cells were incubated under polarizing conditions for 4 days at 37°C with 5% CO_2.

Table 1: Cytokine and antibody concentration used for T cell differentiation

Th0 cells		Th1 cells		Th2 cells	
Reagent	Final conc.	Reagent	Final conc.	Reagent	Final conc.
α-IFNγ	10 µg/mL	IFNγ	10 ng/mL	α-IFNγ	10 µg/mL
IL-2	20 ng/mL	IL-2	20 ng/mL	IL-2	20 ng/mL
α-IL-4	10 µg/mL	α-IL-4	2 µg/mL	IL-4	100 ng/mL
		IL-12	20 ng/mL		

2.5.2.3 Restimulation of differentiated T cells

Due to the PMA mediated downregulation of CD4 surface molecules, differentiated T cells were stained for cell surface molecules CD4 and CD3ε prior stimulation (284). After 4 days differentiation, cells were centrifuged (8 min, 300 x g, RT) and supernatant was collected. Cells were washed with 200 µL PBS and transferred into new round bottom wells of 96-well plate and re-stained with CD4 and CD3ε antibodies for 20 min at 4°C. Cells were washed 1x with PBS. After centrifugation (8 min, 300 x g, RT), T cell medium supplemented with Brefeldin A and PMA/ionomycin cell stimulation cocktail was added to the cells. Cells were stimulated for 4 h at 37°C. For non-stimulated controls, normal T cell medium was used.

2.5.2.4 Flow cytometry staining

Cells were washed with PBS then stained with a fixable viability dye for 15 min at 4°C. After two PBS washing steps, cells were fixed in 200 µL with 2% PFA (methanol-free) for 10 min on ice. Next, cell samples were washed 2x with 1x Permeabilisation buffer and intracellularly stained for CD4 and IFNγ or CD4 and IL-4 for 30 min at RT. After washing with 1x Permeabilisation buffer, cells were fixed with 1x Fixation/Permeabilisation buffer for 1 h at RT. Samples were washed with 1x Permeabilisation buffer and transcription factors including Tbet or GATA3 were stained for 30 min at RT, followed by one washing step with 1x Permeabilisation buffer and one washing step with PBS. All staining steps included a separate fluorescence minus one (FMO) control. Samples were analysed on a BD Symphony cytometer.

2.5.2.5 Metabolic analysis

The cellular glycolysis and oxidative phosphorylation were assessed using Seahorse XFe96 Analyzer (Agilent Technologies). One day prior to the experiment, a sensor cartridge (Agilent Technologies) was hydrated at 37°C without CO_2. 3 x 10^5 CD4+ T cells were seeded in a volume of 180 µL on pre-coated poly-L-lysine wells of Seahorse XF96 cell culture microplates (Agilent Technologies) and centrifuged for 1 min at 200 x g. Cells were incubated for 1 h at 37°C without CO_2. Meanwhile cartridge ports were loaded with different stimulation reagents. A volume of 20 µL was used for the first injection, 22 µL for the second injection and 25 µL for the third injection. The cartridge was calibrated accordingly to manufacturers' instructions, then a plate with cells was inserted into the Seahorse XF Analyzer, and the ECAR and OCR were measured. To normalize the ECAR and OCR values to the cell numbers, crystal violet (Sigma Aldrich) staining was performed after Seahorse measurements. Cells were fixed with 2% PFA, followed by the addition of 0.05% (w/v) crystal violet solution for 30 min at RT. Cells were washed 2X with double distilled water, air-dried, resuspended in 200 µL methanol and transferred to a new cell culture 96-well plate (Sarstedt). The absorbance at 590 nm was measured at the infinite M200 plate reader (Tecan).

2.6 *In vivo* experiments

2.6.1 Assessment of immune responses following *L. pneumophila* infection and bacterial load in murine lung

Experiments investigating the innate and adaptive immune responses to *L. pneumophila* infection in mice involved the quantification of leukocytes, determination of *L. pneumophila* positive phagocytes and assessment of *L. pneumophila* CFU in murine lung.

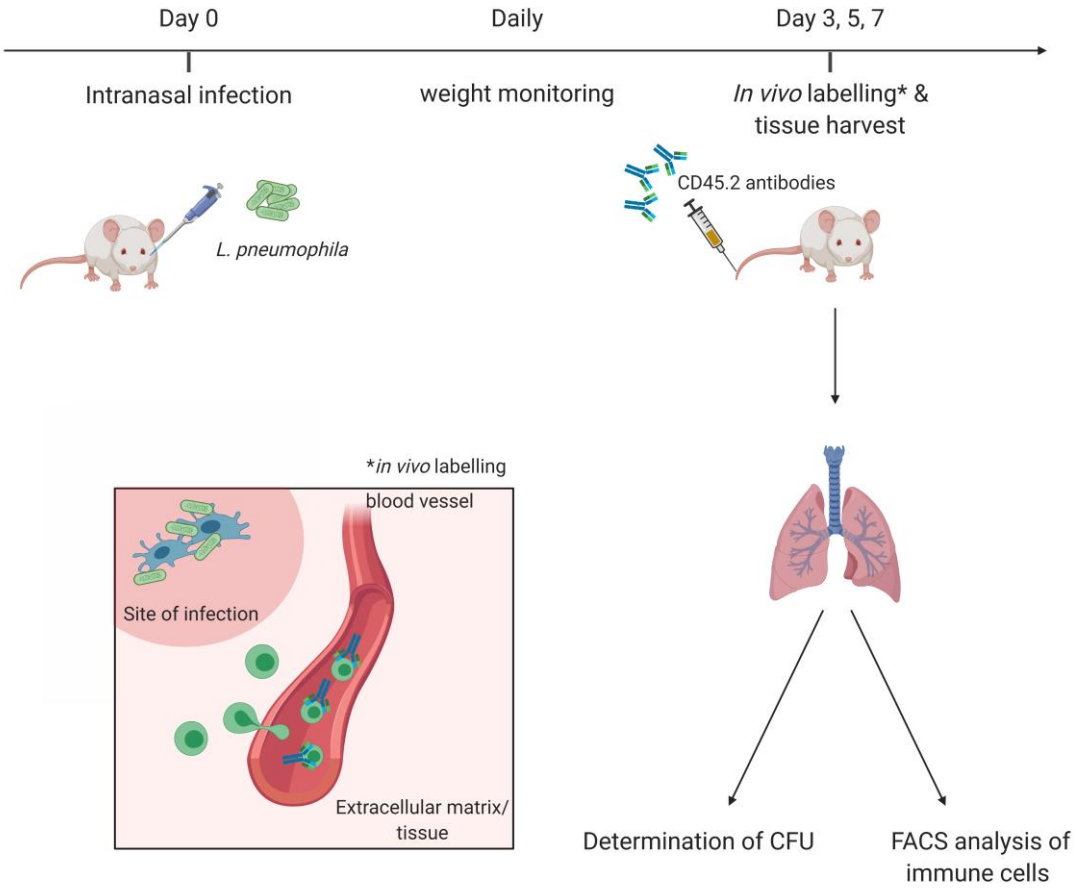

Figure 2.1.: Schematic illustration of experimental timeline and procedures to assess immune responses and bacterial load in murine lung following *L. pneumophila* infection. Mice were infected intranasally with *L. pneumophila*. Mice were weighted daily. Prior to killing and tissue harvest, CD45.2 antibody

solution was injected intravenously into mice to *in vivo* label vasculature-associated leukocytes. This method allowed discrimination of immune cells resident in the lung and those which have successfully infiltrated the lung tissue (site of infection) from immune cells located in the vasculature. Additionally, lung tissue was further processed to determine the CFU.

2.6.1.1 *L. pneumophila* challenge

Colonies of *Legionella* were picked from agar plates and transferred into sterile PBS. For infection inoculum, bacteria density was adjusted via UV-spectroscopy to 5 x 10^7 CFU/mL. A CFU of 2.5 x 10^6 was administrated in 50 µL via intranasal route to each mouse as described in 2.3.3.2. For mock infection sterile PBS was used. The accuracy of the actual inoculum dose was checked by plating the inoculum solution in serial dilutions onto BCYE agar plates, followed by the determination of CFU.

2.6.1.2 Quantitation of *L. pneumophila* CFU in lung tissue

At indicated time points, right lung lobes were harvested from mice as described in 2.3.3.3 and collected in 10 mL conical tubes containing 2.5 mL sterile PBS. This tissue was further homogenised using a tissue homogeniser (Kinematica Polytron) with a 10 mm EasyCare generator at 22,000 rpm for several seconds until completely homogenised. Between different samples the probe was sterilized with 80% ethanol and subsequently rinsed with PBS. Tissue and homogenates were kept on ice during these procedures.

One mL aliquot of each homogenate samples was transferred into microfuge tubes and 0.1% (w/v) saponin solution (Sigma Aldrich) was added. Saponin mediated lysis was performed for 30 min at 37°C. Each lung sample was serially diluted 10-fold in sterile PBS. For the timepoints 3 days p.i. 1/10, 1/100 and 1/1000 dilutions were plated, while for 5 days p.i. 1/10 and 1/100 dilutions were used and for timepoints 7 days p.i. the homogenates were plated neat (not diluted). 100 µL of each dilution was equally distributed on selective agar media by spreading with an ethanol-sterilised glass spreader. All samples were plated in

duplicate and were incubated at 37°C for 3-4 days. The number of colonies of each plate was manually counted and the CFU of *L. pneumophila* in lung tissue was extrapolated accordingly to the dilutions used. In general, plates with more than or equal to 30 colonies present were used for quantification.

2.6.1.3 Preparation of single cell suspensions from lung tissue

Left lung lobes were collected from infected mice as described in 2.3.3.3 and prepared to single cell suspensions via enzymatic digestion. Lung tissue were finely minced using scissors in a petri dish and collected in 3.5 mL tissue digestion buffer (RPMI 1640 medium supplemented with DNAseI and Collagenase III) in a 10 mL conical tube. These samples were incubated for 30 min at 37°C and were mixed by pipetting every ~5 min to dissociate cells from tissue. After the addition of 6.5 mL FACS buffer, the suspension was filtered through a 70 µm nylon strainer (Miltenyi Biotech). The filtrate was pelleted at 400 x g for 5 minutes at 4°C and cells were used for subsequent procedures.

2.6.1.4 Staining of cell surface proteins and erythrocyte lysis

Cell surface proteins of distinct cell types were stained with fluorescent antibodies for flow cytometry analysis. Cells obtained from 2.6.1.3 were split into two FACS tubes and stained with a master-mix cocktail containing a specific panel of antibodies to stain for myeloid cells or lymphocytes. 50 µL of antibody cocktail was added to each sample and samples were vortexed briefly and incubated for 20 min at 4°C. Erythrocytes were lysed for 5 min by adding 500 µL of FACS lysing buffer (BD Biosciences) to the antibody-cell mixture. After, samples were washed with FACS buffer. If necessary, staining of secondary antibody was performed by adding 50 µL of secondary antibody mix then incubating for 15 min at 4°C followed by removal by washing with FACS buffer. In order to stain for viable cells, samples were washed with PBS, 50 µL of fixable viability dye in PBS was added and samples were incubated for 30 min at RT. If no intracellular staining was required, samples were fixed with 2% PFA for 30 min at RT. Samples were then washed and resuspended in FACS buffer. All steps were performed under light-protected conditions. All centrifugation steps were performed at 400 x g for 5 min.

2.6.1.5 Intracellular staining of *L. pneumophila*

Intracellular staining was utilized to detect *L. pneumophila* within different phagocytes. Accordingly the manufacturer's instructions, 200 µL 1x Fixation/Permeabilisation Buffer (eBioscience) was added to the samples following cell surface and viability staining (2.6.1.4), and samples incubated for 30 min at 4°C. Subsequently, samples were washed with 1x Permeabilisation Buffer. FITC conjugated *Legionalla* antibody was diluted in 1x Permeabilisation buffer and in a volume of 50 µL was added to the cells. Cells were incubated for 30 min at 4°C followed by one washing step with 1x Permeabilisation Buffer and then washing step with FACS buffer. Samples were resuspended in FACS buffer and were stored at 4°C till further procedure. All steps were performed under light-protected conditions.

2.6.1.6 APC-labelled microbeads

APC-labelled polymethylmethacrylate microbeads (BD Calibrite) were utilized in flow cytometry analysis to quantify different immune cell populations within tissues. 2 x 10^4 APC-labelled microbeads diluted in FACS buffer were added to the samples prior to sample acquisition on a flow cytometer. After sample acquisition, the factor difference between the recorded events of microbeads and the total added number of microbeads within the sample was used to extrapolate the number of events recorded to the cells present in the full sample. This number within the sample was then further extrapolated to the cell number in the whole lung.

2.6.1.7 Cytokine measurement using cytometric bead array

To determine cytokine and chemokine concentrations, cytometric bead array kit (CBA; BD Biosciences) was used. In this way, a custom CBA panel was designed with CBA flex sets for IL-1α, IL-2, IL-6, IL-17A, IL-12p70, IFNγ, TNFα, GM-CSF and MCP-1. Bronchoalveolar liquid of mice challenged with *L. pneumophila* for 1-3 days was collected as described in 2.3.3.4. CBA was performed according to manufacturer's instructions except using 10-fold less volume of samples and reagents.

2.6.1.8 β-lactamase based effector translocation assay

The principle of the applied effector translocation is based on GeneBLAzer™ technology using CCF2-AM dye (Thermofisher) (248, 285). CCF2-AM is cleaved in the presence of β-lactamase which can be measured spectrophotometrically (**Figure 2.2**). Therefore, mice were infected intranasally (2.3.3.2) with a *L. pneumophila* strain genetically modified to express an effector protein fused to β-lactamase or *L. pneumophila* control strains. One day post infection, bronchoalveolar liquid was harvested as described in 2.3.3.4. Cells obtained from the BAL were pelleted and erythrocyte lysis was performed. Next, cells were washed with 4 mL FACS buffer and 2 x 10^5 cells were transferred into a 5 mL tube. Cells were pelleted and resuspended in 100 µL HBSS (PAN Biotech). Standard loading solution was prepared accordingly to manufacturer's instructions and 20 µL was added to each sample. Samples were incubated for 1 h at RT. After washing with 1 mL HBSS, cells were pelleted and stained with fixable viability dye, antibodies against surface proteins and fixed as above (2.6.1.4). Samples were immediately acquired on the flow cytometer.

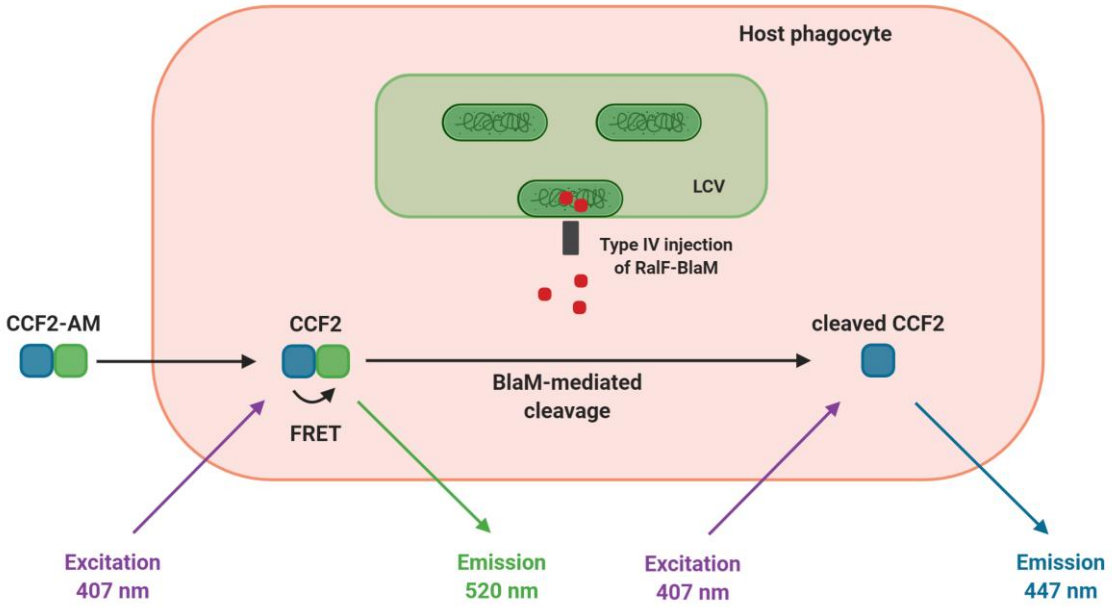

Figure 2.2: Graphical illustration of *L. pneumophila* effector translocation assay. *L. pneumophila* utilizes type IV secretion system to inject effectors such as RalF-BlaM. CCF2-AM dye diffuses into host cell and when excited at 407nm, its emission can be detected at 520 nm. BlaM mediates the cleavage of CCF2 and the product is now detected at 447 nm.

2.6.2 Analysis of T cell responses following influenza A virus challenge

CD8+ T cell responses to influenza A virus were analysed in mice in collaboration with the laboratory of Sammy Bedoui (**Figure 2.3**). Different effector CD8+ T cell subtypes in lung and spleen were quantified following 8 days infection. Additionally, cellular effector functions of splenic antigen-specific CD8+ T cell responses were assessed following *in vitro* restimulation.

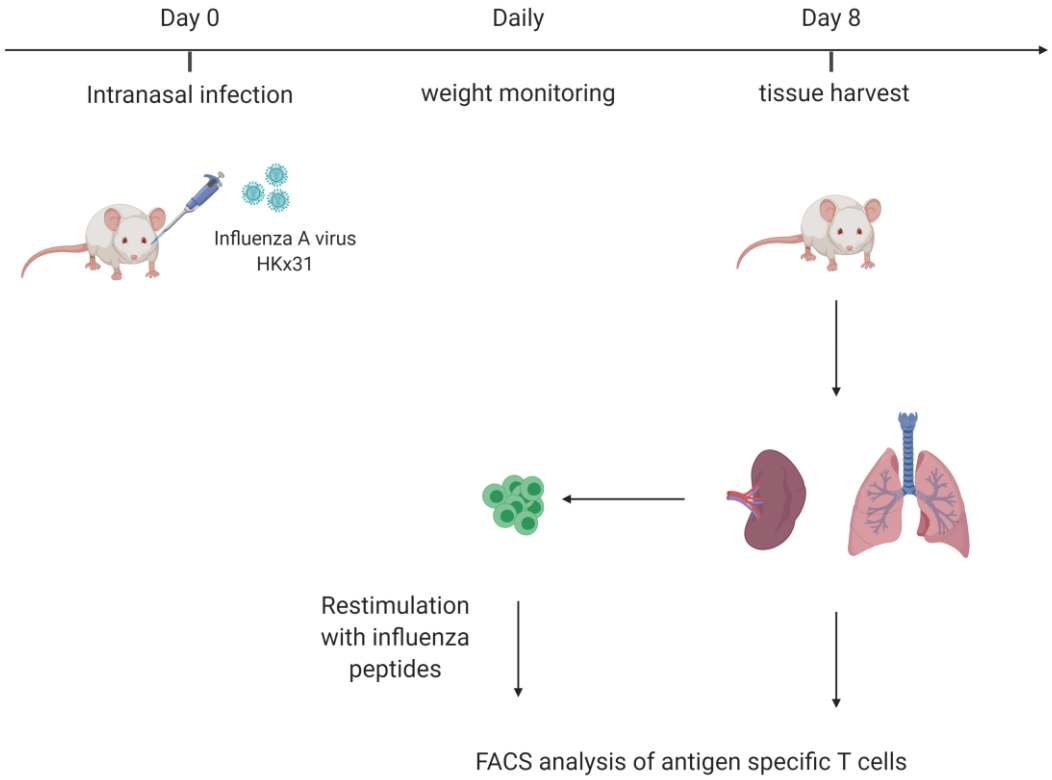

Figure 2.3: Schematic illustration of experimental timeline and procedures to analyse antigen-specific T cell immune responses to influenza A virus infection in mice. Mice were infected intranasally with influenza A virus (HKx31). Mice were weighted daily. Spleen and lung tissues were harvested after 8 days of infection. Spleen and lung tissues were further processed, stained for influenza-specific CD8+ T cells and analysed via flow cytometer. Additionally, splenocytes were *in vitro* stimulated with influenza peptides and the cytokine response of antigen-specific effector T cells was determined.

2.6.3 Influenza A virus challenge

In similar fashion to the *Legionella* challenge described in 2.6.1.1, mice were infected intranasally with HKx31 influenza A virus. Therefore, virus stock solution (3.75 x 10^8 PFU/ml) was diluted in PBS to 2x10^5 PFU/mL. 10^4 PFU in 50 µL was then administrated to each mouse as described in 2.3.3.4.

2.6.3.1 Preparation of single cell suspensions from lung and spleen tissue

Following CO_2 asphyxiation, whole lung and spleen tissue were harvested from mice as described in 2.3.3.3. For single cell suspensions, lung tissue was digested enzymatically as in 2.6.1.3, while spleen tissue was processed to single cell suspension and erythrocyte lysis was performed (analogous to 2.5.1.1). Lung samples were resuspended in a volume of 5 mL T cell medium and spleen samples in a volume of 8 mL T cell medium.

2.6.3.2 Tetramer and cell surface protein staining

200 µL of each cell suspension was transferred into a 96-well tissue culture plate. Cells were pelleted and resuspended in a volume of 50 µL of tetramer mastermix cocktail followed by 30-45 min incubation at 37°C with 6.5% CO_2. After, cells were washed with 100 µL FACS buffer and following centrifugation, resuspended in 50 µL of antibody mix cocktail to stain T cell surface molecules. Antibody staining was performed for 30 min at 4°C. Next, cells were washed with 100 µL FACS buffer and after centrifugation resuspended in 50 µL of propidium iodide (PI) solution to stain for dead cells. Similarly to 2.6.1.6, 2 x 10^4 fluorescent-labelled microbeads were added to each sample to quantify different cell types within lung and spleen tissue.

2.6.3.3 Restimulation of influenza-specific CD8+ T cells

200 µL of splenic cell suspension (2.6.3.1) were transferred into a 96-well tissue culture plate and cells were pelleted. Cells were resuspended in 200 µL of T cell medium containing influenza peptides and samples were incubated for 1 h at 37°C with 6.5% CO_2. Next, Brefeldin A solution was added to the cells and cells were incubated for additional 4 h at 37°C with 6.5% CO_2. For non-stimulated controls, cells were stimulated with pure T cell medium. After restimulation, samples were washed with FACS buffer and stained for flow cytometry.

2.6.3.4 Intracellular staining for cytokines

Prior intracellular staining, samples from 2.6.3.3 were stained first for cell surface markers. Therefore, cells were pelleted and resuspended in a volume of 50 µL of master-mix antibody and fixable viability dye cocktail. Cells were stained for cell surface markers for 30 min at 4°C and washed afterwards with FACS buffer. For fixation, 75 µL of cytofix/cytoperm buffer were added to the cells and samples were incubated for 20 min at 4°C. After 3 washing steps with 1x Permeabilisation buffer, cells were resuspended in 100 µL of cytokine antibody mix diluted in 1x Permeabilisation buffer and left at 4°C for overnight staining. After intracellular staining, samples were washed with 150 µL FACS buffer and 100 µL fluorescent-labelled microbeads were added to the samples prior flow cytometry analysis (2.6.1.6). All staining steps were performed under light protected conditions.

2.7 Flow cytometer analysis

The acquisition of FACS samples was performed on either BD LSRFortessa™ or BD FACSymphony™ cytometers.

2.8 Software

Following software was used within this PhD thesis: FlowJo (V10; 10.5.3), GraphPad Prism 6.0 or 7.0, Inkscape (0.92.4) and BioRender.

2.9 Statistical analysis

Statistical analyses were performed using GraphPad Prism 6.0 or 7.0. software. Data of this study were analysed using two-tailed Mann-Whitney U-test or two-tailed Student's t-test. Differences with p values <0.05 were considered statistically significant.

3. The role of cytohesins in the innate immune response to *Legionella pneumophila* infection

3.1 Introduction

Studies over the past years have revealed the Arf-guanine exchange factors of the protein family cytohesin to exert diverse functions within the immune system and its responses. Through associating to β2 integrins, cytohesins can influence the adhesive and migrating properties of leukocytes, which are essential processes in the innate and adaptive immune response to pathogenic threat or injury (covered in 1.4.4). Another relevant aspect of cytohesins in the regulation of immune responses is their involvement in bactericidal properties of phagocytes including ROS production and phagocytosis (172, 286) . Because of the distinct and broad role of cytohesins in immune cells, they are targeted by several pathogens to evade host immune defence (covered in section 1.4.6). Therefore, cytohesins may be key elements in the coordination and regulation of mammalian immune responses.

However, most observations on the role of cytohesins in immunity are derived from *in vitro* studies and cover only particular aspects of cytohesin function in distinct immune processes. The impact of cytohesins on a multifaceted *in vivo* immune response and primary underlying mechanism(s) are not understood. Studies of this chapter analysed the overall impact of cytohesins in *L. pneumophila* infection *in vitro* and *in vivo* using an *in vitro* cultured macrophages and an *in vivo* murine lung infection model.

Efficient replication of *L. pneumophila* in macrophages follows a series of sequential events that requires both host and bacterial factors. Following uptake, *L. pneumophila* translocates more than 300 effector proteins into the host cell via the Dot/Icm secretion system (178-181). These effector proteins interfere with host cell structure and function in order to evade the cell intrinsic immune response and establish a replicative vacuole termed *Legionella*-containing vacuole (LCV) (182, 183).

In vivo, in mice and humans, a rapid and robust innate cytokine and phagocyte response to *L. pneumophila* follows uptake by alveolar macrophages and this is essential to control the infection. In this context, different phagocytes migrate to the infected site and infiltrate the lung to clear the organism from the pathogenic threat. By using different single knockout (KO) mice for several members of the cytohesin family, the functions of individual cytohesins in the immune response during respiratory infection were assessed, including bacterial load, immune cell recruitment and phagocytosis.

3.2 Results

3.2.1 The GEF function of cytohesins is not required for intracellular replication of *L. pneumophila in vitro*

L. pneumophila replicate intracellularly in alveolar macrophages at the primary site of infection. The establishment of a replicative vacuole within the host cell is required for an efficient replication of *L. pneumophila* (covered in section 1.5). To avoid the murine Naip5 inflammasome response which restricts bacterial replication in the cells or lungs of C57BL/6 mice, an aflagellated *L. pneumophila* mutant (Δ*flaA*) derived from wildtype *L. pneumophila* strain 130b was used (covered in section 1.5.2).

Diverse studies have implicated cytohesins in the invasion and intracellular replication of different bacterial pathogens in host cells (covered in section 1.4.6), yet, it is unknown whether the GEF function of cytohesins is required for the intracellular replication of *L. pneumophila* in macrophages.

To assess whether *L. pneumophila* uptake and/or intracellular replication in macrophages is influenced by the GEF activity of the cytohesins, the GEF function of all cytohesins was pharmacologically inhibited by SecinH3. SecinH3 inhibits se-

lectively the Sec7 domain of only cytohesin proteins. Here, the established concentration of SecinH3 used in the laboratory has elicited inhibition in many systems. Immortalized (iBMDM) as well as primary bone marrow-derived macrophages (pBMDM) were treated 24 hours prior to infection with SecinH3 or the vehicle control (DMSO). iBMDM or pBMDM were inoculated with *L. pneumophila* Δ*flaA* and left for two hours to allow phagocytosis followed by gentamicin treatment to kill extracellular bacteria. iBMDM or pBMDM were maintained in SecinH3 or DMSO supplemented medium until determination of the number of colony-forming units (CFU) of *L. pneumophila* on BYCE agar at specific time points after infection.

Over 48 hours of infection, the inhibition of cytohesin GEF function did not alter *L. pneumophila* replication in iBMDM, with comparable colony-forming units (CFU) observed in DMSO and SecinH3 treated cells (**Figure 3.1A**). The proportion of internalised *L. pneumophila* versus the initial inoculum also did not differ significantly in SecinH3-inhibited macrophages compared to the DMSO control (**Figure 3.1B**). Furthermore, the fold change of the bacterial load in relation to actual inoculum dose increased similarly at 24 and 48 hours after infection in SecinH3-treated cells relative to the DMSO control (**Figure 3.1C**).

A similar picture could be observed in SecinH3 treated pBMDM. *L. pneumophila* replication in SecinH3-treated pBMDM was similar to control pBMDM (**Figure 3.2A**) and SecinH3 treatment also did not affect uptake of the bacteria in pBMDM (**Figure 3.2B**), resulting in a comparable fold increase in bacterial numbers 24 and 48 hours after infection (**Figure 3.2C**).

These results suggested that the GEF activity of cytohesin was not required for efficient replication of *L. pneumophila* in BMDM *in vitro.*

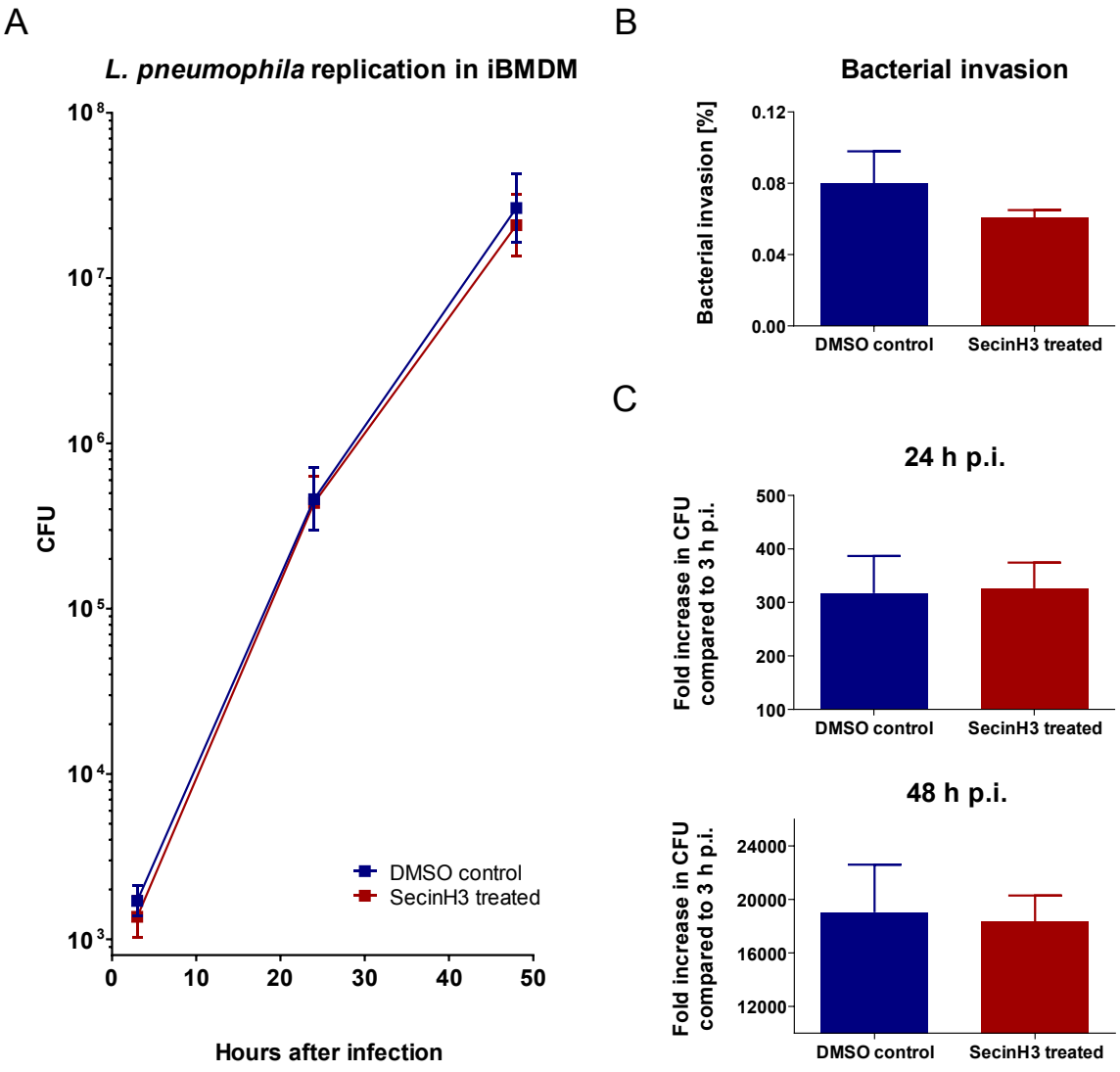

Figure 3.1: Replication of *L. pneumophila* in SecinH3-treated iBMDM. iBMDM were treated with 10 µM SecinH3 or DMSO (vehicle) and infected with *L. pneumophila ΔflaA* for 2 h. Gentamicin was added to kill extracellular bacteria for 1 h and then replaced by media supplemented with SecinH3 or DMSO. iBMDM were lysed with digitonin at different time points (3, 24, 48 h post-infection (p.i.)) and CFU assessed by plating cell lysates onto BCYE agar plates. **A**. Bacterial load in iBMDM following *L. pneumophila* infection. **B**. Percentage of *L. pneumophila* internalised by iBMDM (3 h p.i.). **C**. Fold increase of CFU at 24 and 48 h p.i. compared to 3 h p.i.. Graphs present the mean with SEM. n=3 per time point and data is pooled from three independent experiments. No significant difference was found between SecinH3 treatment and vehicle control (threshold $p<0.05$; unpaired two tailed student t-test).

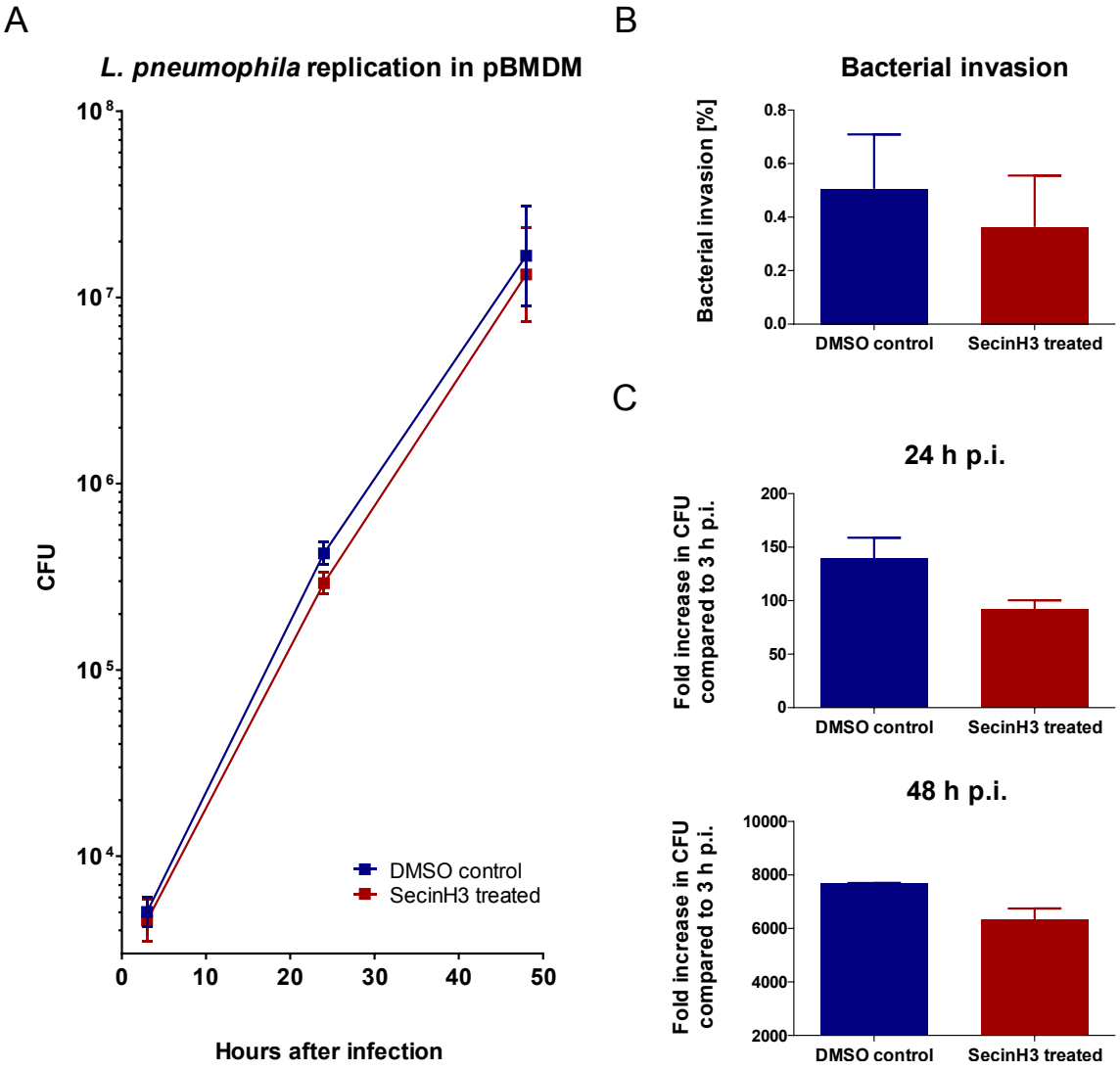

Figure 3.2: Replication of *L. pneumophila* in SecinH3-treated pBMDM. pBMDM were treated with 10 µM SecinH3 or DMSO (vehicle) and infected with *L. pneumophila ΔflaA* for 2 h. Gentamicin was added to kill extracellular bacteria for 1 h and then replaced by media supplemented with SecinH3 or DMSO. pBMDM were lysed with digitonin at different time points (3, 24, 48 h post-infection (p.i.)) and CFU assessed by plating cell lysates onto BCYE agar plates. **A**. Bacterial load in pBMDM following *L. pneumophila* infection. **B**. Percentage of *L. pneumophila* internalised by pBMDM (3 h p.i.). **C**. Fold increase of CFU at 24 and 48 h p.i. compared to 3 h p.i.. Graphs present the mean with SEM. n=3 per time point and data is pooled from three independent experiments. No significant difference was found between SecinH3 treatment and vehicle control (threshold $p<0.05$; unpaired two tailed student t-test).

3.2.2 Cytohesin-1 and -3 are not required for LCV biogenesis

In section 3.2.1 the requirement of cytohesin GEF activity in the efficient invasion and propagation of *L. pneumophila* in BMDM *in vitro* was examined. Experiments in this section aimed to elucidate whether cytohesin-1 or cytohesin-3 are important host factors for LCV biogenesis in phagocytes *in vivo* (287). The method utilizes the effector protein, RalF, that is translationally fused to a β-lactamase reporter (BlaM). The form of BlaM utilised lacks a signal peptide for secretion and hence is only secreted into the host cell cytosol by *L. pneumophila* if fused to an effector protein. Cytosolic BlaM can be detected with the substrate, CCF2. In the presence of BlaM, CCF2 is cleaved into two products which leads to a shift in the fluorescence emission of CCF2 from green to blue (see section 2.6.1.8).

Mice were infected with different *L. pneumophila* strains including *L. pneumophila ΔflaA* transformed with pXDC61 expressing RalF-BlaM, or the control strains *L. pneumophila ΔflaA*, *L. pneumophila ΔflaA* transformed with empty pXDC61 vector and a *L. pneumophila ΔflaAΔdotA* double mutant transformed with pXDC61 expressing RalF-BlaM. *L. pneumophila ΔflaAΔdotA* expresses RalF-BlaM but lacks a functional Dot/Icm secretion system, and so cannot translocate effectors into phagocytes. One day after infection, cells were collected from the BAL and stained with CCF2 to analyse the translocation of bacterial effectors into individual phagocytes identified using antibodies to cell specific markers.

Figure 3.3 shows the translocation of RalF-BlaM in AM of *Cyth1*$^{-/-}$ and *Cyth3*$^{-/-}$ as well as WT mice. Mice that were infected with *L. pneumophila ΔflaA* with pXDC61 RalF-BlaM displayed a conversion of CCF2 from green to blue in AM (**Figure 3.3A**), whereas AM from mice that have received the *dotA* mutant presented no conversion of CCF2 to blue, emphasizing that translocation of *L. pneumophila* effector proteins depends on a functional Dot/Icm type IV secretion system (**Figure 3.3B**). Also, no significant conversion was found in other controls for cells

infected with *L. pneumophila ΔflaA* or *L. pneumophila ΔflaA* transformed with empty pXDC61 vector (not shown).

In AM from WT mice the percentage of CCF2 blue-converted cells accounted for 8.1% in average which was in the range that has been published previously (288). In *Cyth1*$^{-/-}$ and *Cyth3*$^{-/-}$ no significant difference was found in the proportions of CCF2 blue-converted AM compared to WT AM. (**Figure 3.3C**).

Consequently, *Cyth1* and *Cyth3* had no influence on the translocation of RalF into AM *in vivo*.

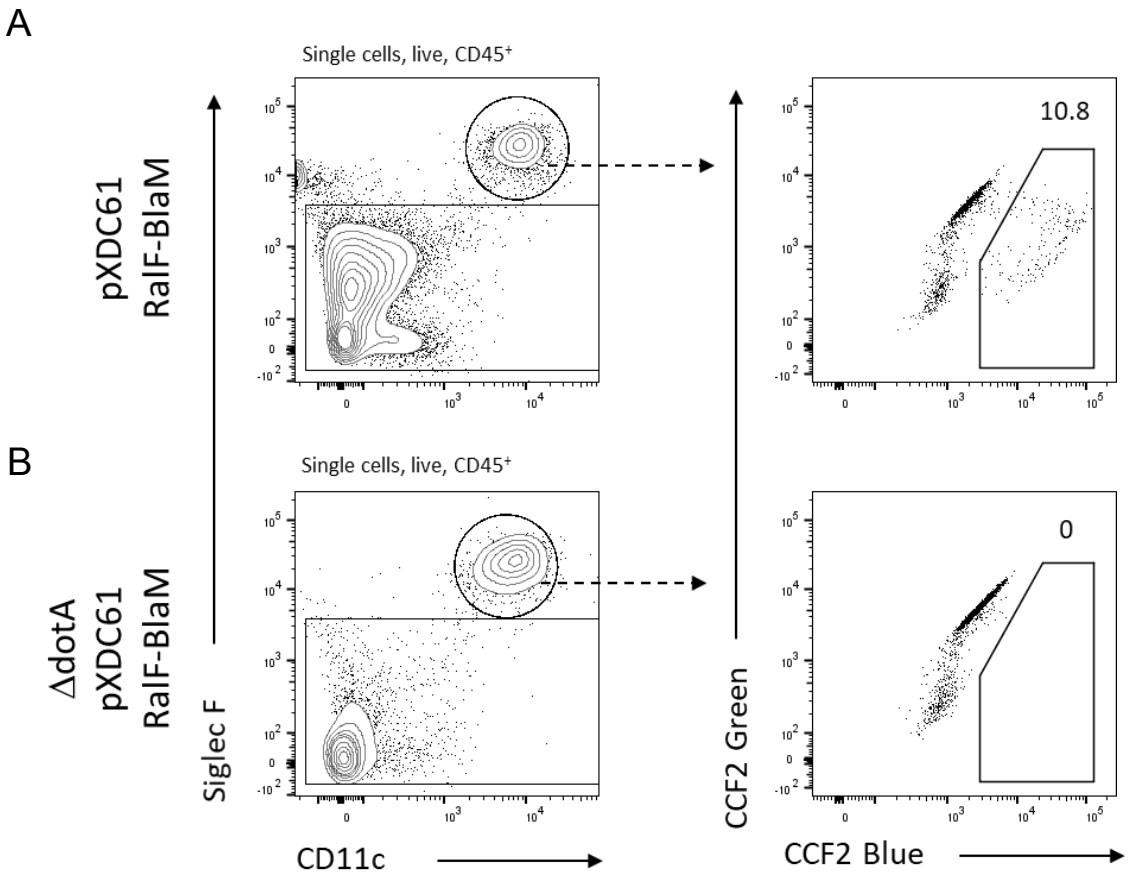
A
Single cells, live, CD45+
pXDC61
RalF-BlaM
10.8
B
Single cells, live, CD45+
ΔdotA
pXDC61
RalF-BlaM
0
Siglec F
CD11c
CCF2 Green
CCF2 Blue

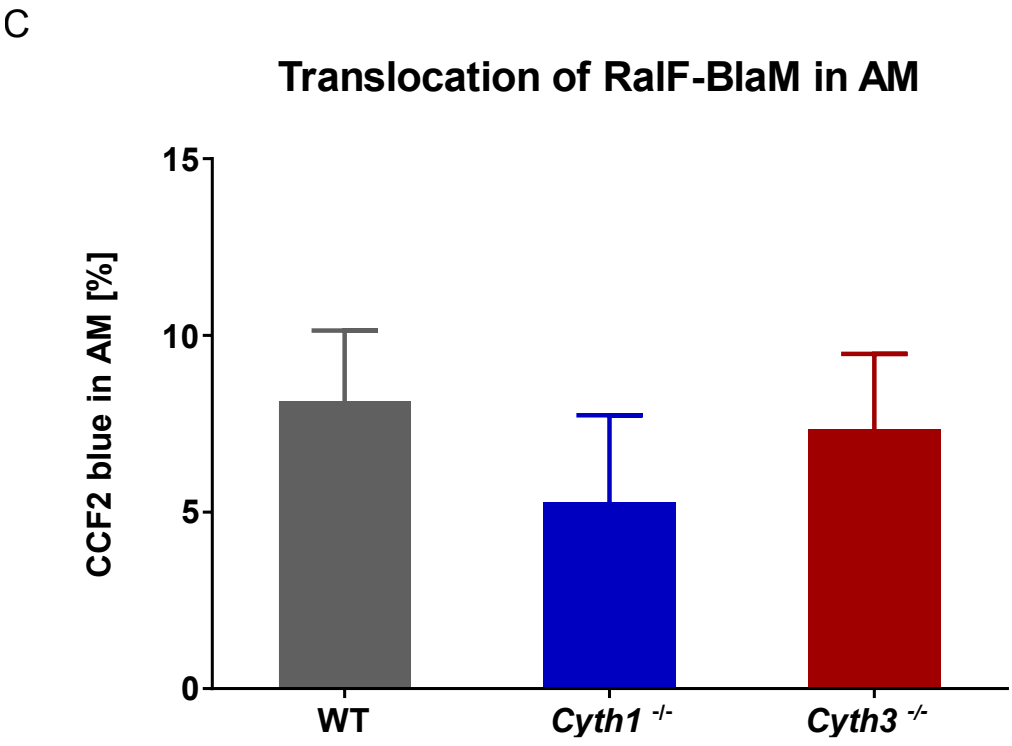
C
Translocation of RalF-BlaM in AM
CCF2 blue in AM [%]
15
10
5
0
WT
Cyth1 -/-
Cyth3 -/-

Figure 3.3: Translocation of *L. pneumophila* effectors in cytohesin-1 or -3 deficient alveolar macrophages *in vivo*. Mice were infected with *L. pneumophila* expressing the translocated effector RalF fused to the reporter protein BlaM (pXDC61 RalF-BlaM) or respective control strains for 1 day. Cells were collected by bronchoalveolar lavage and stained with CCF2-AM dye, which is cleaved by translocated RalF-BlaM resulting in a spectral shift from green to blue. **A**. Gating strategy to identify alveolar macrophages with cleaved CCF2 (blue). Number represents percentage of AM with translocated RalF as measured by CCF2-blue fluorescence. **B**. Cells from mice infected with control *L. pneumophila ΔflaAΔdotA* strain containing pxDC61 plasmid expressing RalF-BlaM shows no translocation. **C**. Percentage of AM with translocated RalF-BlaM measured by CCF2-blue fluorescence from C57BL/6 (WT), cytohesin-1 (*Cyth1*$^{-/-}$) and cytohesin-3 (*Cyth3*$^{-/-}$) mice. Graphs present the mean with SEM. n=3 from one experiment. No significant difference was found between wildtype and knockout mice (threshold $p<0.05$; unpaired two-tailed student t-test).

Although AM are considered to be the key phagocyte that supports the intracellular replication of *L. pneumophila*, the pathogen is also able to translocate effector proteins into neutrophils, although they do not appear to support intracellular replication (288). Similar to AM, translocation of *L. pneumophila* effectors into neutrophils depended on the formation of a functional Dot/Icm type IV secretion system representing 2% of CCF2 Blue-converted neutrophils infected with *L. pneumophila ΔflaA* carrying pXDC61 encoding RalF-BlaM (**Figure 3.4A**) and 0% of CCF2 conversion in neutrophils infected with *L. pneumophila ΔflaAΔdotA* expressing RalF-BlaM (**Figure 3.4B**).

The percentage of neutrophils that converted to CCF2 blue did not statistically differ among *Cyth1*$^{-/-}$, *Cyth3*$^{-/-}$ and WT neutrophils (**Figure 3.4C**) indicating that *Cyth1* and *Cyth3* were not required for the translocation of RalF by *L. pneumophila* in neutrophils.

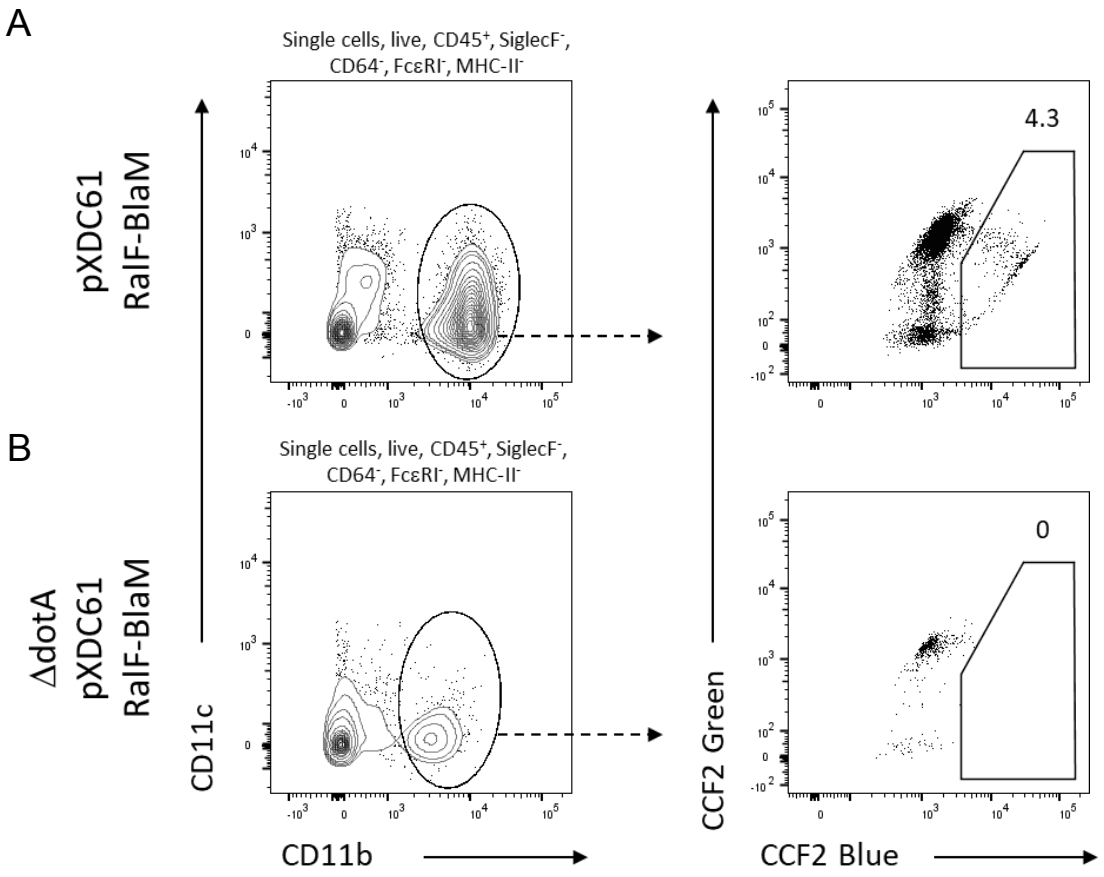
A
Single cells, live, CD45+, SiglecF-, CD64-, FcεRI-, MHC-II-
pXDC61 RalF-BlaM
4.3
B
Single cells, live, CD45+, SiglecF-, CD64-, FcεRI-, MHC-II-
ΔdotA pXDC61 RalF-BlaM
0
CD11c
CD11b
CCF2 Green
CCF2 Blue

C

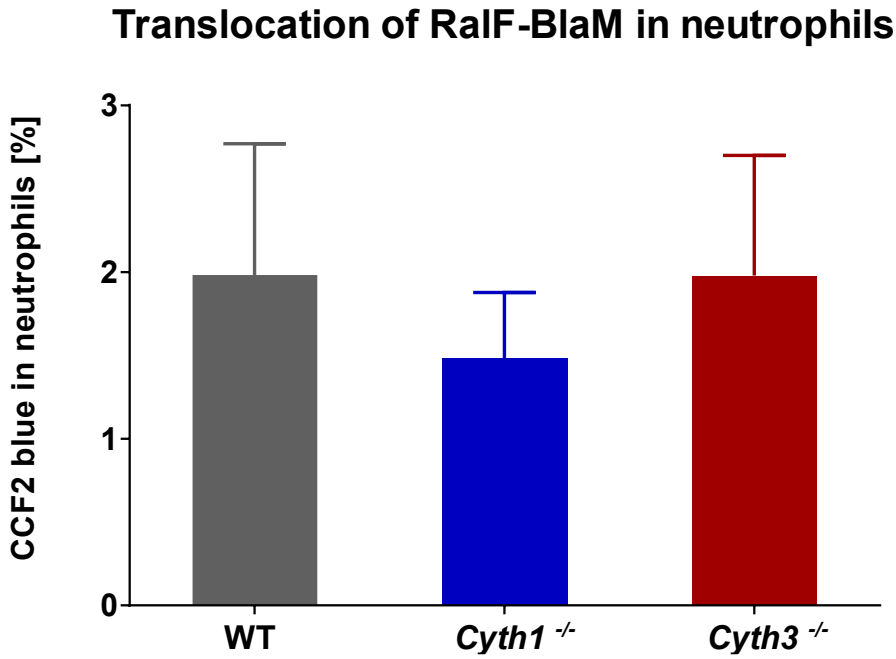
Translocation of RalF-BlaM in neutrophils
CCF2 blue in neutrophils [%]
0
1
2
3
WT
Cyth1 -/-
Cyth3 -/-

Figure 3.4: Translocation of *L. pneumophila* effectors in cytohesin-1 or -3 deficient neutrophils *in vivo*. Mice were infected with *L. pneumophila ΔflaA* expressing the translocated effector RalF fused to the reporter protein BlaM (pXDC61 RalF-BlaM) or respective control strains for 1 day. Cells were collected by bronchoalveolar lavage and stained with CCF2-AM dye, which is cleaved by translocated RalF-BlaM resulting in a spectral shift from green to blue. **A**. Gating strategy to identify neutrophils with cleaved CCF2 (blue). Number represents percentage of neutrophils with translocated RalF as measured by CCF2-blue fluorescence. **B**. Cells from mice infected with control *L. pneumophila ΔflaAΔdotA* strain containing pxDC61 plasmid expressing RalF-BlaM shows no translocation. **C**. Percentage of neutrophils with translocated RalF-BlaM measured by CCF2-blue fluorescence from C57BL/6 (WT), cytohesin-1 (*Cyth1*$^{-/-}$) and cytohesin-3 (*Cyth3*$^{-/-}$) mice. Graphs present the mean with SEM. n=3 from one experiment. No significant difference was found between wildtype and knockout mice (threshold $p<0.05$; unpaired two-tailed student t-test).

The blue conversion of CCF2 by translocated RalF- BlaM in MCs was also investigated. One day after infection, few MCs had infiltrated the bronchoalveolar space. However, mice that were infected with *L. pneumophila ΔflaA* expressing RalF-BlaM showed similar translocation levels in MCs as neutrophils (**Figure 3.5A)**. MCs from mice infected with *L. pneumophila ΔflaAΔdotA* mutant did not show any shift in CCF2 green to blue emission (**Figure 3.5B**).

As in previous analyses, no statistically significant difference was observed in the translocation of RalF-BlaM into MCs in *Cyth1* or *Cyth3* deficient mice (**Figure 3.5C**). Therefore, *Cyth1* and *Cyth3* deficiency did not alter the translocation of RalF-BlaM in MCs.

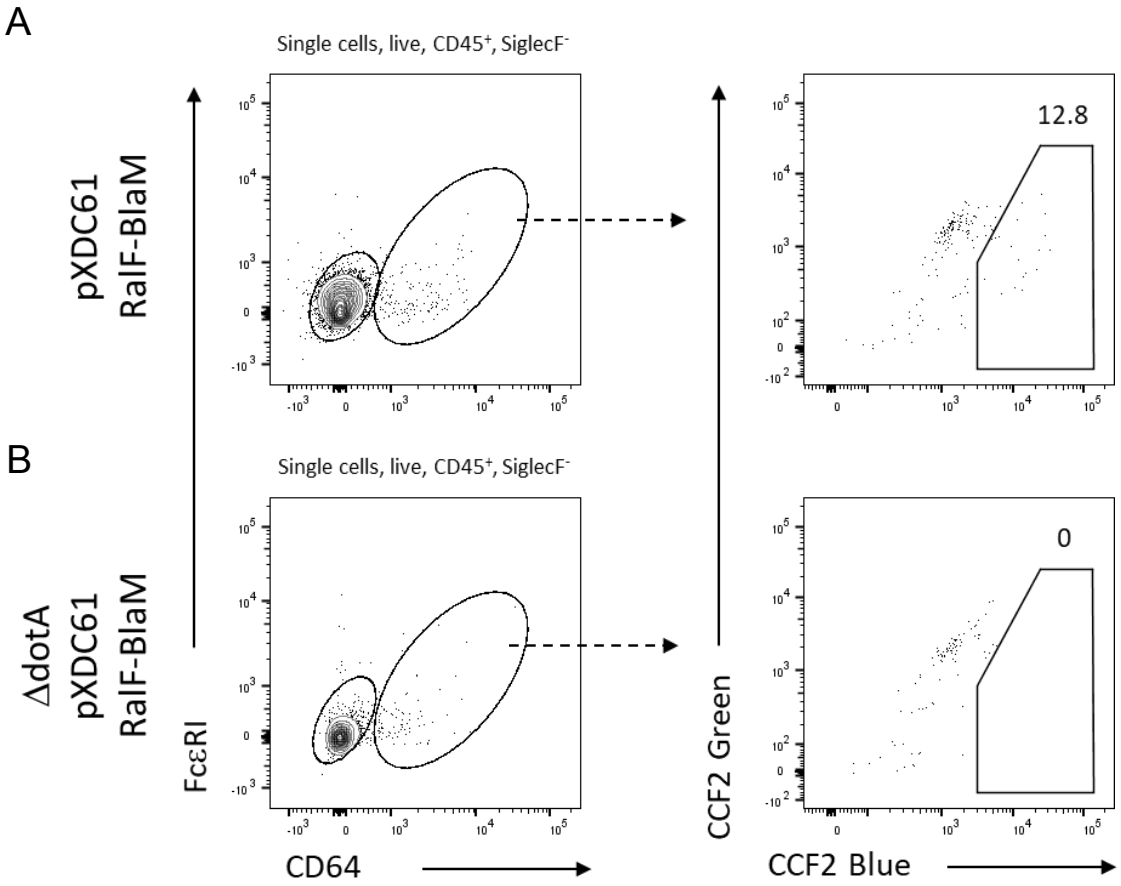
A
Single cells, live, CD45+, SiglecF-
pXDC61
RalF-BlaM
12.8
B
Single cells, live, CD45+, SiglecF-
ΔdotA
pXDC61
RalF-BlaM
0
FcεRI
CD64
CCF2 Green
CCF2 Blue

C

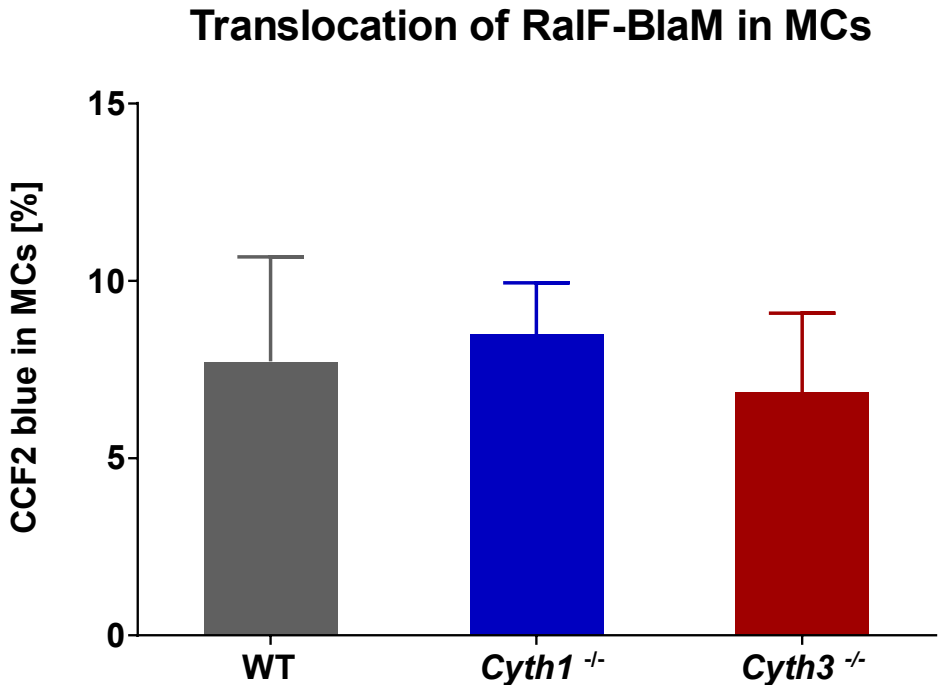
Translocation of RalF-BlaM in MCs
CCF2 blue in MCs [%]
15
10
5
0
WT
Cyth1 -/-
Cyth3 -/-

Figure 3.5: Translocation of *L. pneumophila* effectors in cytohesin-1 or -3 deficient monocyte-derived cells *in vivo*. Mice were infected with *L. pneumophila ΔflaA* expressing the translocated effector RalF fused to the reporter protein BlaM (pXDC61 RalF-BlaM) or respective control strains for 1 day. Cells were collected by bronchoalveolar lavage and stained with CCF2-AM dye, which is cleaved by translocated RalF-BlaM resulting in a spectral shift from green to blue. **A**. Gating strategy to identify monocyte-derived cells with cleaved CCF2 (blue). Number represents percentage of MCs with translocated RalF as measured by CCF2-blue fluorescence. **B**. Cells from mice infected with control *L. pneumophila ΔflaAΔdotA* strain containing pxDC61 plasmid expressing RalF-BlaM shows no translocation. **C**. Percentage of MCs with translocated RalF-BlaM measured by CCF2-blue fluorescence from C57BL/6 (WT), cytohesin-1 (*Cyth1*$^{-/-}$) and cytohesin-3 (*Cyth3*$^{-/-}$) mice. Graphs present the mean with SEM. n=3 from one experiment. No significant difference was found between wildtype and knockout mice (threshold $p<0.05$; unpaired two-tailed student t-test).

In summary, the efficiency of *L. pneumophila* effector translocation was measured in the main pulmonary phagocytes known to internalise *L. pneumophila* during infection *in vivo*. Neither cytohesin-1 nor cytohesin-3 altered the efficiency of effector translocation and were therefore unlikely to influence LCV biogenesis.

3.2.3 Cytohesin-3 contributes to weight recovery after *L. pneumophila* infection

The phenotype of different cytohesin knockout (KO) mice challenged with *L. pneumophila* was assessed to elucidate the overall effect of cytohesin deficiency on the immune response to respiratory infection. The specific mouse strains utilized were cytohesin-1 (*Cyth1*) and cytohesin-3 (*Cyth3*) germline knockout (KO) strains, and conditional (cond.) cytohesin-2 (*Cyth2*) KO mice, which contains both floxed *Cyth2* alleles and a single $Lyz2^{Cre}$ allele resulting in deletion of *Cyth2* in certain myeloid cells. The expression of Cre recombinase by the *Lyz2* promoter generates deletion of *Cyth2* only in myeloid cell populations. The latter strain was used because germline knockout of *Cyth2* results in neonatal lethality (Jux, B., unpublished). Although a fourth member of the cytohesin family exists (*Cyth4)*, this was not investigated in these studies as knockout animals have not yet been generated.

In order to assess the overall phenotype during *Legionella* infection, control mice (see below) and cytohesin KO mice were challenged with aflagellated *L. pneumophila* then assessed over a 7 day period where body weight was monitored daily. For the control groups, wildtype C57BL/6 (WT) mice were used for *Cyth1* and *Cyth3* KO experiments, while myeloid-specific *Cyth2* KO experiments required the controls, *Cyth2* floxed Cre-recombinase negative mice and *Cyth2* wildtype Cre-recombinase positive mice to account for the hemizygous deletion of *Lyz2* gene.

The expected phenotype for the *L. pneumophila* infection model in C57BL/6 mice is weight loss in the early stages of infection (1-3 days) (established model in our laboratory). After the third day, when the innate immune response peaks and bacterial burden drops, mice typically start to regain weight. The phenotype observed in these experiments was consistent with this for WT mice (**Figure 3.6**).

On day 1 post-infection (p.i.), $Cyth1^{-/-}$ *and* $Cyth3^{-/-}$ mice exhibited a minor increase in weight loss compared to WT (**Figure 3.6A**). However, this normalized by day 2. More interestingly, $Cyth3^{-/-}$ mice displayed a significantly delayed and reduced

weight recovery that manifested after 3 days p.i.. Notably, after 7 days, infected *Cyth3*$^{-/-}$ mice still had not fully regained initial body weight in contrast to *Cyth1*$^{-/-}$ and WT mice.

During *L. pneumophila* infection in *Cyth2* mice, myeloid-specific *Cyth2* KO mice showed comparable weight reduction as the control mice (**Figure 3.6B**). In addition, weight gain among these groups proceeded in similar fashion till day 5 p.i.. Intriguingly, by day 7 p.i. myeloid-specific *Cyth2* KO mice had gained significantly more weight compared to *Cyth2*$^{fl/fl}$ mice (**Figure 3.6B**).

These results demonstrated that loss of *Cyth1* or myeloid deletion of *Cyth2* did not affect the overall health of animals as measured by weight upon *Legionella* infection. In contrast, loss of *Cyth3* had strong impact on the recovery of mice following *L. pneumophila* infection.

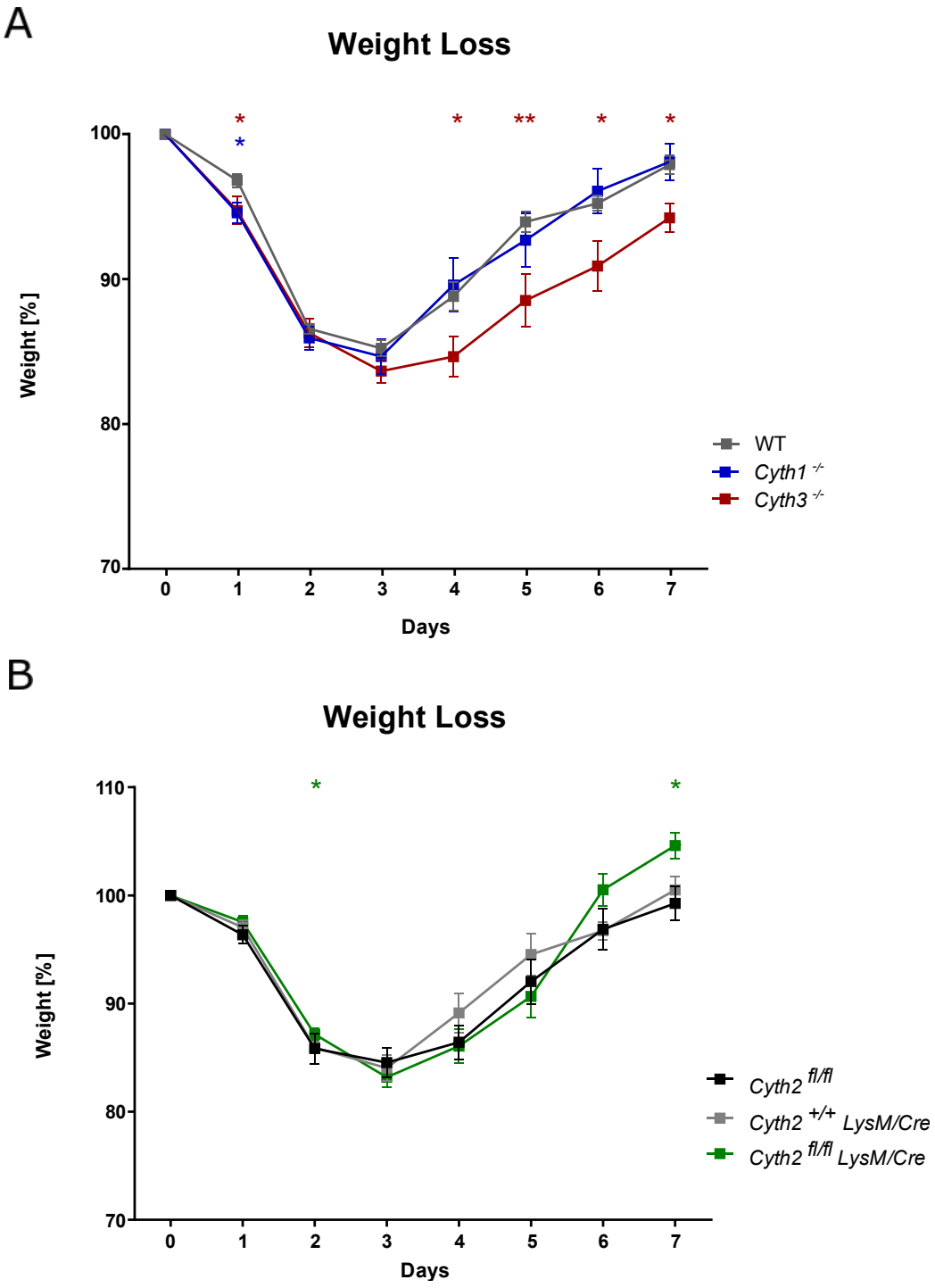

Figure 3.6: Body weights of cytohesin-1 and cytohesin-3 knockout mice and cytohesin-2 conditional knockout mice following *L. pneumophila* infection. C57BL/6 (WT), cytohesin-1 (*Cyth1*$^{-/-}$) and cytohesin-3 (*Cyth3*$^{-/-}$) knockout mice (**A**.) and cytohesin-2 conditional knockout (*Cyth2*$^{fl/fl}$ *LysM/Cre*), floxed cytohesin-2 (*Cyth2*$^{fl/fl}$) and LysM/Cre (*Cyth2*$^{+/+}$ *LysM/Cre*) control mice (**B**.) were challenged with *L. pneumophila ΔflaA* and weighed daily. Graphs present the mean with SEM. n≥7 pooled from n≥2 independent experiments (*, p<0.05; **, p<0.01; two-tailed Mann-Whitney U-test).

3.2.4 Cytohesins are not required for pulmonary clearance of *L. pneumophila*

To determine if genetic loss of the cytohesins affected pulmonary clearance of *L. pneumophila*, the bacterial burden in cytohesin KO mice was assessed over the course of the 7 days. Lungs were collected and the number of colony-forming units were determined from lung homogenates (as described in 2.6.1).

The typical kinetics of bacterial load observed in this model are that bacterial burden increases within the first 2 days, followed by gradual clearance (established model in our laboratory). This is consistent with what was observed in these experiments (**Figure 3.7A**).

In the course of *L. pneumophila* infection assessed here, none of cytohesin-1, cytohesin-2 or cytohesin-3 had any effect on bacterial load, with *Cyth1*$^{-/-}$ and *Cyth3*$^{-/-}$ mice showing same trend of bacterial burden as WT mice (**Figure 3.7A**). Hemizygous replacement of the original *Lyz2* gene resulted in a minor reduction in bacterial load on day 5, which is consistent with a role for lysozyme in clearing bacterial infection. However, the additional deletion of *Cyth2* did not alter the bacterial burden in comparison to *Cyth2*$^{+/+}$ *LysM/Cre* (**Figure 3.7B**).

Overall, none of the cytohesins analysed had an effect on pulmonary clearance of *L. pneumophila* in mice.

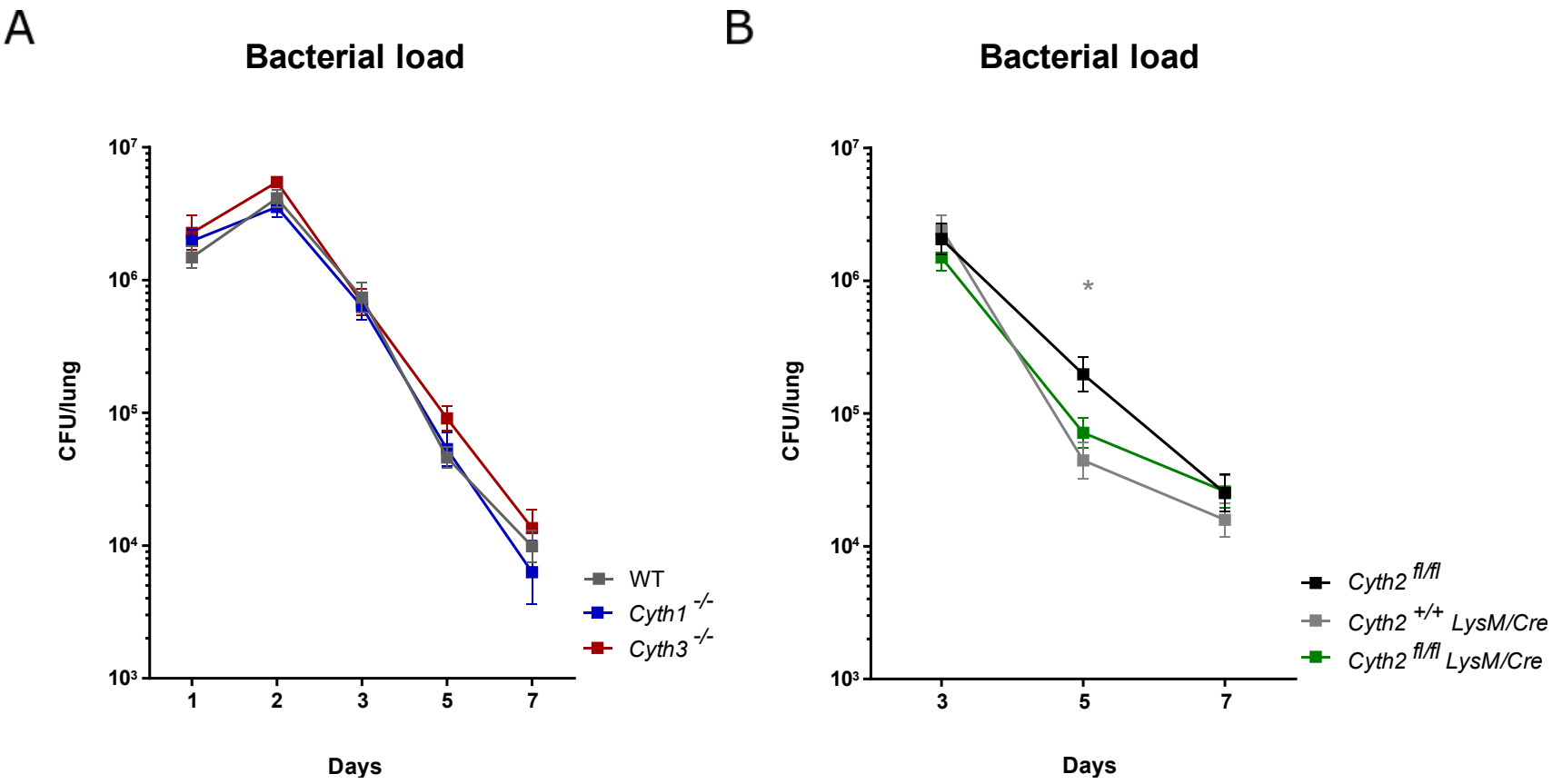

Figure 3.7: Bacterial burden in the lungs of cytohesin-1 and cytohesin-3 knockout and cytohesin-2 cond. knockout mice following *L. pneumophila* infection. C57BL/6 (WT), cytohesin-1 (*Cyth1*$^{-/-}$) and cytohesin-3 (*Cyth3*$^{-/-}$) knockout mice (**A**.) and cytohesin-2 conditional knockout (*Cyth2*$^{fl/fl}$ *LysM/Cre*), floxed cytohesin-2 (*Cyth2*$^{fl/fl}$) and LysM/Cre (*Cyth2*$^{+/+}$ *LysM/Cre*) control mice (**B**.) were challenged with ~2.5 × 10^6 *L. pneumophila ΔflaA*. At indicated time points, lungs were collected, homogenized, cells lysed with saponin and serial dilutions of lysates plated on BCYE agar plates to determine total CFU. n≥7 pooled from n≥2 independent experiments (*, $p<0.05$; two-tailed Mann-Whitney U-test).

3.2.5 Cytohesin-1 and cytohesin-3 deficiency leads to elevated pulmonary cytokine release, while cytohesin-2 conditional knockout results in partially decreased cytokine levels

Respiratory infection with *L. pneumophila* leads to acute inflammation in the murine lung resulting in strong cytokine production by tissue resident and infiltrated immune and non-immune cells at the primary site of infection (182, 289). The release of IFNγ, TNF and IL-12 at the site of infection leads to an enhanced bactericidal activity of certain innate immune cells and in this way, drives the bacterial clearance (244, 290, 291). Furthermore, IL-6 exerts pro- and anti-inflammatory functions and additionally to IL-17A, IL-10 and IL-12 it shapes T cell responses (292-296). Moreover, monocyte chemoattractant protein-1 (MCP-1) plays an important role in the recruitment of monocytes, neutrophils and lymphocytes to the site of infection (297). To analyse the effect of cytohesins on the cytokine response upon *L. pneumophila* infection, BAL were collected from cytohesin KO and control mice after *L. pneumophila* infection. Levels of IFNγ, TNF, MCP-1, IL-12, IL-6, IL-17A and IL-10 were determined using cytometric bead array.

Overall, the cytokine response appeared to peak on the second day of infection, which is consistent with previous descriptions of this model (**Figure 3.8**) (established model in our laboratory). Interestingly, cytohesin deficiency in mice showed an effect on pulmonary cytokine levels in a time-dependent manner.

In the early stages of *L. pneumophila* infection *Cyth1*$^{-/-}$ mice displayed significantly elevated levels of pulmonary TNF on day 1 post-infection (p.i) and enhanced levels of IFNγ, IL-12 and IL-17A on day 2 p.i.. No effect of *Cyth1* deficiency was observed in the release of MCP-1, IL-10 and IL-6 (**Figure 3.8**).

In the BAL of *Cyth3*$^{-/-}$ mice IL-12 and IL-6 were elevated on day 2 p.i. but no significant alterations in the secretion of pulmonary IFNγ, TNF IL-17A, MCP-1 and IL-10 was observed in *Cyth3* deficient animals (**Figure 3.8**).

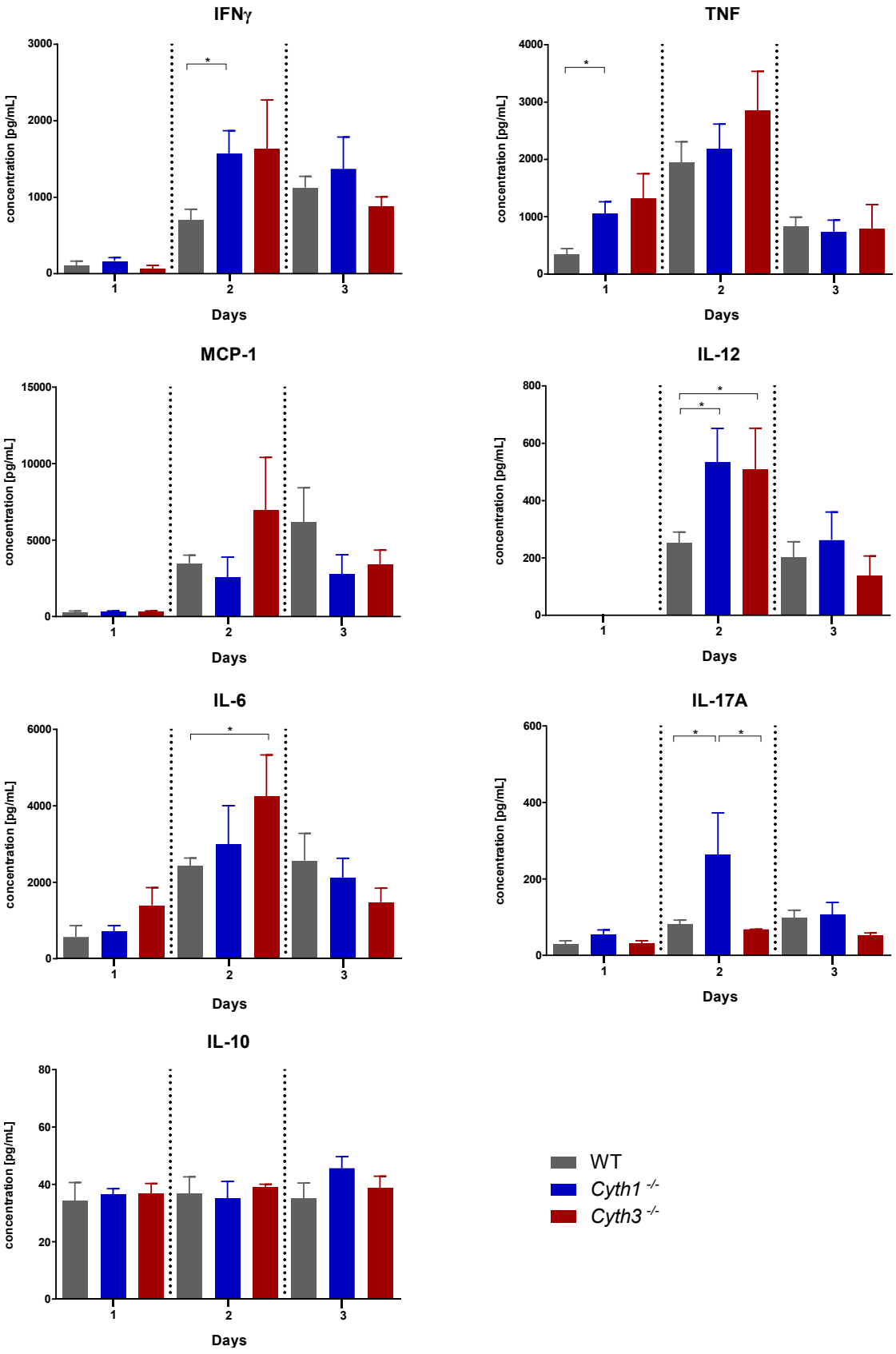
IFNγ
TNF
MCP-1
IL-12
IL-6
IL-17A
IL-10
concentration [pg/mL]
Days
WT
Cyth1 -/-
Cyth3 -/-

Figure 3.8: Pulmonary cytokine levels in *L. pneumophila* infected cytohesin-1 and cytohesin-3 knockout mice. C57BL/6 (WT), cytohesin-1 (*Cyth1*$^{-/-}$) and cytohesin-3 (*Cyth3*$^{-/-}$) knockout mice were infected with *L. pneumophila ⊿flaA* and bronchoalveolar lavages performed at the indicated timepoints. Levels of IFNγ, TNF, MCP-1, IL-12, IL-6, IL-17A and IL-10 were measured by cytometric bead array. Graphs present the mean and SEM. n=3-7 pooled from ≥ 2 experiments (*, $p<0.05$;**, $p<0.01$; unpaired two tailed student t-test).

In myeloid-specific *Cyth2* KO, a significantly reduced amount of pulmonary IFNγ was observed relative to floxed and Cre-recombinase controls on day 2 and 3 p.i., as well as reductions in IL-12 and IL-17A levels on day 2. In contrast, MCP-1 levels and IL-6 appeared to be elevated in the BAL of myeloid-specific *Cyth2* KO mice, whereas IL-10 and TNF concentrations were similar among the analysed groups (**Figure 3.9**).

These results showed that cytohesins differentially affect the release of specific cytokines in the bronchoalveolar space following *L. pneumophila* infection. The strongest effects on the cytokine response was observed in the BAL of *Cyth1*$^{-/-}$ mice. Deletion of *Cyth1* led to elevated levels of IFNγ, TNF, IL-12 and IL-17A. Additionally, deficiency of *Cyth3* resulted in an enhanced release of pulmonary IL-12 and IL-6 and conditional KO of *Cyth2* affected the release of IL-6 and MCP-1. However, this KO had mostly an inhibitory effect on the secretion of IFNγ, IL-12 and IL-17A. Given that the alterations in cytokine levels were observed at specific time points p.i., this suggested a temporal regulation of cytokine release by cytohesins.

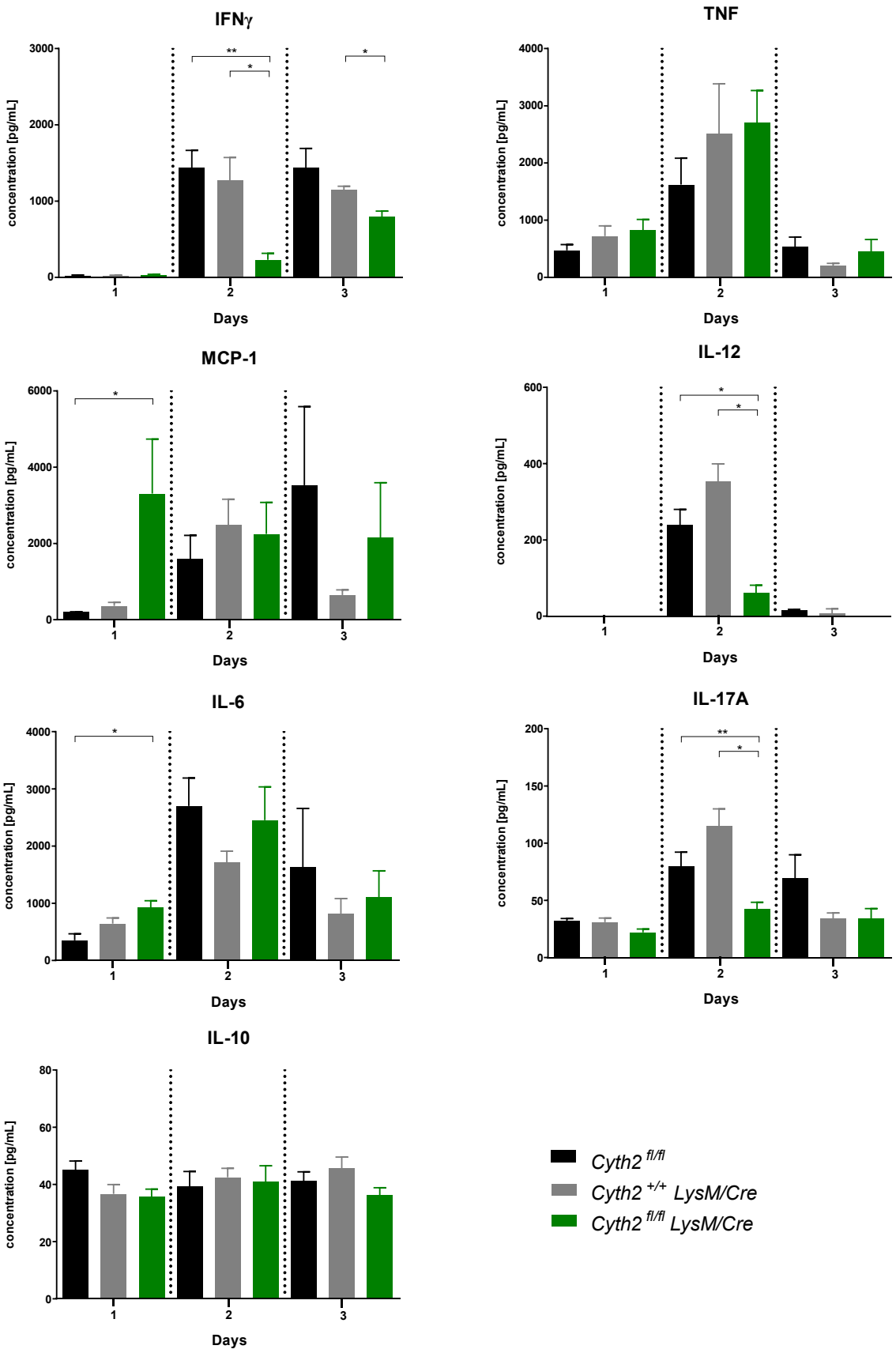
IFNγ
concentration [pg/mL]
Days
TNF
MCP-1
IL-12
IL-6
IL-17A
IL-10
Cyth2 fl/fl
Cyth2 +/+ LysM/Cre
Cyth2 fl/fl LysM/Cre

Figure 3.9: Pulmonary cytokine levels in *L. pneumophila* infected cytohesin-2 conditional knockout mice. Cytohesin-2 conditional knockout (*Cyth2$^{fl/fl}$ LysM/Cre*), floxed cytohesin-2 (*Cyth2$^{fl/fl}$*) and LysM/Cre (*Cyth2$^{+/+}$ LysM/Cre*) control mice were infected with *L. pneumophila ΔflaA* and bronchoalveolar lavages performed at the indicated timepoints. Levels of IFNγ, TNF, MCP-1, IL-12, IL-6, IL-17A and IL-10 were measured by cytometric bead array. Graphs present the mean and SEM. n=3-7 pooled from ≥ 2 experiments (*, $p<0.05$;**, $p<0.01$; unpaired two tailed student t-test).

3.2.6 Phagocyte transmigration after *L. pneumophila* infection

The alterations in cytokine response observed in 3.2.5 could result in differential recruitment of leukocytes to the lung in cytohesin KO mice. Additionally, it is established that cytohesins have roles in cell adhesion and cell migration. Therefore, the studies in this section examined the impact of cytohesin-deficiency on the recruitment and transmigration of different phagocyte populations.

In order to investigate the effect of cytohesins on phagocyte recruitment to the site of inflamed tissue following *L. pneumophila* infection, control mice and cytohesin KO mice were challenged with *L. pneumophila ⊿flaA* over a 7-day period and the number of phagocytes were enumerated at certain time points during the infection. To investigate the transmigratory properties of leukocytes and to distinguish lung-infiltrated immune cells in cytohesin deficient mice, a CD45.2 antibody was injected into the tail vein prior to killing to label all leucocytes in the vasculature (see illustration **Figure 2.1**). Leukocytes that did not stain with CD45.2 antibody were considered to have infiltrated into the lung. After harvesting the lung and processing to single cell suspension, cells were stained with an antibody mix that included a second CD45 antibody, which recognizes a distinct epitope, to discriminate individual types of phagocytes. For correct identification of CD45.2 positivity, a WT control mouse was injected with PBS (vehicle) instead of CD45.2 antibody in each experiment to indicate true CD45.2 negativity (**Figure 3.10B, Figure 3.11B, Figure 3.12B**).

3.2.6.1 Cytohesins in neutrophil recruitment

Upon infection, neutrophils rapidly infiltrate the lungs of mice and represent one of the dominant cell types in the innate response to *L. pneumophila* (244).

During *L. pneumophila ΔflaA* infection, neutrophils showed a 30-fold increase 3 days p.i compared to steady state in WT mice (**Figure 3.10C** left). At 3 days p.i. around 80% of the recruited neutrophils were located within the lung tissue as opposed to remaining in the lung vasculature (**Figure 3.10C** right). By day 7 p.i. the number of tissue located neutrophils had dropped, but high numbers of neutrophils still remained in the whole lung vasculature (**Figure 3.10C**).

The neutrophil kinetics in whole lung (**Figure 3.10C** left) and lung tissue (**Figure 3.10.C** right) of *Cyth1*$^{-/-}$ and *Cyth3*$^{-/-}$ mice were similar to WT mice following infection. The proportion of neutrophils that transmigrated into the tissue in relation to whole lung was also similar among the groups (**Figure 3.10E**), indicating that *Cyth1* and *Cyth3* did not participate in neutrophil recruitment and their extravasation into the lung tissue.

Neutrophil kinetics in *Cyth2* mice presented the same trend as the controls (**Figure 3.10D**) showing a similar amount of neutrophils entered the lung (**Figure 3.10E**). Notably, *Cyth2*$^{fl/fl}$ control mice displayed a significantly enhanced number of total and infiltrated neutrophils compared to the other groups on day 5 p.i. suggesting that heterozygosity of the *LysM* gene alone could affect phagocyte numbers (**Figure 3.10D**). The enhanced neutrophil count reflected the higher bacterial burden observed in 3.2.4 for this time point. On day 7 p.i., myeloid-specific KO *Cyth2* mice showed a minor elevation in the total neutrophil number compared to the controls, but this was small and unlikely to have physiological effect (**Figure 3.10D**).

Consequently, deficiency in *Cyth1, Cyth2 and Cyth3* did not strongly affect the migration properties of neutrophils.

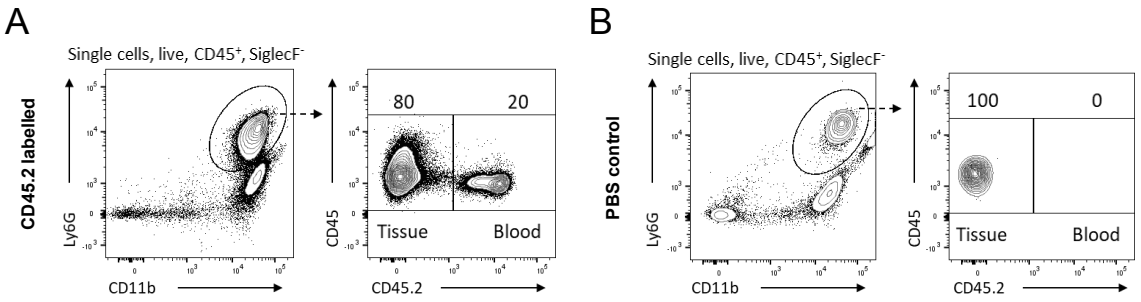
A
Single cells, live, CD45+, SiglecF-
CD45.2 labelled
Ly6G
CD11b
80
20
CD45
Tissue
Blood
CD45.2
B
Single cells, live, CD45+, SiglecF-
PBS control
Ly6G
CD11b
100
0
CD45
Tissue
Blood
CD45.2

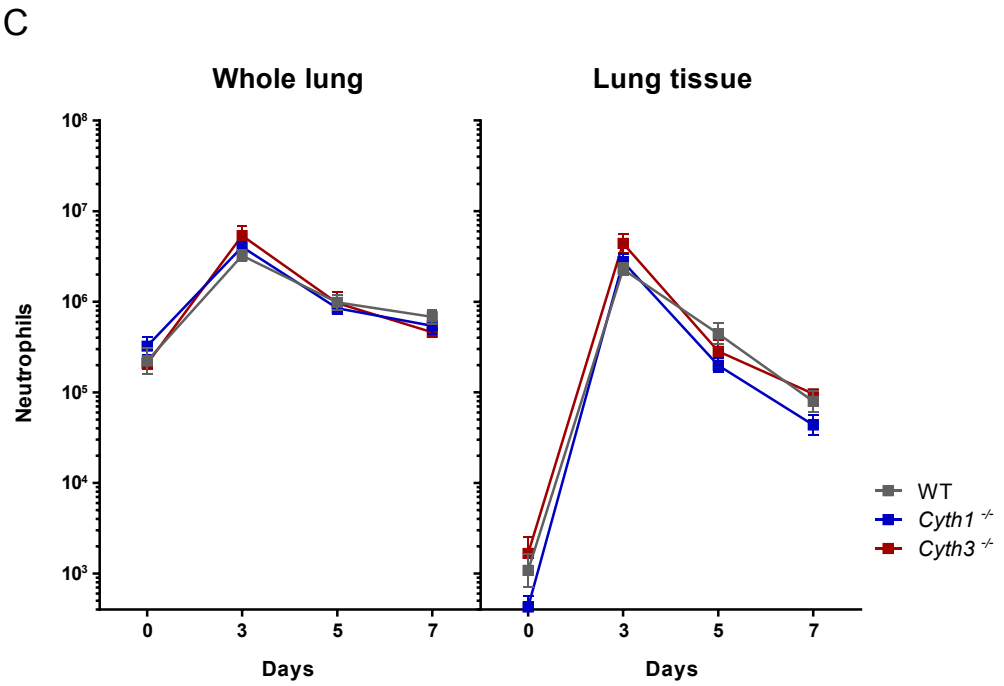
C
Whole lung
Lung tissue
Neutrophils
Days
WT
Cyth1 -/-
Cyth3 -/-

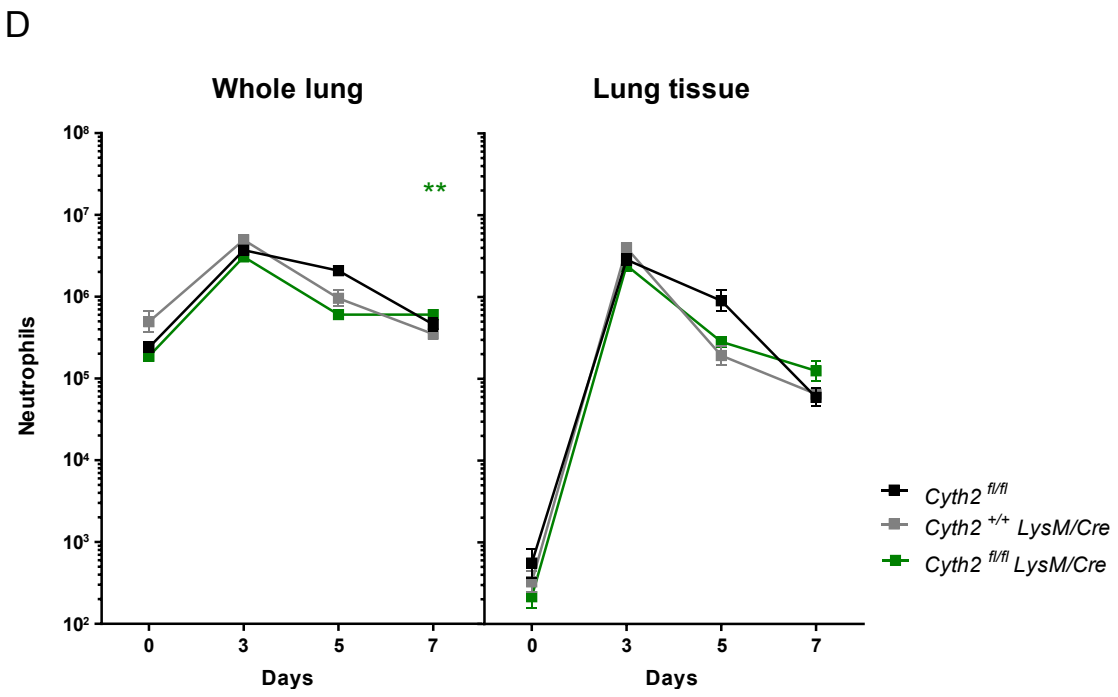
D
Whole lung
Lung tissue
**
Neutrophils
Days
Cyth2 fl/fl
Cyth2 +/+ LysM/Cre
Cyth2 fl/fl LysM/Cre

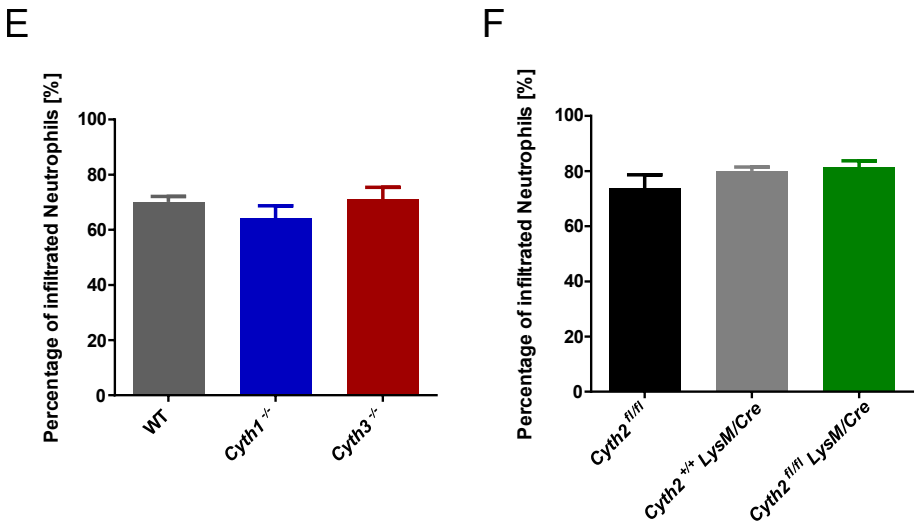

Figure 3.10: Kinetics of neutrophil recruitment in the lungs of cytohesin knockout mice following *L. pneumophila* infection. Mice were infected with *L. pneumophila ΔflaA*, then injected with CD45.2 antibody i.v. to label cells in the vasculature prior to analysing lung cells by flow cytometry at indicated timepoints. **A**. and **B**. Simplified gating strategy for neutrophils in murine lung after CD45.2 antibody (A.) or PBS (B.) injection following 3 days infection. Dotted arrows indicate sequential gating. **C**. Enumeration of neutrophils in C57BL/6 (WT), cytohesin-1 (*Cyth1*$^{-/-}$) and cytohesin-3 (*Cyth3*$^{-/-}$) knockout mice. **D**. Enumeration of neutrophils in cytohesin-2 conditional knockout (*Cyth2*$^{fl/fl}$ *LysM/Cre*), floxed cytohesin-2 (*Cyth2*$^{fl/fl}$) and LysM/Cre (*Cyth2*$^{+/+}$ *LysM/Cre*) control mice. Left panels present the neutrophil count in the whole lung with vasculature, right panels present the cell count of infiltrated neutrophils into the lung tissue. **E**. and **F**. Percentage of lung-infiltrated vs total neutrophils in the lung after 3 days infection. Graphs present the mean with SEM. n≥8 pooled from n≥2 independent experiments. Significant differences were found between *Cyth2*$^{fl/fl}$ *LysMCre* and *Cyth2*$^{+/+}$ *LysM/Cre* (day 7) and *Cyth2*$^{fl/fl}$ between *Cyth2*$^{fl/fl}$ *LysMCre* and *Cyth2*$^{+/+}$ *LysM/Cre* (day 5, not indicated) in whole lung (**, p<0.01; two-tailed Mann-Whitney U-test).

3.2.6.2 Cytohesins in monocyte recruitment

Given their plasticity, differentiated monocytes overlap in function and morphology with tissue-resident macrophages and cDCs, and therefore, are termed as monocyte derived cells (MCs) (26-28). Early in *L. pneumophila* infection, MCs migrate into the lung in large numbers and are one of the main contributors to the clearance of *L. pneumophila* infection (244).

MC numbers increased 200-fold from steady state 3 days p.i with *L. pneumophila ⊿flaA* (**Figure 3.11C**). In the later stages of infection, the number of MCs slowly decreased but, in contrast to neutrophils, MCs still stayed relatively high which is consistent with previous reports (244).

The analysis of MCs in infected *Cyth1*$^{-/-}$ mice showed similar overall kinetics as WT mice, except for day 3 p.i. where the MC count was slightly elevated in *Cyth1*$^{-/-}$ compared to WT mice (**Figure 3.11C**). *Cyth3*$^{-/-}$ mice also displayed similar MC kinetics relative to WT upon *L. pneumophila* infection (**Figure 3.11C**). Again, infected *Cyth2* mice showed equal infiltration and kinetics of MCs relative to the controls (**Figure 3.11D**).

In summary, among the analysed cytohesins only *Cyth1* had any effect on MC recruitment. However, this was minor and likely does not have any biological significance.

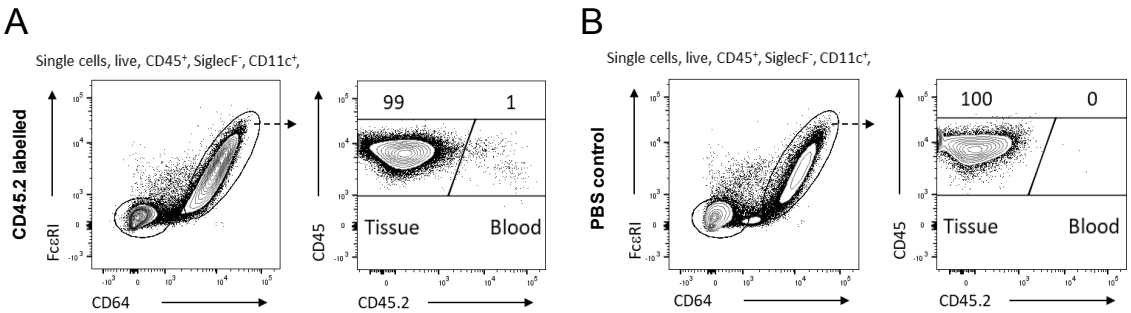
A
Single cells, live, CD45+, SiglecF-, CD11c+,
CD45.2 labelled
FcεRI
CD64
99
1
CD45
Tissue
Blood
CD45.2
B
Single cells, live, CD45+, SiglecF-, CD11c+,
PBS control
FcεRI
CD64
100
0
CD45
Tissue
Blood
CD45.2

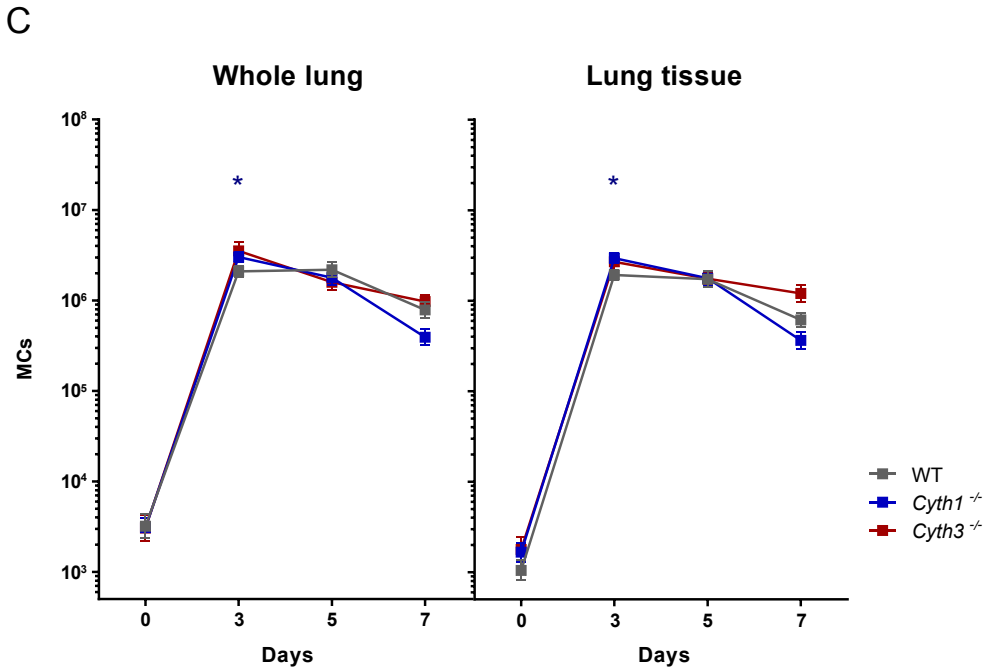
C
Whole lung
Lung tissue
MCs
Days
WT
Cyth1 -/-
Cyth3 -/-

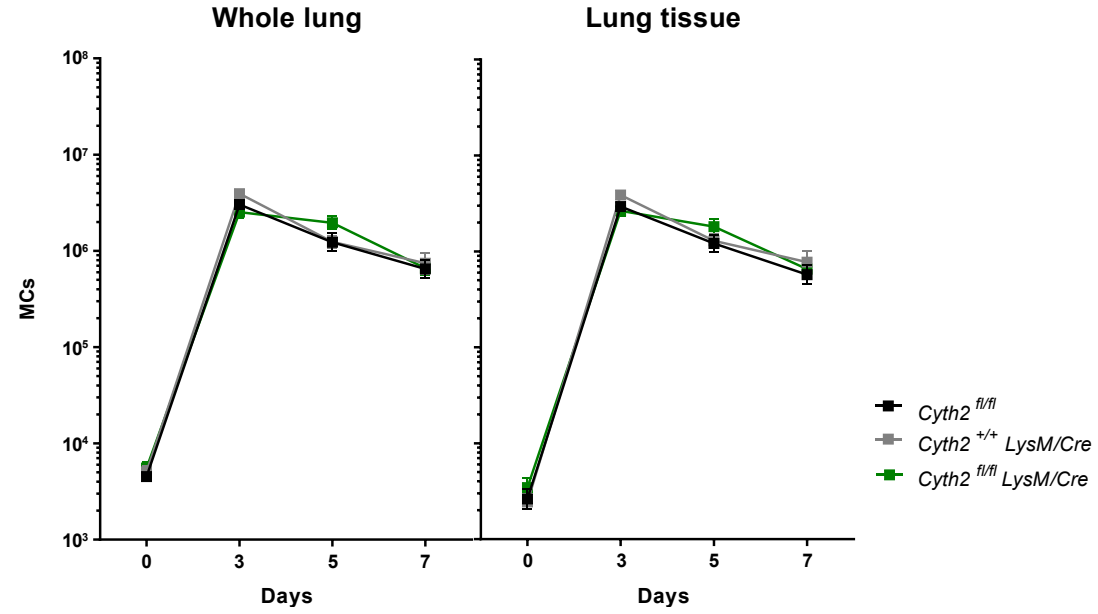
D
Whole lung
Lung tissue
MCs
Days
Cyth2 fl/fl
Cyth2 +/+ LysM/Cre
Cyth2 fl/fl LysM/Cre

Figure 3.11: Kinetics of monocyte-derived cell recruitment in the lungs of cytohesin knockout mice following *L. pneumophila* infection. Mice were infected with *L. pneumophila ⊿flaA*, then injected with CD45.2 antibody i.v. to label cells in the vasculature prior to analysing lung cells by flow cytometry at indicated timepoints. **A**. and **B**. Simplified gating strategy for monocyte-derived cells (MCs) in murine lung after CD45.2 antibody (*A.*) or PBS (*B.*) injection following 3 days infection. Dotted arrows indicate sequential gating. **C**. Enumeration of MCs in C57BL/6 (WT), cytohesin-1 (*Cyth1*$^{-/-}$) and cytohesin-3 (*Cyth3*$^{-/-}$) knockout mice. **D**. Enumeration of MCs in cytohesin-2 conditional knockout (*Cyth2*$^{fl/fl}$ *LysM/Cre*), floxed cytohesin-2 (*Cyth2*$^{fl/fl}$) and LysM/Cre (*Cyth2*$^{+/+}$ *LysM/Cre*) control mice. Left panels present the MC count in the whole lung with vasculature, right panels present the cell count of infiltrated MCs into the lung tissue. Graphs are shown the mean with SEM. n≥8 pooled from n≥2 independent experiments. Significant differences were found between *Cyth1*$^{-/-}$ and WT in whole lung and lung tissue on day 3 p.i. (*, $p<0.05$; two-tailed Mann-Whitney U-test).

3.2.6.3 Cytohesins in cDC kinetics

There are two populations of cDCs described in the lung. cDC1 can be identified by high CD103 expression, and are typically present on the basolateral face of the epithelia in the alveolar space. cDC2 express CD11b, and are located deeper in the lung parenchyma (32, 223, 245-247). This study did not discriminate the two populations but rather investigated the total number of all cDCs in the lung.

In the course of infection, the number of cDCs increased 10-fold (3 days p.i.) compared to steady state and reached its peak by day 5 (**Figure 3.12C**).

Similar to MCs, the cDC levels were significantly increased in *Cyth1*$^{-/-}$ mice whereas *Cyth3*$^{-/-}$ mice showed identical cDC kinetics as WT mice (**Figure 3.12C**). In contrast, lack of *Cyth2* led to a transient lower cDC count on day 3 compared to the controls (**Figure 3.12D**).

Consequently, only *Cyth1* and *Cyth2* affected cDC numbers which could indicate an alteration in T cell priming in these mice upon infection.

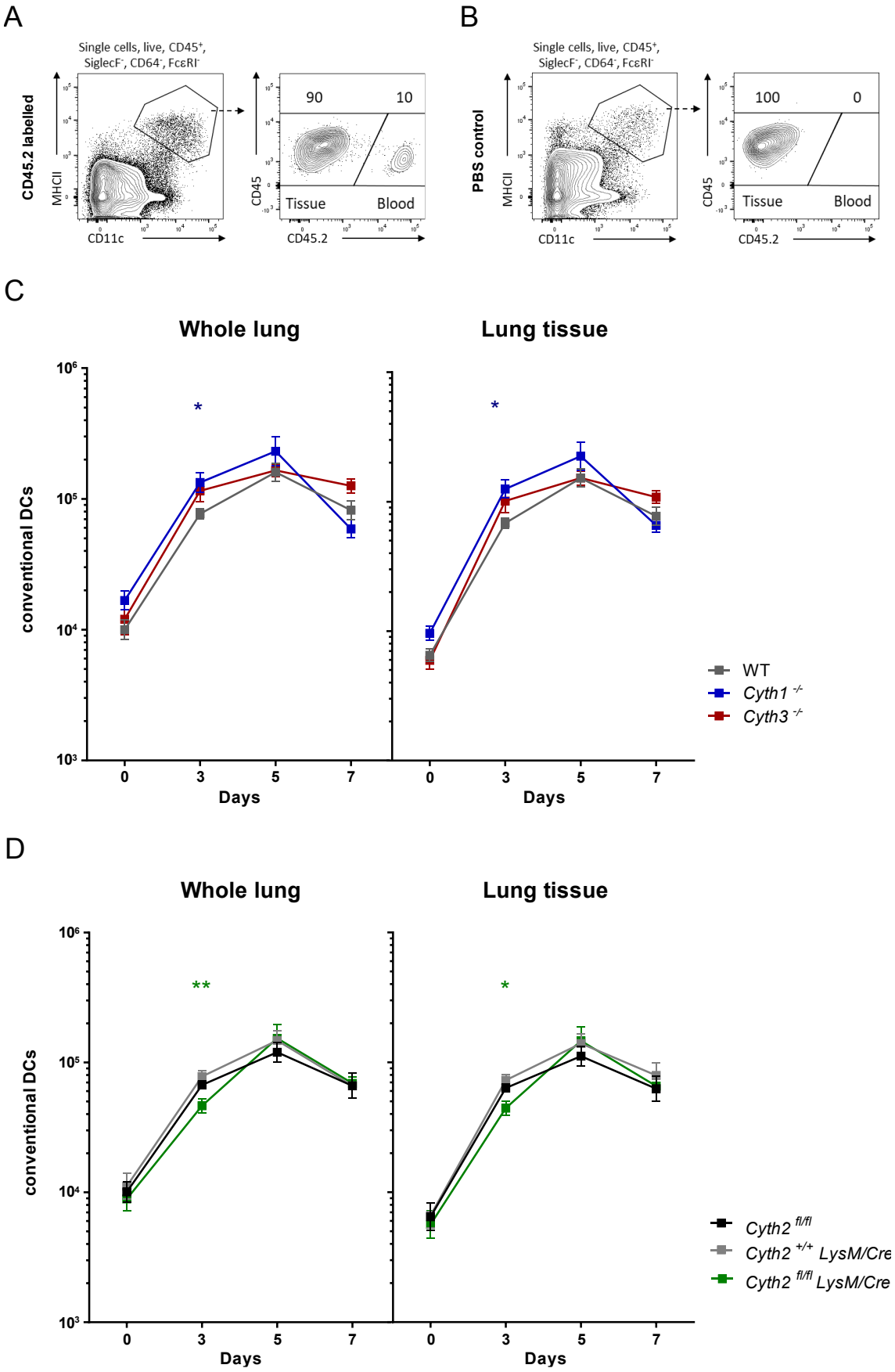
A
Single cells, live, CD45+, SiglecF-, CD64-, FcεRI-
CD45.2 labelled
MHCII
CD11c
CD45
CD45.2
90
10
Tissue
Blood
B
Single cells, live, CD45+, SiglecF-, CD64-, FcεRI-
PBS control
MHCII
CD11c
CD45
CD45.2
100
0
Tissue
Blood
C
Whole lung
Lung tissue
conventional DCs
Days
WT
Cyth1 -/-
Cyth3 -/-
D
Whole lung
Lung tissue
conventional DCs
Days
Cyth2 fl/fl
Cyth2 +/+ LysM/Cre
Cyth2 fl/fl LysM/Cre

Figure 3.12: Kinetics of conventional dendritic cell recruitment in the lungs of cytohesin knockout mice following *L. pneumophila* infection. Mice were infected with *L. pneumophila ⊿flaA*, then injected with CD45.2 antibody i.v. to label cells in the vasculature prior to analysing lung cells by flow cytometry at indicated timepoints. **A**. and **B**. Simplified gating strategy for conventional dendritic cells (cDCs) in murine lung after CD45.2 antibody (A.) or PBS (B.) injection following 3 days infection. Dotted arrows indicate sequential gating. **C**. Enumeration of cDCs in C57BL/6 (WT), cytohesin-1 (*Cyth1*$^{-/-}$) and cytohesin-3 (*Cyth3*$^{-/-}$) knockout mice. **D**. Enumeration of cDCs in cytohesin-2 conditional knockout (*Cyth2*$^{fl/fl}$ *LysM/Cre*), floxed cytohesin-2 (*Cyth2*$^{fl/fl}$) and LysM/Cre (*Cyth2*$^{+/+}$ *LysM/Cre*) control mice. Left panels present the cDC count in the whole lung with vasculature, right panels present the cell count of infiltrated cDCs into the lung tissue. Graphs present the mean with SEM. n≥8 pooled from n≥2 independent experiments. Significant differences were found between *Cyth1*$^{-/-}$ and WT in whole lung and lung tissue, *Cyth2*$^{fl/fl}$ *LysM/Cre* and *Cyth2*$^{+/+}$ *LysM/Cre* and *Cyth2*$^{fl/fl}$ in whole lung and in lung tissue (*, $p<0.05$; **, $p<0.01$ two-tailed Mann-Whitney U-test).

3.2.6.4 Cytohesins in AM kinetics

Alveolar macrophages (AM) are the most abundant cell type of lung-tissue-resident macrophages and are found at the epithelia of the alveolar space (32, 223). Therefore, this cell population is stained negative for the intravenously injected CD45.2 antibody. Because AM are the replicative niche for *L. pneumophila,* it is assumed that bacterial replication and subsequent cell lysis led to a decrease in AM number after infection (**Figure 3.13A**) (established model in our laboratory). As the bacteria were cleared and the bacterial burden in the lung declined, AM slowly replenished and increased in cell number from 5 day p.i..

Overall, *Cyth1*, *Cyth3* (**Figure 3.13B**) or *Cyth2* (**Figure 3.13C**) deficiency did not influence AM number prior or post infection.

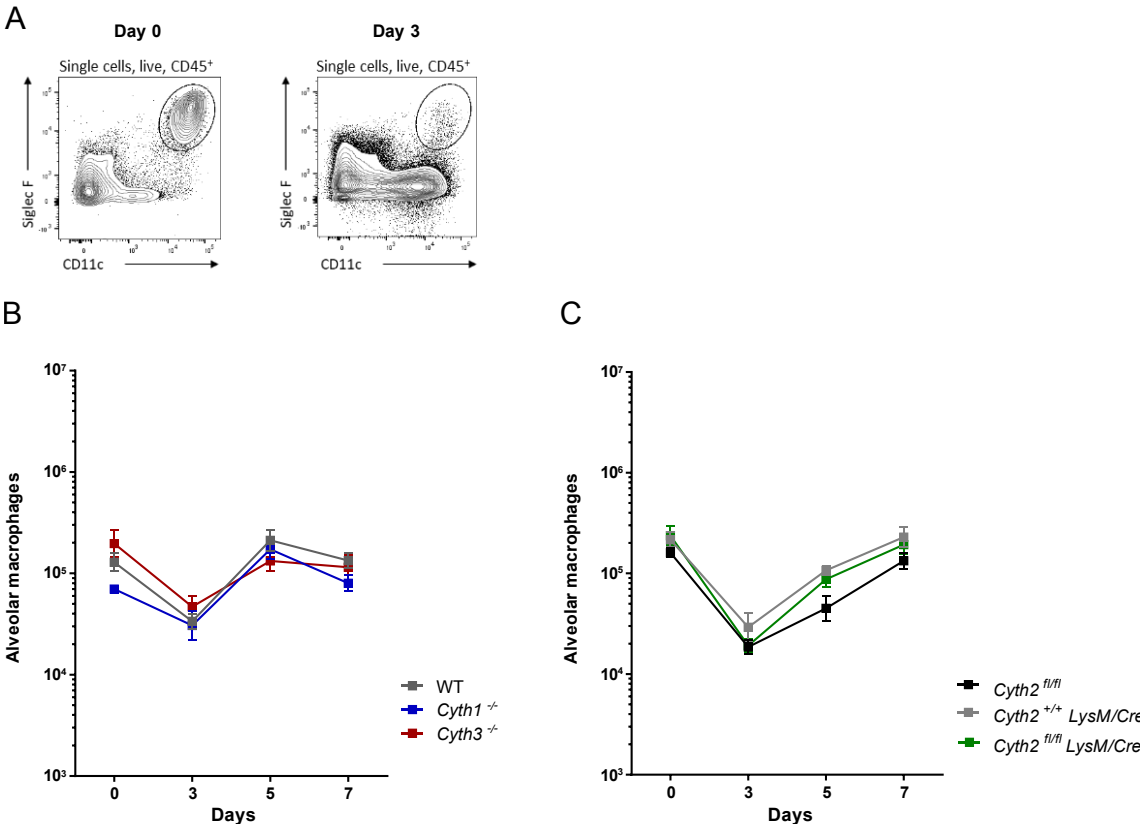

Figure 3.13: Kinetics of alveolar macrophages in the lungs of cytohesin knockout mice following *L. pneumophila* infection. Mice were infected with *L. pneumophila ΔflaA* and alveolar macrophages (AM) quantified by flow cytometry at indicated timepoints. **A**. Simplified gating for alveolar macrophages in murine lung before (Day 0, *left*) or after (Day 3, *right*) infection. **B**. Enumeration of AM in C57BL/6 (WT), cytohesin-1 (*Cyth1*$^{-/-}$) and cytohesin-3 (*Cyth3*$^{-/-}$) knockout mice. **C**. Enumeration of AM in cytohesin-2 conditional knockout (*Cyth2*$^{fl/fl}$ *LysM/Cre*), floxed cytohesin-2 (*Cyth2*$^{fl/fl}$) and LysM/Cre (*Cyth2*$^{+/+}$ *LysM/Cre*) control mice. Graphs present the mean with SEM. n≥8 pooled from n≥2 independent experiments. Significant differences were found for *Cyth2*$^{fl/fl}$ control on day 5 (not indicated,**, p<0.01 two-tailed Mann-Whitney U-test).

3.2.7 Phagocytosis of *L. pneumophila* by different myeloid cells

To elucidate whether cytohesins played a role in the phagocytic processes of different myeloid populations, intracellular *L. pneumophila* were stained with a *L. pneumophila* specific antibody in lung phagocytes (298). It is important to note that this antibody does not discriminate viable bacteria and also stains free antigens and/or degraded bacteria. The phagocytes stained positive for *L. pneumophila* (*L.pn*$^{+}$) in the lung tissue were enumerated and the percentage of *L.pn*$^{+}$ of total phagocyte population in the tissue determined.

After 3 days of infection, the number of *L.pn*$^{+}$ neutrophils decreased due to gradual clearance of the pathogen (**Figure 3.14B**). In the early stages of infection, around 30% of lung-located neutrophils were *L. pneumophila* positive and 4 days later the percentage of *L.pn*$^{+}$ neutrophils declined to ~10% (**Figure 3.14C**).

In *Cyth1*$^{-/-}$ mice the absolute count of tissue *L.pn*$^{+}$ neutrophils did not statistically differ compared to WT mice over the course of infection (**Figure 3.14B**). However, in relation to the total number of neutrophils in the lung, the proportion of *L.pn*$^{+}$ neutrophils in *Cyth1*$^{-/-}$ mice was slightly decreased on day 3 p.i. compared to WT mice (**Figure 3.14C**).

In *Cyth3*$^{-/-}$ mice, there were increased numbers of *L.pn*$^{+}$ neutrophils in the later stages of infection compared to WT mice (**Figure 3.14B**). However, the proportion of neutrophils that were *L.pn*+ was percentage-wise not significantly different in *Cyth3*$^{-/-}$ mice on day 7 (**Figure 3.14C**).

The absolute number of *L.pn*$^{+}$ neutrophils in myeloid-specific *Cyth2* KO mice were similar to controls (**Figure 3.14B**). However, percentage-wise *L.pn*$^{+}$ neutrophils were slightly lower in these mice on day 7 p.i. (**Figure 3.14C**).

These results indicated that deletion of *Cyth1*, *Cyth2* and *Cyth3* in neutrophils did not drastically alter the phagocytic processes upon *L. pneumophila* infection.

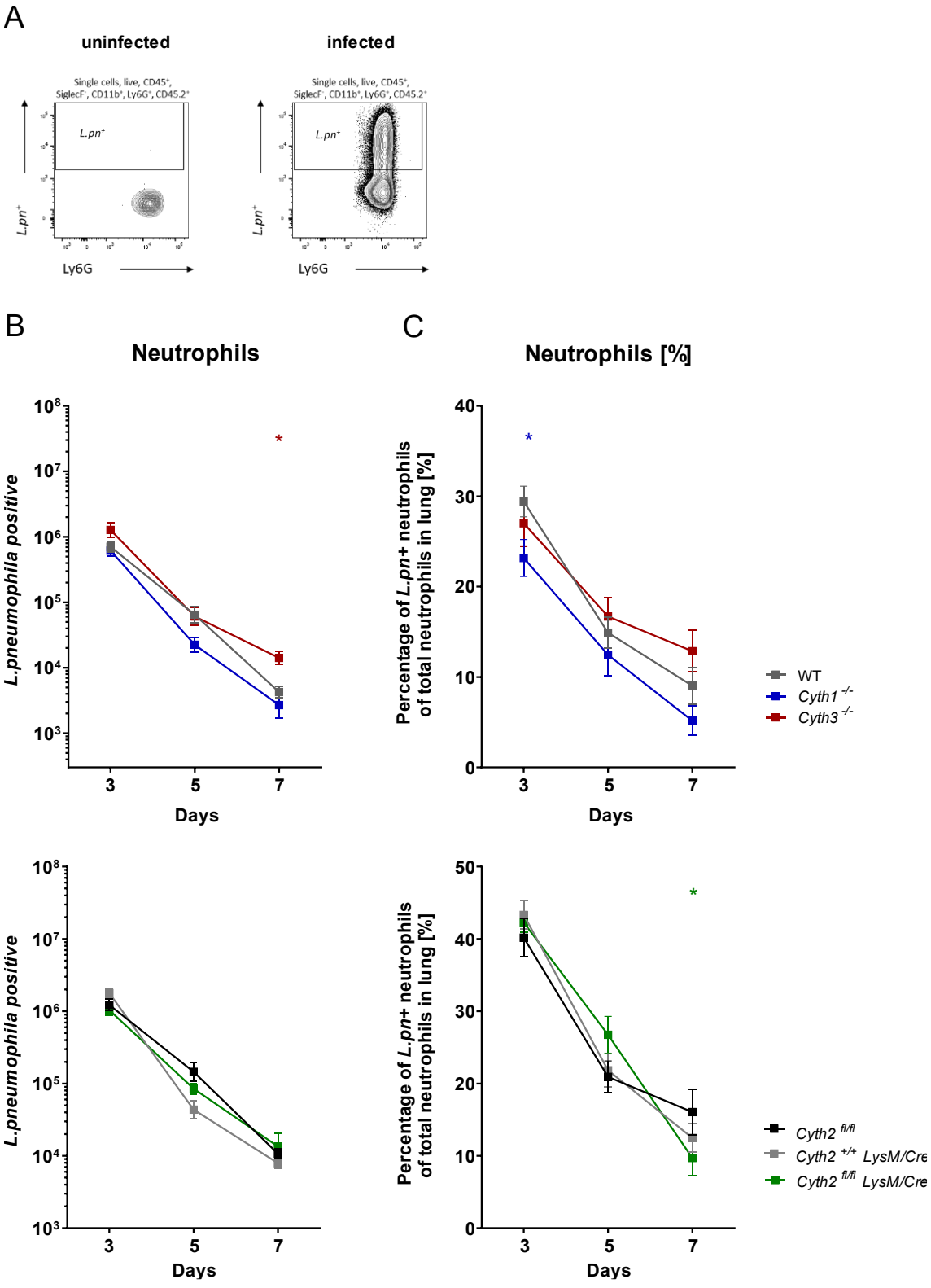

Figure 3.14: Enumeration of *L. pneumophila*⁺ neutrophils in the lung of cytohesin knockout mice after infection. C57BL/6 (WT), cytohesin-1 (*Cyth1*$^{-/-}$) and cytohesin-3 (*Cyth3*$^{-/-}$) knockout mice, as well as cytohesin-2 conditional knockout (*Cyth2*$^{fl/fl}$ *LysM/Cre*), floxed cytohesin-2 (*Cyth2*$^{fl/fl}$) and LysM/Cre

(*Cyth2*$^{+/+}$ *LysM/Cre*) control mice were challenged with *L. pneumophila ⊿flaA* over a 7 day time course. Murine lung was collected to different time points and *L. pneumophila*$^{+}$(*L.pn*$^{+}$) neutrophils were identified and quantified via flow cytometry analysis as in **Figure 3.10A** with the use of an antibody that stains *L.pn* LPS. **A**. Simplified gating for *L.pn*$^{+}$ neutrophils in murine lung 3 days after infection and not infected mice (control). **B***.* Enumeration of *L.pn*$^{+}$ neutrophils presented lung tissue. **C***.* Percentage of *L.pn*$^{+}$ neutrophils of all neutrophils in the lung tissue. Graphs present the mean with SEM. n≥8 pooled from n≥2 independent experiments (*, p<0.05; two-tailed Mann-Whitney U-test).

After infection, MCs engulf *L. pneumophila* and the number of *L.pn*$^{+}$ MCs decreases slowly over time **Figure 3.15B**. Notably, the percentage of *L.pn*$^{+}$ MC in relation to all lung tissue MCs increased from ~50% to ~80% (**Figure 3.15C**).

Cyth1$^{-/-}$ mice displayed a lower number of *L.pn*$^{+}$ MCs on day 7 p.i. (**Figure 3.15B**), although proportionally they did not alter compared to WT *L.pn*$^{+}$ MCs (**Figure 3.15C**).

Moreover, *Cyth3*$^{-/-}$ *L.pn*$^{+}$ MCs were numerically increased versus WT *L.pn*$^{+}$ MCs in the early stage (**Figure 3.15B**). However, these differences were not significant when calculated as a percentage of total lung infiltrated MCs in these mice (**Figure 3.15C**).

In *Cyth2* experiments the *Cyth2*$^{+/+}$ *LysM/Cre* control mice showed elevation of *L.pn*$^{+}$ MCs compared to myeloid-specific *Cyth2* KO mice (**Figure 3.15B**), which was not significantly different percentage-wise (**Figure 3.15C**). However, similar to *L.pn*$^{+}$ neutrophils, *L.pn*$^{+}$ MCs in myeloid-specific *Cyth2* KO were proportionally lower compared to the controls on day 7 (**Figure 3.15C**).

Therefore, deletion of either *Cyth1*, *Cyth2* or *Cyth3* did not remarkably modify the phagocytosis of *L. pneumophila* by MCs.

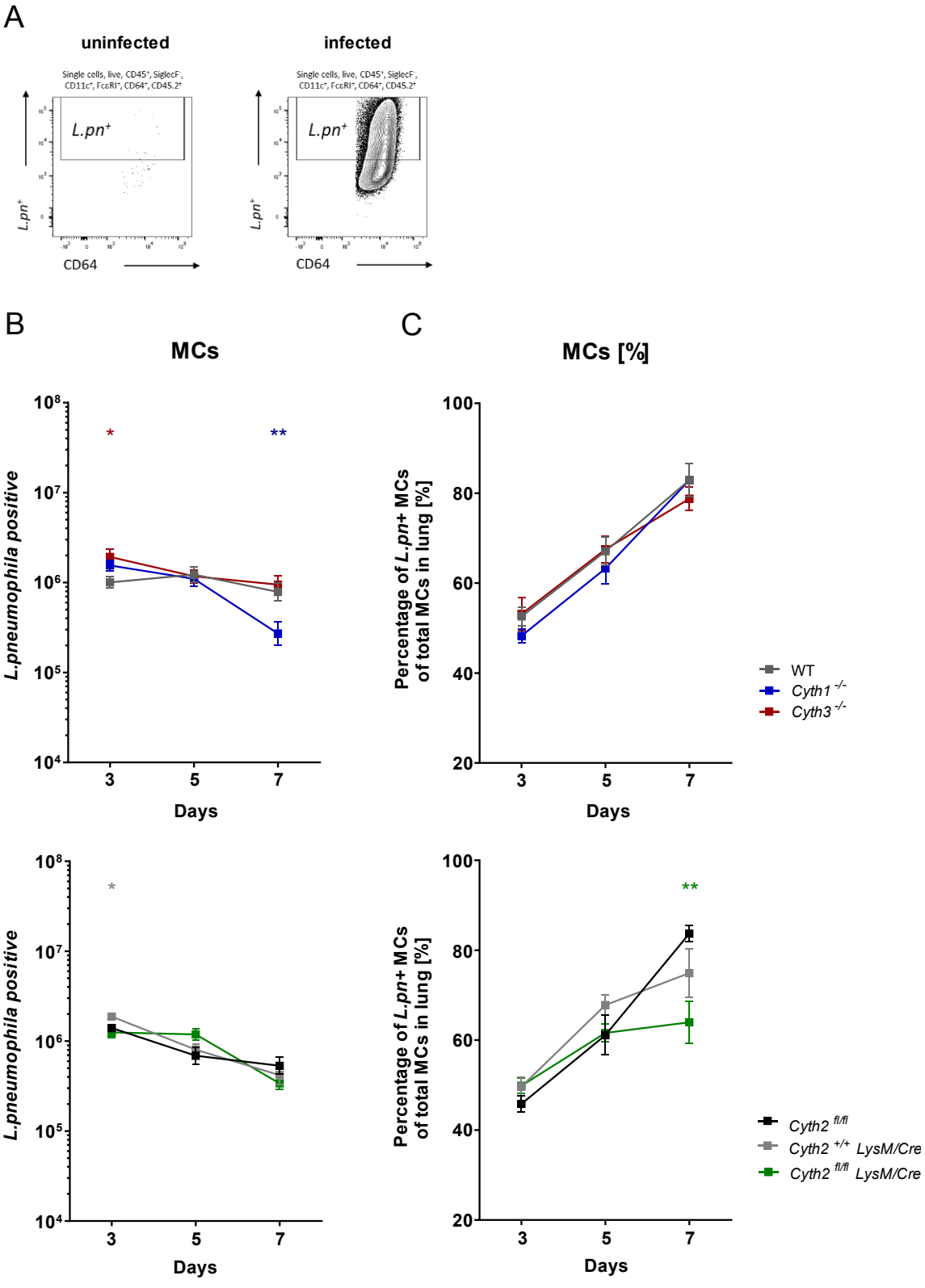

Figure 3.15: Enumeration of *L. pneumophila*⁺ monocyte-derived cells in the lung of cytohesin knockout mice after infection. C57BL/6 (WT), cytohesin-1 (*Cyth1*$^{-/-}$) and cytohesin-3 (*Cyth3*$^{-/-}$) knockout mice, as well as cytohesin-2 conditional knockout (*Cyth2*$^{fl/fl}$ *LysM/Cre*), floxed cytohesin-2 (*Cyth2*$^{fl/fl}$) and LysM/Cre

(*Cyth2*$^{+/+}$ *LysM/Cre*) control mice were challenged with *L. pneumophila ⊿flaA* over a 7 day time course. Murine lung was collected to different time points and *L. pneumophila*$^{+}$ MCs were identified and quantified via flow cytometry analysis as in **Figure 3.11A** with the use of an antibody that stains *L.pn* LPS. **A**. Simplified gating for *L.pn*$^{+}$ MCs in murine lung 3 days after infection and not infected mice (control). **B**. Enumeration of *L.pn*$^{+}$ MCs presented lung tissue. **C**. Percentage of *L.pn*$^{+}$ MCs of all MCs in the lung tissue. Graphs present the mean with SEM. n≥8 pooled from n≥2 independent experiments (*, $p<0.05$; **, $p<0.01$; two-tailed Mann-Whitney U-test).

The number of cDCs which engulfed *L. pneumophila* in the course of infection was lower than other phagocytes, with only 4-8% of all lung located cDCs staining positive for *L. pneumophila* (**Figure 3.16**).

Following infection, *Cyth1*$^{-/-}$ mice displayed similar absolute counts (**Figure 3.16B**) and percentage (**Figure 3.16C**) of *L.pn*$^{+}$ cDC compared to WT mice. Similar to neutrophils, the absolute count of *L.pn*$^{+}$ cDC was increased in *Cyth3*$^{-/-}$ mice (**Figure 3.16B**), but was not different as a proportion of total cDCs (**Figure 3.16C**).

Decreased numbers of *L.pn*$^{+}$ cDC were observed in myeloid-specific *Cyth2* KO mice on day 3 (**Figure 3.16B**). However, this was in line with generally lower numbers of cDCs (see **Figure 3.12**) and was not significantly different as a proportion of total cDC (**Figure 3.16C**). The percentage of *L.pn*$^{+}$ cDC in these mice was inconsistent and showed a higher percentage of *L.pn*$^{+}$ cDCs on day 5 and lower on day 7 p.i. (**Figure 3.16C**). It therefore seems unlikely that phagocytosis by cDCs is altered overall in myeloid-specific *Cyth2* KO mice.

In conclusion, this data suggests that *Cyth1*, *Cyth2* or *Cyth3* did not heavily impact the uptake of *L. pneumophila* in cDCs.

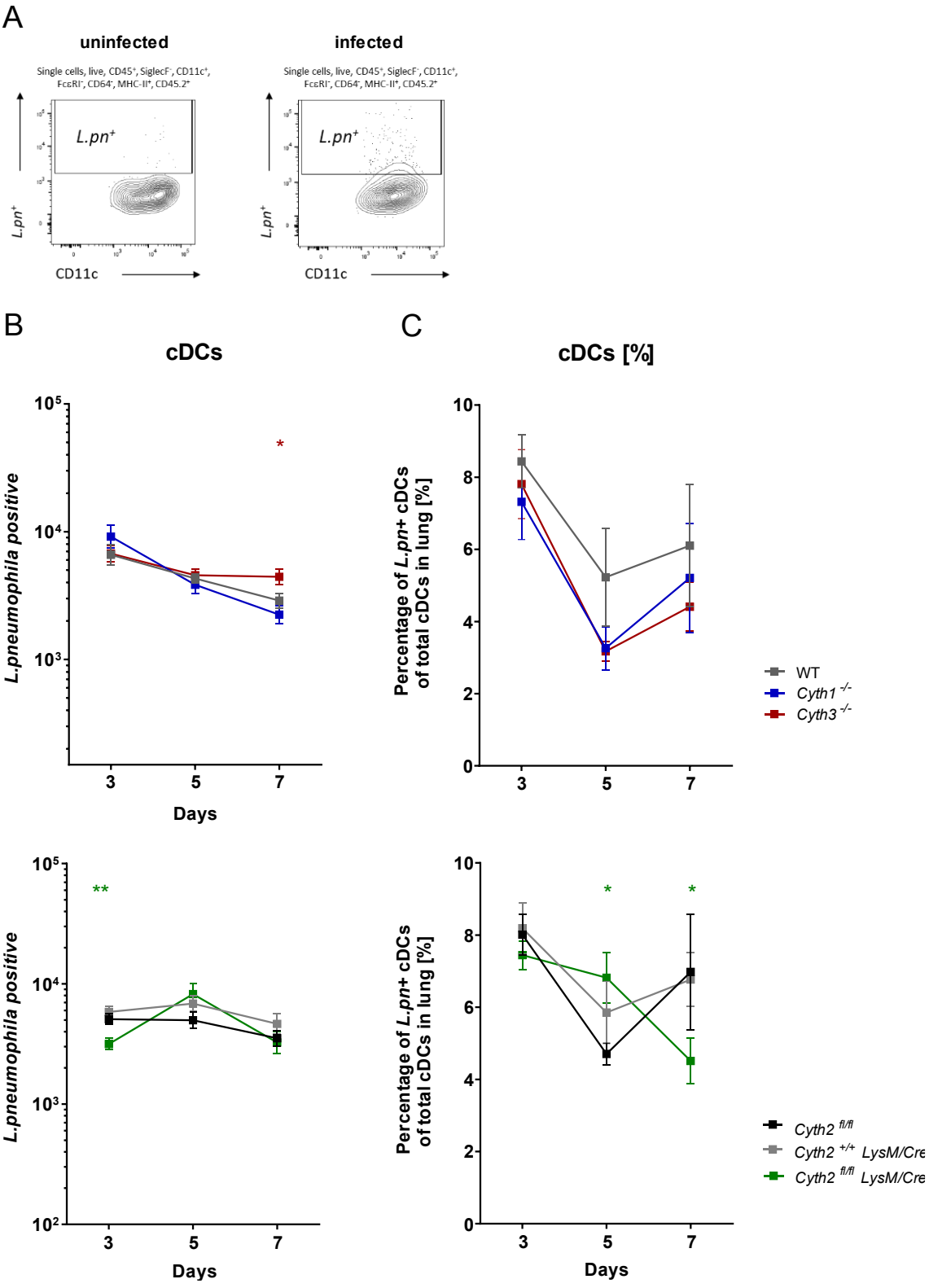

Figure 3.16: Enumeration of *L. pneumophila*⁺ cDCs in the lung of cytohesin knockout mice after infection. C57BL/6 (WT), cytohesin-1 (*Cyth1*$^{-/-}$) and cytohesin-3 (*Cyth3*$^{-/-}$) knockout mice, as well as cytohesin-2 conditional knockout (*Cyth2*$^{fl/fl}$ *LysM/Cre*), floxed cytohesin-2 (*Cyth2*$^{fl/fl}$) and LysM/Cre (*Cyth2*$^{+/+}$

LysM/Cre) control mice were challenged with *L. pneumophila ΔflaA* over a 7 day time course. Murine lung was collected to different time points and *L. pneumophila*$^+$ cDCs were identified and quantified via flow cytometry analysis as in **Figure 3.12A** with the use of an antibody that stains *L.pn* LPS. **A**. Simplified gating for *L.pn*$^+$ cDCs in murine lung 3 days after infection and not infected mice (control). **B**. Enumeration of *L.pn*$^+$ cDCs presented lung tissue. **C**. Percentage of *L.pn*$^+$ cDCs of all cDCs in the lung tissue. Graphs present the mean with SEM. n≥8 pooled from n≥2 independent experiments (*, $p<0.05$; **, $p<0.01$; two-tailed Mann-Whitney U-test).

Although the AM population decreased in the early stages of infection, the number of *L.pn*$^+$ AM consistently increased, possibly because of the uptake of bacterial debris and *Legionella* antigens (**Figure 3.17B**). Approximately 50-85% of AM were stained positive for *L.pn* and therefore, represented the phagocyte with the highest *L. pneumophila* content (**Figure 3.17C**).

During the course of infection, no significant differences were found in the absolute (**Figure 3.17B**) and relative number (**Figure 3.17C**) for *L.pn*$^+$ AM among *Cyth1*$^{-/-}$, *Cyth3*$^{-/-}$ and WT mice.

Similarly, in *Cyth2* experiments the absolute values for *L.pn*$^+$ AM were equal to the controls (**Figure 3.17B**). However, on day 7 p.i. the percentage of *L.pn*$^+$ AM in myeloid-specific *Cyth2* KO mice was much lower than in the controls (**Figure 3.17C**) which could indicate that there were less *L.pn* antigens present in these mice by this time point.

In summary, *Cyth1*, *Cyth2* or *Cyth3* were not required in the phagocytosis of *L. pneumophila* in AM upon infection in mice.

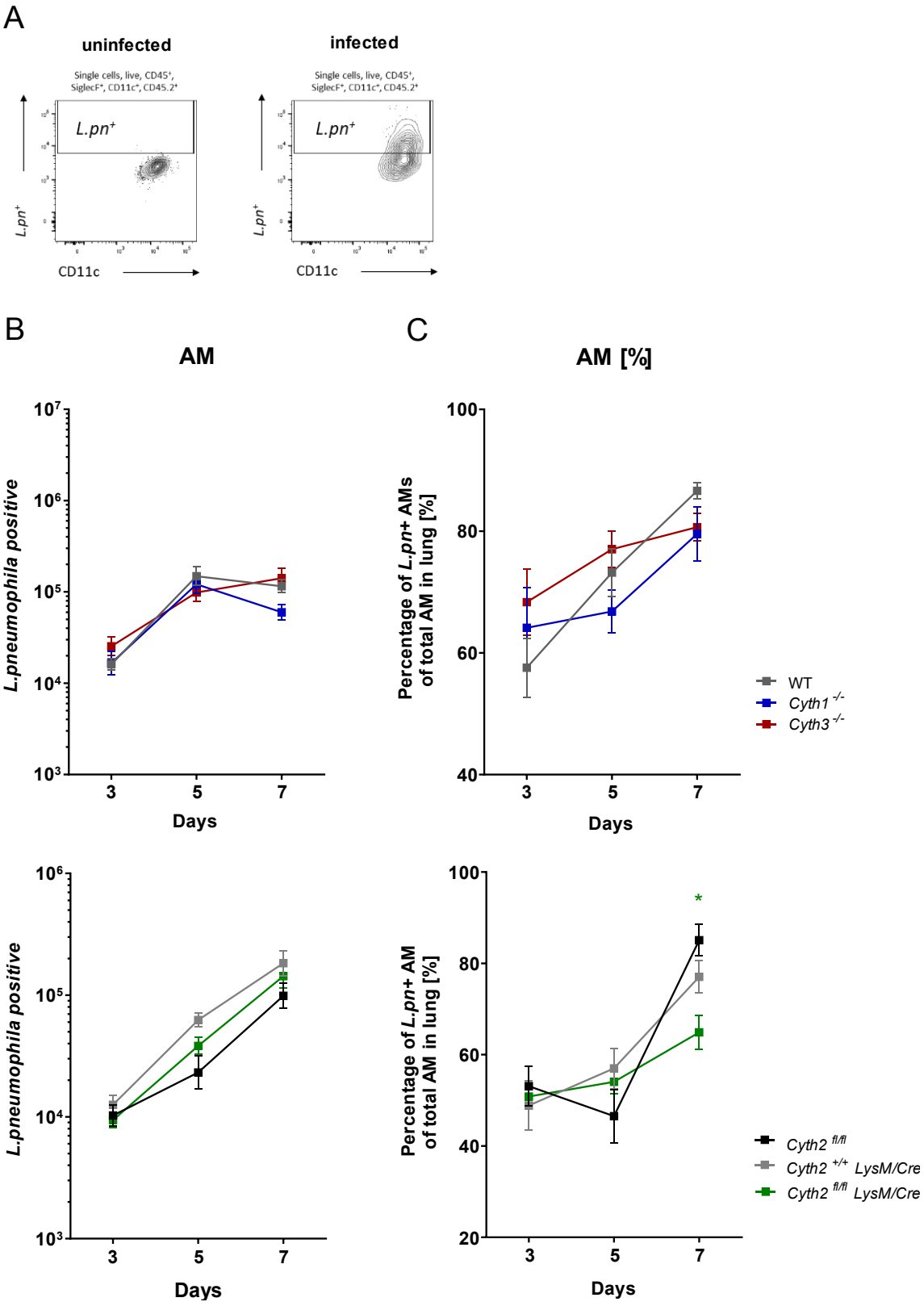

Figure 3.17: Enumeration of *L. pneumophila*⁺ alveolar macrophages in the lung of cytohesin knockout mice after infection. C57BL/6 (WT), cytohesin-1 (*Cyth1*$^{-/-}$) and cytohesin-3 (*Cyth3*$^{-/-}$) knockout mice, as well as cytohesin-2 condi-

tional knockout (*Cyth2$^{fl/fl}$ LysM/Cre*), floxed cytohesin-2 (*Cyth2$^{fl/fl}$*) and LysM/Cre (*Cyth2$^{+/+}$ LysM/Cre*) control mice were challenged with *L. pneumophila ⊿flaA* over a 7 day time course. Murine lung was collected to different time points and *L. pneumophila*$^{+}$ alveolar macrophages (AM) were identified and quantified via flow cytometry analysis as in **Figure 3.13A** with the use of an antibody that stains *L.pn* LPS. **A**. Simplified gating for *L.pn*$^{+}$ AM in murine lung 3 days after infection and not infected mice (control). **B**. Enumeration of *L.pn*$^{+}$ AM presented lung tissue. ***C.*** Percentage of *L.pn*$^{+}$ AM of all AM in the lung tissue. Graphs present the mean with SEM. n≥8 pooled from n≥2 independent experiments (*, p<0.05; two-tailed Mann-Whitney U-test).

In summary, deletion of *Cyth1$^{-/-}$* led to a reduction in the absolute count of *L.pn*$^{+}$ neutrophils and *L.pn*$^{+}$ MCs, while *Cyth3$^{-/-}$* deficiency caused an increase in the absolute count of *L.pn*$^{+}$ neutrophils, *L.pn*$^{+}$ MCs and *L.pn*$^{+}$ cDCs at certain time points during *L. pneumophila* infection. Nonetheless, these alterations were not present when calculated as a percentage of the total number of the respective myeloid population present in the lung tissue, indicating that phagocytosis in these cell populations was not altered in the absence of *Cyth1* of *Cyth3,* and any difference was potentially due to differences in cell numbers present.

Myeloid-specific *Cyth2* KO mice appeared to have a reduced percentage of phagocytes positive for *L. pneumophila* when compared to the cell amount in the lung tissue in the late stage of infection. However, these alterations were not dramatic and did not lead to changes in the overall bacterial burden in the lung of myeloid-specific *Cyth2* KO mice. This suggested that *Cyth2* does not play an essential role in the phagocytosis of *L. pneumophila* in mice.

3.3 Discussion

Increasing evidence over the last several years supported the idea of a regulatory role of cytohesins in cell adhesion and migration (reviewed in section 1.4.4), which suggests they may control recruitment of leukocytes during inflammation. Additionally, cytohesins are known to be involved in phagocytosis (reviewed in section 1.4.6), suggesting that the also play a role in innate immunity. However, whether modulation of these processes affects the outcome of infection *in vivo* has never previously been assessed. This study provides the first comprehensive *in vivo* analysis of the individual genes of the cytohesin Arf-GEF family during infection. Specifically, a *L. pneumophila* respiratory infection model was used to dissect the function of cytohesin-1, cytohesin-2 and cytohesin-3 in bacterial invasion, replication, clearance, as well as transmigration of different immune cell types to the infected lung tissue.

3.3.1 Cytohesins are not required in *L. pneumophila* infection life cycle

A potential role for cytohesins in the life cycle of *L. pneumophila* was considered possible, as host Arf1 is an important factor in early LCV biogenesis (299, 300) and cytohesin-1, -2 and -3 act all as GEFs for Arf1 (130, 132, 145, 146). However, no evidence was found for the modulation of replication of *L. pneumophila* within phagocytes by the cytohesins.

Experiments of this chapter demonstrated that SecinH3 inhibition of cytohesin GEF activity did not result in any alteration in the invasion and intracellular replication of *L. pneumophila* in either immortalized or primary bone marrow-derived macrophages indicating that the GEF function of cytohesins were not required in this process (see results 3.2.1). This might be explained by the fact that *L. pneumophila* likely expresses its own Arf-GEFs, which apparently do not cooperate with endogenous exchange factors of the cytohesin family. Some of the effectors that are injected into the host cell which act as GEF proteins themselves are RalF, LidA, DrrA, and Lpg0393 (301-304), with RalF displaying a Sec7 domain, which is the enzymatic domain for the Arf-GEF activity. RalF is secreted into the host

cytosol in the early stages of the intracellular life cycle of *L. pneumophila* and the Sec7 domain shares 47% sequence homology with eukaryotic Arf-GEFs (305). This suggests that *L. pneumophila* does not depend on the guanine nucleotide exchange activity by host Arf-GEFs such as cytohesins.

In *Shigella* and *Salmonella*, which both exploit cytohesins for invasion into host cells, translocation of the cytohesin to the cytosolic side of the host plasma membrane is necessary to mediate the sequential recruitment of other effectors to trigger bacterial entry (169, 171). These findings raise the question of whether cytohesins might operate as adapter proteins during bacterial invasion and in early LCV biogenesis. A translocation assay was used to measure the efficiency of effector secretion into different pulmonary phagocytes in the early stage of infection (section 3.2.2). However, the conducted data suggested that cytohesin-1 and cytohesin-3 were not essential in the translocation processes and were unlikely to significantly contribute to LCV biogenesis in pulmonary AM, neutrophils and MCs.

In summary, *L. pneumophila* does not depend on the presence of host derived cytohesin-1 and -3, as well as cytohesin enzymatic activity, for bacterial invasion and for intracellular replication.

3.3.2 Cytohesin-1 does not affect the innate immune response following *L. pneumophila* infection

The data based on *in vivo* infection experiments of this chapter suggested cytohesin-1 was not a critical factor for the clearance of *L. pneumophila* in murine lung. Mice deficient for cytohesin-1 efficiently cleared bacteria and recovered from the infection within one week similar to wildtype mice. This finding was also in accordance with the overall observation that the cell recruitment of key phagocytes to the inflamed lung was not strongly affected in the absence of cytohesin-1. Therefore, cytohesin-1 did not play an essential role in the coordination and recruitment of myeloid cells in this infection model. Additionally, deletion of cytohe-

sin-1 did not influence the capability of myeloid cells to phagocytose the bacteria which is consistent with the lack of influence on *L. pneumophila* clearance.

Interestingly, cytohesin-1 deficient mice showed an elevated response of proinflammatory cytokines in the bronchoalveolar space in the early stages of infection. This was accompanied by a slightly higher drop in weight on the first day of infection, which could be linked to increased release of TNF or IFNγ. The release of both cytokines has been associated with body weight loss in different infection models (306-309). In the course of *L. pneumophila* infection, IFNγ is secreted by lymphocytes such as NK cells, natural killer T (NKT) cells, Th1 cells, CD8+ effector T cells and γδ T cells and potentially by neutrophils, although this is controversially discussed (202, 291). TNF on the other hand is produced by MCs, neutrophils, cDCs and by bystander macrophages (237, 290, 291). MCs and cDCs also release IL-12 (212, 244). The latter two cell types were found slightly elevated in the early stages of infection in *Cyth1*$^{-/-}$ mice and could be the source of enhanced IL-12 levels (244, 291). However, an exact identification of the cellular origin for the distinct cytokines was not assessed here. It is likely that these observed events are coupled and the result of a positive feedback-loop previously described by our laboratory (244). In this loop, IL-12 induces the expression of IFNγ and IL-17A in a non-cognate manner from lymphocytes, which in turn stimulates the release of other proinflammatory cytokines. However, the observed elevation of these cytokines seems to happen in a time-restricted manner in *Cyth1*$^{-/-}$ mice, only being present on the first two days after infection and normalising thereafter. In this way, these alterations in cytohesin-1 deficiency do not affect the outcome of this disease in mice. Hence, it would need further evaluation and investigation whether the cytokines might affect cells other than myeloid cells (e.g. lymphocytes).

In conclusion, no evidence was found to support a significant role of cytohesin-1 in the innate immune response towards pulmonary *L. pneumophila* infection.

3.3.3 Myeloid-specific cytohesin-2 knockout leads to increased weight gain in mice in the late stages of infection

Following *L. pneumophila* infection, myeloid-specific cytohesin-2 knockout mice presented a similar phenotype in bacterial clearance and cell recruitment as the controls. This result strongly suggests that myeloid-specific knockout of cytohesin-2 does not impact the innate immune responses in *Legionella* infection. Notably, cDC numbers in the lungs of these mice were found to be slightly decreased in the early stages of infection, which normalized relative to the controls in later phases of infection. However, this alteration did not seem to strongly affect the general innate immune response to *L. pneumophila*, although it may suggest that cytohesin-2 has a minor intrinsic role in cDC recruitment.

Intriguingly, cytohesin-2 appeared to positively regulate cytokine responses in myeloid cells. The deletion of cytohesin-2 led to a decreased amount of certain pro-inflammatory cytokines including IL-12, IFNγ and IL-17A. Whether this observation is caused by only one specific cell type (e.g. decreased cDC numbers might result a lower IL-12 response) or if this effect is present in all myeloid cells remains unknown. Notably, this effect on cytokines is opposite to the findings in *Cyth1*$^{-/-}$ mice. Some members of the cytohesin family have been identified to act in an antagonistic manner on various cellular functions (310). Therefore, it is possible that the same reciprocal influences may regulate cytokine production. Moreover, similar to the observation in *Cyth1*$^{-/-}$ mice, downregulation of the cytokine response in myeloid-specific *Cyth2* KO mice only occurred at specific time points.

Another interesting observation was that myeloid-specific *Cyth2* KO mice recovered in body weight faster than controls in the late stages of infection, gaining even more than their initial body weight. This is quite intriguing, as there was no difference in the immune response or bacterial loads at these timepoints. Additionally, deletion of *Cyth2* was restricted to myeloid cells, and consequently, this effect must be attributable only to these cells. In this context, the role of adipose tissue resident macrophages regulating obesity has been intensively studied in the past (311). It is tempting to postulate that cytohesin-2 might fulfil a regulatory

function in metabolic processes in adipose tissue macrophages that is triggered by infection. This is consistent with the findings that cytohesin-2 reacts to metabolic stimuli showing an insulin-dependent translocation to the plasma membrane in adipocytes (136). Although speculative, it is possible that lack of cytohesin-2 may lead to a dysregulation in metabolism after an infection or insult. However, this hypothesis will require extensive further studies to corroborate, which could involve analysis of how cytohesin-2 deficient macrophages react to metabolic stress.

In summary, these results demonstrate that cytohesin-2 is also not required for the myeloid immune response towards *L. pneumophila.* However, it is possible that cytohesin-2 might fulfil a regulatory function in the metabolic equilibration after infection.

3.3.4 Cytohesin-3 is an important factor in the recovery following infection

The overall phenotype of cytohesin-3 deficient mice was the most pronounced of the cytohesin deficient mice examined, suggesting that cytohesin-3 may be the cytohesin most relevant to the response to infection. Mice deficient in cytohesin-3 displayed a drastically impaired weight recovery indicating that the progression of the disease was worse compared to mice with functional cytohesin-3.

Interestingly, this phenotype could not be explained by an impaired bacterial clearance as lack of cytohesin-3 did not have any strong impact on innate immune responses to the pathogen. Although *Cyth3*$^{-/-}$ mice had slightly elevated pulmonary IL-6 and IL-12 levels at the early time points of infection, this did not correlate with an altered cell kinetics and was temporally segregated from when more severe disease was observed, suggesting that this effect was not pronounced enough to significantly alter pathogenesis.

One possible explanation for the increased disease signs is the postulated role of cytohesin-3 in insulin signalling, metabolism and lipogenesis (covered in section 1.4.3), which has been demonstrated by our laboratory (149). Under challenge, such as aging or high fat diet, deletion of cytohesin-3 seems to lead to an

impaired metabolic homeostasis and regulation in mice accompanied by reduced weight gain due to impaired insulin-receptor signalling (149). In a similar fashion, abrogated insulin-receptor signalling in the absence of cytohesin-3 might lead to delayed weight recovery in mice following infection. This hypothesis can be tested by comparing the phenotypes of insulin-receptor deficient mice with insulin-receptor/cytohesin-3 double knockout mice under bacterial challenge.

Nevertheless, it is unknown if the given phenotype arose from specific tissue or distinct cell types. Therefore, the use of tissue specific cytohesin-3 knockout mice (e.g. liver specific KO) in further studies could shed more light on the mechanism of action of cytohesin-3 and its (metabolic) function. With reference to the observed phenotype in myeloid-specific *Cyth2* KO mice, the alterations in cytohesin-3 knockout mice could arise from certain immune cells (e.g. myeloid cells). In this scenario, cytohesin-2 and cytohesin-3 might also work in an antagonistic fashion as has been described for other cellular functions (162). However, this would require further evaluation including the use of a myeloid-specific cytohesin-3 knockout or a double cytohesin-2/-3 conditional knockout mice. The latter should then revert the phenotype to wildtype.

The impaired recovery might also indicate an aberrant immune activity in the absence of cytohesin-3. However, the extent of this abnormality is unclear as *Cyth3*$^{-/-}$ mice still clear the bacterial threat. The lack of any obvious effects of cytohesin-3 on the replication of *L. pneumophila* or innate immune responses analysed here, suggests that the underlying reason for any phenotype is either not immune-related or may be related to adaptive responses. The latter is further investigated in Chapter 4.

In summary, the results in this chapter suggest cytohesin-3 is the most important cytohesin in the response to infection and resulting disease. Consequently, a dysfunctional or absent cytohesin-3 protein may have significant implications for the outcome of infection with more virulent pathogens of viral, parasitic or bacterial origin.

4. The role of cytohesins in T cell responses

4.1 Introduction

In Chapter 3 distinct cytohesins were found to modulate the recovery from *L. pneumophila* infection, although only minor and temporally restricted effects were found in the cytokine and innate immune responses. Additionally, no effect was observed on bacterial clearance in these mice. One possibility that could reconcile these observations is cytohesin's involvement in the adaptive immune system. Increasing evidence over the past years supported the idea of a regulatory function of cytohesins in T cell immunity in particular (covered in section 1.4.5). The experiments in this chapter elucidated whether individual cytohesin KO mice had altered T cell recruitment or activation. Additionally, the role of cytohesins in T cell responses was investigated using influenza A infection, a model which relies heavily on T cells to clear infection.

4.2 Results

4.2.1 Cytohesins regulate T cell recruitment following *L. pneumophila* infection

A similar approach was used to the transmigration experiments performed in Chapter 3, where CD45.2 was injected i.v. to label vasculature-associated leukocytes. Only T cells within lung tissue were investigated. In addition to antibodies targeting T cell specific markers, antibodies against CD44 and CD62L were also utilized to determine effector and memory T cell subtypes (**Figure 4.1A**, **Figure 4.2B**).

T cells expressing only CD62L are referred as naïve T cells, the co-expression of CD62L and CD44 determines a central memory T cell phenotype, and the exclusive expression of CD44 defines effector memory T cells (312, 313).

Typically, in *L. pneumophila* infection, the number of CD4+ and CD8+ T cells within the lung increases gradually over time which is consistent with the phenotype observed in these experiments (**Figure 4.1**, **Figure 4.2**) (established model in our laboratory). During early infection, T cells are primarily non-cognate, whereas in the later phase of infection *Legionella*-specific T cells accumulate in the lung (244).

Following infection, *Cyth1*$^{-/-}$ mice showed fewer transmigrated CD4+ T cells relative to WT mice; this effect was especially significant in the late phase of infection (**Figure 4.1B**). Moreover, this trend was represented within central (**Figure 4.1C**) and effector memory (**Figure 4.1D**) CD4+ T cell subpopulations.

Cyth3$^{-/-}$ mice displayed higher recruitment of CD4+ T cells compared to WT mice that was statistically significant on day 7 p.i.. Here, central (**Figure 4.1C**) and effector memory (**Figure 4.1D**) CD4+ T cells were found to be numerically enhanced, with significantly higher counts of effector memory cells on day 7.

Furthermore, in myeloid-specific *Cyth2* KO mice total CD4+ T cells (**Figure 4.1B**) and both memory CD4+ T cell subtypes (**Figure 4.1C and D**) showed a transiently lower count on day 5 p.i..

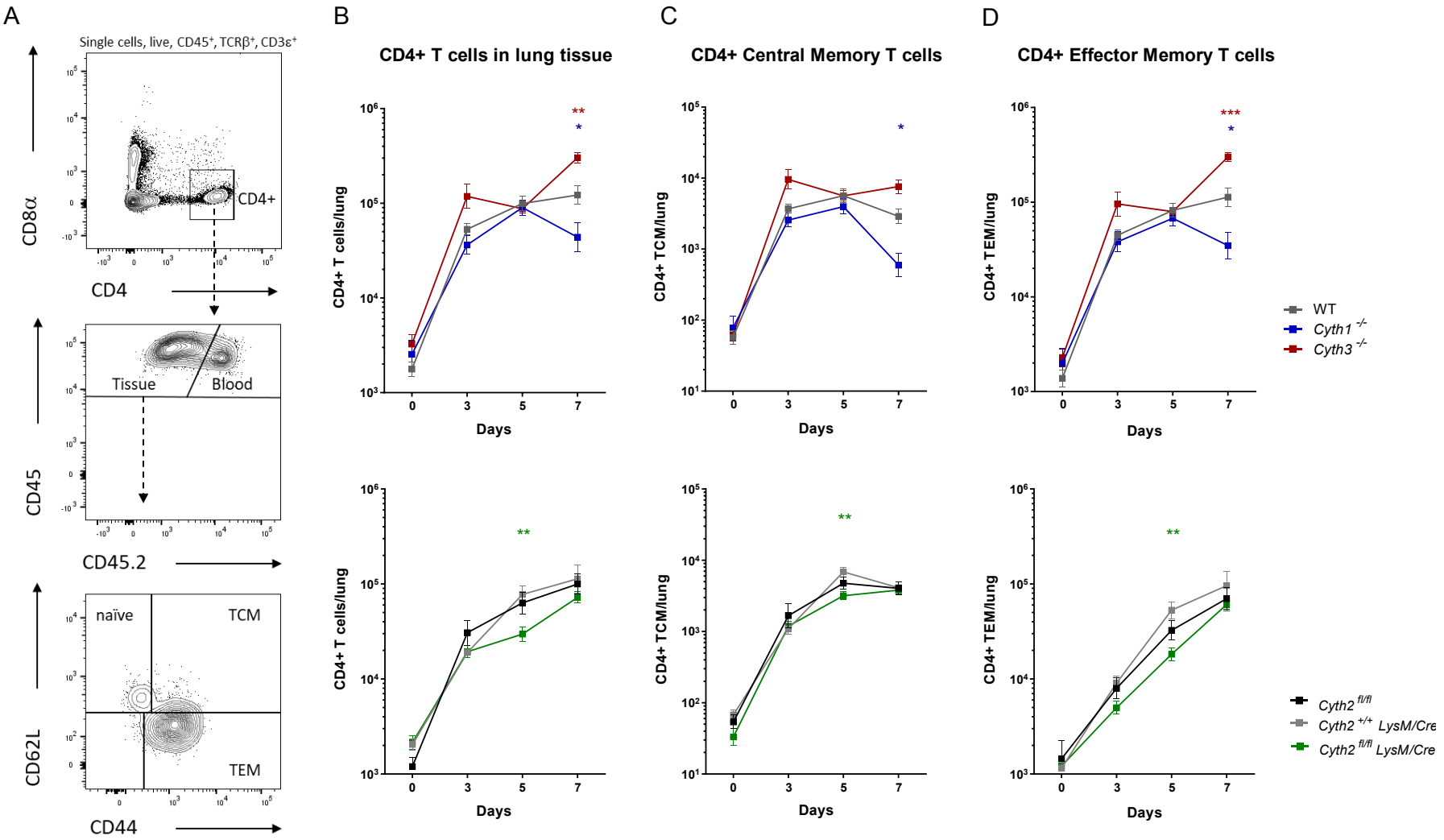
A
Single cells, live, CD45+, TCRβ+, CD3ε+
CD8α
CD4+
CD4
Tissue
Blood
CD45
CD45.2
naïve
TCM
TEM
CD62L
CD44
B
CD4+ T cells in lung tissue
CD4+ T cells/lung
Days
C
CD4+ Central Memory T cells
CD4+ TCM/lung
Days
D
CD4+ Effector Memory T cells
CD4+ TEM/lung
Days
WT
Cyth1 -/-
Cyth3 -/-
Cyth2 fl/fl
Cyth2 +/+ LysM/Cre
Cyth2 fl/fl LysM/Cre

Figure 4.1: Enumeration of CD4+ T cell populations in cytohesin knockout mice following *L. pneumophila* infection. Mice were infected with *L. pneumophila ⊿flaA*, then injected with CD45.2 antibody i.v. to label cells in the vasculature prior to analysing lung cells by flow cytometry at indicated timepoints. **A**. Different T cell subsets gated on CD4+CD44-CD62L+ for naïve, CD4+CD44+ CD62L+ for central memory (TCM) and CD4+CD44+CD62L- for effector memory (TEM) CD4+ T cells in murine lung following 5 days infection. **B**. Enumeration of total CD4+ T cells, **C**. TCM and **D**. TEM cells in the lungs of C57BL/6 (WT), cytohesin-1 (*Cyth1*$^{-/-}$) and cytohesin-3 (*Cyth3*$^{-/-}$) knockout mice (*upper panels*) and of cytohesin-2 conditional knockout (*Cyth2*$^{fl/fl}$ *LysM/Cre*), floxed cytohesin-2 (*Cyth2*$^{fl/fl}$) and LysM/Cre (*Cyth2*$^{+/+}$ *LysM/Cre*) control mice (*lower panels*). Graphs present the mean with SEM. n≥8 pooled from n≥2 independent experiments. Significant differences were found between *Cyth1*$^{-/-}$ and WT, *Cyth3*$^{-/-}$ and WT in total CD4+ T cells, TCM and TEM, *Cyth2*$^{fl/fl}$ *LysM/Cre* and *Cyth2*$^{+/+}$ *LysM/Cre* in total CD4+ T cells, TCM and TEM (*, p<0.05; **, p<0.01; ***, p<0.001; two-tailed Mann-Whitney U-test).

Similar observations to CD4+ T cell kinetics were made of CD8+ T cells in *Cyth1*, *Cyth2* and *Cyth3* knockout mice following *L. pneumophila* infection (**Figure 4.2**).

The CD8+ T cell response in *Cyth1*$^{-/-}$ mice was decreased compared to WT mice (**Figure 4.2B**) and a lower number of central (**Figure 4.2C**) and effector (**Figure 4.2D**) CD8+ T cells were observed in the late stages of infection.

The total CD8+ T cell number in *Cyth3*$^{-/-}$ mice was found elevated on day 7 p.i relative to WT mice (**Figure 4.2B**). Additionally, the counts for central (**Figure 4.2C**) and effector memory (**Figure 4.2D**) CD8+ T cells were elevated in *Cyth3*$^{-/-}$ mice compared to WT.

Mice with myeloid-specific *Cyth2* KO had less total CD8+ T cells on day 3 and 5 p.i. (**Figure 4.2B**), with decreased numbers of central memory T cells on day 5 (**Figure 4.2C**) and effector memory T cells on day 3 (**Figure 4.2D**).

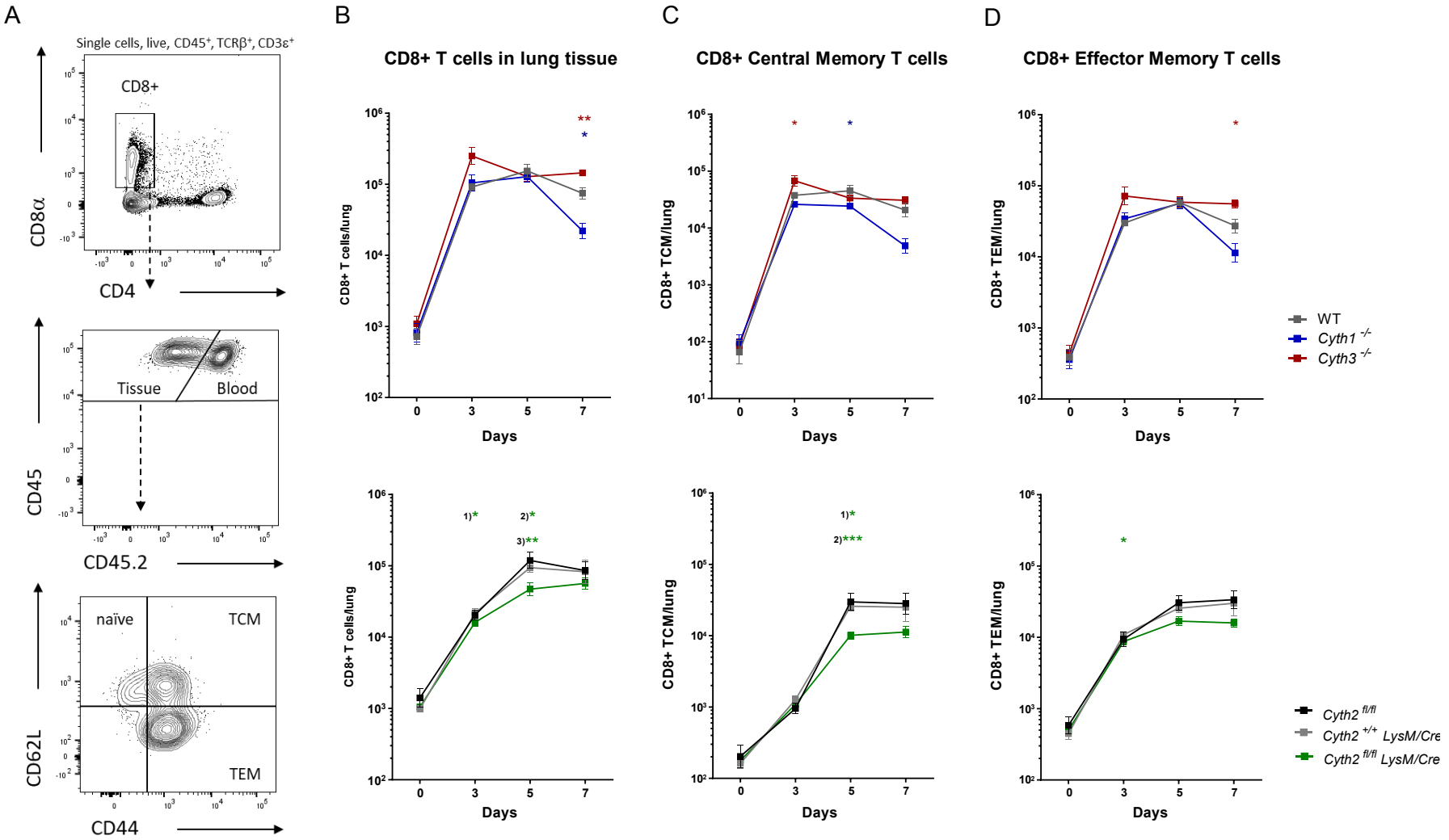
A
Single cells, live, CD45+, TCRβ+, CD3ε+
CD8+
CD8α
CD4
Tissue
Blood
CD45
CD45.2
naïve
TCM
TEM
CD62L
CD44
B
CD8+ T cells in lung tissue
CD8+ T cells/lung
Days
C
CD8+ Central Memory T cells
CD8+ TCM/lung
Days
D
CD8+ Effector Memory T cells
CD8+ TEM/lung
Days
WT
Cyth1 -/-
Cyth3 -/-
Cyth2 fl/fl
Cyth2 +/+ LysM/Cre
Cyth2 fl/fl LysM/Cre

Figure 4.2: Enumeration of CD8+ T cell populations in cytohesin knockout mice during *L. pneumophila* infection. Mice were infected with *L. pneumophila ⊿flaA*, then injected with CD45.2 antibody i.v. to label cells in the vasculature prior to analysing lung cells by flow cytometry at indicated timepoints. **A***.* Different T cell subsets gated on CD8+CD44-CD62L+ for naïve, CD8+CD44+CD62L+ for central memory (TCM) and CD8+CD44+CD62L- for effector memory (TEM) CD8+ T cells in murine lung following 5 days infection. **B***.* Enumeration of total CD8+ T cells, **C**. TCM and **D***.* TEM cells in the lungs of C57BL/6 (WT), cytohesin-1 (*Cyth1*$^{-/-}$) and cytohesin-3 (*Cyth3*$^{-/-}$) knockout mice (*upper panels*) and of cytohesin-2 conditional knockout (*Cyth2*$^{fl/fl}$ *LysM/Cre*), floxed cytohesin-2 (*Cyth2*$^{fl/fl}$) and LysM/Cre (*Cyth2*$^{+/+}$ *LysM/Cre*) control mice (*lower panels*). Graphs present the mean with SEM. n≥8 pooled from n≥2 independent experiments. Significant differences in total CD8+ T cells, TCM and TEM found between *Cyth1*$^{-/-}$ and WT, *Cyth3*$^{-/-}$ and WT, also in total CD8+ T cells between [1)] *Cyth2*$^{fl/fl}$ *LysM/Cre* and *Cyth2*$^{+/+}$ *LysM/Cre*, [2)] *Cyth2*$^{fl/fl}$ *LysM/Cre* and *Cyth2*$^{fl/fl}$, [3)] *Cyth2*$^{fl/fl}$ *LysM/Cre* and *Cyth2*$^{+/+}$ *LysM/Cre*; further in TCM between [1)] *Cyth2*$^{fl/fl}$ *LysM/Cre* and *Cyth2*$^{fl/fl}$, [2)] *Cyth2*$^{fl/fl}$ *LysM/Cre* and *Cyth2*$^{+/+}$ *LysM/Cre* and in TEM between *Cyth2*$^{fl/fl}$ *LysM/Cre* and *Cyth2*$^{+/+}$ *LysM/Cre* (*, p<0.05; **, p<0.01; ***, p<0.001; two-tailed Mann-Whitney U-test).

In summary, the responses of CD4+ and CD8+ T cells among cytohesin deficient mice were quite diverse. *Cyth1*$^{-/-}$ mice displayed a lower number of central and effector memory CD4+ and CD8+ T cells, which resulted in lower overall counts of T cells in the lung. Interestingly, *Cyth3*$^{-/-}$ mice displayed the opposite phenotype of *Cyth1*$^{-/-}$ mice, demonstrating enhanced recruitment of central and effector memory CD4+ and CD8+ T cells to the lung. These effects were especially obvious in the late stage of infection. In contrast, *Cyth2* cond. KO led only to a transiently weaker CD4+ and CD8+ T cell response in the middle stages of infection.

4.2.2 Pulmonary and splenic CD8+ T cell counts are not altered in cytohesin deficient mice following influenza infection

The results in the previous section demonstrated divergent influence of T cell responses by different cytohesins following bacterial infection. However, in this infection model T cells have less of a major role in the clearance of *L. pneumophila* than innate cells. The strongest differences in the T cell kinetics were found among *Cyth1*$^{-/-}$ and *Cyth3*$^{-/-}$ mice in late infection, raising the question of whether effects were due to *Legionella*-specific effector T cells. Therefore, the studies of this subchapter elucidated antigen-specific CD8+ T cell responses upon challenge with influenza A virus. This was performed in collaboration with the laboratory of Sammy Bedoui, the University of Melbourne.

Cytohesin-deficient mice and control mice were infected intranasally with HKx31 influenza A virus and after 8 days infection, the number of total leukocytes and CD8+ T cells in lung and spleen tissue was determined.

After 8 days infection, no significant difference was found in the number of either total leukocytes or total CD8+ T cells in lung or spleen of any cytohesin deficient mice (**Figure 4.3**).

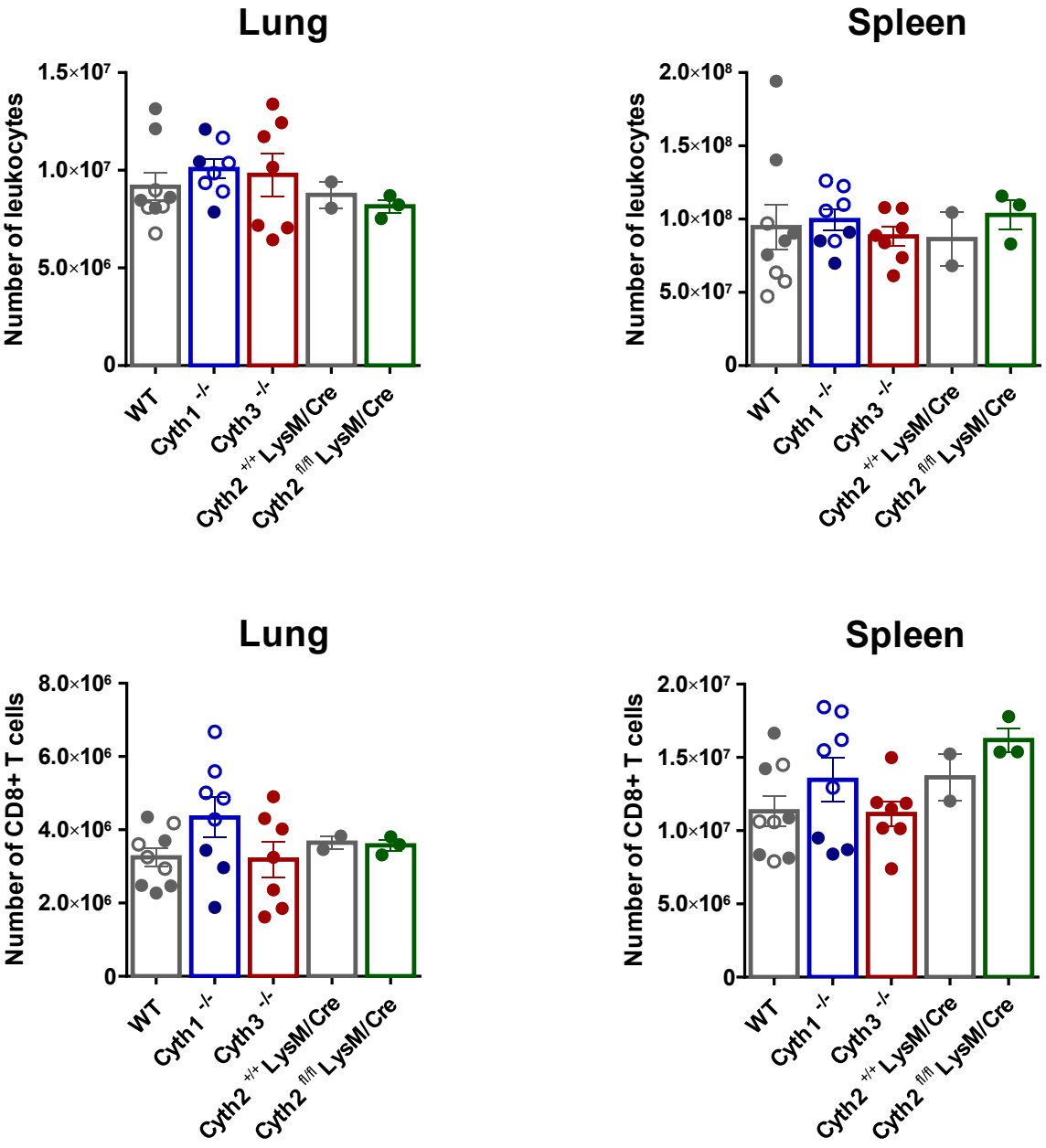

Figure 4.3: Enumeration of leukocytes and CD8+ T cells in lung and spleen of cytohesin knockout mice following influenza infection. C57BL/6 (WT), cytohesin-1 (*Cyth1*$^{-/-}$) and cytohesin-3 (*Cyth3*$^{-/-}$) knockout mice, as well as cytohesin-2 conditional knockout (*Cyth2*$^{fl/fl}$ *LysM/Cre*) and *LysM/Cre* (*Cyth2*$^{+/+}$ *LysM/Cre*) control mice were infected intranasally with HKx31 influenza A virus for 8 days. Lungs and spleens were collected to determine the total leukocyte count (*upper panels*) and total CD8+ T cell count (*lower panels*) via flow cytometry. Each dot represents one mouse and bars present the mean with SEM. Filled and unfilled datapoints distinguish individual experiments. No significant differences were found in cytohesin transgenic mice compared to wildtype control (threshold, $p<0.05$; two-tailed Mann-Whitney U-test).

4.2.3 Cytohesin-1 and -3 modulate the ratio of antigen-specific CD8+ T cells

Intranasal infection with HKx31 influenza A virus leads in mice to two predominant CD8+ T cell populations that recognize specific epitopes of the viral nucleoprotein ($NP_{366-374}$; NP366) and the PA polymerase ($PA_{224-233}$; PA224) presented on H-$2D^b$ (314, 315).

Using tetrameric complexes of H-$2D^b$ and either NP366 or PA224 peptides, CD8+ T cells with TCRs recognizing these epitopes were labelled and assessed via flow cytometry (**Figure 4.4A**).

The proportion of PA224-specific CD8+ T cells in spleen of *Cyth1*$^{-/-}$ mice were significantly decreased compared to WT CD8+ T cells (**Figure 4.4B**). Although not statistically significant, a similar trend for the equivalent population was found in lung (**Figure 4.4B**) and for NP366-specific CD8+ T cells in spleen (**Figure 4.4C**) of *Cyth1*$^{-/-}$ mice. No difference was observed in the pulmonary NP366-specific CD8+ T cell population (**Figure 4.4C**).

The opposite effect was found in *Cyth3*$^{-/-}$ mice. The ratio of PA224-specific CD8+ T cells, especially in the spleen, was enhanced in *Cyth3*$^{-/-}$ mice relative to WT mice (**Figure 4.4B**). No significant difference was found in NP366-specific CD8+ T cells in lung and spleen of *Cyth3*$^{-/-}$ mice.

No effect of myeloid-specific cytohesin-2-deficiency was observed on influenza-specific CD8+ T cells (**Figure 4.4B, C**).

In conclusion, lack of *Cyth1* or *Cyth3* had a significant effect on the proportion of PA224-specific CD8+ T cells in the spleen.

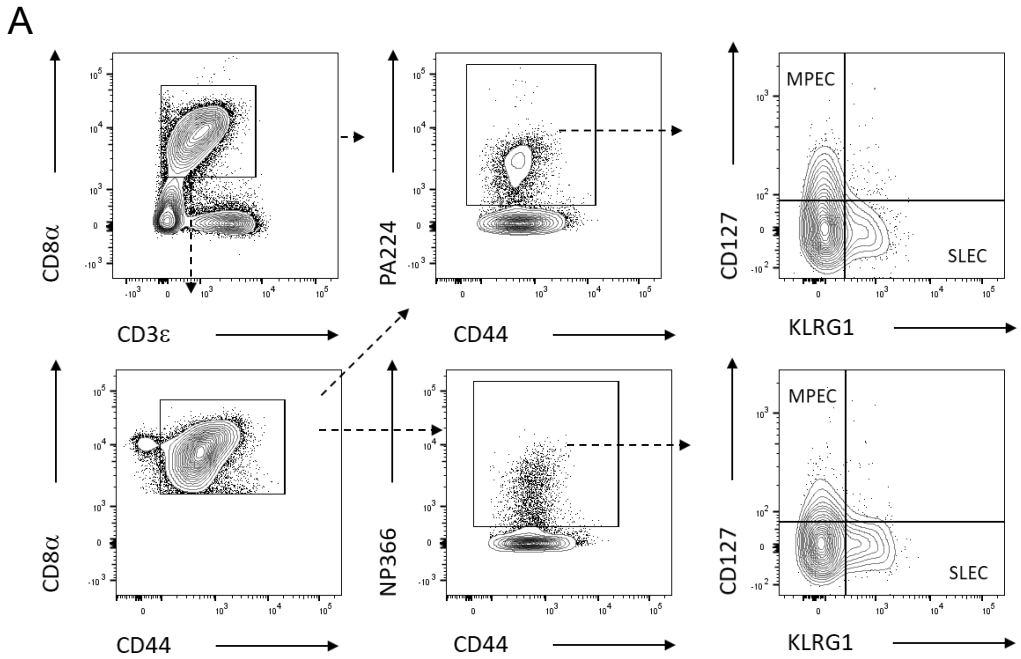
A
CD8α
CD3ε
PA224
CD44
CD127
KLRG1
MPEC
SLEC
CD8α
CD44
NP366
CD44
CD127
KLRG1
MPEC
SLEC

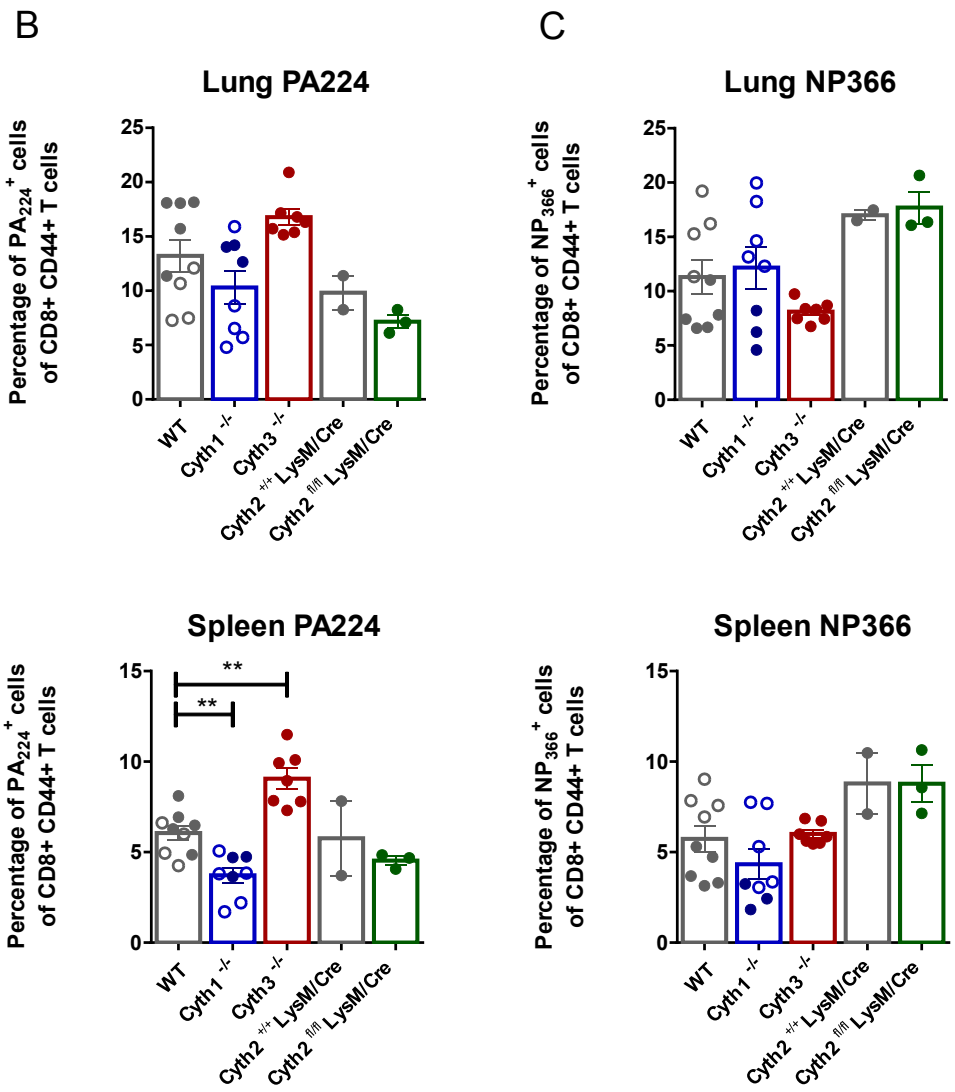
B
Lung PA224
Percentage of PA224+ cells of CD8+ CD44+ T cells
C
Lung NP366
Percentage of NP366+ cells of CD8+ CD44+ T cells
Spleen PA224
Percentage of PA224+ cells of CD8+ CD44+ T cells
Spleen NP366
Percentage of NP366+ cells of CD8+ CD44+ T cells
WT
Cyth1 -/-
Cyth3 -/-
Cyth2 +/+ LysM/Cre
Cyth2 fl/fl LysM/Cre
**
**

Figure 4.4: Antigen-specific effector CD8+ T cells in lung and spleen of cytohesin knockout mice following influenza infection. C57BL/6 (WT), cytohesin-1 (*Cyth1*$^{-/-}$) and cytohesin-3 (*Cyth3*$^{-/-}$) knockout mice, as well as cytohesin-2 conditional knockout (*Cyth2*$^{fl/fl}$ *LysM/Cre*) and *LysM/Cre* (*Cyth2*$^{+/+}$ *LysM/Cre*) control mice were infected intranasally with HKx31 influenza A virus for 8 days. The populations of PA_{224}^{+} and NP_{366}^{+} specific effector CD8+ T cells were determined in lung and spleen using a tetrameric complex of the H-2D^{b} glycoprotein and the respective epitopes via flow cytometry. **A**. Simplified gating strategy for influenza-specific effector CD8+ T cells after 8 days infection. Percentage of **B**. PA_{224}^{+} and **C**. NP_{366}^{+} specific CD8+ T cells of total effector CD8+ T cells in lung (*upper panels*) and spleen (*lower panels*). Bars present the mean with SEM. Each dot represents one mouse. Unfilled data points indicate second experiment. Significant differences found in PA_{224}^{+} effector CD8+ T cell population in *Cyth1*$^{-/-}$ and *Cyth3*$^{-/-}$ compared to WT mice in spleen (**, p<0.01; two-tailed Mann-Whitney U-test).

4.2.4 Cytohesin-1 influences the differentiation of short-lived effector T cells in lung

Given the differences in the proportions of antigen-specific CD8+ T cells, the subpopulations within the antigen-specific CD8+ T cell pool were determined using antibodies targeting CD127 and Killer cell lectin-like receptor subfamily G member 1 (KLRG1) (see gating of **Figure 4.4A**). CD8+ T cells expressing CD127^{high} KLRG1^{low} represent memory precursor effector cells (MPEC) (316). These MPEC considered as long-lived memory T cells. In contrast, CD127^{low} KLRG1^{high} CD8+ T cells define a short-lived effector cell (SLEC) phenotype (316). The latter population diminishes in size after successful pathogen clearance (316). However, both populations exhibit similar cellular effector functions in terms of cytokine response and cytotoxicity (317).

In the lungs of *Cyth1*$^{-/-}$ mice SLEC populations within PA224- and NP366-specific CD8+ T cells were proportionally decreased compared to wildtype T cells which is quite interesting as the results in previous section showed no statistically sig-

nificant difference in the frequency of total influenza-specific CD8+ T cells indicating that cytohesin-1 function targets specific cell subsets in the lung. In *Cyth1*$^{-/-}$ spleens no alterations in these subpopulations were found (**Figure 4.5**).

No significant difference in the ratios of MPEC and SLEC were determined in the lungs and spleens of *Cyth3* and myeloid-specific *Cyth2* KO mice (**Figure 4.5**).

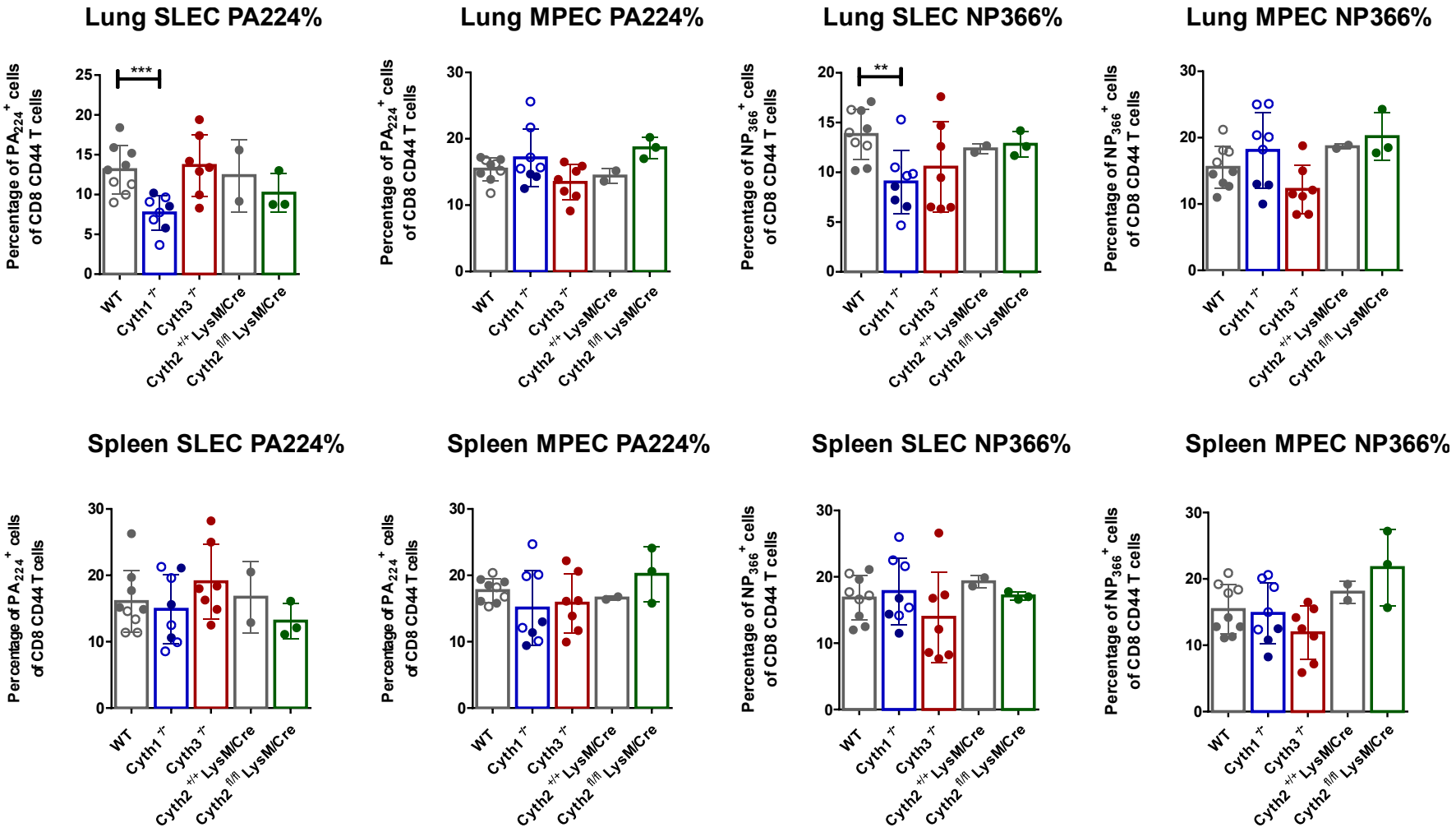
Lung SLEC PA224%
Percentage of PA224+ cells of CD8 CD44 T cells
***
Lung MPEC PA224%
Lung SLEC NP366%
**
Lung MPEC NP366%
Percentage of NP366+ cells of CD8 CD44 T cells
Spleen SLEC PA224%
Spleen MPEC PA224%
Spleen SLEC NP366%
Spleen MPEC NP366%
WT
Cyth1-/-
Cyth3-/-
Cyth2+/+ LysMCre
Cyth2fl/fl LysMCre

Figure 4.5: Frequencies of short-lived and memory precursor effector cells of antigen-specific CD8+ T cell populations in lung and spleen of cytohesin knockout mice following influenza infection. C57BL/6 (WT), cytohesin-1 (*Cyth1*$^{-/-}$) and cytohesin-3 (*Cyth3*$^{-/-}$) knockout mice, as well as cytohesin-2 conditional knockout (*Cyth2*$^{fl/fl}$ *LysM/Cre*) and *LysM/Cre* (*Cyth2*$^{+/+}$ *LysM/Cre*) control mice were infected with HKx31 influenza A virus for 8 days. Short-lived (SLEC) and memory precursor effector cells (MPEC) of PA_{224}^{+} and NP_{366}^{+} specific effector CD8+ T cell population were determined in lung (*upper panels*) and spleen (*lower panels*) via flow cytometry as shown in **Figure 4.4A.** Each dot represents one mouse and bars present the mean with SEM. Filled and unfilled datapoints distinguish individual experiments. Significant differences were found in SLEC of PA_{224}^{+} effector CD8+ T cell population among *Cyth1*$^{-/-}$ and WT mice in lung (**, $p<0.01$; ***, $p<0.001$; two-tailed Mann-Whitney U-test).

4.2.5 Cytohesin-1 and -3 reciprocally regulate cytokine responses of influenza-specific CD8+ T cells

Alterations in the relative amount of influenza-specific CD8+ T cells and effector subtypes among cytohesin-1 and cytohesin-3 KO mice raised the question whether the effector functions of these CD8+ T cells may differ. IFNγ and TNF secretion, which is important in the elimination of influenza-infected cells, was investigated to analyse the functional ability of single cells (318).

Splenocytes of cytohesin-deficient mice were isolated following 8 days infection, and *in vitro* restimulated with immunogenic epitopes to induce a cytokine response in influenza-specific CD8+ T cells. These immunogenic epitopes are peptides of influenza antigens and include NP366, PA224, non-structural protein 2 ($NS2_{114\text{-}121;}$ NS2) and polymerase basic protein 1 ($PB1_{703\text{-}711}$; PB1). The production of IFNγ and TNF was assessed via intracellular staining and flow cytometry.

Cyth1$^{-/-}$ samples had proportionally less IFNγ-secreting effector CD8+ T cells to all immunogenic peptides used compared to WT samples (**Figure 4.6A**). Addi-

tionally, coexpression of TNF was decreased in *Cyth1*$^{-/-}$ effector CD8+ T cells when stimulated with PB1 and NS2 epitopes (**Figure 4.6B**).

In contrast, expression of IFNγ (**Figure 4.6A**) and TNF (**Figure 4.6B**) was increased in all *Cyth3*$^{-/-}$ influenza-specific T cells in comparison to WT T cells.

In myeloid-specific *Cyth2* KO no effect was observed in the cytokine production of effector CD8+ T cells after restimulation among all used epitopes.

In conclusion, deletion of cytohesin-1 impaired the cellular response in effector CD8+ T cells after restimulation with their cognate epitopes. In contrast, lack of cytohesin-3 resulted in stronger cytokine response in all restimulated influenza-specific CD8+ T cells.

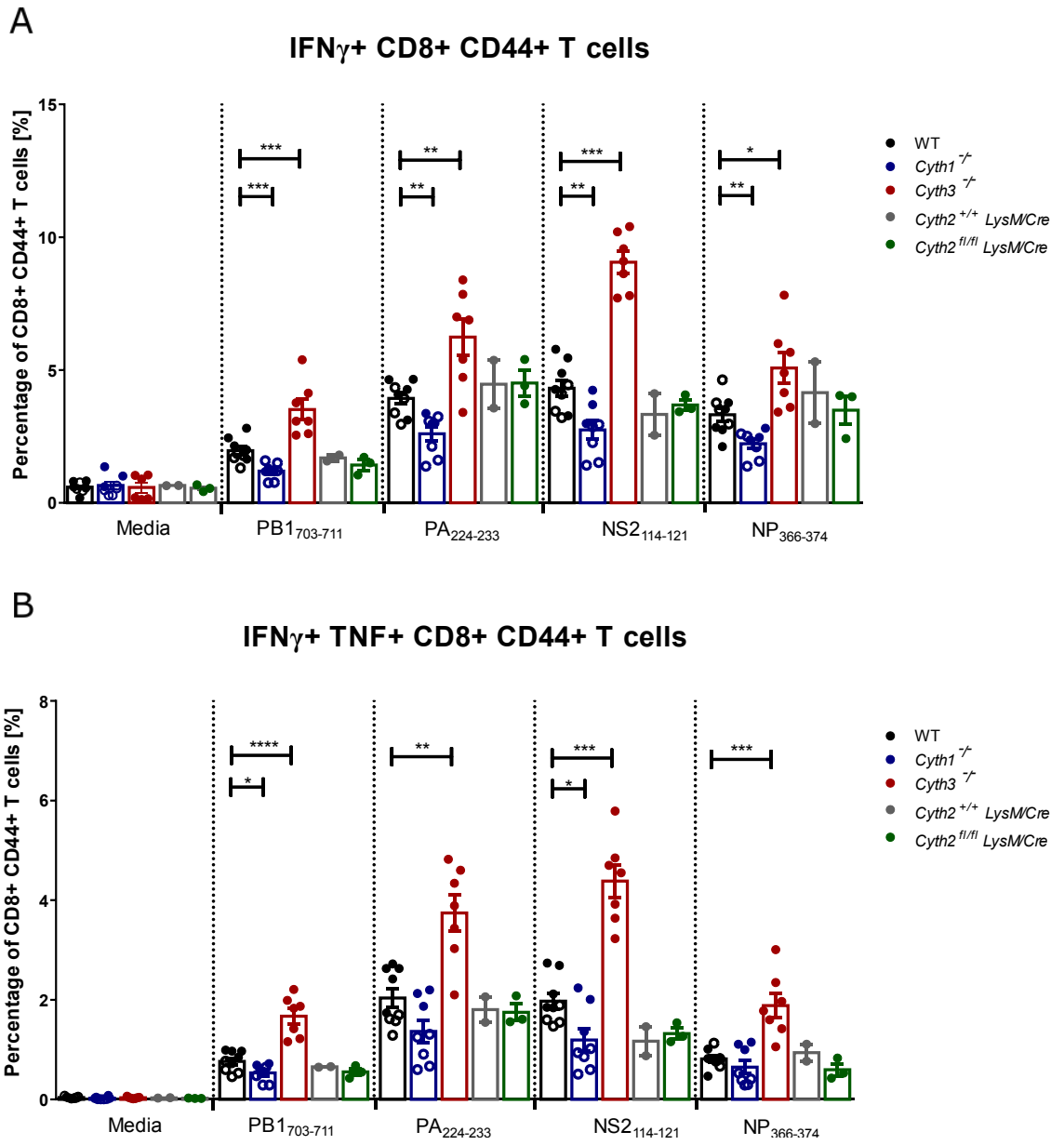

Figure 4.6: IFNγ and TNF response of antigen-specific effector CD8+ T cells after *in vitro* restimulation. C57BL/6 (WT), cytohesin-1 (*Cyth1*$^{-/-}$) and cytohesin-3 (*Cyth3*$^{-/-}$) knockout mice, as well as cytohesin-2 conditional knockout (*Cyth2*$^{fl/fl}$ *LysM/Cre*) and *LysM/Cre* (*Cyth2*$^{+/+}$ *LysM/Cre*) control mice were infected with HKx31 influenza A virus for 8 days. Splenocytes were isolated and restimulated *in vitro* with immunogenic peptides ($PB1_{703-711}$, $PA_{224-233}$, $NS2_{114-121}$, $NS2_{366-374}$) or media control to induce cytokine release. The expression of IFNγ and TNF in CD8+ effector cells was determined via flow cytometry after intracellular cytokine staining. Each dot represents one mouse and bars present the mean with SEM. Filled and unfilled datapoints distinguish individual experiments. Significant differences were found in IFNγ+ and TNF+ CD8+ effector cells of *Cyth1*$^{-/-}$ and *Cyth3*$^{-/-}$ compared to WT samples (*, $p<0.05$; **, $p<0.01$; ***, $p<0.001$; two-tailed Mann-Whitney U-test).

4.3 Discussion

The analyses presented in this chapter clearly demonstrate that the primary role of cytohesins during pulmonary infection is restricted to T cell responses. Here, all cytohesin deficient mice displayed phenotypes in CD4+ and CD8+ T cell kinetics in response to *L. pneumophila* infection. This was distributed in all analysed memory T cell subtypes. Remarkably, cytohesin-1 and cytohesin-3 exerted opposing effects on T cell responses. The dichotomy between cytohesin-1 and cytohesin-3 functions was also corroborated by their respective contributions to the development and regulation of effector functions of influenza-specific CD8+ T cells. The results demonstrate for the first time *in vivo* how these proteins not only impact the recruitment of different T cells to the inflamed tissue, but also regulate T cell effector functions.

4.3.1 Cytohesin-1 promotes antigen-specific T cell responses

Mice deficient in cytohesin-1 showed weaker CD4+ and CD8+ T cell responses following *L. pneumophila* infection, implying that cytohesin-1 promotes T cell immunity. Because this phenotype arose in the late stages of *L. pneumophila* infection, a likely explanation may be that cytohesin-1 contributes to cognate T cell responses. In support of this, cytohesin-1 affected influenza-specific CD8+ T cell responses, as demonstrated by an impaired acquisition of antigen-specific CD8+ T cells in the absence of cytohesin-1. Additionally, optimal cellular responses to antigen-specific stimuli depended on a functional cytohesin-1, underlining the importance of cytohesin-1 in the optimal effector functions of T cells

The exact mechanism of the involvement of cytohesin-1 in the T cell biology is still unclear. Cytohesin-1 has been shown to facilitate LFA-1 signalling and thereby increase T cell activation and Th1 differentiation in collaboration to TCR stimulation (167). In cooperation with LFA-1, cytohesin-1 lowers the signal threshold that is required for proper T cell activation (167). Consequently, lack of cytohesin-1 may lead to less responsive T cells and inefficient T cell priming within lymphoid tissues resulting in fewer T cells acquiring effector functions. Further-

more, our laboratory demonstrated that cytohesin-1 expression enhances IL-2 promoter activity in Jurkat T cells (Paul, B., PhD thesis). IL-2 is essential in T cell expansion and the differentiation to different effector T cells (319). Therefore, decreased IL-2 levels in the absence of cytohesin-1 might lead to decreased T cell proliferation and differentiation in the course of infection.

The notion that cytohesin-1 affects the threshold of T cell activation and in the resulting effect on T cell priming may explain why some of the functional effects of cytohesin-1 ablation appear stronger in settings where T cells are exposed to suboptimal antigenic stimulation. Specifically, *Cyth1*$^{-/-}$ mice showed a stronger phenotype in influenza-specific CD8+ T cell populations of the spleen compared to the lung, an organ of presumably low antigenic density. Furthermore, the PA224-specific T cell population was more affected by the lack of cytohesin-1 in comparison to NP366-specific T cells. PA224-epitopes are presented by APC in lower levels than NP366-epitopes (280). This favours the idea that cytohesin-1 deficient T cells require stronger stimulus with higher antigen-encounter for a proper T cell activation. Therefore, T cells that recognize more rarely presented antigens (e.g. PA224-epitopes) are more strongly affected by the lack of cytohesin-1.

Furthermore, cytohesin-1 appears to coordinate the differentiation of distinct effector cell subtypes leading to fewer SLEC in the lack of cytohesin-1. The cell-fate decision of activated T cell to differentiate to SLEC or MPEC subtype depends on different factors including antigen load, co-stimulation, cytokine milieu, metabolic signals and strength of TCR engagement (320). Here, exposure to high IL-2 levels, as well strong interaction of TCR with the epitope presented on the MHC molecule favours the differentiation towards SLEC (320-322). With respect to the role of LFA-1 in the formation of the immune synapse upon TCR priming (323), one might speculate that cytohesin-1 deficiency weakens the attachment of LFA-1 to its agonist on APC leading to weaker contact during TCR ligation and consequently, resulting in fewer SLEC. In order to gain a better understanding of the function of cytohesin-1 in T cell activation, further studies might address the

role of the protein in the formation of the immune synapse and investigate events occurring in T cell priming within infected *Cyth1*$^{-/-}$ mice.

In conclusion, these results demonstrate that cytohesin-1 positively regulates T cell immune responses and is required for optimal acquisition of antigen-specific effector functions following pulmonary infections.

4.3.2 Myeloid-specific deletion of cytohesin-2 only slightly impacts T cell responses

Myeloid-specific cytohesin-2 deficient mice showed a transient effect in CD4+ and CD8+ T cell responses in *L. pneumophila* infection indicating that the T cell-APC interaction might be perturbed. In this context, these mice displayed a transiently lower cDC number in lung (3.2.6.3) raising the possibility that the alteration of T cell responses might be due to altered distribution of cDCs. As T cell responses are also induced in the draining lymph nodes, further investigation of immune responses in this tissue might elucidate whether trafficking of activated cytohesin-2 deficient cDCs towards lymphoid tissues is altered. Notably, no phenotype in CD8+ T cell responses was observed in the influenza infection model. However, it is possible that earlier transient effects were missed because this experiment only examined one time point.

In summary, myeloid-specific cytohesin-2 transiently alters T cell responses following bacterial challenge, which might be due to effects on cDC biology. However, these impacts are not pronounced enough to result in major changes in the T cell response and therefore do not influence the outcome of the disease.

4.3.3 Cytohesin-3 inhibits T cell responses

Overall T cell responses were amplified following *L. pneumophila* infection in *Cyth3*$^{-/-}$ mice, indicating that deletion of cytohesin-3 leads to a general hyperactivation of all T cell subtypes. Increased influenza-specific CD8+ T cell activity in the absence of cytohesin-3 was also observed, emphasizing the prominent role of cytohesin-3 in T cell mediated responses.

Interestingly, the T cell phenotype in *Cyth3*$^{-/-}$ T cells was converse to the phenotype of *Cyth1*$^{-/-}$ T cells, which implies that these two cytohesins act in an antagonistic manner, although this counterregulation must not necessarily affect the same pathway. In this regard, functions of cytohesin-3 impact global T cell immune responses, whereas function of cytohesin-1 seems to target specific effector CD8+ T cell subtypes as seen in the SLEC differentiation. Furthermore, the quantitative phenotype of cytohesin-3 ablation was more profound than that of other cytohesins, indicating that cytohesin-3 has the most prominent role of all cytohesin genes in T cell biology.

In this context, the relevance of coordinated function of cytohesin-3 in T cell biology is supported by the finding that cytohesin-3 expression is tightly regulated in T cells: its expression is suppressed following T cell activation and increased in T cell anergy (153)(Tolksdorf, F., PhD thesis). This evidence supports the possible function of cytohesin-3 as an immune checkpoint that suppresses T cell activation and induces peripheral tolerance. In accordance with this idea, our laboratory demonstrated induction of cytohesin-3 mRNA and protein expression in anergic T cells, which was dependent on the ligation of PD-1, one of the most important immune checkpoint control factors (Paul, B. PhD thesis). PD-1 counteracts proximal T cell signalling upon T cell activation leading to inhibition of T cell proliferation and suppression of proinflammatory T cell responses (324, 325).

Thus, it is possible that cytohesin-3 is part of the PD-1 inhibitory signalling machinery. Classically, PD-1 engagement with PD-L1 or PD-L2 recruit tyrosine phosphatases SHP-1 and SHP-2 to the cytoplasmatic tail of PD-1, which subse-

quently inhibit downstream effectors in the TCR signalling cascade such as CD3ζ, ZAP70 and PKCθ (326, 327). Additionally, PD-1 signalling blocks the CD28-mediated activation of PI3K and its downstream target Akt impairing the release of IL-2 and IFNγ (328).

On the basis of other *in vitro* observations, a strong involvement of cytohesin-3 in the inhibition of TCR and CD28 signalling is also likely. In this context, our laboratory demonstrated that the addition of CD28 ligand inhibited the induced expression of cytohesin-3 in anergic T cells (Paul, B., PhD thesis). Therefore, CD28 signalling which is required for a proper T cell activation, seems to silence the function of cytohesin-3. Furthermore, overexpression of cytohesin-3 in Jurkat T cells interfered with TCR signalling and supressed phosphorylation of downstream effector Akt (Tolksdorf, F., PhD Thesis). Consequently, lack of cytohesin-3 might lead to an enhanced TCR/CD28 signalling axis, resulting in increased cytokine release which is indeed observed in cytohesin-3 deficient T cells.

Notably, deletion of other components of the PD-1 inhibitory signalling in T cells results in a phenotype which is comparable to that of cytohesin-3 deficient mice. Specifically, deletion of SHP-2 in T cells leads to a hyperactivated TCR signalling resulting in increased IFNγ response and increased activity of cytotoxic T cells in different *in vivo* models (329, 330). In similar fashion, cytohesin-3 deficiency might lead to a more reactive TCR signalling due to the lack of a putative inhibitory immune checkpoint.

As important regulators of the immune responses, one major function of immune checkpoints is to suppress autoreactive immune activity and control inflammation. The importance of a functional and balanced regulation of immune responses becomes clear when dysregulation results in chronic inflammation leading to tissue destruction as well as autoimmune disorders including rheumatoid arthritis and type 1 diabetes mellitus (331-334).

Intriguingly, *Cyth3*$^{-/-}$ mice display impaired recovery following *L. pneumophila* infection which strongly correlates with the T cell phenotype. Dysregulated T cell

responses which result in increased T cell infiltration and reactivity as observed in the absence of cytohesin-3 might result in an overall stronger pulmonary inflammation with potential tissue destruction. Therefore, further studies might test whether T cell-specific deletion of cytohesin-3 phenocopies the full ablation of cytohesin-3 in mice.

In conclusion, these results highlight that cytohesin-3 is a crucial element in balanced and controlled T cell immune responses, possibly via exhibiting a suppressive function in T cell activation signalling and might contribute to the inhibitory immune checkpoint function. The extent of the dysregulation in T cell responses in the absence of cytohesin-3 appears to affect the overall recovery of mice to pulmonary infection, which identifies cytohesin-3 as the most important single member of the cytohesin family for the regulation of *in vivo* immune responses:

5. The role of cytohesins in T cell differentiation and metabolism

5.1 Introduction

The results of Chapter 4 identified cytohesin-1 and cytohesin-3 as regulators of T cell immunity in response to bacterial and viral infection in mice. Interestingly, cytohesin-1 and cytohesin-3 intervene in T cell immune activity in opposing manners. Cytohesin-1 appears to be important in antigen-specific T cell immune responses, whereas the lack of cytohesin-3 results in a general hyperactivation of T cells, eventually leading to delayed recovery of mice from infection. Therefore, the experiments in this chapter aimed to understand specifically how these cytohesins modulate T cell immune responses.

5.2 Results

5.2.1 Cytohesin-1 and cytohesin-3 reciprocally orchestrate the differentiation of naïve CD4+ T cells to effector T helper subtypes

In the course of infection, naïve CD4+ T cells can differentiate to several helper cell types that mediate distinct effector functions (reviewed in section 1.2.2). Th1 cells occur predominantly in response to intracellular pathogens and provide help in the clearance (335). Th2 cells are important in the combat of extracellular parasites and they also support B cell immune responses (336). Perez *et al*. described that LFA-1 signalling preferably induces the polarization towards Th1 phenotype following stimulation (167). Whereas PD-1 ligation which might be possible component in the cytohesin-3 signalling has been shown to induce the transition towards Th2 cell type (337). The involvement of cytohesin-1 and cytohesin-3 in the polarization processes of T cells has not been defined yet.

In order to investigate whether cytohesin-1 or cytohesin-3 affect the differentiation of naïve CD4+ T cells (Th0), naïve CD4+ T cells were isolated from *Cyth1*$^{-/-}$ and *Cyth3*$^{-/-}$ mice and wildtype littermates, then cultured under Th1 and Th2 polarizing conditions for 4 days prior restimulation with phorbol 12-myristate 13-acetate (PMA) and ionomycin. The expression of defining cytokines and transcription factors specific for Th1 and Th2 cell types were assessed in differentiated T cells after intracellular staining via flow cytometry (**Figure 5.1**). Th1 cells can be characterized by the high expression of transcription factor Tbet (*Tbx21*) and IFNγ, while Th2 subtype is identified by the increased expression of GATA3 and IL-4 (338). Undifferentiated Th0 cells and non-restimulated but differentiated T cells were used as controls to check the differentiation efficiency (**Figure 5.1**).

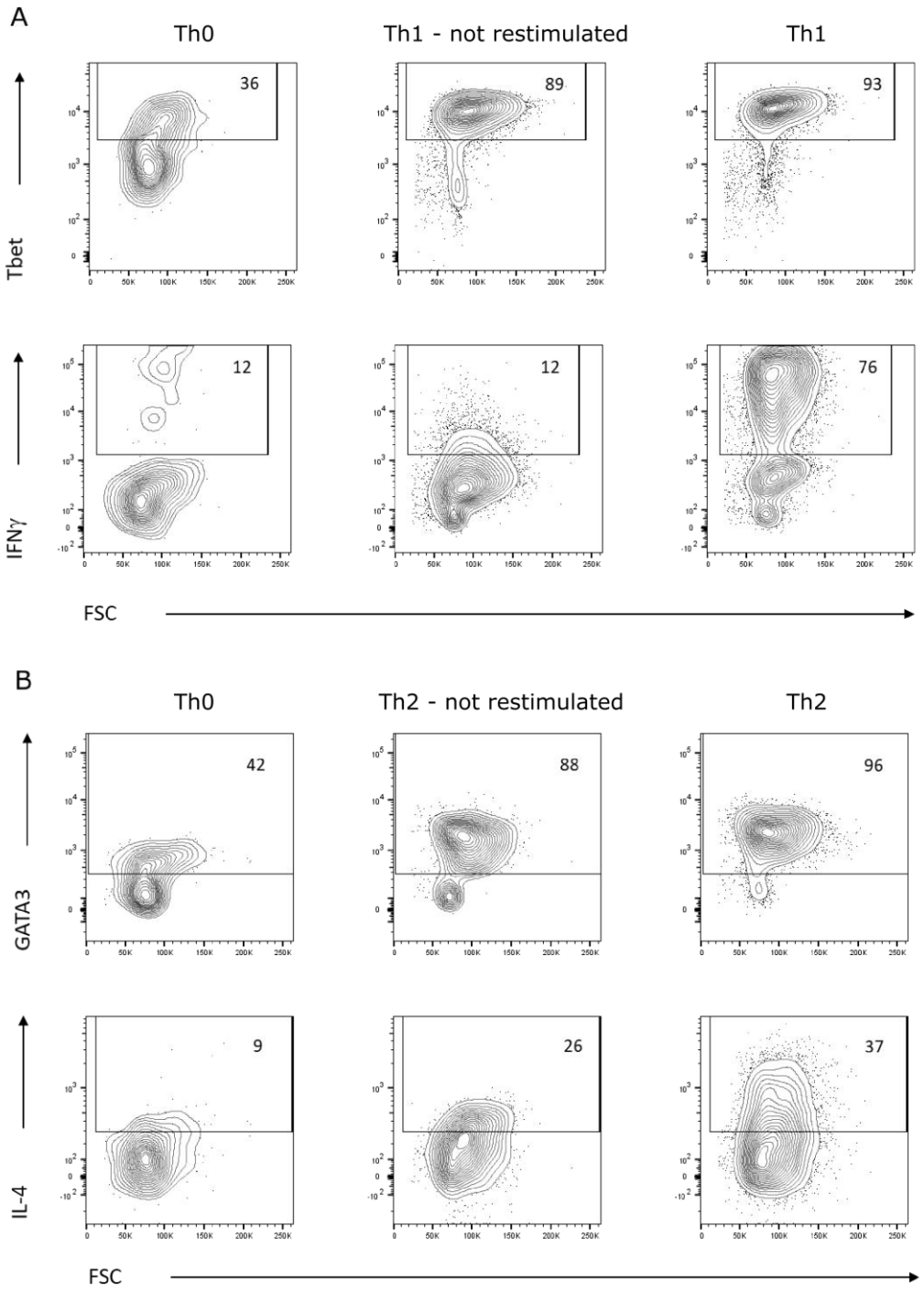

Figure 5.1: *In vitro* differentiation of naïve CD4+ T cells to Th1 and Th2 subtypes. Naïve CD4+ T cells (Th0) from murine spleen and lymph nodes were isolated via MACS and differentiated under polarizing conditions to **A.** Th1 or **B.** Th2 cell types for 4 days. Cells were restimulated with PMA/ionomycin and the transcription factors as well cytokine response intracellularly determined by flow cytometry. Plots represent simplified gating strategy of restimulated Th1 or Th2 cells (*right panels*), not-restimulated control (*middle panels*) and naïve CD4+ (*left panels*) control from wildtype mice pre-gated on live CD4+CD3ε+ cells.

Following differentiation, *Cyth1*$^{-/-}$ CD4+ T cells displayed a lower frequency of differentiated Th2 cells compared to wildtype T cells, with fewer cells expressing GATA3 and IL-4 (**Figure 5.2A**). Although a trend towards less Th1 polarization in *Cyth1*$^{-/-}$ CD4+ T cells was observed relative to wildtype T cells, no statistically significance could be identified (**Figure 5.2A**).

The opposite results were obtained for *Cyth3*$^{-/-}$ CD4+ T cells, with more differentiated Th1 cells obtained compared to wildtype control (**Figure 5.2B**). The proportion of Th2 cells also appeared to be elevated, although not statistically significant, compared to wildtype T cells (**Figure 5.2B**).

In conclusion, cytohesin-1 appears to be a positive factor in the differentiation of naïve CD4+ T cells towards Th2 cell type, whereas cytohesin-3 negatively regulates the polarization towards Th1 cells.

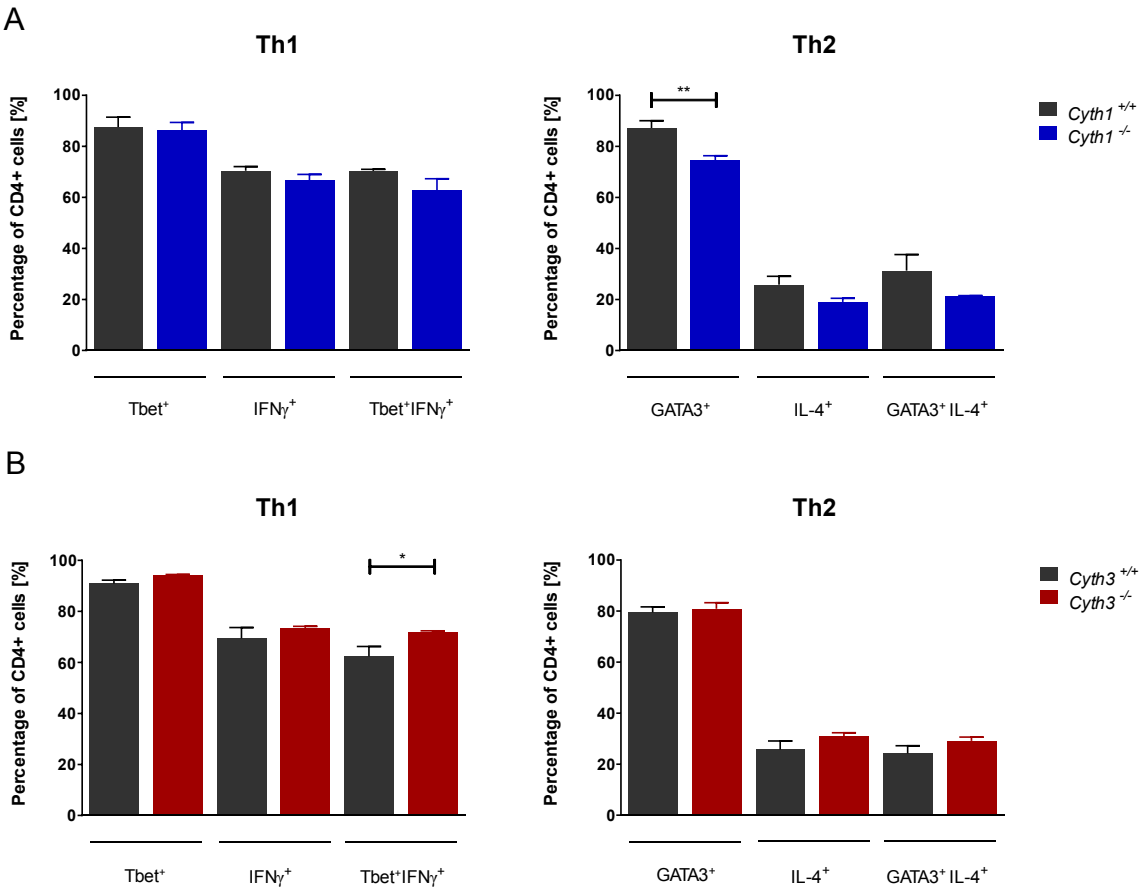

Figure 5.2: *In vitro* differentiation of cytohesin-1 or cytohesin-3 deficient CD4+ T cells to Th1 and Th2 subtypes. Naïve CD4+ T cells from murine spleen and lymph nodes were isolated via MACS and differentiated under polarizing conditions to Th1 (*left panels*) or Th2 (*right panels*) subtypes for 4 days. Restimulation was performed using PMA/ionomycin in the presence of BrefeldinA. The expression of Th1 or Th2 cell-specific transcription factors and cytokines of **A.** *Cyth1*$^{+/+}$ or *Cyth1*$^{-/-}$ T cells and **B.** *Cyth3*$^{+/+}$ or *Cyth3*$^{-/-}$ T cells was determined via flow cytometry. Bars present the mean (n=3) with SEM. Significant differences were found between *Cyth1*$^{-/-}$ and *Cyth1*$^{+/+}$ in GATA3^{+} Th2 cells and between *Cyth3*$^{-/-}$ and *Cyth3*$^{+/+}$ Tbet^{+}IFNγ^{+} Th1 cells (*, $p<0.05$; unpaired two tailed student t-test).

5.2.2 Cytohesin-1 intervenes in metabolic processes following T cell stimulation

Metabolic reprogramming of T cells following activation is an important component assuring optimal and rapid immune responses (reviewed in section 1.2.6). Because of the prominent function of cytohesin-3 in metabolic processes (see section 1.4.3) it was considered that the metabolic fitness of cytohesin-deficient T cells might differ which may account for the observed alterations in T cell responses. Therefore, T cells were stimulated with defined mitogens, and the cellular glycolytic as well as mitochondrial respiratory responses were analysed.

Isolated naïve CD4+ T cells of *Cyth1*$^{-/-}$ and *Cyth3*$^{-/-}$ mice were stimulated with either α-CD3 and α-CD28 antibodies, PMA and ionomycin or glucose. Following stimulation the extracellular acidification rate (ECAR) which serves as a readout for the glycolytic activity, as well as the cellular oxygen consumption rate (OCR), a correlate for mitochondrial respiration were measured using a Seahorse Analyzer. The addition of α-CD3 and α-CD28 antibodies results in the activation of the TCR and CD28 signalling (339). In contrast stimulation with PMA/Ionomycin bypasses the TCR signalling resulting in direct activation of protein kinase C (PKC) and an increase in intracellular calcium concentrations (340, 341). The stimulation with glucose was used to determine the ability of cells to take up essential sources for glycolysis which is mediated by different glucose transporters such as Glut1 (342). Following these stimulations oligomycin as well as 2-deoxy-D-glucose (2-DG) were injected. Oligomycin inhibits ATP synthase in the mitochondrial ATP production shifting the ECAR to the maximum glycolytic capacity (343, 344). The final injection of 2-DG results in the inhibition of glycolysis by inhibiting competitively hexokinase (345).

5.2.2.1 Cytohesin-1 affects the ability of naïve T cells to react to TCR stimulation

Injection α-CD3/CD28 did not lead to an immediate change in ECAR (**Figure 5.3A** and **C** *left panel*) and OCR (**Figure 5.3B** and **D** *left panel*) of *Cyth1*$^{-/-}$ T cells in contrast to WT T cells. However, addition of oligomycin led to similar glycolytic capacity in *Cyth1*$^{-/-}$ and *Cyth1*$^{+/+}$ T cells showing the same increase in ECAR and decrease in OCR (**Figure 5.3C** and **D** *middle panel*). Interestingly, even though 2-DG injection resulted in the same initial drop in the ECAR among *Cyth1*$^{-/-}$ and *Cyth1*$^{+/+}$ T cells, *Cyth1*$^{-/-}$ T cells displayed a further delayed decrease in ECAR which was not observed for the wildtype counterpart (**Figure 5.3C**, *right panel*).

A

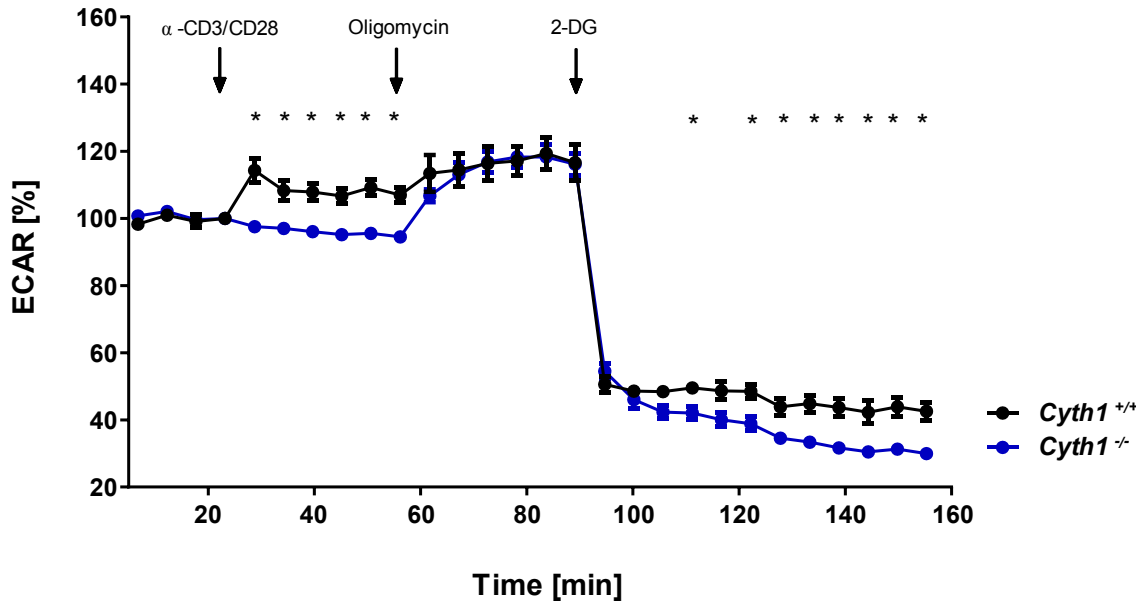
ECAR during TCR stimulation
α -CD3/CD28
Oligomycin
2-DG
ECAR [%]
Time [min]
Cyth1 +/+
Cyth1 -/-

B

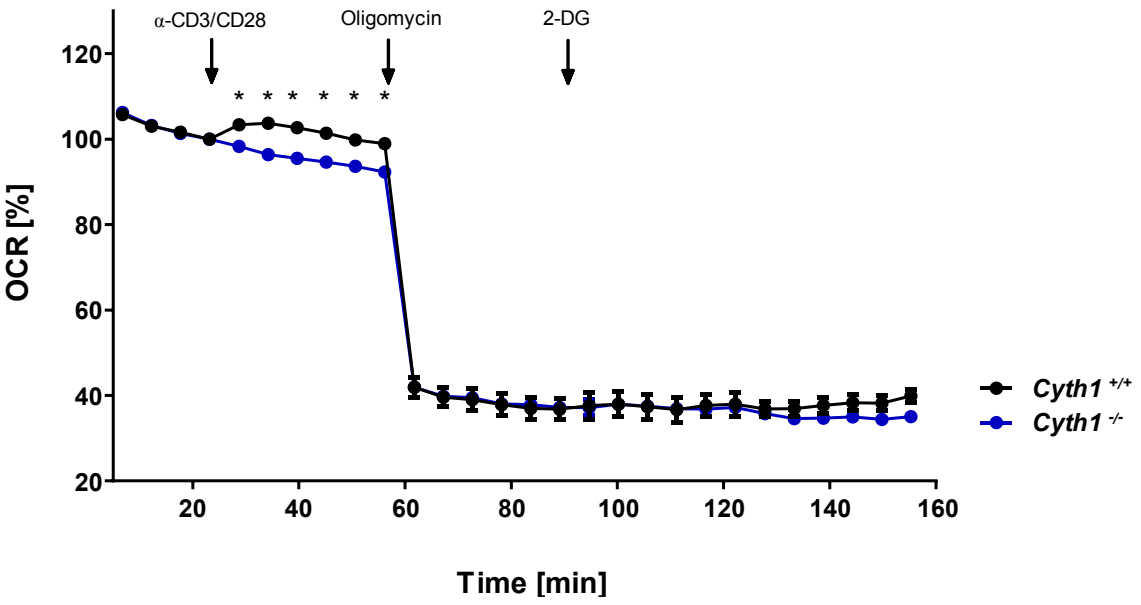
OCR during TCR stimulation
α-CD3/CD28
Oligomycin
2-DG
OCR [%]
Time [min]
Cyth1 +/+
Cyth1 -/-

C

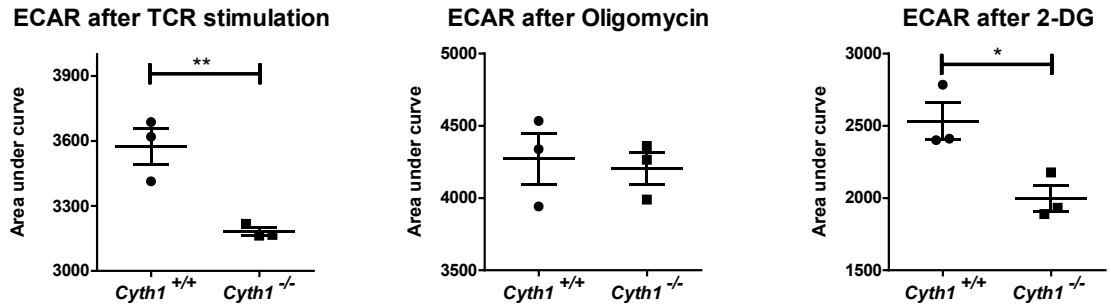

D

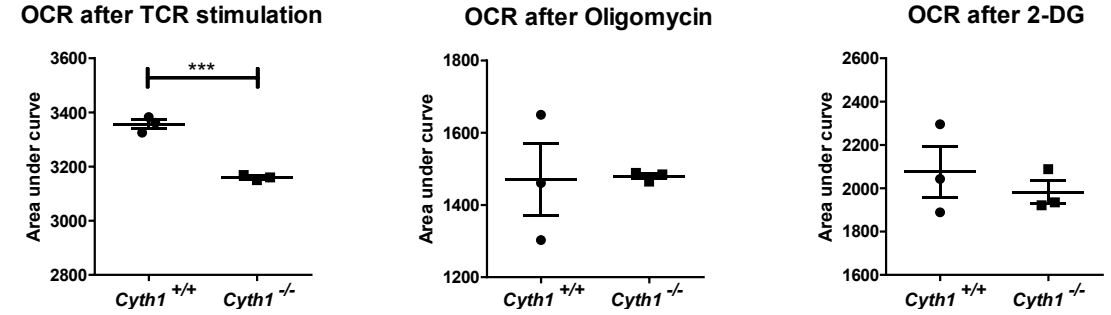

Figure 5.3: Glycolysis and mitochondrial respiration of cytohesin-1 deficient naïve CD4+ T cells following TCR stimulation. A. Extracellular acidification rate (ECAR) and **B**. Oxygen consumption rate (OCR) after injection (indicated by arrows) of α-CD3/CD28 antibodies, oligomycin and 2-deoxy-D-glucose (2-DG). Graphs present the mean (n=3) with SEM and is normalized to cell number with background correction. Baseline is set to the timepoint prior first injection. Calculated area under curve of **C***.* ECAR and **D**. OCR for α-CD3/CD28 antibodies stimulation after α-CD3/CD28 antibodies and prior oligomycin injection (*left panels*), for oligomycin after oligomycin and prior 2-DG injection (*middle panels*) and for 2-DG after 2-DG injection (*right panels*). Graphs present the mean (n=3) with SEM (*, $p<0.05$; **, $p<0.01$; ***, $p<0.001$; unpaired student's t-test).

5.2.2.2 Cytohesin-1 intervenes in the metabolic switch following PMA/ionomycin stimulation

Injection of PMA/ionomycin led immediately to a dramatic change in the ECAR (**Figure 5.4A**) and OCR (**Figure 5.4B**) giving comparable high levels in *Cyth1*$^{-/-}$ and *Cyth1*$^{+/+}$ T cells. However, the drop in ECAR and OCR after the initial stimulus occurred in *Cyth1*$^{-/-}$ T cells was more drastic than wildtype controls (**Figure 5.4C**,**D** *left panel*). The subsequent addition of oligomycin led to a drop in ECAR and OCR, however the relative change of ECAR and OCR in *Cyth1*$^{-/-}$ T cells was not as strong as in *Cyth1*$^{+/+}$ T cells (**Figure 5.4C**,**D** *middle panel*). Small but significant differences were observed in the ECAR and OCR following 2-DG injection (**Figure 5.4C**,**D** *right panel*).

A

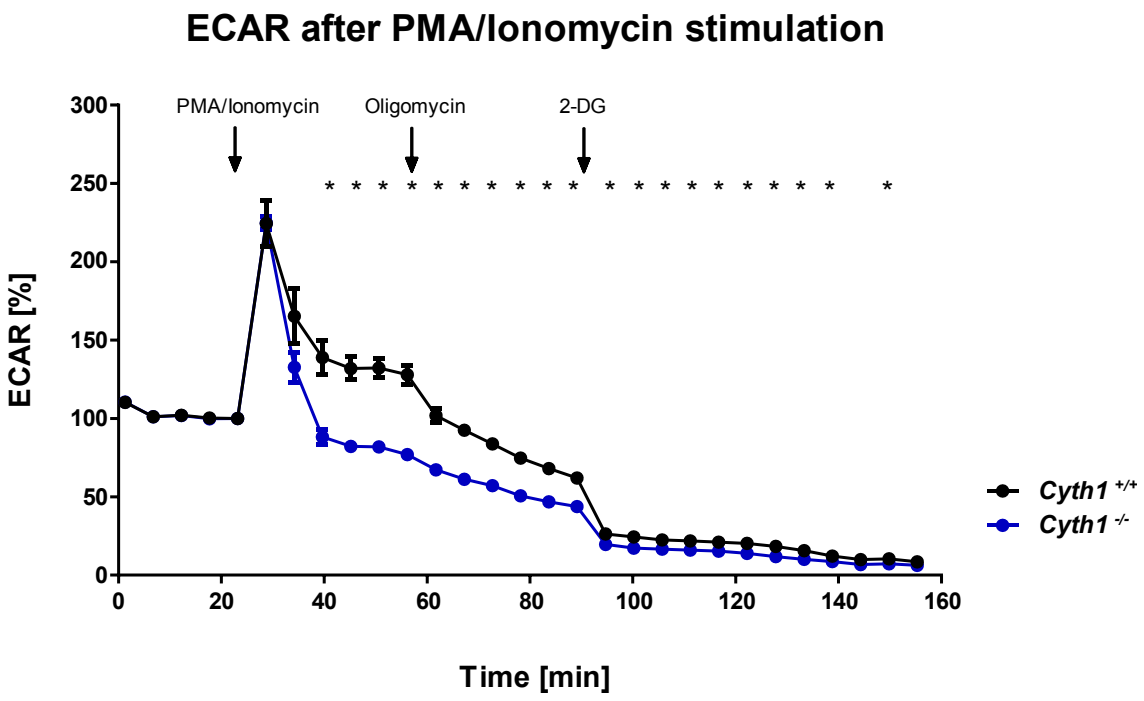
ECAR after PMA/Ionomycin stimulation
PMA/Ionomycin
Oligomycin
2-DG
ECAR [%]
Time [min]
Cyth1 +/+
Cyth1 -/-

B

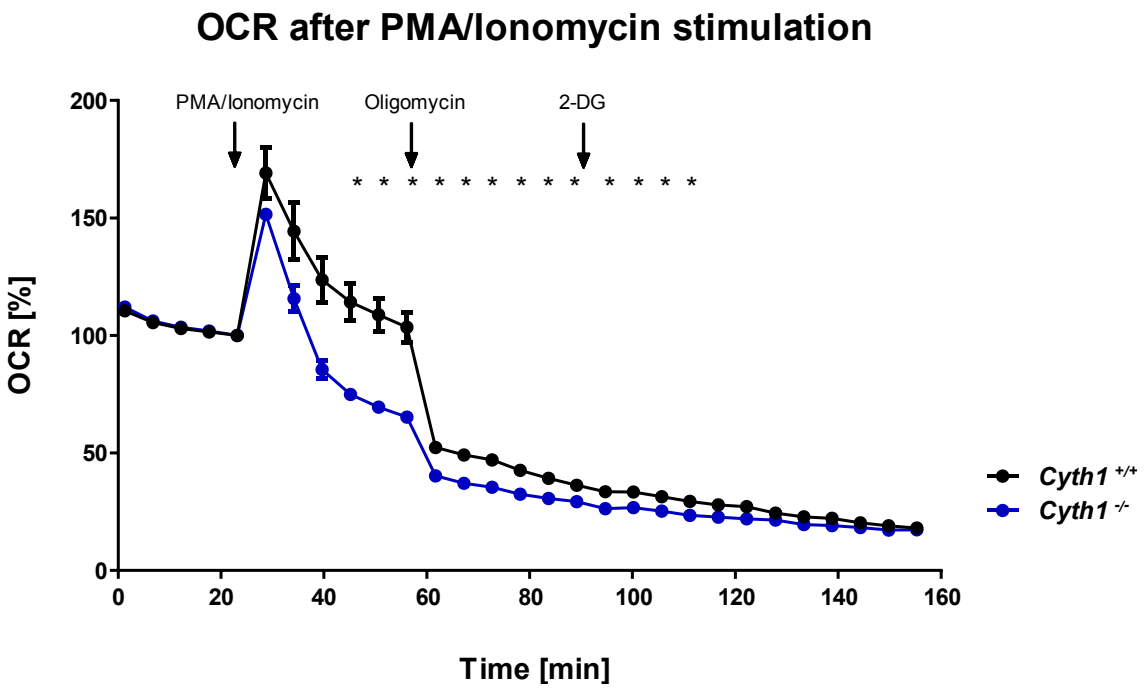
OCR after PMA/Ionomycin stimulation
PMA/Ionomycin
Oligomycin
2-DG
OCR [%]
Time [min]
Cyth1 +/+
Cyth1 -/-

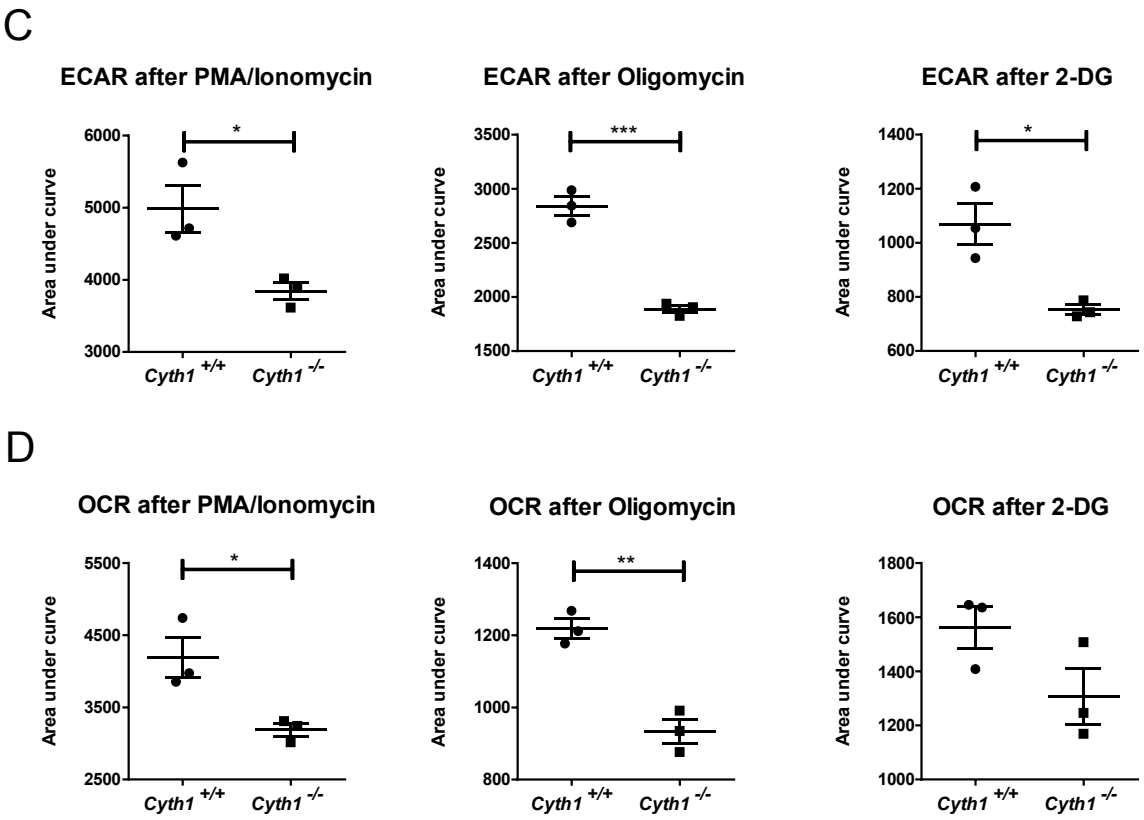

Figure 5.4: Glycolysis and mitochondrial respiration of cytohesin-1 deficient naïve CD4+ T cells following PMA/ionomycin stimulation. A. Extracellular acidification rate (ECAR) and **B**. Oxygen consumption rate (OCR) after injection (indicated by arrows) of PMA/ionomycin mix, oligomycin and 2-deoxy-D-glucose (2-DG). Graphs present the mean (n=3) with SEM and is normalized to cell number with background correction. Baseline is set to the timepoint prior first injection. Calculated area under curve of **C**. ECAR and **D**. OCR for PMA/ionomycin stimulation after PMA/ionomycin and prior oligomycin injection (*left panels*), for oligomycin after oligomycin and prior 2-DG injection (*middle panels*) and for 2-DG after 2-DG injection (*right panels*). Graphs present the mean (n=3) with SEM (*, $p<0.05$; **, $p<0.01$; ***, $p<0.001$; unpaired student's t-test).

5.2.2.3 Cytohesin-1 does not affect glycolysis following glucose injection

Following glucose injection *Cyth1*$^{-/-}$ and *Cyth1*$^{+/+}$ T cells displayed comparable increase in ECAR (**Figure 5.5A**,**C**). Further, *Cyth1*$^{-/-}$ T cells displayed a trend to a lower OCR relative to *Cyth1*$^{+/+}$ T cells (**Figure 5.5B**,**D**).

A

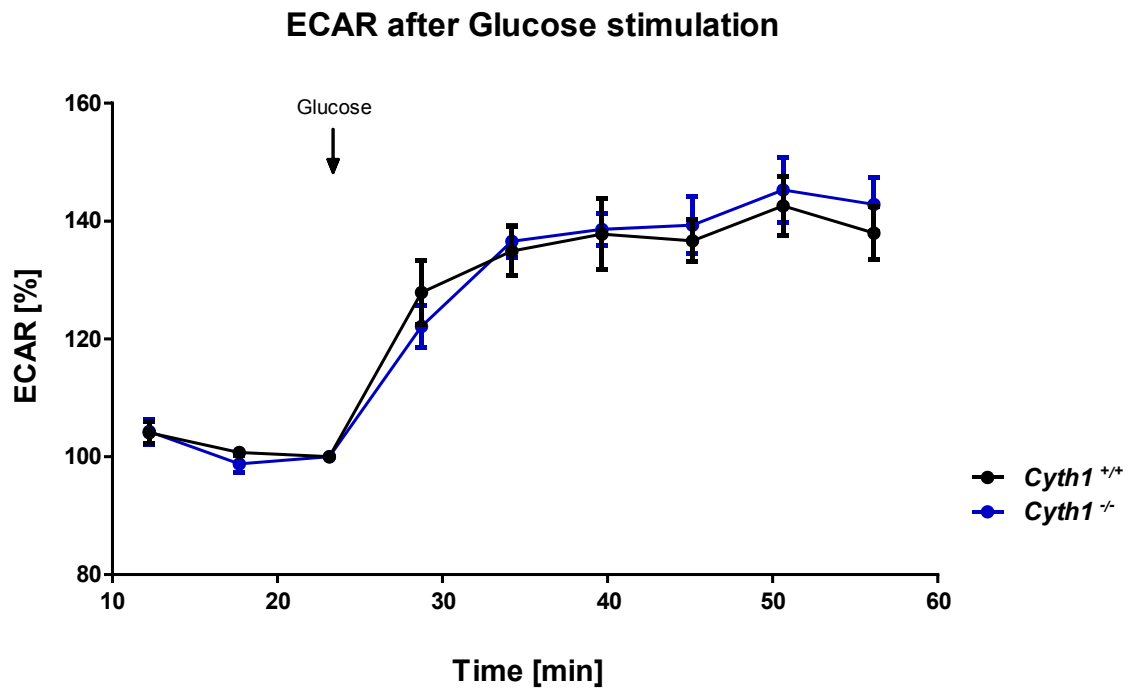
ECAR after Glucose stimulation
Glucose
ECAR [%]
160
140
120
100
80
10
20
30
40
50
60
Time [min]
Cyth1 +/+
Cyth1 -/-

B

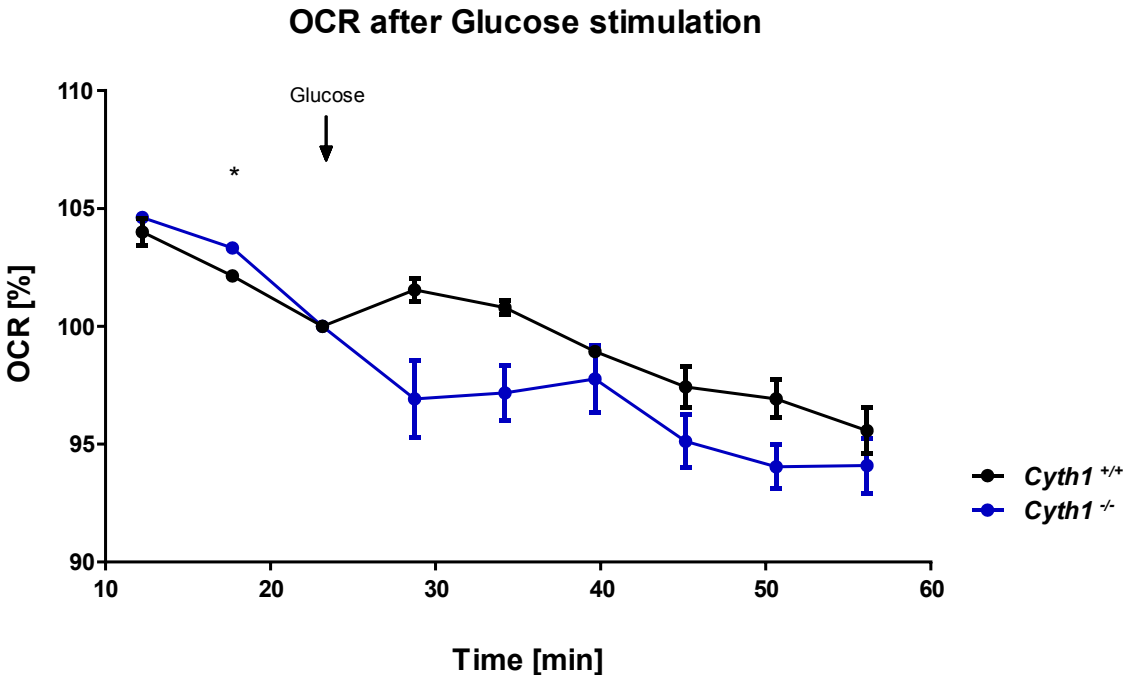
OCR after Glucose stimulation
Glucose
*
OCR [%]
110
105
100
95
90
10
20
30
40
50
60
Time [min]
Cyth1 +/+
Cyth1 -/-

C

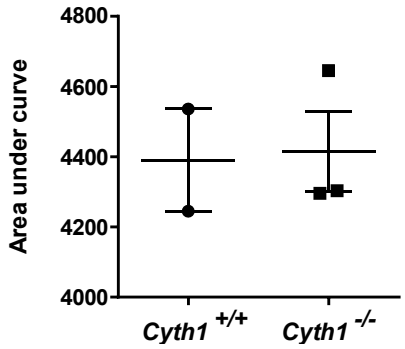

D

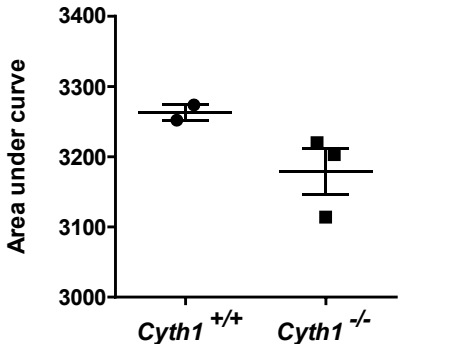

Figure 5.5: Glycolysis and mitochondrial respiration of cytohesin-1 deficient naïve CD4+ T cells following glucose stimulation. A. Extracellular acidification rate (ECAR) and **B**. Oxygen consumption rate (OCR) after injection (indicated by arrows) of glucose. Graphs present the mean (n=3) with SEM and is normalized to cell number with background correction. Baseline is set to the timepoint prior first injection. Calculated area under curve of **C**. ECAR and **D**. OCR for glucose stimulation after glucose Graphs present the mean (n=2-3) with SEM (*, $p<0.05$; unpaired student's t-test).

In conclusion lack of cytohesin-1 impaired metabolic capacity in naïve CD4+ T cells following stimulation of the TCR complex or its downstream effectors. No strong effect was given for sole glucose stimulation in cytohesin-1 deficient naïve CD4+ T cells.

5.2.2.4 Cytohesin-3 does not impact the metabolic switch of naïve T cells

Following α-CD3/CD28 stimulation *Cyth3*$^{-/-}$ naïve CD4+ T cells displayed a similar increase in ECAR (**Figure 5.6A** and **C** *left panel*) and OCR (**Figure 5.6B** and **D** *left panel*) as *Cyth3*$^{+/+}$ T cells. Although *Cyth3*$^{-/-}$ T cells appeared to have a relatively lower ECAR (**Figure 5.6A**) and OCR (**Figure 5.6B**) compared to *Cyth3*$^{+/+}$ T cells, no statistically significant difference was found in ECAR and OCR following oligomycin (**Figure 5.6C**,**D** *middle panels*) and 2-DG (**Figure 5.6C**,**D** *right panels*) injections.

A

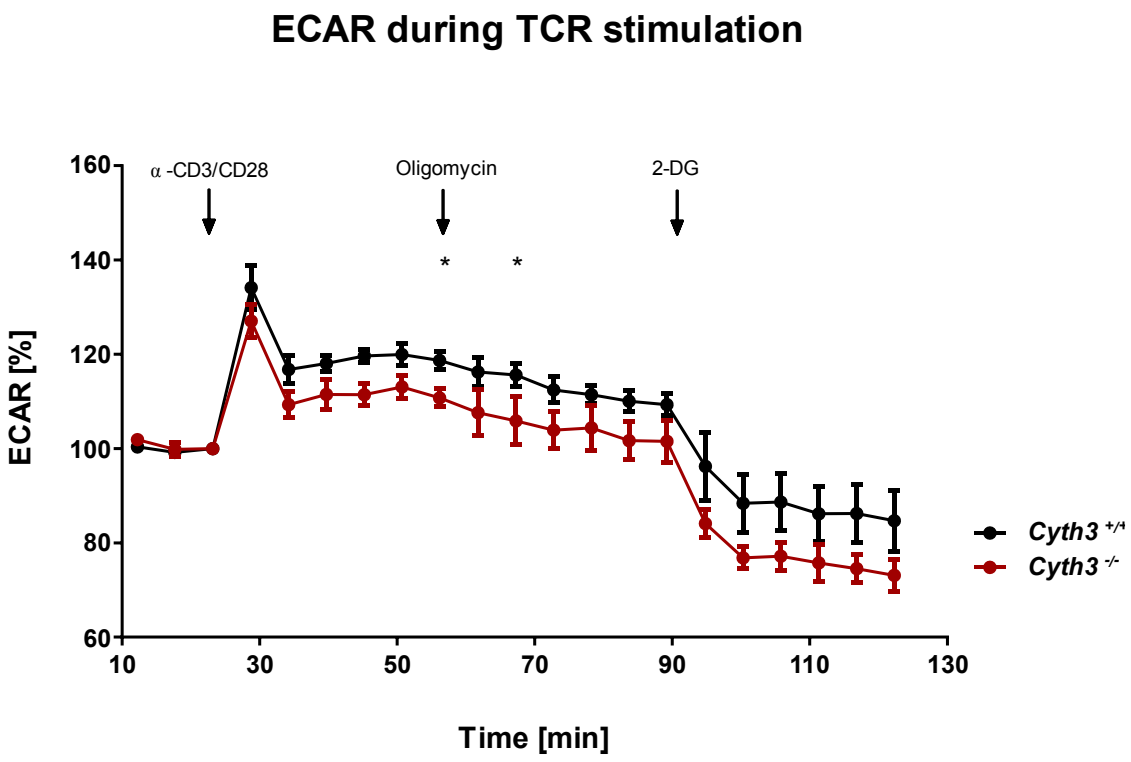
ECAR during TCR stimulation
α -CD3/CD28
Oligomycin
2-DG
*
*
ECAR [%]
160
140
120
100
80
60
10
30
50
70
90
110
130
Time [min]
Cyth3 +/+
Cyth3 -/-

B

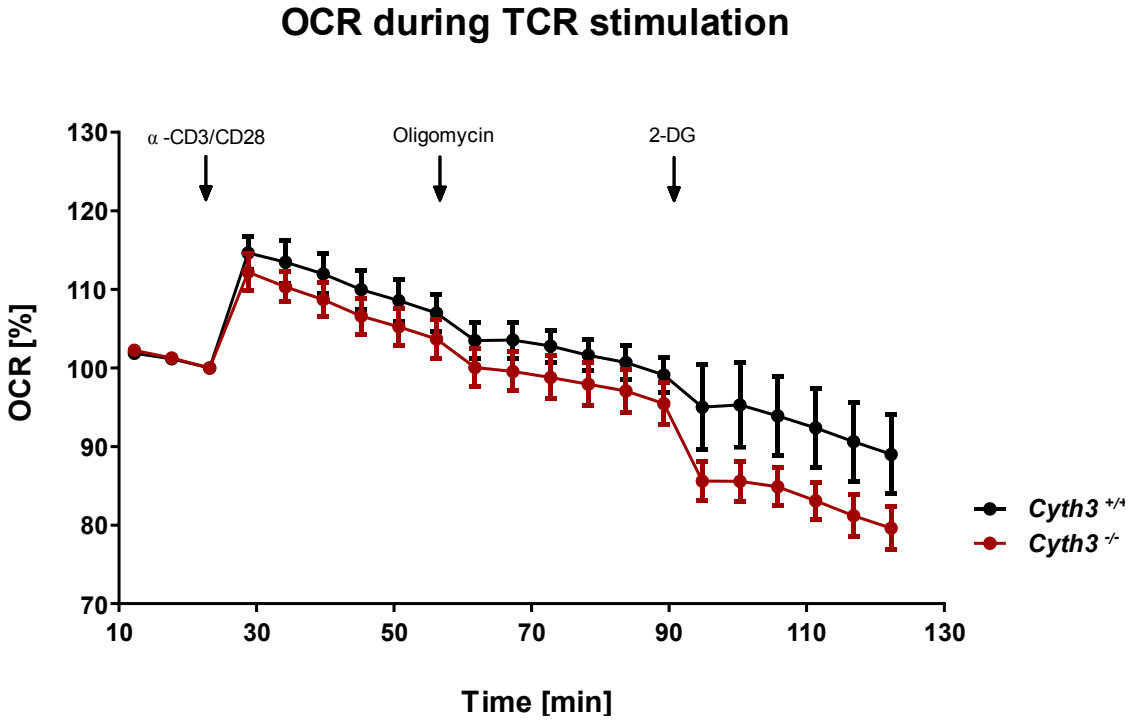
OCR during TCR stimulation
α -CD3/CD28
Oligomycin
2-DG
OCR [%]
130
120
110
100
90
80
70
10
30
50
70
90
110
130
Time [min]
Cyth3 +/+
Cyth3 -/-

C

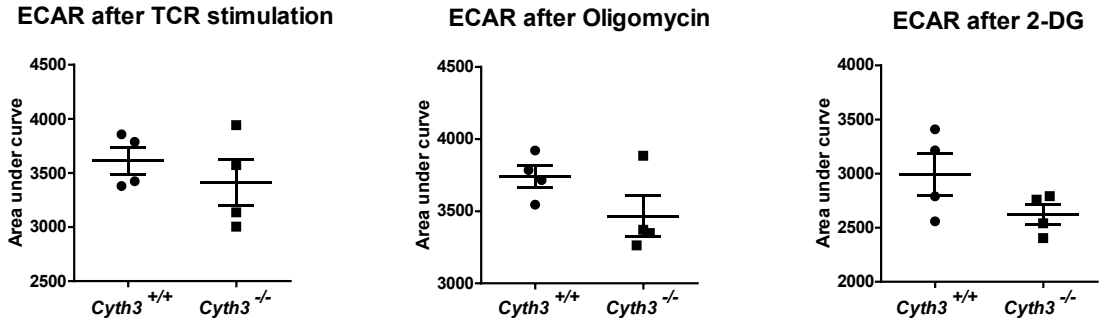

D

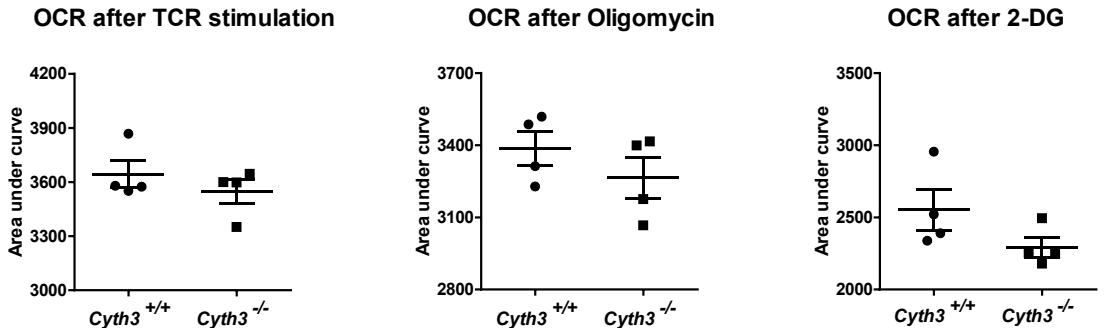

Figure 5.6: Glycolysis and mitochondrial respiration of cytohesin-3 deficient naïve CD4+ T cells following TCR stimulation. A. Extracellular acidification rate (ECAR) and **B**. Oxygen consumption rate (OCR) after injection (indicated by arrows) of α-CD3/CD28 antibodies, oligomycin and 2-deoxy-D-glucose (2-DG). Graphs present the mean (n=3) with SEM and is normalized to cell number with background correction. Baseline is set to the timepoint prior first injection. Calculated area under curve of **C***.* ECAR and **D**. OCR for α-CD3/CD28 antibodies stimulation after α-CD3/CD28 antibodies and prior oligomycin injection (*left panels*), for oligomycin after oligomycin and prior 2-DG injection (*middle panels*) and for 2-DG after 2-DG injection (*right panels*). Graphs present the mean (n=4) with SEM (threshold *, $p<0.05$ unpaired student's t-test).

Following PMA and ionomycin injection, lack of cytohesin-3 did not alter glycolysis or mitochondrial respiration compared to wildtype control, with equivalent ECAR (**Figure 5.7A**) and OCR (**Figure 5.7B**) observed. Similar observations were made following the addition of oligomycin and 2-DG.

A

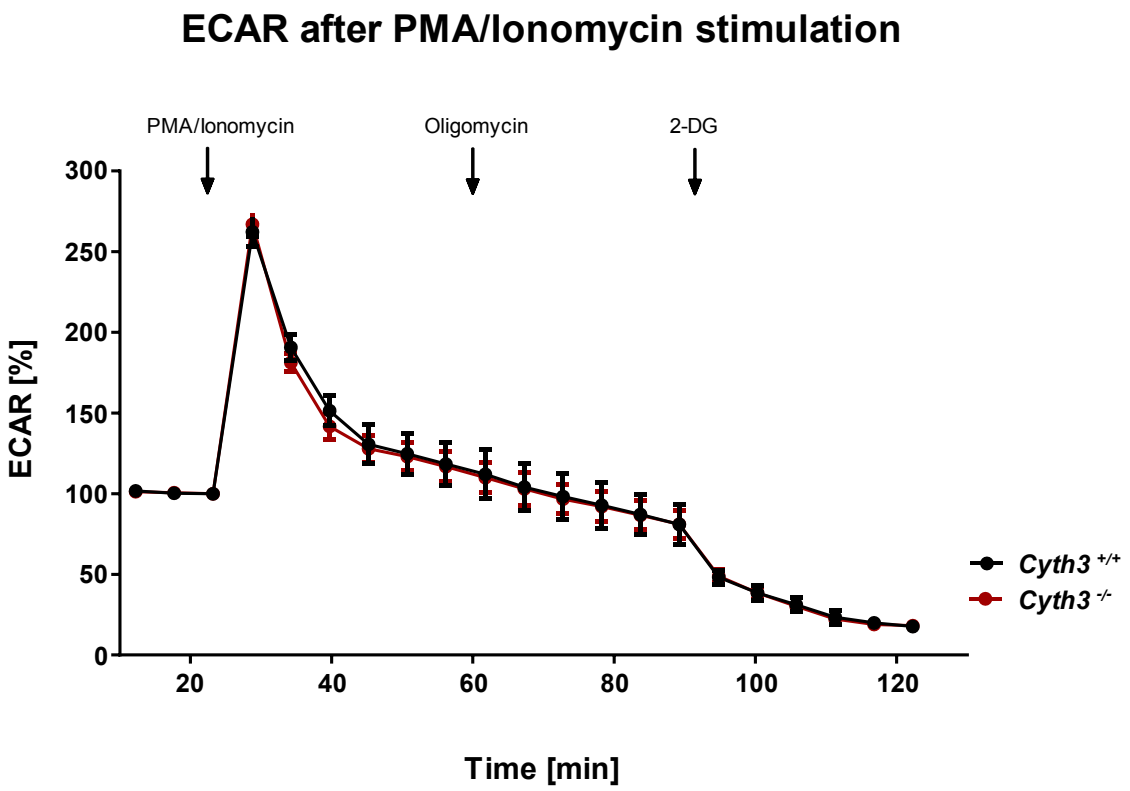
ECAR after PMA/Ionomycin stimulation
PMA/Ionomycin
Oligomycin
2-DG
ECAR [%]
300
250
200
150
100
50
0
20
40
60
80
100
120
Time [min]
Cyth3 +/+
Cyth3 -/-

B

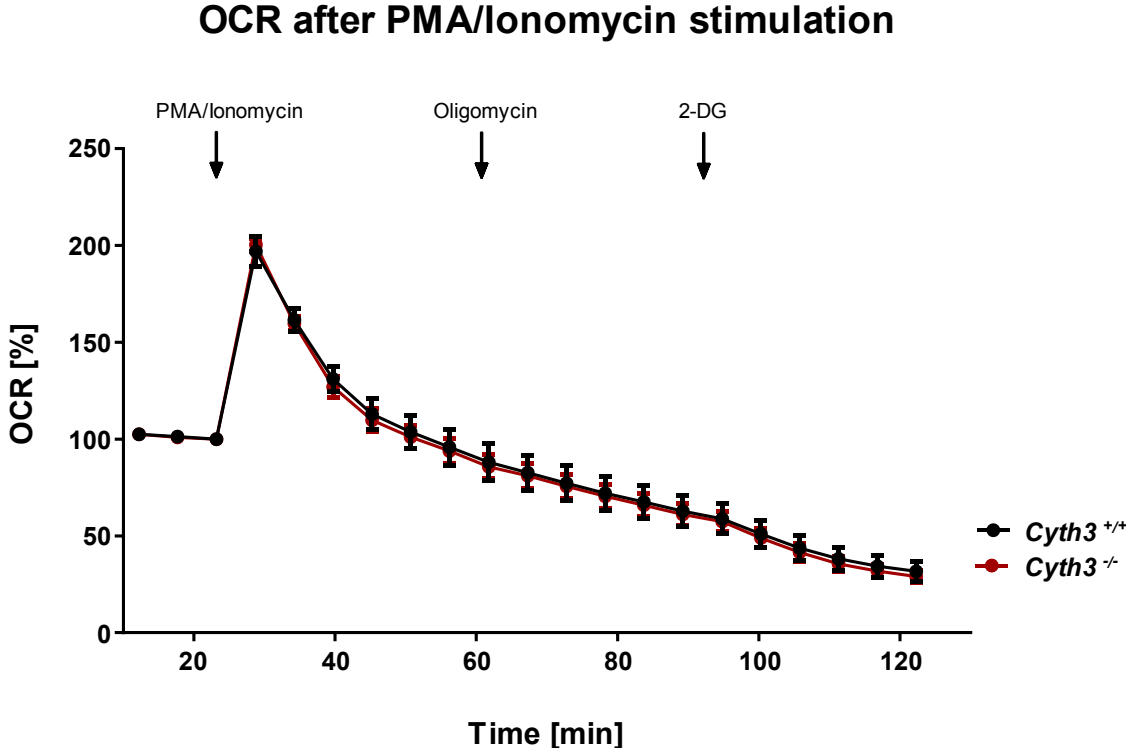
OCR after PMA/Ionomycin stimulation
PMA/Ionomycin
Oligomycin
2-DG
OCR [%]
250
200
150
100
50
0
20
40
60
80
100
120
Time [min]
Cyth3 +/+
Cyth3 -/-

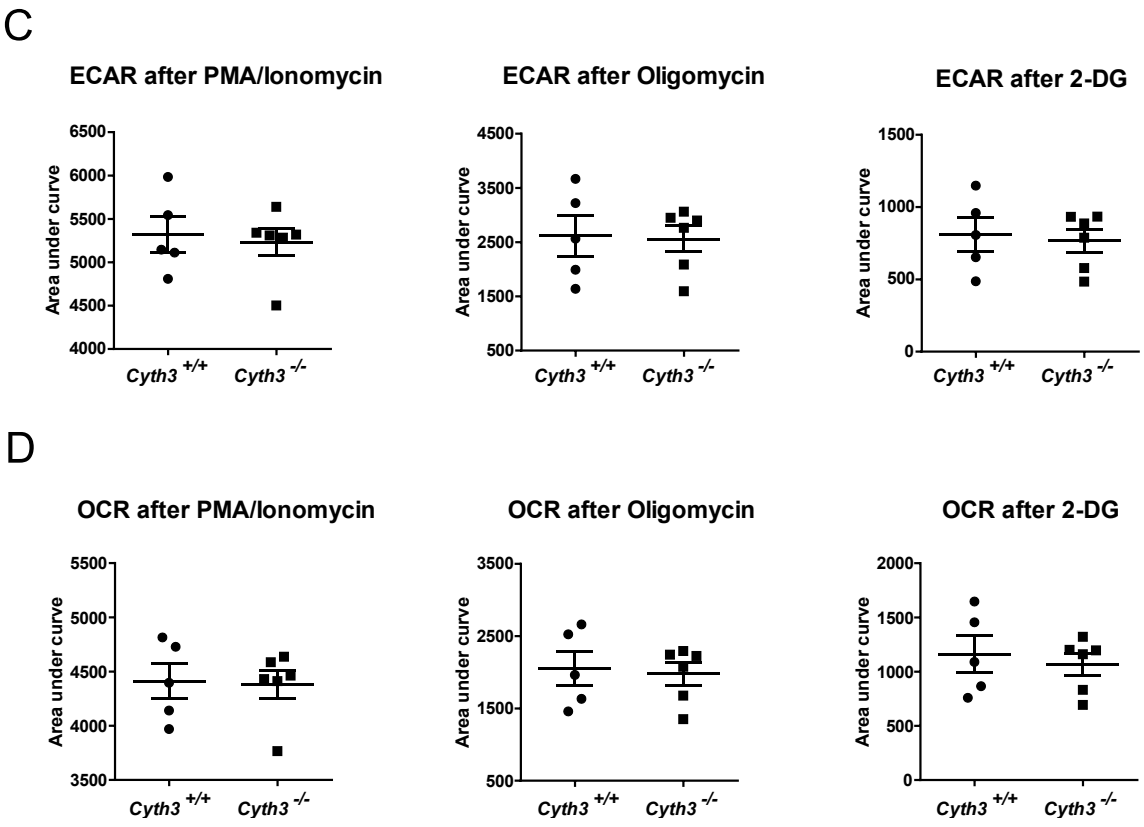

Figure 5.7: Glycolysis and mitochondrial respiration of cytohesin-3 deficient naïve CD4+ T cells following PMA/ionomycin stimulation. A. Extracellular acidification rate (ECAR) and **B**. Oxygen consumption rate (OCR) after injection (indicated by arrows) of PMA/ionomycin mix, oligomycin and 2-deoxy-D-glucose (2-DG). Graphs present the mean (n=3) with SEM and is normalized to cell number with background correction. Baseline is set to the timepoint prior first injection. Calculated area under curve of **C***.* ECAR and **D**. OCR for PMA/ionomycin stimulation after PMA/ionomycin and prior oligomycin injection (*left panels*), for oligomycin after oligomycin and prior 2-DG injection (*middle panels*) and for 2-DG after 2-DG injection (*right panels*). Graphs present the mean (n=5) with SEM (threshold *, $p<0.05$ unpaired student's t-test).

Cyth3$^{-/-}$ and *Cyth3*$^{+/+}$ T cells demonstrated comparable increases in ECAR following the addition of glucose (**Figure 5.8A**). The values for OCR were also unchanged in the absence of cytohesin-3 (**Figure 5.8B**). Similar to previous results, the injection of oligomycin (**Figure 5.8C**,**D** *middle panels*) and 2-DG (**Figure 5.8C**,**D** *right panels*) did not display any alteration in ECAR and OCR among *Cyth3*$^{-/-}$ and *Cyth3*$^{+/+}$ T cells.

A

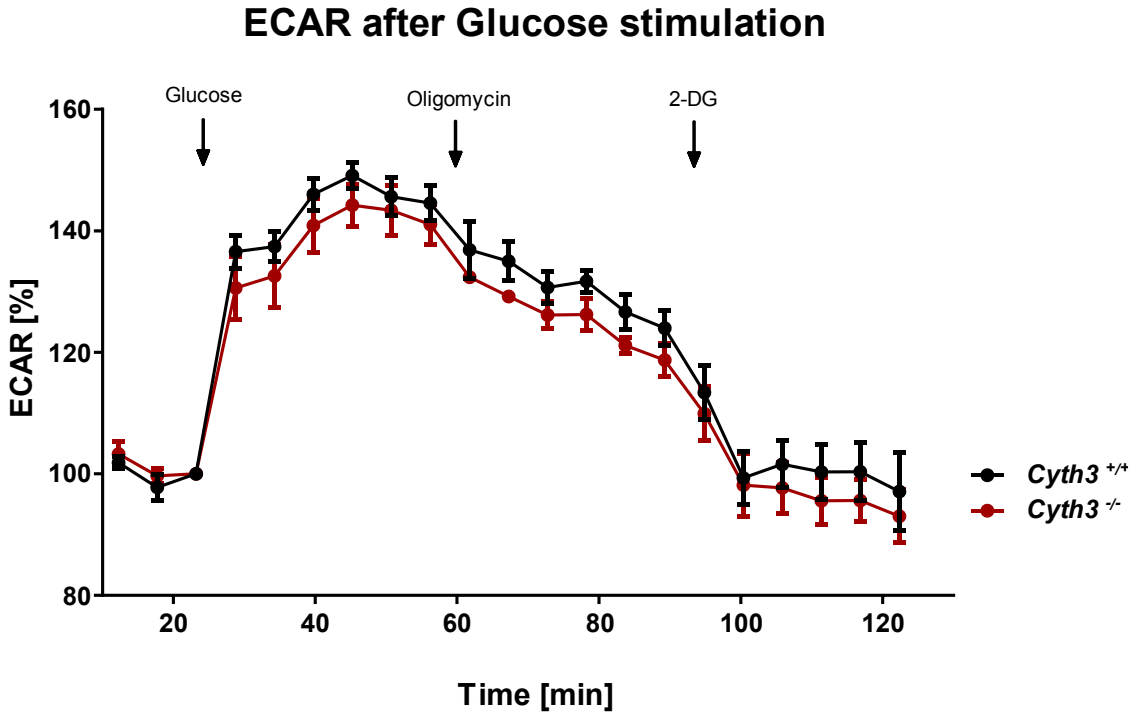
ECAR after Glucose stimulation
Glucose
Oligomycin
2-DG
ECAR [%]
160
140
120
100
80
20
40
60
80
100
120
Time [min]
Cyth3 +/+
Cyth3 -/-

B

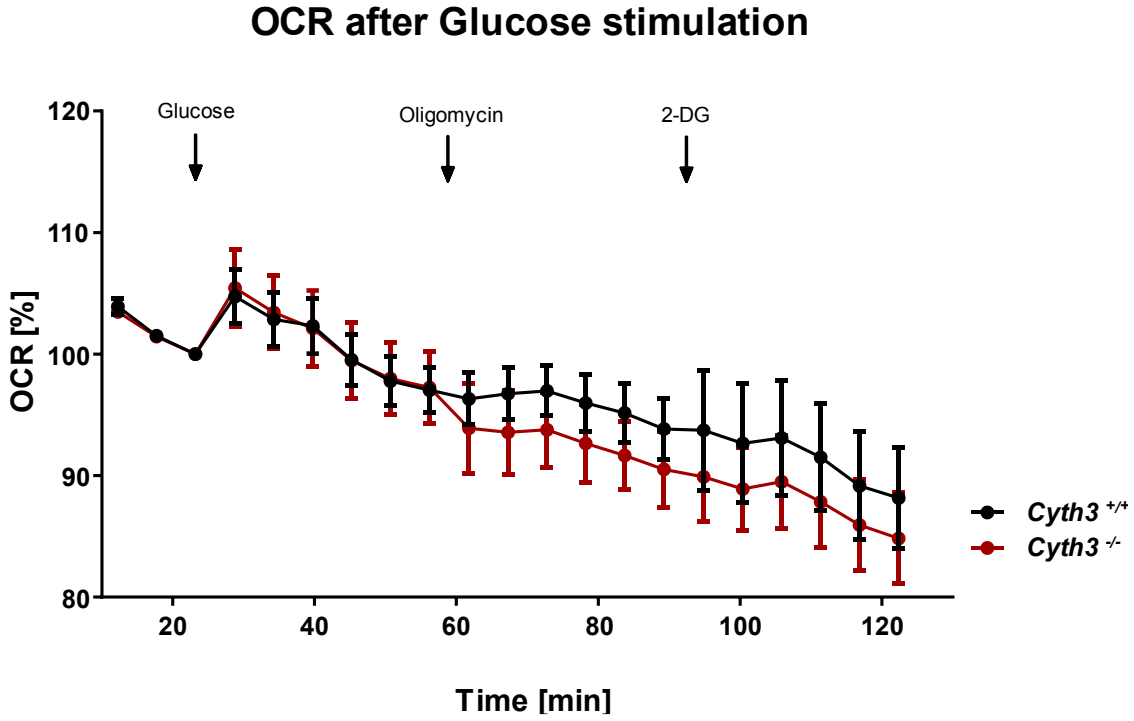
OCR after Glucose stimulation
Glucose
Oligomycin
2-DG
OCR [%]
120
110
100
90
80
20
40
60
80
100
120
Time [min]
Cyth3 +/+
Cyth3 -/-

C

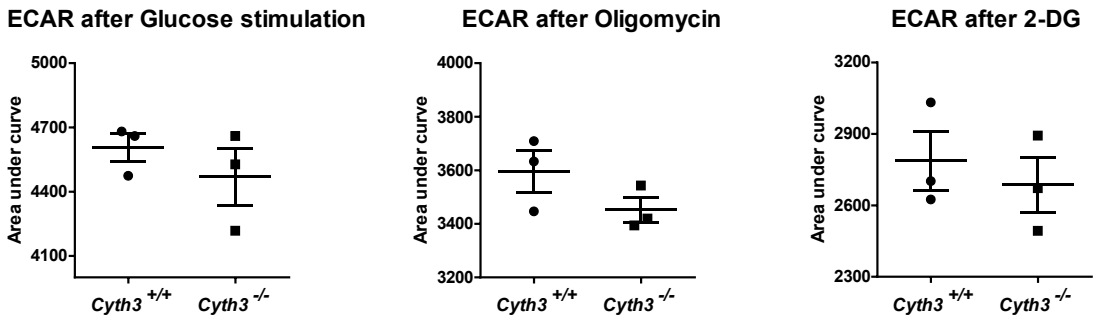

D

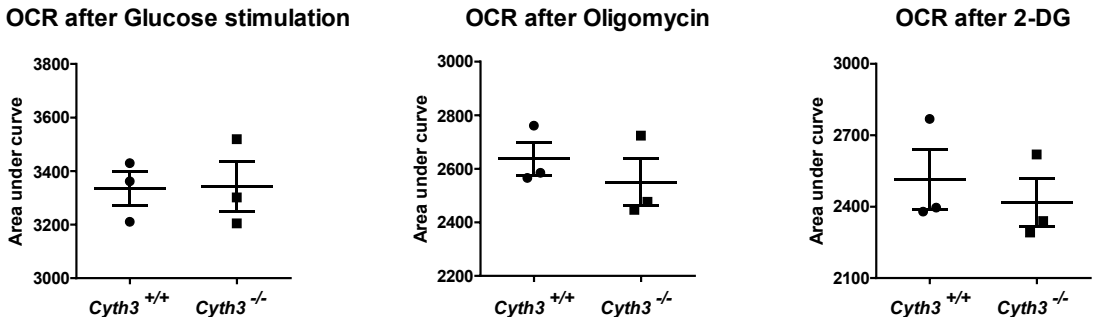

Figure 5.8: Glycolysis and mitochondrial respiration of cytohesin-3 deficient naïve CD4+ T cells following glucose stimulation. A. Extracellular acidification rate (ECAR) and **B**. Oxygen consumption rate (OCR) after injection (indicated by arrows) of glucose, oligomycin and 2-deoxy-D-glucose (2-DG). Graphs present the mean (n=3-4) with SEM and is normalized to cell number with background correction. Baseline is set to the timepoint prior first injection. Calculated area under curve of **C**. ECAR and **D**. OCR for glucose stimulation after glucose and prior oligomycin injection (*left panels*), for oligomycin after oligomycin and prior 2-DG injection (*middle panels*) and for 2-DG after 2-DG injection (*right panels*). Graphs present the mean (n=3-4) with SEM (threshold *, $p<0.05$ unpaired student's t-test).

5.3 Discussion

The analyses presented in this chapter examined the mechanistic involvement of cytohesins in T helper cell polarization and metabolic switching during T cell stimulation, demonstrated once again a dichotomy between cytohesin-1 and cytohesin-3. Interesting, the results presented here also provide the first evidence that cytohesin-1 contributes to immunometabolic processes of naïve CD4+ T cells.

5.3.1 Cytohesin-1 is required for efficient metabolic reprogramming in naïve CD4+ T cells and promotes the polarization to Th2 cell type

Cytohesin-1 deficient naïve T cells were characterized by a significant alteration of their metabolic signature following T cell activation, suggesting that cytohesin-1 is an important factor for metabolic switching in the initial stages of activation. Furthermore, *in vitro* differentiation of naïve CD4+ T cells towards effector helper T cells, especially towards Th2 cell subset, was impaired by the lack of the cytohesin-1 gene underlying its role in the efficient transition of naïve T cells to their effector cell subsets.

Generally, naïve T cells become highly proliferative following T cell activation, undergo differentiation and acquire effector functions (reviewed in section 1.2.6). This requires metabolic adaptations in order to meet the arising bioenergetic and biosynthetic demands. Therefore, cells become highly glycolytic and increase mitochondrial respiration, which can be measured by tracing cellular acidification and of the oxygen levels within the medium (346-349). Therefore, both processes are typically upregulated immediately after antigen encounter or T cell stimulation, as observed here (350). However, following TCR/CD28 ligation, cytohesin-1 deficient naïve CD4+ T cells retained a quiescent and more metabolically inactive state, suggesting that cytohesin-1 deficient T cells are less responsive to the given TCR stimulus. Consequently, these T cells might fall short of their bioenergetic needs to support efficient proliferation and subsequent differentiation. This is in line with the overall cytohesin-1 T cell phenotypes observed across all chap-

ters. Moreover, this result also suggests that function of cytohesin-1 is required in the initial phase of T cell activation.

Interestingly, cytohesin-1 deficient T cells still presented the same maximum glycolytic capacity as wildtype T cells, which was measured by the injection of oligomycin that blocks mitochondrial respiration and shifts glycolysis to its maximum capacity (**Figure 5.3**). The inhibition of glycolytic processes by introducing 2-DG, which inhibits one enzyme in the glucose breakdown process, leads to a drop in the ECAR in KO and WT cells. However, after the 2-DG-mediated drop in the ECAR cytohesin-1 deficient cells displayed a continuous decrease in the ECAR, which suggests that these cells continue to shutdown processes that are leading to proton efflux. Apart from the classical glycolysis, tetracarboxylic acid cycle (TCA)-derived CO_2 has been described to contribute to non-glycolytic acidification through the formation of carbonic acid (351). In this way, CO_2 is generated in the biosynthesis of intermediates within TCA (352). Consequently, these observations suggest that the TCA might be limited in the absence of cytohesin-1, which may mean that cytohesin-1 deficient T cells lack biosynthetic precursors for optimal effector functions.

An even stronger suppression effect of metabolic activities was observed following PMA and ionomycin stimulation in the absence of cytohesin-1 (**Figure 5.4**). Normally, the addition of PMA and ionomycin results in a strong increase in ECAR and OCR as it bypasses TCR stimulation and acts directly on the downstream intracellular signalling pathways. Here, PMA/ionomycin stimulation resulted in the same immediate metabolic response in KO and WT suggesting either that cytohesin-1 interferes with the immediate events downstream of TCR/CD28 complex and upstream of PMA/ionomycin pathways, or that cytohesin-1 deficient CD4+ T cells are capable of upregulating glycolysis and mitochondrial respiration similar to wildtype CD4+ T cells if exposed to a sufficiently strong stimulus.

Nevertheless, the dramatic shutdown of glycolysis and mitochondrial respiration in *Cyth1*$^{-/-}$ cells following the increase of ECAR and OCR in response to PMA/ionomycin stimulation indicates that regulatory feedback mechanisms might

be imbalanced in the absence of cytohesin-1. Important signalling pathways in metabolic activation include the mammalian target of rapamycin (mTOR) and Akt proteins, which are both activated by PMA and through CD3/CD28 ligation (349, 353-358). mTOR can be further subdivided into mTOR complex 1 (mTORC1) and complex 2 (mTORC2) (359). The function of mTORC1 as effector protein in biosynthesis, metabolism, cell proliferation and survival is well established, in contrast the mechanism of mTORC2 is not well understood (359). However, mTORC2 has been shown to exert differential effects on the differentiation of Th1 and Th2 cell types by different mechanisms (360). On the one hand, mTORC2-regulated PKC mediates the transcription of GATA3 and the development of Th2 cell type, on the other hand mTORC2 enhances Akt activity following TCR/CD28 stimulation leading to expansion of Th1 cells (360). As the differentiation of Th2 lineage was more affected by cytohesin-1, it might be speculated that cytohesin-1 is implicated in the mTORC2-PKC signalling axis.

In conclusion, cytohesin-1 is important for the metabolic fitness of naïve T cells and required for efficient T cell activation providing the metabolic adaptation following TCR and CD28 stimulation. Further, these data suggest that cytohesin-1 enables CD4+ T cells to sustain metabolic demands for efficient and successful proliferation and acquisition of effector functions.

5.3.2 Cytohesin-3 suppresses Th1 differentiation

In contrast to cytohesin-1, ablation of cytohesin-3 led to a stronger differentiation of Th1 cells, suggesting that cytohesin-3 negatively regulates an aspect of the differentiation process in naïve CD4+ T cells. Interestingly, this was not accompanied by a different metabolic fitness of naïve CD4+ T cells, since stimulation of cytohesin-3 deficient naïve CD4+ T cells with different mitogens did not show alterations in glycolysis and mitochondrial respiration compared to wildtype cells. This suggests that cytohesin-3 is not essential for the initial metabolic reprogramming of naïve CD4+ T cells following stimulation. However, cytohesin-3 might

mediate metabolic functions at latter time points of T cell activation than measured here.

The exact mechanism of how cytohesin-3 regulates the transition of distinct helper T cell is elusive. IFNγ and IL-12 are crucial cytokines for proper Th1 polarization (361, 362). In the previous chapter cytohesin-3 deficient antigen-specific CD8+ T cells were more reactive to stimulation and expressed higher levels of IFNγ (see results 4.2.5). Therefore, a possible explanation may involve increased autocrine IFNγ or IL-12 stimulation leading to enhanced Th1 polarization. Furthermore, cytohesin-3 may interfere with Th1 differentiation, e.g. by suppressing transcription factors such as STAT1 and STAT4 (51, 363). Therefore, the assessment of different STAT protein levels in cytohesin-3 deficient T cells might be the subject of future work.

Another important aspect to mention is the potential involvement of cytohesin-3 in the PD-1 inhibitory signalling pathway (discussed in section 4.3.3). The effects of cytohesin-3 ablation are comparable to that of SHP-2 deletion, which has a similar impact on the Th1 differentiation in a tumour microenvironment, supporting a role for cytohesin-3 in this signalling pathways (364). Notably, due to its immunoregulatory function, PD-1 is associated with the promotion and expansion of Tregs (365, 366). Blockage of PD-1 leads to increased IL-6 levels and has been shown to favour the differentiation of Th1 and Th17 lineages (367, 368). In this way, IL-6 is an important cytokine inducing Th17 differentiation and suppressing Treg polarization (369). Therefore, future studies might elucidate if cytohesin-3 mediates Treg differentiation in different *in vitro* and *in vivo* scenarios. Some evidence already points towards a possible dysregulation of Tregs as pulmonary IL-6 levels were found elevated in cytohesin-3 deficient mice in the course of *L. pneumophila* infection (**Figure 3.8**).

Taken together, these observations suggest that the development of different T helper lineages in the course of infection are imbalanced in the absence of cytohesin-3.

In conclusion, the *in vitro* data presented in this chapter are consistent with the T cell phenotypes observed with the *in vivo* infection experiments, which further underscores that cytohesin-1 supports efficient development of distinct helper T cells, while cytohesin-3 negatively regulates the differentiation of helper T cell functions. Furthermore, these results suggest that, cytohesin-3 does not participate in the initial metabolic responses in naïve CD4+ T cells following stimulation, in contrast to cytohesin-1.

6. Conclusion and perspectives

Cytohesins are GEFs for Arf proteins providing the switch to GTP-bound active Arf form. Over the past decades, more evidence has accumulated that cytohesins fulfil a prominent role in the immune system and its responses. In particular, through their association with integral membrane proteins, such as integrins, cytohesins have been suggested to affect the adhesive and migratory properties of leukocytes, which are essential processes for the establishment of efficient innate and adaptive immune responses *in vivo*. This PhD study aimed at providing a better understanding of how the cytohesins impact on the regulation and coordination of the immune responses upon respiratory infections in mice.

6.1 Cytohesins are not required for effective innate immune responses to *L. pneumophila* infection

The initial experiments in this study analysed the role of cytohesins in the migration of different myeloid populations to the site of inflammation in response to *L. pneumophila* infection. Cytohesin-2 has been previously identified as an important factor for Salmonella, Shigella and EPEC/EHEC pathogenesis, being either involved in the process of establishing an intracellular niche for replication, or in modulating innate immune responses (169, 171, 172). Furthermore, cytohesin-1 has been shown to affect migrating properties of different myeloid cells as well as their phagocytic capacity (159, 370-372). However, in this study deletion of different cytohesins did not significantly affect cell recruitment and transmigration of phagocytes during *L. pneumophila* infection. This study also showed that *L. pneumophila* does not rely on GEF function of cytohesins or the presence of cytohesin-1 or -3 to establish a replication niche within cells.

However, it is possible that cytohesins play a stronger role in the gastrointestinal tract, as *Salmonella, Shigella* and EPEC/EHEC are all intestinal pathogens. Alternatively, these pathogens may trigger a particular innate immune circuit that is more quiescent during *L. pneumophila* infection. Even though the findings of

these studies provide no evidence for a significant role of the cytohesins in innate immune response against respiratory bacterial infection, they contribute to a greater understanding of how they function during infections.

6.2 Cytohesin-1 promotes T cell responses by setting an efficient threshold for T cell activation

The results of this study demonstrated that cytohesin-1 is required for optimal responses of CD4+ and CD8+ T cells. The implications by the deletion of cytohesin-1 were prominent in the later phases of *L. pneumophila* infection indicating that cytohesin-1 is important for the establishment of cognate T cell responses. This was verified by making use of the influenza infection model, in which a decrease of antigen-specific CD8+ T cell populations in the absence of cytohesin-1 was observed.

The observations of this study suggest that cytohesin-1 provides the right threshold for an efficient signal input in T cell signalling which was also described in an *in vitro* setting (167). Consistently, cytohesin-1 deficient naïve CD4+ T cells were impaired in shifting their metabolism following CD3/CD28 stimulation, which suggests that cytohesin-1 is important for the induction of early signalling pathways (**Figure 5.3**). However, a strong stimulation by PMA and ionomycin led to similar metabolic responses among analysed groups, indicating that cytohesin-1 deficient T cells are able to react sufficiently at saturating levels of stimulation. Consequently, cytohesin-1 appears to amplify the T cell signalling events in various types of T cells, but the absence of cytohesin-1 has stronger consequences in situations of suboptimal antigenic stimulation (see discussion 4.3.1). Modulation of T cell responses by cytohesin-1 may thus be more important for specific subsets, such as short-lived effector cells and Th2 cells (see 4.2.4 and 5.3.1).

Furthermore, cytohesin-1 appears not only to be important in the initial T cell activation but is also essential for intact T cell effector functions. In this way, cytohesin-1 was required to sustain the metabolic activity and to fulfil the bioenergetic demands of T cells (see discussion 5.3.1). As cytohesin-1 deficient T cells

showed impaired metabolic response following activation, it is likely that they were not able to produce enough energy and metabolic intermediates to properly respond to infections. This hypothesis is consistent with the observation of lower cellular responses of influenza-specific *Cyth1*$^{-/-}$ CD8+ T cells following antigen restimulation (**Figure 4.6**).

Cytohesin-1 might furthermore play a role in the longevity of memory T cell populations. Cytohesin-1 deficient mice were characterized by a decrease in memory T cell populations during *L. pneumophila* infection (section 4.2.1). The establishment of T cell memory also require distinct metabolic adaptations (373, 374). In reference to the function of cytohesin-1 in metabolic regulation of T cell immune responses, one may speculate, that altered memory T cell populations in cytohesin-1 deficient mice can lead to impaired adaptive immunity upon secondary infection. Therefore, future work might involve the analysis of cytohesin-1 in immunization studies.

In conclusion, cytohesin-1 is an important element in the activation of T cells and in the promotion of T cell effector functions by potentially enhancing T cell signalling and providing the bioenergetic demands following activation. In this regard, a functional cytohesin-1 might be a crucial factor in the combat of more severe infections that rely on rapid and robust T cell responses.

6.3 Cytohesin-2 transiently regulates cDC and cytokine responses

In previous studies, cytohesin-2 has been shown to regulate the motility of non-immune cells (158, 375). The essential, but poorly understood function of cytohesin-2 during embryonic development makes it impossible to work with full knockout mice because they die within the first hours after birth. In this study, myeloid-specific cytohesin-2 deficient mice were used, because *L. pneumophila* infection is primarily controlled by the innate immune system. However, myeloid-

specific function of cytohesin-2 was not required for the efficient control of *L. pneumophila*.

In the early *L. pneumophila* infection cytohesin-2 was found to positively regulate pulmonary cytokine response. A possible explanation for this is that cytohesin-2 might function as a mediator in the MyD88 signalling cascade as it has been found to engage to the adapter protein MyD88 in endothelial cells (376). Activation of TLR4 initiates MyD88 signalling which results in IL-12 expression in cDCs (377). Consequently, ablation of *Cyth2* might impair MyD88 signalling upon TLR activation and subsequently, decrease IL-12 production in cDCs. In addition, cDC numbers in myeloid-specific cytohesin-2 KO mice were decreased in the initial stages following infection which might also account for the overall decreased cytokine production. The role of cytohesin-2 in cDCs has not been deeply investigated. However, novel findings by Rafiq *et al.* and our group identified cytohesin-2 to control podosome formation (Namislo, A., PhD thesis)(163). Podosomes are found in diverse leukocytes including immature DCs where they participate in diapedesis (164-166). Work by Namislo showed a selective regulation of podosome formation by cytohesin-2 (Namislo, unpublished). Therefore, a possible regulation of cytohesin-2 on cDC trafficking might be attributed to its role in actin organization and remodelling.

These results demonstrate that cytohesin-2 likely plays a role in regulating pulmonary cytokine and cDC responses. Because the results of this study show that cytohesin-1 and -3 have major roles in T cell responses, it is possible that cytohesin-2 might play a more dramatic role in T cells than what was identified here. Future prospective studies might employ T cell-specific cytohesin-2 KO mice to this end.

6.4 Inhibitory functions of cytohesin-3 are comparable to an immune checkpoint

Cytohesin-3 deficiency resulted in an overall stronger T cell response in all subtypes, implying that absence of cytohesin-3 leads to a general hyperactivation of T cells. The data demonstrate that cytohesin-3 suppresses CD4+ and CD8+ T cell responses following bacterial infection as well as influenza-specific T cell responses. Furthermore, cytohesin-3 selectively affected *in vitro* differentiation of Th1 cells, which would explain why a prominent phenotype was observed with both *L. pneumophila* and Influenza A virus, as these are both Th1-inducing infections (**Figure 6.1**).

Due to the association of cytohesin-3 with PD-1 signalling, a proposed model is that cytohesin-3 might act as an inhibitory immune checkpoint (see discussion 4.3.3). T cell-specific deletion of SHP-2, an intermediate in the PD-1 signalling pathway, elicits a similar phenotype as cytohesin-3 deficiency (329), suggesting that cytohesin-3 has a comparable position in this signalling chain. Possible suppressive mechanisms may be mediated by the regulation of Akt. In this regard, cytohesin-3 overexpression was shown to suppress phosphorylation of downstream Akt in the T cell signalling cascade (Tolksdorf, F., PhD Thesis). Interestingly, CD28 ligation counteracts cytohesin-3 expression indicating that function of cytohesin-3 needs to be silenced for proper T cell activation (Tolksdorf, F., PhD thesis). Both observations strengthen the notion of a suppressive function of cytohesin-3 in T cell activation. Consequently, deletion of cytohesin-3 leads to amplified TCR signalling making T cells more reactive to stimuli as was observed in the cellular T cell response against influenza antigens (**Figure 4.6**) (see discussion 4.3.3).

Although not investigated here, cytohesin-3 expression also correlates with T cell anergy, suggesting that cytohesin-3 might promote peripheral tolerance, which is also maintained by immune checkpoints such as PD-1 (153, 378). In this way, PD-1 signalling promotes Treg homeostasis (378). Prospective studies might therefore focus on the role of cytohesin-3 role in regulatory mechanisms, e.g. by investigating whether Treg development and their responses are altered in cyto-

hesin-3 deficient mice. This may produce interesting phenotypes of cytohesin-3 deficient mice in chronic viral infection or tumour models. If cytohesin-3 strongly modulates T cell regulation, it may eventually emerge as a viable therapeutic target for the treatment of chronic viral infection and cancer.

In summary, these results highlight that cytohesin-3 is essential in preventing hyperactivation of T cells to produce optimal immune responses by potentially acting as an immune checkpoint.

6.5 Reciprocal regulation of immune responses by cytohesins

Fascinatingly, cytohesin-1 and cytohesin-3 appear to orchestrate T cell responses in an opposing fashion. This was consistently observed throughout this study, in both bacterial and viral infection models, as well as in *in vitro* assays (**Figure 6.1**). It seems likely that these two proteins have evolved to act as an antagonistic pair of regulatory factors in T cell activation.

How these highly homologous proteins (88% sequence similarity) interact in such different ways is not understood. Differences in the cytohesin biology are found in their regulation and isoforms. Cytohesin-1 is mostly expressed in the so-called triglycine form, while cytohesin-3 is mostly expressed as a diglycine variant (132, 139). These are splice variants of the coding sequences of the respective PH domains which have differential affinity and specificity for phosphoinositides. The diglycine isoform has high affinity to PIP_3, whereas triglycine isoform has lower affinity to PIP_3 and may require the polybasic region or adapter protein for its plasma membrane association (131, 138, 139). Consequently, PI3K regulates the translocation of cytohesins to the plasma membrane (136, 147, 379, 380). Furthermore, cytohesin-1 harbors phosphorylation sites within the polybasic region (138). Phosphorylation of these sites have been shown to promote the attachment to the plasma membrane (138, 381). In this way, phosphorylation of cytohesin-1 by PKC has been demonstrated to be important for its function in

LFA-1 and T cell activation (382) (Paul, B., PhD thesis). In contrast, cytohesin-3 was not found to be phosphorylated following PMA-initiated T cell activation (382). The results suggest that cytohesins' cellular distribution and activity might be regulated differently by signalling molecules such as PKC and PI3K which both are important components of the T cell signalling cascade.

Interestingly, previous results of our laboratory demonstrated that overexpression of cytohesin-3 reduces PMA-initiated phosphorylation of cytohesin-1 (Paul, B., PhD thesis), supporting the idea that cytohesins suppress each other's function and act in an antagonistic fashion. The concept of antagonistic roles by highly homologous proteins is a common theme for several different protein families including STATs (383). Possible antagonistic mechanisms might be investigated for cytohesins by using cytohesin-1 and cytohesin-3 double knockout mice. Logically, the double knockout would result in the neutralization of these antagonistic effects in common signalling pathways of the T cell response.

Differential regulation by cytohesins may also involve common downstream effectors such as Arf proteins. Arf6 is an important player in diverse cellular processes including endocytosis, phagocytosis and actin reorganization (384-386). Furthermore, Arf6 activates the lipid modifying enzymes like PIP_5 kinase and PLD, which are important effectors following extracellular stimuli, and is also involved in TLR-signalling pathways (385, 387). Therefore, differential regulation of Arf6 by individual cytohesins might lead to altered signal transduction and divergent cytokine responses via altered TLR-signalling, or migratory properties via reciprocal actin reorganization. However, a more comprehensive understanding of these processes and cross regulations by cytohesins will require further mechanistic studies of the involved signalling events. Apart from using multiple KO of cytohesins to study antagonistic regulations, another approach to identify the different roles of cytohesins might involve phosphoproteomics which would give a more detailed picture of cytohesins' signalling pathways (388).

6.6 Concluding remarks

This study analysed the role of individual cytohesins in the innate and adaptive immune responses following respiratory infections, and identified cytohesin-1 and cytohesin-3 to be particularly important regulators in T cell responses with both acting in an opposite manner. Deletion of cytohesin-1 inhibited T cell responses to bacterial and viral infections. T cells deficient in cytohesin-1 were impaired to mediate metabolic switch following T cell activation and were not able to fully exert their effector functions. In contrast, ablation of cytohesin-3 led to hyperactivated T cells and amplified T cell responses to bacterial and viral infections. The results of this PhD study substantially enhance the knowledge on how individual cytohesins modulate immune responses following infection.

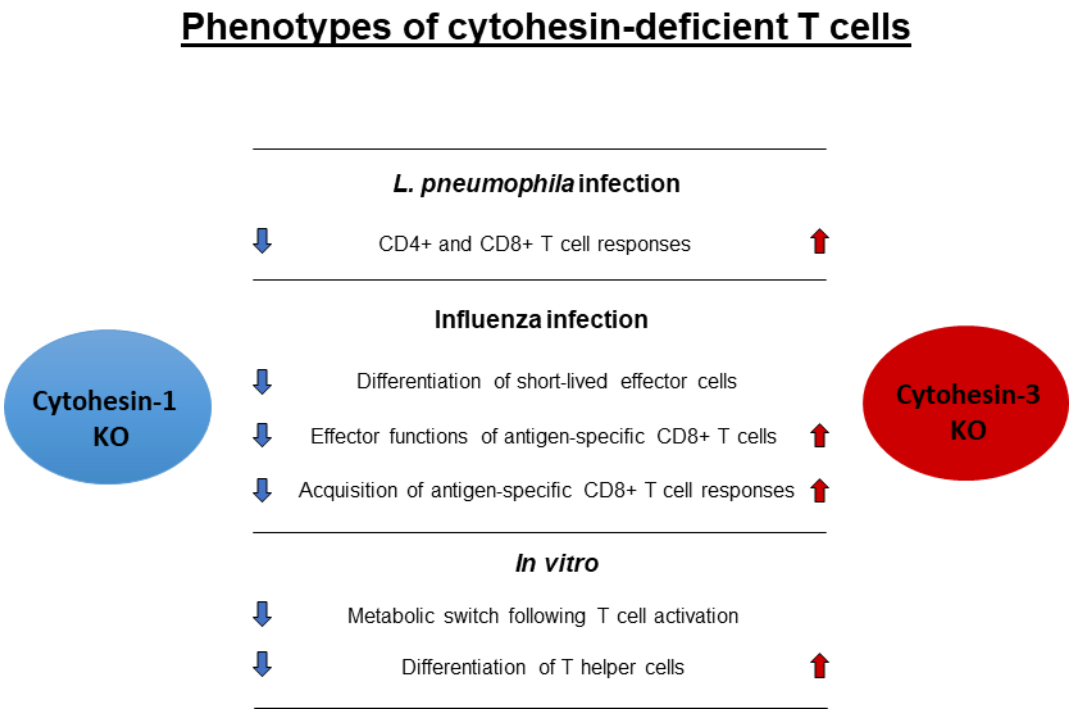

Figure 6.1: Overview of T cell phenotypes observed in cytohesin-1 and cytohesin-3 deficiency in *in vivo* and *in vitro* settings. Arrow up illustrates increased activity, arrow down illustrates decreased activity. Blue colour indicates effects caused by the deletion of cytohesin-1, red colour indicates effects caused by the deletion of cytohesin-3.

7. References

1. Sun J-J, Lan J-F, Zhao X-F, Vasta GR, Wang J-X. Binding of a C-type lectin's coiled-coil domain to the Domeless receptor directly activates the JAK/STAT pathway in the shrimp immune response to bacterial infection. PLOS Pathogens. 2017;13(9):e1006626.

2. Loo Y-M, Gale M, Jr. Immune signaling by RIG-I-like receptors. Immunity. 2011;34(5):680-92.

3. Nakaya Y, Lilue J, Stavrou S, Moran EA, Ross SR. AIM2-Like Receptors Positively and Negatively Regulate the Interferon Response Induced by Cytosolic DNA. mBio. 2017;8(4):e00944-17.

4. Barton GM, Medzhitov RJS. Toll-like receptor signaling pathways. 2003;300(5625):1524-5.

5. Akira S, Hemmi H. Recognition of pathogen-associated molecular patterns by TLR family. Immunology Letters. 2003;85(2):85-95.

6. Deguine J, Barton GMJFr. MyD88: a central player in innate immune signaling. 2014;6.

7. Moynagh PN. TLR signalling and activation of IRFs: revisiting old friends from the NF-κB pathway. Trends in Immunology. 2005;26(9):469-76.

8. Ting JP-Y, Lovering RC, Alnemri ES, Bertin J, Boss JM, Davis BK, et al. The NLR gene family: a standard nomenclature. 2008;28(3):285-7.

9. Girardin SE, Boneca IG, Carneiro LA, Antignac A, Jehanno M, Viala J, et al. Nod1 detects a unique muropeptide from gram-negative bacterial peptidoglycan. Science. 2003;300(5625):1584-7.

10. Girardin SE, Boneca IG, Viala J, Chamaillard M, Labigne A, Thomas G, et al. Nod2 is a general sensor of peptidoglycan through muramyl dipeptide (MDP) detection. 2003;278(11):8869-72.

11. Davis BK, Wen H, Ting JP. The inflammasome NLRs in immunity, inflammation, and associated diseases. Annu Rev Immunol. 2011;29:707-35.

12. Amer A, Franchi L, Kanneganti TD, Body-Malapel M, Ozoren N, Brady G, et al. Regulation of Legionella phagosome maturation and infection through flagellin and host Ipaf. J Biol Chem. 2006;281(46):35217-23.

13. Kofoed EM, Vance RE. Innate immune recognition of bacterial ligands by NAIPs determines inflammasome specificity. Nature. 2011;477(7366):592-5.

14. Zhong Y, Kinio A, Saleh M. Functions of NOD-Like Receptors in Human Diseases. Frontiers in immunology. 2013;4:333.

15. Zamboni DS, Kobayashi KS, Kohlsdorf T, Ogura Y, Long EM, Vance RE, et al. The Birc1e cytosolic pattern-recognition receptor contributes to the detection and control of Legionella pneumophila infection. 2006;7(3):318.

16. Furze RC, Rankin SM. Neutrophil mobilization and clearance in the bone marrow. Immunology. 2008;125(3):281-8.

17. Futosi K, Fodor S, Mócsai A. Neutrophil cell surface receptors and their intracellular signal transduction pathways. Int Immunopharmacol. 2013;17(3):638-50.

18. Faurschou M, Borregaard N. Neutrophil granules and secretory vesicles in inflammation. Microbes and infection. 2003;5(14):1317-27.

19. Falloon J, Gallin JI. Neutrophil granules in health and disease. The Journal of allergy and clinical immunology. 1986;77(5):653-62.

20. Dahlgren C, Karlsson A. Respiratory burst in human neutrophils. Journal of Immunological Methods. 1999;232(1):3-14.

21. Rossi F. The O2−-forming NADPH oxidase of the phagocytes: nature, mechanisms of activation and function. Biochimica et Biophysica Acta (BBA) - Reviews on Bioenergetics. 1986;853(1):65-89.

22. Sampath P, Moideen K, Ranganathan UD, Bethunaickan R. Monocyte Subsets: Phenotypes and Function in Tuberculosis Infection. 2018;9(1726).

23. Guilliams M, Mildner A, Yona S. Developmental and Functional Heterogeneity of Monocytes. Immunity. 2018;49(4):595-613.

24. Geissmann F, Jung S, Littman DR. Blood monocytes consist of two principal subsets with distinct migratory properties. Immunity. 2003;19(1):71-82.

25. Mitchell AJ, Roediger B, Weninger W. Monocyte homeostasis and the plasticity of inflammatory monocytes. Cellular immunology. 2014;291(1):22-31.

26. Mascarenhas DP, Pereira MS, Manin GZ, Hori JI, Zamboni DS. Interleukin 1 Receptor–Driven Neutrophil Recruitment Accounts to MyD88–Dependent Pulmonary Clearance of Legionella pneumophila Infection In Vivo. The Journal of infectious diseases. 2014;211(2):322-30.

27. Horwitz MA. The Legionnaires' disease bacterium (Legionella pneumophila) inhibits phagosome-lysosome fusion in human monocytes. Journal of Experimental Medicine. 1983;158(6):2108-26.

28. Hespel C, Moser M. Role of inflammatory dendritic cells in innate and adaptive immunity. European journal of immunology. 2012;42(10):2535-43.

29. Jakubzick CV, Randolph GJ, Henson PMJNRI. Monocyte differentiation and antigen-presenting functions. 2017;17(6):349.

30. Murray PJ. Immune regulation by monocytes. Seminars in immunology. 2018;35:12-8.

31. Ginhoux F, Jung S. Monocytes and macrophages: developmental pathways and tissue homeostasis. Nature Reviews Immunology. 2014;14(6):392-404.

32. Guilliams M, Lambrecht B, Hammad H. Division of labor between lung dendritic cells and macrophages in the defense against pulmonary infections. Mucosal immunology. 2013;6(3):464.

33. Elhelu MAJJotNMA. The role of macrophages in immunology. 1983;75(3):314.

34. Kappler JW, Marrack PC. Helper T cells recognize antigen and macrophage surface components simultaneously. Nature. 1976;262(5571):797-9.

35. Underhill DM, Bassetti M, Rudensky A, Aderem AJJoEM. Dynamic interactions of macrophages with T cells during antigen presentation. 1999;190(12):1909-14.

36. e Sousa CRJNRI. Dendritic cells in a mature age. 2006;6(6):476.

37. Förster R, Schubel A, Breitfeld D, Kremmer E, Renner-Müller I, Wolf E, et al. CCR7 coordinates the primary immune response by establishing functional microenvironments in secondary lymphoid organs. 1999;99(1):23-33.

38. Ohl L, Mohaupt M, Czeloth N, Hintzen G, Kiafard Z, Zwirner J, et al. CCR7 governs skin dendritic cell migration under inflammatory and steady-state conditions. 2004;21(2):279-88.

39. Sallusto F, Schaerli P, Loetscher P, Schaniel C, Lenig D, Mackay CR, et al. Rapid and coordinated switch in chemokine receptor expression during dendritic cell maturation. 1998;28(9):2760-9.

40. Dalod M, Chelbi R, Malissen B, Lawrence T. Dendritic cell maturation: functional specialization through signaling specificity and transcriptional programming. The EMBO journal. 2014;33(10):1104-16.

41. Worbs T, Hammerschmidt SI, Förster R. Dendritic cell migration in health and disease. Nature Reviews Immunology. 2016;17:30.

42. Tai Y, Wang Q, Korner H, Zhang L, Wei W. Molecular Mechanisms of T Cells Activation by Dendritic Cells in Autoimmune Diseases. Front Pharmacol. 2018;9:642-.

43. Mempel TR, Henrickson SE, Von Andrian UH. T-cell priming by dendritic cells in lymph nodes occurs in three distinct phases. Nature. 2004;427(6970):154-9.

44. Janeway CA Jr TP, Walport M, et al. Immunobiology: The Immune System in Health and Disease. 5th edition. New York: Garland Science; 2001.

45. Starr TK, Jameson SC, Hogquist KA. Positive and negative selection of T cells. Annu Rev Immunol. 2003;21:139-76.

46. Kreslavsky T, Gleimer M, Garbe AI, Von Boehmer HJIr. αβ versus γδ fate choice: counting the T-cell lineages at the branch point. 2010;238(1):169-81.

47. Bluestone JA, Khattri R, Sciammas R, Sperling AI. TCR gamma delta cells: a specialized T-cell subset in the immune system. Annu Rev Cell Dev Biol. 1995;11:307-53.

48. Trinchieri G, Pflanz S, Kastelein RA. The IL-12 family of heterodimeric cytokines: new players in the regulation of T cell responses. Immunity. 2003;19(5):641-4.

49. Iwasaki A, Medzhitov R. Toll-like receptor control of the adaptive immune responses. Nature immunology. 2004;5(10):987-95.

50. Trinchieri G, Sher A. Cooperation of Toll-like receptor signals in innate immune defence. Nat Rev Immunol. 2007;7(3):179-90.

51. Afkarian M, Sedy JR, Yang J, Jacobson NG, Cereb N, Yang SY, et al. T-bet is a STAT1-induced regulator of IL-12R expression in naive CD4+ T cells. Nature immunology. 2002;3(6):549-57.

52. Lazarevic V, Chen X, Shim JH, Hwang ES, Jang E, Bolm AN, et al. T-bet represses T(H)17 differentiation by preventing Runx1-mediated activation of the gene encoding RORgammat. Nature immunology. 2011;12(1):96-104.

53. Lugo-Villarino G, Maldonado-Lopez R, Possemato R, Penaranda C, Glimcher LH. T-bet is required for optimal production of IFN-gamma and antigen-specific T cell activation by dendritic cells. Proc Natl Acad Sci U S A. 2003;100(13):7749-54.

54. Zhu J, Yamane H, Cote-Sierra J, Guo L, Paul WE. GATA-3 promotes Th2 responses through three different mechanisms: induction of Th2 cytokine production, selective growth of Th2 cells and inhibition of Th1 cell-specific factors. Cell Res. 2006;16(1):3-10.

55. Zhu J, Guo L, Watson CJ, Hu-Li J, Paul WE. Stat6 is necessary and sufficient for IL-4's role in Th2 differentiation and cell expansion. Journal of immunology. 2001;166(12):7276-81.

56. Kaplan MH, Schindler U, Smiley ST, Grusby MJ. Stat6 is required for mediating responses to IL-4 and for development of Th2 cells. Immunity. 1996;4(3):313-9.

57. Sokol CL, Chu NQ, Yu S, Nish SA, Laufer TM, Medzhitov R. Basophils function as antigen-presenting cells for an allergen-induced T helper type 2 response. Nature immunology. 2009;10(7):713-20.

58. Del Prete G. Human Th1 and Th2 lymphocytes: their role in the pathophysiology of atopy. Allergy. 1992;47(5):450-5.

59. Ivanov, II, McKenzie BS, Zhou L, Tadokoro CE, Lepelley A, Lafaille JJ, et al. The orphan nuclear receptor RORgammat directs the differentiation program of proinflammatory IL-17+ T helper cells. Cell. 2006;126(6):1121-33.

60. Annunziato F, Cosmi L, Santarlasci V, Maggi L, Liotta F, Mazzinghi B, et al. Phenotypic and functional features of human Th17 cells. J Exp Med. 2007;204(8):1849-61.

61. Moseley TA, Haudenschild DR, Rose L, Reddi AH. Interleukin-17 family and IL-17 receptors. Cytokine & growth factor reviews. 2003;14(2):155-74.

62. Chen W, Jin W, Hardegen N, Lei KJ, Li L, Marinos N, et al. Conversion of peripheral CD4+CD25- naive T cells to CD4+CD25+ regulatory T cells by TGF-beta induction of transcription factor Foxp3. J Exp Med. 2003;198(12):1875-86.

63. Yoshimura A, Muto G. TGF-beta function in immune suppression. Curr Top Microbiol Immunol. 2011;350:127-47.

64. Fujio K, Okamura T, Yamamoto K. The Family of IL-10-secreting CD4+ T cells. Advances in immunology. 2010;105:99-130.

65. Ouyang W, Rutz S, Crellin NK, Valdez PA, Hymowitz SG. Regulation and functions of the IL-10 family of cytokines in inflammation and disease. Annu Rev Immunol. 2011;29:71-109.

66. Wodarz D, Jansen VA. The role of T cell help for anti-viral CTL responses. Journal of theoretical biology. 2001;211(4):419-32.

67. Andersen MH, Schrama D, thor Straten P, Becker JC. Cytotoxic T Cells. Journal of Investigative Dermatology. 2006;126(1):32-41.

68. Nagata S. Fas-mediated apoptosis. Mechanisms of Lymphocyte Activation and Immune Regulation VI: Springer; 1996. p. 119-24.

69. Trapani JA, Smyth MJJNRI. Functional significance of the perforin/granzyme cell death pathway. 2002;2(10):735.

70. König R, Huang L-Y, Germain RN. MHC class II interaction with CD4 mediated by a region analogous to the MHC class I binding site for CD8. Nature. 1992;356(6372):796-8.

71. Alarcón B, Mestre D, Martínez-Martín NJI. The immunological synapse: a cause or consequence of T-cell receptor triggering? 2011;133(4):420-5.

72. Dustin ML. The immunological synapse. Cancer immunology research. 2014;2(11):1023-33.

73. Guy CS, Vignali DAA. Organization of proximal signal initiation at the TCR:CD3 complex. 2009;232(1):7-21.

74. Love PE, Hayes SM. ITAM-mediated Signaling by the T-Cell Antigen Receptor. 2010;2(6).

75. Wang H, Kadlecek TA, Au-Yeung BB, Goodfellow HES, Hsu L-Y, Freedman TS, et al. ZAP-70: an essential kinase in T-cell signaling. 2010;2(5):a002279.

76. Li Y, Mariuzza RJFii. Structural and biophysical insights into the role of CD4 and CD8 in T cell activation. 2013;4:206.

77. Cocco L, Follo MY, Manzoli L, Suh P-GJJolr. Phosphoinositide-specific phospholipase C in health and disease. 2015;56(10):1853-60.

78. Jayaraman T, Ondriasova E, Ondrias K, Harnick DJ, Marks ARJPotNAoS. The inositol 1, 4, 5-trisphosphate receptor is essential for T-cell receptor signaling. 1995;92(13):6007-11.

79. Liu JOJIr. Calmodulin-dependent phosphatase, kinases, and transcriptional corepressors involved in T-cell activation. 2009;228(1):184-98.

80. Zanoni I, Granucci FJEjoi. Regulation and dysregulation of innate immunity by NFAT signaling downstream of pattern recognition receptors (PRRs). 2012;42(8):1924-31.

81. Roose JP, Mollenauer M, Gupta VA, Stone J, Weiss AJM, biology c. A diacylglycerol-protein kinase C-RasGRP1 pathway directs Ras activation upon antigen receptor stimulation of T cells. 2005;25(11):4426-41.

82. Leevers SJ, Paterson HF, Marshall CJJN. Requirement for Ras in Raf activation is overcome by targeting Raf to the plasma membrane. 1994;369(6479):411.

83. Chang F, Steelman LS, Lee JT, Shelton JG, Navolanic PM, Blalock WL, et al. Signal transduction mediated by the Ras/Raf/MEK/ERK pathway from cytokine receptors to transcription factors: potential targeting for therapeutic intervention. Leukemia. 2003;17(7):1263-93.

84. Shaul YD, Seger R. The MEK/ERK cascade: From signaling specificity to diverse functions. Biochimica et Biophysica Acta (BBA) - Molecular Cell Research. 2007;1773(8):1213-26.

85. Karin M. The Regulation of AP-1 Activity by Mitogen-activated Protein Kinases. 1995;270(28):16483-6.

86. Steffan NM, Bren GD, Frantz B, Tocci MJ, O'Neill EA, Paya CV. Regulation of IkB alpha phosphorylation by PKC- and Ca(2+)-dependent signal transduction pathways. Journal of immunology. 1995;155(10):4685-91.

87. Lallena M-J, Diaz-Meco MT, Bren G, Payá CV, Moscat JJM, Biology C. Activation of IκB kinase β by protein kinase C isoforms. 1999;19(3):2180-8.

88. Gilmore TD. Introduction to NF-κB: players, pathways, perspectives. Oncogene. 2006;25(51):6680-4.

89. Hemmings BA, Restuccia DF. PI3K-PKB/Akt Pathway. 2012;4(9).

90. Sadra A, Cinek T, Arellano JL, Shi J, Truitt KE, Imboden JB. Identification of tyrosine phosphorylation sites in the CD28 cytoplasmic domain and their role in the costimulation of Jurkat T cells. Journal of immunology. 1999;162(4):1966-73.

91. Lemmon MA. Pleckstrin homology (PH) domains and phosphoinositides. Biochemical Society symposium. 2007(74):81-93.

92. Nossal GJ, Pike BL. Clonal anergy: persistence in tolerant mice of antigen-binding B lymphocytes incapable of responding to antigen or mitogen. Proc Natl Acad Sci U S A. 1980;77(3):1602-6.

93. Schwartz RH. T Cell Anergy. 2003;21(1):305-34.

94. Appleman LJ, Boussiotis VA. T cell anergy and costimulation. Immunological reviews. 2003;192:161-80.

95. DeSilva DR, Urdahl KB, Jenkins MK. Clonal anergy is induced in vitro by T cell receptor occupancy in the absence of proliferation. Journal of immunology. 1991;147(10):3261-7.

96. Lechler R, Chai JG, Marelli-Berg F, Lombardi GJI. The contributions of T-cell anergy to peripheral T-cell tolerance. 2001;103(3):262-9.

97. Ishida Y, Agata Y, Shibahara K, Honjo T. Induced expression of PD-1, a novel member of the immunoglobulin gene superfamily, upon programmed cell death. Embo j. 1992;11(11):3887-95.

98. McCoy KD, Le Gros GJI, biology c. The role of CTLA-4 in the regulation of T cell immune responses. 1999;77(1):1-10.

99. Pardoll DM. The blockade of immune checkpoints in cancer immunotherapy. Nature Reviews Cancer. 2012;12:252.

100. Wei SC, Duffy CR, Allison JP. Fundamental Mechanisms of Immune Checkpoint Blockade Therapy. 2018;8(9):1069-86.

101. Seidel JA, Otsuka A, Kabashima KJFio. Anti-PD-1 and anti-CTLA-4 therapies in cancer: mechanisms of action, efficacy, and limitations. 2018;8:86.

102. Frauwirth KA, Riley JL, Harris MH, Parry RV, Rathmell JC, Plas DR, et al. The CD28 signaling pathway regulates glucose metabolism. 2002;16(6):769-77.

103. Sena LA, Li S, Jairaman A, Prakriya M, Ezponda T, Hildeman DA, et al. Mitochondria are required for antigen-specific T cell activation through reactive oxygen species signaling. 2013;38(2):225-36.

104. Yusuf I, Fruman DAJTii. Regulation of quiescence in lymphocytes. 2003;24(7):380-6.

105. Gubser PM, Bantug GR, Razik L, Fischer M, Dimeloe S, Hoenger G, et al. Rapid effector function of memory CD8+ T cells requires an immediate-early glycolytic switch. 2013;14(10):1064.

106. Berod L, Friedrich C, Nandan A, Freitag J, Hagemann S, Harmrolfs K, et al. De novo fatty acid synthesis controls the fate between regulatory T and T helper 17 cells. 2014;20(11):1327.

107. Michalek RD, Gerriets VA, Jacobs SR, Macintyre AN, MacIver NJ, Mason EF, et al. Cutting edge: distinct glycolytic and lipid oxidative metabolic programs are essential for effector and regulatory CD4+ T cell subsets. 2011;186(6):3299-303.

108. Endo Y, Asou HK, Matsugae N, Hirahara K, Shinoda K, Tumes DJ, et al. Obesity drives Th17 cell differentiation by inducing the lipid metabolic kinase, ACC1. 2015;12(6):1042-55.

109. Schimmel L, Heemskerk N, van Buul JDJSG. Leukocyte transendothelial migration: a local affair. 2017;8(1):1-15.

110. Nourshargh S, Alon R. Leukocyte Migration into Inflamed Tissues. Immunity. 2014;41(5):694-707.

111. McEver RPJCr. Selectins: initiators of leucocyte adhesion and signalling at the vascular wall. 2015;107(3):331-9.

112. Lefort CT, Ley KJFii. Neutrophil arrest by LFA-1 activation. 2012;3:157.

113. Petri B, Bixel MG. Molecular events during leukocyte diapedesis. 2006;273(19):4399-407.

114. Campbell ID, Humphries MJ. Integrin Structure, Activation, and Interactions. 2011;3(3).

115. Frelinger AL, 3rd, Cohen I, Plow EF, Smith MA, Roberts J, Lam SC, et al. Selective inhibition of integrin function by antibodies specific for ligand-occupied receptor conformers. J Biol Chem. 1990;265(11):6346-52.

116. Askari JA, Buckley PA, Mould AP, Humphries MJ. Linking integrin conformation to function. Journal of cell science. 2009;122(Pt 2):165-70.

117. Faull RJ, Ginsberg MH. Inside-out signaling through integrins. Journal of the American Society of Nephrology : JASN. 1996;7(8):1091-7.

118. D'Souza-Schorey C, Chavrier P. ARF proteins: roles in membrane traffic and beyond. Nature Reviews Molecular Cell Biology. 2006;7(5):347-58.

119. Nie Z, Hirsch DS, Randazzo PA. Arf and its many interactors. Current Opinion in Cell Biology. 2003;15(4):396-404.

120. Donaldson JG, Jackson CL. ARF family G proteins and their regulators: roles in membrane transport, development and disease. Nature reviews Molecular cell biology. 2011;12(6):362-75.

121. Claude A, Zhao BP, Kuziemsky CE, Dahan S, Berger SJ, Yan JP, et al. GBF1: A novel Golgi-associated BFA-resistant guanine nucleotide exchange factor that displays specificity for ADP-ribosylation factor 5. J Cell Biol. 1999;146(1):71-84.

122. D'Souza-Schorey C, Li G, Colombo MI, Stahl PD. A regulatory role for ARF6 in receptor-mediated endocytosis. Science. 1995;267(5201):1175-8.

123. Brown HA, Gutowski S, Moomaw CR, Slaughter C, Sternwels PCJC. ADP-ribosylation factor, a small GTP-dependent regulatory protein, stimulates phospholipase D activity. 1993;75(6):1137-44.

124. Peters PJ, Hsu VW, Ooi CE, Finazzi D, Teal SB, Oorschot V, et al. Overexpression of wild-type and mutant ARF1 and ARF6: distinct perturbations of nonoverlapping membrane compartments. 1995;128(6):1003-17.

125. Goldberg J. Structural Basis for Activation of ARF GTPase: Mechanisms of Guanine Nucleotide Exchange and GTP–Myristoyl Switching. Cell. 1998;95(2):237-48.

126. Bos JL, Rehmann H, Wittinghofer A. GEFs and GAPs: critical elements in the control of small G proteins. Cell. 2007;129(5):865-77.

127. Schlacht A, Mowbrey K, Elias M, Kahn RA, Dacks JB. Ancient Complexity, Opisthokont Plasticity, and Discovery of the 11th Subfamily of Arf GAP Proteins. 2013;14(6):636-49.

128. Jackson CL, Bouvet S. Arfs at a Glance. 2014;127(19):4103-9.

129. Kolanus W, Nagel W, Schiller B, Zeitlmann L, Godar S, Stockinger H, et al. Alpha L beta 2 integrin/LFA-1 binding to ICAM-1 induced by cytohesin-1, a cytoplasmic regulatory molecule. Cell. 1996;86(2):233-42.

130. Chardin P, Paris S, Antonny B, Robineau S, Beraud-Dufour S, Jackson CL, et al. A human exchange factor for ARF contains Sec7- and pleckstrin-homology domains. Nature. 1996;384(6608):481-4.

131. Klarlund JK, Guilherme A, Holik JJ, Virbasius JV, Chawla A, Czech MP. Signaling by phosphoinositide-3, 4, 5-trisphosphate through proteins containing pleckstrin and Sec7 homology domains. Science. 1997;275(5308):1927-30.

132. Ogasawara M, Kim SC, Adamik R, Togawa A, Ferrans VJ, Takeda K, et al. Similarities in function and gene structure of cytohesin-4 and cytohesin-1, guanine nucleotide-exchange proteins for ADP-ribosylation factors. J Biol Chem. 2000;275(5):3221-30.

133. Mansour M, Lee SY, Pohajdak B. The N-terminal coiled coil domain of the cytohesin/ARNO family of guanine nucleotide exchange factors interacts with the scaffolding protein CASP. Journal of Biological Chemistry. 2002;277(35):32302-9.

134. Hafner M, Schmitz A, Grune I, Srivatsan SG, Paul B, Kolanus W, et al. Inhibition of cytohesins by SecinH3 leads to hepatic insulin resistance. Nature. 2006;444(7121):941-4.

135. Nagel W, Schilcher P, Zeitlmann L, Kolanus W. The PH domain and the polybasic c domain of cytohesin-1 cooperate specifically in plasma membrane association and cellular function. Molecular biology of the cell. 1998;9(8):1981-94.

136. Venkateswarlu K, Oatey PB, Tavaré JM, Cullen PJ. Insulin-dependent translocation of ARNO to the plasma membrane of adipocytes requires phosphatidylinositol 3-kinase. Current biology. 1998;8(8):463-6.

137. Nagel W, Zeitlmann L, Schilcher P, Geiger C, Kolanus J, Kolanus W. Phosphoinositide 3-OH kinase activates the beta2 integrin adhesion pathway and induces membrane recruitment of cytohesin-1. J Biol Chem. 1998;273(24):14853-61.

138. Cronin TC, DiNitto JP, Czech MP, Lambright DG. Structural determinants of phosphoinositide selectivity in splice variants of Grp1 family PH domains. The EMBO journal. 2004;23(19):3711-20.

139. Klarlund JK, Tsiaras W, Holik JJ, Chawla A, Czech MP. Distinct Polyphosphoinositide Binding Selectivities for Pleckstrin Homology Domains of GRP1-like Proteins Based on DiglycineVersus Triglycine Motifs. Journal of Biological Chemistry. 2000;275(42):32816-21.

140. Hofmann I, Thompson A, Sanderson CM, Munro S. The Arl4 family of small G proteins can recruit the cytohesin Arf6 exchange factors to the plasma membrane. Current biology. 2007;17(8):711-6.

141. Cohen LA, Honda A, Varnai P, Brown FD, Balla T, Donaldson JGJMbotc. Active Arf6 recruits ARNO/cytohesin GEFs to the PM by binding their PH domains. 2007;18(6):2244-53.

142. Nagel W, Schilcher P, Zeitlmann L, Kolanus W. The PH domain and the polybasic c domain of cytohesin-1 cooperate specifically in plasma membrane association and cellular function. Molecular biology of the cell. 1998;9(8):1981-94.

143. Santy LC, Frank SR, Hatfield JC, Casanova JEJCb. Regulation of ARNO nucleotide exchange by a PH domain electrostatic switch. 1999;9(20):1173-6.

144. Kolanus WJIr. Guanine nucleotide exchange factors of the cytohesin family and their roles in signal transduction. 2007;218(1):102-13.

145. Meacci E, Tsai S-C, Adamik R, Moss J, Vaughan MJPotNAoS. Cytohesin-1, a cytosolic guanine nucleotide-exchange protein for ADP-ribosylation factor. 1997;94(5):1745-8.

146. Franco M, Boretto J, Robineau S, Monier S, Goud B, Chardin P, et al. ARNO3, a Sec7-domain guanine nucleotide exchange factor for ADP ribosylation factor 1, is involved in the control of Golgi structure and function. Proc Natl Acad Sci U S A. 1998;95(17):9926-31.

147. Fuss B, Becker T, Zinke I, Hoch MJN. The cytohesin Steppke is essential for insulin signalling in Drosophila. 2006;444(7121):945.

148. Hafner M, Schmitz A, Grüne I, Srivatsan SG, Bianca P, Kolanus W, et al. Inhibition of cytohesins by SecinH3 leads to hepatic insulin resistance. Nature. 2006;444(7121):941.

149. Jux B, Gosejacob D, Tolksdorf F, Mandel C, Rieck M, Namislo A, et al. Cytohesin-3 is required for full insulin receptor signaling and controls body weight via lipid excretion. 2019;9(1):3442.

150. Weber KS, Weber C, Ostermann G, Dierks H, Nagel W, Kolanus W. Cytohesin-1 is a dynamic regulator of distinct LFA-1 functions in leukocyte arrest and transmigration triggered by chemokines. Current biology : CB. 2001;11(24):1969-74.

151. Geiger C, Nagel W, Boehm T, van Kooyk Y, Figdor CG, Kremmer E, et al. Cytohesin-1 regulates beta-2 integrin-mediated adhesion through both ARF-GEF function and interaction with LFA-1. EMBO J. 2000;19(11):2525-36.

152. Frank SR, Hatfield JC, Casanova JE. Remodeling of the actin cytoskeleton is coordinately regulated by protein kinase C and the ADP-ribosylation factor nucleotide exchange factor ARNO. Molecular biology of the cell. 1998;9(11):3133-46.

153. Korthauer U, Nagel W, Davis EM, Le Beau MM, Menon RS, Mitchell EO, et al. Anergic T lymphocytes selectively express an integrin regulatory protein of the cytohesin family. Journal of immunology. 2000;164(1):308-18.

154. Quast T, Tappertzhofen B, Schild C, Grell J, Czeloth N, Forster R, et al. Cytohesin-1 controls the activation of RhoA and modulates integrin-dependent adhesion and migration of dendritic cells. Blood. 2009;113(23):5801-10.

155. Quast T, Tappertzhofen B, Schild C, Grell J, Czeloth N, Förster R, et al. Cytohesin-1 controls the activation of RhoA and modulates integrin-dependent adhesion and migration of dendritic cells. Blood. 2009;113(23):5801-10.

156. Radhakrishna H, Al-Awar O, Khachikian Z, Donaldson JG. ARF6 requirement for Rac ruffling suggests a role for membrane trafficking in cortical actin rearrangements. Journal of cell science. 1999;112(6):855-66.

157. Norman J, Jones D, Barry S, Holt M, Cockcroft S, Critchley D. ARF1 mediates paxillin recruitment to focal adhesions and potentiates Rho-stimulated stress fiber formation in intact and permeabilized Swiss 3T3 fibroblasts. J Cell Biol. 1998;143(7):1981-95.

158. Santy LC, Casanova JE. Activation of ARF6 by ARNO stimulates epithelial cell migration through downstream activation of both Rac1 and phospholipase D. The Journal of cell biology. 2001;154(3):599-610.

159. El Azreq MA, Garceau V, Bourgoin SG. Cytohesin-1 regulates fMLF-mediated activation and functions of the beta2 integrin Mac-1 in human neutrophils. Journal of leukocyte biology. 2011;89(6):823-36.

160. El Azreq M-A, Bourgoin SG. Cytohesin-1 regulates human blood neutrophil adhesion to endothelial cells through β2 integrin activation. Molecular immunology. 2011;48(12):1408-16.

161. Phillipson M, Heit B, Colarusso P, Liu L, Ballantyne CM, Kubes P. Intraluminal crawling of neutrophils to emigration sites: a molecularly distinct process from adhesion in the recruitment cascade. Journal of Experimental Medicine. 2006;203(12):2569-75.

162. Oh SJ, Santy LC. Differential effects of cytohesins 2 and 3 on β1 integrin recycling. Journal of Biological Chemistry. 2010;285(19):14610-6.

163. Rafiq NBM, Lieu ZZ, Jiang T, Yu C-h, Matsudaira P, Jones GE, et al. Podosome assembly is controlled by the GTPase ARF1 and its nucleotide exchange factor ARNO. 2017;216(1):181-97.

164. Gaidano G, Bergui L, Schena M, Gaboli M, Cremona O, Marchisio PC, et al. Integrin distribution and cytoskeleton organization in normal and malignant monocytes. 1990;4(10):682-7.

165. Marchisio PC, Bergui L, Corbascio GC, Cremona O, D'Urso N, Schena M, et al. Vinculin, talin, and integrins are localized at specific adhesion sites of malignant B lymphocytes. 1988;72(2):830-3.

166. Hiura K, Lim SS, Little SP, Lin S, Sato MJCm, cytoskeleton t. Differentiation dependent expression of tensin and cortactin in chicken osteoclasts. 1995;30(4):272-84.

167. Perez OD, Mitchell D, Jager GC, South S, Murriel C, McBride J, et al. Leukocyte functional antigen 1 lowers T cell activation thresholds and signaling through cytohesin-1 and Jun-activating binding protein 1. Nature immunology. 2003;4(11):1083.

168. Korthäuer U, Nagel W, Davis EM, Le Beau MM, Menon RS, Mitchell EO, et al. Anergic T lymphocytes selectively express an integrin regulatory protein of the cytohesin family. The Journal of Immunology. 2000;164(1):308-18.

169. Humphreys D, Davidson A, Hume PJ, Koronakis V. Salmonella virulence effector SopE and Host GEF ARNO cooperate to recruit and activate WAVE to trigger bacterial invasion. Cell host & microbe. 2012;11(2):129-39.

170. Humphreys D, Davidson AC, Hume PJ, Makin LE, Koronakis V. Arf6 coordinates actin assembly through the WAVE complex, a mechanism usurped by Salmonella to invade host cells. Proc Natl Acad Sci U S A. 2013;110(42):16880-5.

171. Garza-Mayers AC, Miller KA, Russo BC, Nagda DV, Goldberg MB. Shigella flexneri regulation of ARF6 activation during bacterial entry via an IpgD-mediated positive feedback loop. mBio. 2015;6(2):e02584.

172. Humphreys D, Singh V, Koronakis V. Inhibition of WAVE regulatory complex activation by a bacterial virulence effector counteracts pathogen phagocytosis. Cell reports. 2016;17(3):697-707.

173. McDade JE, Shepard CC, Fraser DW, Tsai TR, Redus MA, Dowdle WR, et al. Legionnaires' disease: isolation of a bacterium and demonstration of its role in other respiratory disease. New England Journal of Medicine. 1977;297(22):1197-203.

174. Fraser DW, Tsai TR, Orenstein W, Parkin WE, Beecham HJ, Sharrar RG, et al. Legionnaires' disease: description of an epidemic of pneumonia. New England Journal of Medicine. 1977;297(22):1189-97.

175. Rowbotham TJ. Preliminary report on the pathogenicity of Legionella pneumophila for freshwater and soil amoebae. Journal of clinical pathology. 1980;33(12):1179-83.

176. Fliermans C, Cherry W, Orrison L, Thacker L. Isolation of Legionella pneumophila from nonepidemic-related aquatic habitats. Applied and environmental microbiology. 1979;37(6):1239-42.

177. Morris GK, Patton CM, Feeley JC, Johnson SE, Gorman G, Martin WT, et al. Isolation of the Legionnaires' disease bacterium from environmental samples. Annals of internal medicine. 1979;90(4):664-6.

178. Marra A, Blander SJ, Horwitz MA, Shuman HA. Identification of a Legionella pneumophila locus required for intracellular multiplication in human

macrophages. Proceedings of the National Academy of Sciences. 1992;89(20):9607-11.

179. Roy CR, Berger KH, Isberg RR. Legionella pneumophila DotA protein is required for early phagosome trafficking decisions that occur within minutes of bacterial uptake. Molecular microbiology. 1998;28(3):663-74.

180. Vogel JP, Andrews HL, Wong SK, Isberg RR. Conjugative transfer by the virulence system of Legionella pneumophila. Science. 1998;279(5352):873-6.

181. Simon S, Hilbi H. Subversion of cell-autonomous immunity and cell migration by Legionella pneumophila effectors. Frontiers in immunology. 2015;6.

182. Newton HJ, Ang DK, van Driel IR, Hartland EL. Molecular pathogenesis of infections caused by Legionella pneumophila. Clinical microbiology reviews. 2010;23(2):274-98.

183. Swanson MS, Isberg RR. Association of Legionella pneumophila with the macrophage endoplasmic reticulum. Infection and immunity. 1995;63(9):3609-20.

184. Isberg RR, O'Connor T, Heidtman M. The Legionella pneumophila replication vacuole: making a cozy niche inside host cells. Nature reviews Microbiology. 2009;7(1):13.

185. Chardin P, Paris S, Antonny B, Robineau S, Béraud-Dufour S, Jackson CL, et al. A human exchange factor for ARF contains Sec7-and pleckstrin-homology domains. Nature. 1996;384(6608):481-4.

186. Machner MP, Isberg RR. Targeting of host Rab GTPase function by the intravacuolar pathogen Legionella pneumophila. Developmental cell. 2006;11(1):47-56.

187. Glavin FL, Winn Jr WC, Craighead JE. Ultrastructure of lung in Legionnaires' disease. Ann Intern Med. 1979;90:555-9.

188. Fields BS, Benson RF, Besser RE. Legionella and Legionnaires' disease: 25 years of investigation. Clinical microbiology reviews. 2002;15(3):506-26.

189. Fitzgeorge R, Baskerville A, Broster M, Hambleton P, Dennis P. Aerosol infection of animals with strains of Legionella pneumophila of different virulence: comparison with intraperitoneal and intranasal routes of infection. Epidemiology & Infection. 1983;90(1):81-9.

190. Brieland J, Freeman P, Kunkel R, Chrisp C, Hurley M, Fantone J, et al. Replicative Legionella pneumophila lung infection in intratracheally inoculated A/J mice. A murine model of human Legionnaires' disease. The American journal of pathology. 1994;145(6):1537.

191. Yoshida S, Goto Y, Mizuguchi Y, Nomoto K, Skamene E. Genetic control of natural resistance in mouse macrophages regulating intracellular Legionella pneumophila multiplication in vitro. Infection and immunity. 1991;59(1):428-32.

192. GLAVIN FL, WINN WC, CRAIGHEAD JEJAoim. Ultrastructure of lung in Legionnaires' disease: observations of three biopsies done during the Vermont epidemic. 1979;90(4):555-9.

193. Lamkanfi M, Dixit VM. Inflammasomes: guardians of cytosolic sanctity. Immunological reviews. 2009;227(1):95-105.

194. Dietrich WF, Damron DM, Isberg RR, Lander ES, Swanson MS. Lgn1, a gene that determines susceptibility to Legionella pneumophila, maps to mouse chromosome 13. Genomics. 1995;26(3):443-50.

195. Beckers M-C, Yoshida S-I, Morgan K, Skamene E, Gros P. Natural resistance to infection with Legionella pneumophila: chromosomal localization of the Lgn1 susceptibility gene. Mammalian Genome. 1995;6(8):540-5.

196. Molofsky AB, Byrne BG, Whitfield NN, Madigan CA, Fuse ET, Tateda K, et al. Cytosolic recognition of flagellin by mouse macrophages restricts Legionella pneumophila infection. Journal of Experimental Medicine. 2006;203(4):1093-104.

197. Ren T, Zamboni DS, Roy CR, Dietrich WF, Vance RE. Flagellin-deficient Legionella mutants evade caspase-1-and Naip5-mediated macrophage immunity. PLoS pathogens. 2006;2(3):e18.

198. Case CL, Shin S, Roy CR. Asc and Ipaf Inflammasomes direct distinct pathways for caspase-1 activation in response to Legionella pneumophila. Infection and immunity. 2009;77(5):1981-91.

199. Archer KA, Alexopoulou L, Flavell RA, Roy CR. Multiple MyD88-dependent responses contribute to pulmonary clearance of Legionella pneumophila. Cellular microbiology. 2009;11(1):21-36.

200. Archer KA, Ader F, Kobayashi KS, Flavell RA, Roy CR. Cooperation between multiple microbial pattern recognition systems is important for host protection against the intracellular pathogen Legionella pneumophila. Infection and immunity. 2010;78(6):2477-87.

201. Berrington WR, Iyer R, Wells RD, Smith KD, Skerrett SJ, Hawn TR. NOD1 and NOD2 regulation of pulmonary innate immunity to Legionella pneumophila. European journal of immunology. 2010;40(12):3519-27.

202. Brown AS, Yang C, Hartland EL, van Driel IR. The regulation of acute immune responses to the bacterial lung pathogen Legionella pneumophila. Journal of leukocyte biology. 2017;101(4):875-86.

203. Brown AS, van Driel IR, Hartland EL. Mouse models of Legionnaires' disease. Molecular Mechanisms in Legionella Pathogenesis: Springer; 2013. p. 271-91.

204. Massis LM, Zamboni DS. Innate immunity to Legionella pneumophila. Frontiers in microbiology. 2011;2.

205. Schuelein R, Ang DK, van Driel IR, Hartland EL. Immune control of Legionella infection: an in vivo perspective. Frontiers in microbiology. 2011;2.

206. Mascarenhas DPA, Pereira MSF, Manin GZ, Hori JI, Zamboni DS. Interleukin 1 Receptor-Driven Neutrophil Recruitment Accounts to MyD88-Dependent Pulmonary Clearance of Legionella pneumophila Infection In Vivo. Journal of Infectious Diseases. 2015;211(2):322-30.

207. Archer KA, Roy CR. MyD88-dependent responses involving toll-like receptor 2 are important for protection and clearance of Legionella pneumophila in a mouse model of Legionnaires' disease. Infection and immunity. 2006;74(6):3325-33.

208. Hawn TR, Smith KD, Aderem A, Skerrett SJ. Myeloid differentiation primary response gene (88)- and toll-like receptor 2-deficient mice are

susceptible to infection with aerosolized Legionella pneumophila. The Journal of infectious diseases. 2006;193(12):1693-702.

209. Sporri R, Joller N, Albers U, Hilbi H, Oxenius A. MyD88-dependent IFN-gamma production by NK cells is key for control of Legionella pneumophila infection. Journal of immunology. 2006;176(10):6162-71.

210. Hawn TR, Berrington WR, Smith IA, Uematsu S, Akira S, Aderem A, et al. Altered inflammatory responses in TLR5-deficient mice infected with Legionella pneumophila. The Journal of Immunology. 2007;179(10):6981-7.

211. Girard R, Pedron T, Uematsu S, Balloy V, Chignard M, Akira S, et al. Lipopolysaccharides from Legionella and Rhizobium stimulate mouse bone marrow granulocytes via Toll-like receptor 2. Journal of cell science. 2003;116(2):293-302.

212. Newton CA, Perkins I, Widen RH, Friedman H, Klein TW. Role of toll-like receptor 9 in Legionella pneumophila-induced interleukin-12 p40 production in bone marrow-derived dendritic cells and macrophages from permissive and nonpermissive mice. Infect Immun. 2007;75(1):146-51.

213. Hayashi F, Smith KD, Ozinsky A, Hawn TR, Yi EC, Goodlett DR, et al. The innate immune response to bacterial flagellin is mediated by Toll-like receptor 5. Nature. 2001;410(6832):1099-103.

214. Smith KD, Ozinsky A. Toll-like receptor-5 and the innate immune response to bacterial flagellin. Curr Top Microbiol Immunol. 2002;270:93-108.

215. Stunz LL, Lenert P, Peckham D, Yi AK, Haxhinasto S, Chang M, et al. Inhibitory oligonucleotides specifically block effects of stimulatory CpG oligonucleotides in B cells. European journal of immunology. 2002;32(5):1212-22.

216. Bhan U, Trujillo G, Lyn-Kew K, Newstead MW, Zeng X, Hogaboam CM, et al. Toll-like receptor 9 regulates the lung macrophage phenotype and host immunity in murine pneumonia caused by Legionella pneumophila. Infection and immunity. 2008;76(7):2895-904.

217. Hawn TR, Berrington WR, Smith IA, Uematsu S, Akira S, Aderem A, et al. Altered inflammatory responses in TLR5-deficient mice infected with Legionella pneumophila. J Immunol. 2007;179(10):6981-7.

218. Archer KA, Alexopoulou L, Flavell RA, Roy CR. Multiple MyD88-dependent responses contribute to pulmonary clearance of Legionella pneumophila. Cellular microbiology. 2009;11(1):21-36.

219. Berrington W, Smith K, Skerrett S, Hawn T. Nucleotide-binding oligomerization domain containing-like receptor family, caspase recruitment domain (CARD) containing 4 (NLRC4) regulates intrapulmonary replication of aerosolized Legionella pneumophila. BMC infectious diseases. 2013;13(1):1-10.

220. Kumagai Y, Takeuchi O, Akira S. Pathogen recognition by innate receptors. Journal of Infection and Chemotherapy. 2008;14(2):86-92.

221. Kawai T, Akira S. The roles of TLRs, RLRs and NLRs in pathogen recognition. International immunology. 2009;21(4):317-37.

222. Frutuoso MS, Hori JI, Pereira MS, Junior DS, Sônego F, Kobayashi KS, et al. The pattern recognition receptors Nod1 and Nod2 account for neutrophil

recruitment to the lungs of mice infected with Legionella pneumophila. Microbes and infection. 2010;12(11):819-27.

223. Kopf M, Schneider C, Nobs SP. The development and function of lung-resident macrophages and dendritic cells. Nature immunology. 2015;16(1):36-44.

224. Allard B, Panariti A, Martin JG. Alveolar Macrophages in the Resolution of Inflammation, Tissue Repair, and Tolerance to Infection. 2018;9(1777).

225. Vlahos R, Bozinovski S. Role of alveolar macrophages in chronic obstructive pulmonary disease. Frontiers in immunology. 2014;5.

226. Koay MA, Delbeck T, Mack M, Ermert M, Ermert L, Blackwell TS, et al. Role of resident alveolar macrophages in leukocyte traffic into the alveolar air space of intact mice. American Journal of Physiology-Lung Cellular and Molecular Physiology. 2002;282(6):L1245-L52.

227. Hussell T, Bell TJ. Alveolar macrophages: plasticity in a tissue-specific context. Nature reviews Immunology. 2014;14(2):81.

228. Gebran SJ, Newton C, Yamamoto Y, Widen R, Klein TW, Friedman H. Macrophage Permissiveness for Legionella-Pneumophila Growth Modulated by Iron. Infection and immunity. 1994;62(2):564-8.

229. Swanson MS, Isberg RR. Association of Legionella-Pneumophila with the Macrophage Endoplasmic-Reticulum. Infection and immunity. 1995;63(9):3609-20.

230. Amer AO, Swanson MS. Autophagy is an immediate macrophage response to Legionella pneumophila. Cellular microbiology. 2005;7(6):765-78.

231. Horenkamp FA, Kauffman KJ, Kohler LJ, Sherwood RK, Krueger KP, Shteyn V, et al. The Legionella anti-autophagy effector RavZ targets the autophagosome via PI3P-and curvature-sensing motifs. 2015;34(5):569-76.

232. Yang A, Pantoom S, Wu Y-WJE. Elucidation of the anti-autophagy mechanism of the Legionella effector RavZ using semisynthetic LC3 proteins. 2017;6:e23905.

233. Choy A, Dancourt J, Mugo B, O'Connor TJ, Isberg RR, Melia TJ, et al. The Legionella effector RavZ inhibits host autophagy through irreversible Atg8 deconjugation. 2012;338(6110):1072-6.

234. Fontana MF, Banga S, Barry KC, Shen X, Tan Y, Luo Z-Q, et al. Secreted bacterial effectors that inhibit host protein synthesis are critical for induction of the innate immune response to virulent Legionella pneumophila. PLoS pathogens. 2011;7(2):e1001289.

235. Asrat S, Dugan AS, Isberg RR. The frustrated host response to Legionella pneumophila is bypassed by MyD88-dependent translation of pro-inflammatory cytokines. PLoS pathogens. 2014;10(7):e1004229.

236. Barry KC, Fontana MF, Portman JL, Dugan AS, Vance RE. IL-1α signaling initiates the inflammatory response to virulent Legionella pneumophila in vivo. The Journal of Immunology. 2013;190(12):6329-39.

237. Copenhaver AM, Casson CN, Nguyen HT, Duda MM, Shin S. IL-1R signaling enables bystander cells to overcome bacterial blockade of host protein synthesis. Proceedings of the National Academy of Sciences. 2015;112(24):7557-62.

238. Mascarenhas DPA, Zamboni DS. Inflammasome biology taught by Legionella pneumophila. 2017;101(4):841-9.

239. Casson CN, Copenhaver AM, Zwack EE, Nguyen HT, Strowig T, Javdan B, et al. Caspase-11 activation in response to bacterial secretion systems that access the host cytosol. 2013;9(6):e1003400.

240. Case CL, Kohler LJ, Lima JB, Strowig T, de Zoete MR, Flavell RA, et al. Caspase-11 stimulates rapid flagellin-independent pyroptosis in response to Legionella pneumophila. 2013;110(5):1851-6.

241. Pilla DM, Hagar JA, Haldar AK, Mason AK, Degrandi D, Pfeffer K, et al. Guanylate binding proteins promote caspase-11–dependent pyroptosis in response to cytoplasmic LPS. 2014;111(16):6046-51.

242. Casson CN, Yu J, Reyes VM, Taschuk FO, Yadav A, Copenhaver AM, et al. Human caspase-4 mediates noncanonical inflammasome activation against gram-negative bacterial pathogens. 2015;112(21):6688-93.

243. Fernandes-Alnemri T, Yu J-W, Datta P, Wu J, Alnemri ESJN. AIM2 activates the inflammasome and cell death in response to cytoplasmic DNA. 2009;458(7237):509.

244. Brown AS, Yang C, Fung KY, Bachem A, Bourges D, Bedoui S, et al. Cooperation between monocyte-derived cells and lymphoid cells in the acute response to a bacterial lung pathogen. PLoS pathogens. 2016;12(6):e1005691.

245. Schlitzer A, McGovern N, Ginhoux F, editors. Dendritic cells and monocyte-derived cells: two complementary and integrated functional systems. Seminars in cell & developmental biology; 2015: Elsevier.

246. Lambrecht BN, Hammad H. Lung dendritic cells in respiratory viral infection and asthma: from protection to immunopathology. Annual review of immunology. 2012;30:243-70.

247. Liu K, Nussenzweig MC. Origin and development of dendritic cells. Immunological reviews. 2010;234(1):45-54.

248. Copenhaver AM, Casson CN, Nguyen HT, Fung TC, Duda MM, Roy CR, et al. Alveolar macrophages and neutrophils are the primary reservoirs for Legionella pneumophila and mediate cytosolic surveillance of type IV secretion. Infection and immunity. 2014;82(10):4325-36.

249. Nogueira CV, Lindsten T, Jamieson AM, Case CL, Shin S, Thompson CB, et al. Rapid pathogen-induced apoptosis: a mechanism used by dendritic cells to limit intracellular replication of Legionella pneumophila. PLoS pathogens. 2009;5(6):e1000478.

250. Frutuoso MS, Hori JI, Pereira MSF, Junior DSL, Sônego F, Kobayashi KS, et al. The pattern recognition receptors Nod1 and Nod2 account for neutrophil recruitment to the lungs of mice infected with Legionella pneumophila. Microbes and infection. 2010;12(11):819-27.

251. Tateda K, Moore TA, Deng JC, Newstead MW, Zeng X, Matsukawa A, et al. Early recruitment of neutrophils determines subsequent T1/T2 host responses in a murine model of Legionella pneumophila pneumonia. The Journal of Immunology. 2001;166(5):3355-61.

252. LeibundGut-Landmann S, Weidner K, Hilbi H, Oxenius A. Nonhematopoietic cells are key players in innate control of bacterial airway infection. The Journal of Immunology. 2011;186(5):3130-7.

253. Tateda K, Moore TA, Newstead MW, Tsai WC, Zeng X, Deng JC, et al. Chemokine-dependent neutrophil recruitment in a murine model of Legionella pneumonia: potential role of neutrophils as immunoregulatory cells. Infection and immunity. 2001;69(4):2017-24.

254. Amulic B, Cazalet C, Hayes GL, Metzler KD, Zychlinsky A. Neutrophil function: from mechanisms to disease. Annual review of immunology. 2012;30:459-89.

255. Cai S, Batra S, Langohr I, Iwakura Y, Jeyaseelan S. IFN-γ induction by neutrophil-derived IL-17A homodimer augments pulmonary antibacterial defense. Mucosal immunology. 2016;9(3):718.

256. Trunk G, Oxenius A. Innate instruction of CD4+ T cell immunity in respiratory bacterial infection. Journal of immunology. 2012;189(2):616-28.

257. Joller N, Sporri R, Hilbi H, Oxenius A. Induction and protective role of antibodies in Legionella pneumophila infection. European journal of immunology. 2007;37(12):3414-23.

258. Krammer F, Smith GJD, Fouchier RAM, Peiris M, Kedzierska K, Doherty PC, et al. Influenza. Nature reviews Disease primers. 2018;4(1):3.

259. Moghadami M. A Narrative Review of Influenza: A Seasonal and Pandemic Disease. Iran J Med Sci. 2017;42(1):2-13.

260. Sellers SA, Hagan RS, Hayden FG, Fischer WAJI, viruses or. The hidden burden of influenza: A review of the extra-pulmonary complications of influenza infection. 2017;11(5):372-93.

261. Kwong JC, Schwartz KL, Campitelli MA, Chung H, Crowcroft NS, Karnauchow T, et al. Acute myocardial infarction after laboratory-confirmed influenza infection. 2018;378(4):345-53.

262. Louie JK, Salibay CJ, Kang M, Glenn-Finer RE, Murray EL, Jamieson DJJO, et al. Pregnancy and severe influenza infection in the 2013–2014 influenza season. 2015;125(1):184-92.

263. Martin A, Cox S, Jamieson DJ, Whiteman MK, Kulkarni A, Tepper NKJM, et al. Respiratory illness hospitalizations among pregnant women during influenza season, 1998–2008. 2013;17(7):1325-31.

264. Cowling BJ, Ip DK, Fang VJ, Suntarattiwong P, Olsen SJ, Levy J, et al. Aerosol transmission is an important mode of influenza A virus spread. 2013;4:1935.

265. Tripp RA, Tompkins SM. Animal models for evaluation of influenza vaccines. Vaccines for Pandemic Influenza: Springer; 2009. p. 397-412.

266. Bouvier NM, Lowen ACJV. Animal models for influenza virus pathogenesis and transmission. 2010;2(8):1530-63.

267. Fukushi M, Ito T, Oka T, Kitazawa T, Miyoshi-Akiyama T, Kirikae T, et al. Serial histopathological examination of the lungs of mice infected with influenza A virus PR8 strain. 2011;6(6):e21207.

268. Knossow M, Skehel JJJI. Variation and infectivity neutralization in influenza. 2006;119(1):1-7.

269. Baumgarth N, Herman OC, Jager GC, Brown LE, Herzenberg LA, Chen JJJoEM. B-1 and B-2 cell–derived immunoglobulin M antibodies are nonredundant components of the protective response to influenza virus infection. 2000;192(2):271-80.

270. Waffarn EE, Baumgarth NJTJoI. Protective B cell responses to flu—no fluke! 2011;186(7):3823-9.

271. Hashimoto G, Wright PF, Karzon DT. Antibody-dependent cell-mediated cytotoxicity against influenza virus-infected cells. The Journal of infectious diseases. 1983;148(5):785-94.

272. Hashimoto G, Wright PF, Karzon DTJI, immunity. Ability of human cord blood lymphocytes to mediate antibody-dependent cellular cytotoxicity against influenza virus-infected cells. 1983;42(1):214-8.

273. van de Sandt CE, Kreijtz JH, Rimmelzwaan GFJV. Evasion of influenza A viruses from innate and adaptive immune responses. 2012;4(9):1438-76.

274. Okoye IS, Wilson MSJI. CD4+ T helper 2 cells–microbial triggers, differentiation requirements and effector functions. 2011;134(4):368-77.

275. Lamb J, Woody J, Hartzman R, Eckels DJTJoI. In vitro influenza virus-specific antibody production in man: antigen-specific and HLA-restricted induction of helper activity mediated by cloned human T lymphocytes. 1982;129(4):1465-70.

276. Zhu J, Paul WEJIr. Peripheral CD4+ T-cell differentiation regulated by networks of cytokines and transcription factors. 2010;238(1):247-62.

277. Moffat JM, Gebhardt T, Doherty PC, Turner SJ, Mintern JDJEjoi. Granzyme A expression reveals distinct cytolytic CTL subsets following influenza A virus infection. 2009;39(5):1203-10.

278. Topham D, Tripp R, Doherty PJTJoI. CD8+ T cells clear influenza virus by perforin or Fas-dependent processes. 1997;159(11):5197-200.

279. Andrade FJIr. Non-cytotoxic antiviral activities of granzymes in the context of the immune antiviral state. 2010;235(1):128-46.

280. La Gruta NL, Turner SJ, Doherty PC. Hierarchies in Cytokine Expression Profiles for Acute and Resolving Influenza Virus-Specific CD8⁺ T Cell Responses: Correlation of Cytokine Profile and TCR Avidity. 2004;172(9):5553-60.

281. Woodland DL, Hogan RJ, Zhong WJIR. Cellular immunity and memory to respiratory virus infections. 2001;24(1):53-67.

282. Sridhar S, Begom S, Bermingham A, Roberts K, Barclay W, Openshaw P, et al. Predominance of heterosubtypic IFN-γ-only-secreting effector memory T cells in pandemic H1N1 naive adults: 431. 2011;135.

283. Feeley JC, Gibson RJ, Gorman GW, Langford NC, Rasheed JK, Mackel DC, et al. Charcoal-yeast extract agar: primary isolation medium for Legionella pneumophila. Journal of clinical microbiology. 1979;10(4):437-41.

284. Bigby M, Wang P, Fierro JF, Sy MS. Phorbol myristate acetate-induced down-modulation of CD4 is dependent on calmodulin and intracellular calcium. Journal of immunology. 1990;144(8):3111-6.

285. Ng GZ, Solomatina A, van Driel IR, Hartland EL. The Mouse as a Model for Pulmonary Legionella Infection. Legionella: Springer; 2019. p. 399-417.

286. El Azreq M-A, Garceau V, Harbour D, Pivot-Pajot C, Bourgoin SG. Cytohesin-1 regulates the Arf6-phospholipase D signaling axis in human neutrophils: impact on superoxide anion production and secretion. The journal of immunology. 2010;184(2):637-49.

287. Zhu W, Luo Z-Q. Methods for Determining Protein Translocation by the Legionella pneumophila Dot/Icm Type IV Secretion System. In: Buchrieser C, Hilbi H, editors. Legionella: Methods and Protocols. Totowa, NJ: Humana Press; 2013. p. 323-32.

288. Copenhaver AM, Casson CN, Nguyen HT, Fung TC, Duda MM, Roy CR, et al. Alveolar macrophages and neutrophils are the primary reservoirs for Legionella pneumophila and mediate cytosolic surveillance of type IV secretion. 2014;82(10):4325-36.

289. Tateda K, Moore TA, Deng JC, Newstead MW, Zeng X, Matsukawa A, et al. Early Recruitment of Neutrophils Determines Subsequent T1/T2 Host Responses in a Murine Model of Legionella pneumophila Pneumonia. 2001;166(5):3355-61.

290. Ziltener P, Reinheckel T, Oxenius A. Neutrophil and Alveolar Macrophage-Mediated Innate Immune Control of Legionella pneumophila Lung Infection via TNF and ROS. PLOS Pathogens. 2016;12(4):e1005591.

291. Casson CN, Doerner JL, Copenhaver AM, Ramirez J, Holmgren AM, Boyer MA, et al. Neutrophils and Ly6Chi monocytes collaborate in generating an optimal cytokine response that protects against pulmonary Legionella pneumophila infection. PLOS Pathogens. 2017;13(4):e1006309.

292. Trinchieri G. Interleukin-12: a cytokine produced by antigen-presenting cells with immunoregulatory functions in the generation of T-helper cells type 1 and cytotoxic lymphocytes. 1994;84(12):4008-27.

293. Ma X, Yan W, Zheng H, Du Q, Zhang L, Ban Y, et al. Regulation of IL-10 and IL-12 production and function in macrophages and dendritic cells. F1000Research. 2015;4.

294. Wolf J, Rose-John S, Garbers CJC. Interleukin-6 and its receptors: a highly regulated and dynamic system. 2014;70(1):11-20.

295. Tanaka T, Narazaki M, Kishimoto TJI. Immunotherapeutic implications of IL-6 blockade for cytokine storm. 2016;8(8):959-70.

296. Garbers C, Aparicio-Siegmund S, Rose-John SJCoii. The IL-6/gp130/STAT3 signaling axis: recent advances towards specific inhibition. 2015;34:75-82.

297. Deshmane SL, Kremlev S, Amini S, Sawaya BEJJoi, research c. Monocyte chemoattractant protein-1 (MCP-1): an overview. 2009;29(6):313-26.

298. Ang DKY, Ong SY, Brown AS, Hartland EL, Van Driel IRJBrn. A method for quantifying pulmonary Legionella pneumophila infection in mouse lungs by flow cytometry. 2012;5(1):448.

299. Beck R, Sun Z, Adolf F, Rutz C, Bassler J, Wild K, et al. Membrane curvature induced by Arf1-GTP is essential for vesicle formation. 2008;105(33):11731-6.

300. Dorer MS, Kirton D, Bader JS, Isberg RRJPp. RNA interference analysis of Legionella in Drosophila cells: exploitation of early secretory apparatus dynamics. 2006;2(4):e34.

301. Cheng W, Yin K, Lu D, Li B, Zhu D, Chen Y, et al. Structural Insights into a Unique Legionella pneumophila Effector LidA Recognizing Both GDP and GTP Bound Rab1 in Their Active State. PLOS Pathogens. 2012;8(3):e1002528.

302. Murata T, Delprato A, Ingmundson A, Toomre DK, Lambright DG, Roy CR. The Legionella pneumophila effector protein DrrA is a Rab1 guanine nucleotide-exchange factor. Nature Cell Biology. 2006;8(9):971-7.

303. Sohn Y-S, Shin H-C, Park WS, Ge J, Kim C-H, Lee BL, et al. Lpg0393 of Legionella pneumophila Is a Guanine-Nucleotide Exchange Factor for Rab5, Rab21 and Rab22. PloS one. 2015;10(3):e0118683.

304. Nagai H, Kagan JC, Zhu X, Kahn RA, Roy CR. A Bacterial Guanine Nucleotide Exchange Factor Activates ARF on Legionella Phagosomes. 2002;295(5555):679-82.

305. Amor JC, Swails J, Zhu X, Roy CR, Nagai H, Ingmundson A, et al. The structure of RalF, an ADP-ribosylation factor guanine nucleotide exchange factor from Legionella pneumophila, reveals the presence of a cap over the active site. J Biol Chem. 2005;280(2):1392-400.

306. Biesmans S, Bouwknecht JA, Ver Donck L, Langlois X, Acton PD, De Haes P, et al. Peripheral Administration of Tumor Necrosis Factor-Alpha Induces Neuroinflammation and Sickness but Not Depressive-Like Behavior in Mice. Biomed Res Int. 2015;2015:716920-.

307. Belisle SE, Tisoncik JR, Korth MJ, Carter VS, Proll SC, Swayne DE, et al. Genomic Profiling of Tumor Necrosis Factor Alpha (TNF-α) Receptor and Interleukin-1 Receptor Knockout Mice Reveals a Link between TNF-α Signaling and Increased Severity of 1918 Pandemic Influenza Virus Infection. 2010;84(24):12576-88.

308. Shaviya N, Budambula V, Webale MK, Were T. Circulating Interferon-Gamma Levels Are Associated with Low Body Weight in Newly Diagnosed Kenyan Non-Substance Using Tuberculosis Individuals %J Interdisciplinary Perspectives on Infectious Diseases. 2016;2016:9.

309. Tsao TCY, Huang CC, Chiou WK, Yang PY, Hsieh MJ, Tsao KC. Levels of interferon-γ and interleukin-2 receptor-α for bronchoalveolar lavage fluid and serum were correlated with clinical grade and treatment of pulmonary tuberculosis. The International Journal of Tuberculosis and Lung Disease. 2002;6(8):720-7.

310. Kolanus W. Guanine nucleotide exchange factors of the cytohesin family and their roles in signal transduction. Immunological reviews. 2007;218:102-13.

311. Russo L, Lumeng CN. Properties and functions of adipose tissue macrophages in obesity. Immunology. 2018;155(4):407-17.

312. Gerberick GF, Cruse LW, Miller CM, Sikorski EE, Ridder GM. Selective Modulation of T Cell Memory Markers CD62L and CD44 on Murine Draining Lymph Node Cells Following Allergen and Irritant Treatment. Toxicology and Applied Pharmacology. 1997;146(1):1-10.

313. Henao-Tamayo MI, Ordway DJ, Irwin SM, Shang S, Shanley C, Orme IM. Phenotypic definition of effector and memory T-lymphocyte subsets in mice chronically infected with Mycobacterium tuberculosis. Clin Vaccine Immunol. 2010;17(4):618-25.

314. Belz GT, Xie W, Altman JD, Doherty PCJJov. A previously unrecognized H-2Db-restricted peptide prominent in the primary influenza A virus-specific CD8+ T-cell response is much less apparent following secondary challenge. 2000;74(8):3486-93.

315. Belz GT, Xie W, Doherty PCJTJoI. Diversity of epitope and cytokine profiles for primary and secondary influenza a virus-specific CD8+ T cell responses. 2001;166(7):4627-33.

316. Kurtulus S, Tripathi P, Hildeman DA. Protecting and rescuing the effectors: roles of differentiation and survival in the control of memory T cell development. Frontiers in immunology. 2013;3:404-.

317. Yuzefpolskiy Y, Baumann FM, Kalia V, Sarkar S. Early CD8 T-cell memory precursors and terminal effectors exhibit equipotent in vivo degranulation. Cell Mol Immunol. 2015;12(4):400-8.

318. Kuwano K, Kawashima T, Arai S. Antiviral effect of TNF-alpha and IFN-gamma secreted from a CD8+ influenza virus-specific CTL clone. Viral immunology. 1993;6(1):1-11.

319. Ross SH, Cantrell DA. Signaling and Function of Interleukin-2 in T Lymphocytes. Annu Rev Immunol. 2018;36:411-33.

320. Chen Y, Zander R, Khatun A, Schauder DM, Cui W. Transcriptional and Epigenetic Regulation of Effector and Memory CD8 T Cell Differentiation. Frontiers in immunology. 2018;9:2826-.

321. Kalia V, Sarkar S, Subramaniam S, Haining WN, Smith KA, Ahmed R. Prolonged interleukin-2Ralpha expression on virus-specific CD8+ T cells favors terminal-effector differentiation in vivo. Immunity. 2010;32(1):91-103.

322. Kastenmuller W, Gasteiger G, Subramanian N, Sparwasser T, Busch DH, Belkaid Y, et al. Regulatory T cells selectively control CD8+ T cell effector pool size via IL-2 restriction. Journal of immunology. 2011;187(6):3186-97.

323. Dustin ML. The immunological synapse. Cancer Immunol Res. 2014;2(11):1023-33.

324. Riley JL. PD-1 signaling in primary T cells. 2009;229(1):114-25.

325. Salmaninejad A, Valilou SF, Shabgah AG, Aslani S, Alimardani M, Pasdar A, et al. PD-1/PD-L1 pathway: Basic biology and role in cancer immunotherapy. 2019;234(10):16824-37.

326. Sheppard KA, Fitz LJ, Lee JM, Benander C, George JA, Wooters J, et al. PD-1 inhibits T-cell receptor induced phosphorylation of the ZAP70/CD3zeta

signalosome and downstream signaling to PKCtheta. FEBS letters. 2004;574(1-3):37-41.

327. Neel BG, Gu H, Pao LJTibs. The 'Shp'ing news: SH2 domain-containing tyrosine phosphatases in cell signaling. 2003;28(6):284-93.

328. Parry RV, Chemnitz JM, Frauwirth KA, Lanfranco AR, Braunstein I, Kobayashi SV, et al. CTLA-4 and PD-1 Receptors Inhibit T-Cell Activation by Distinct Mechanisms. 2005;25(21):9543-53.

329. Liu W, Guo W, Shen L, Chen Z, Luo Q, Luo X, et al. T lymphocyte SHP2-deficiency triggers anti-tumor immunity to inhibit colitis-associated cancer in mice. 2017;8(5):7586.

330. Zhao M, Guo W, Wu Y, Yang C, Zhong L, Deng G, et al. SHP2 inhibition triggers anti-tumor immunity and synergizes with PD-1 blockade. Acta Pharmaceutica Sinica B. 2019;9(2):304-15.

331. Itariu BK, Stulnig TM. Autoimmune Aspects of Type 2 Diabetes Mellitus - A Mini-Review. Gerontology. 2014;60(3):189-96.

332. Guo Q, Wang Y, Xu D, Nossent J, Pavlos NJ, Xu J. Rheumatoid arthritis: pathological mechanisms and modern pharmacologic therapies. Bone Res. 2018;6:15-.

333. Gajendran M, Loganathan P, Catinella AP, Hashash JG. A comprehensive review and update on Crohn's disease. Disease-a-month : DM. 2018;64(2):20-57.

334. Katsarou A, Gudbjörnsdottir S, Rawshani A, Dabelea D, Bonifacio E, Anderson BJ, et al. Type 1 diabetes mellitus. Nature Reviews Disease Primers. 2017;3:17016.

335. Leung S, Liu X, Fang L, Chen X, Guo T, Zhang J. The cytokine milieu in the interplay of pathogenic Th1/Th17 cells and regulatory T cells in autoimmune disease. Cell Mol Immunol. 2010;7(3):182-9.

336. Smith KM, Pottage L, Thomas ER, Leishman AJ, Doig TN, Xu D, et al. Th1 and Th2 CD4⁺ T Cells Provide Help for B Cell Clonal Expansion and Antibody Synthesis in a Similar Manner In Vivo. 2000;165(6):3136-44.

337. McAlees JW, Lajoie S, Dienger K, Sproles AA, Richgels PK, Yang Y, et al. Differential control of CD4(+) T-cell subsets by the PD-1/PD-L1 axis in a mouse model of allergic asthma. European journal of immunology. 2015;45(4):1019-29.

338. Kanhere A, Hertweck A, Bhatia U, Gokmen MR, Perucha E, Jackson I, et al. T-bet and GATA3 orchestrate Th1 and Th2 differentiation through lineage-specific targeting of distal regulatory elements. Nature communications. 2012;3:1268.

339. Trickett A, Kwan YL. T cell stimulation and expansion using anti-CD3/CD28 beads. Journal of Immunological Methods. 2003;275(1):251-5.

340. Ohtsuka T, Kaziro Y, Satoh T. Analysis of the T-cell activation signaling pathway mediated by tyrosine kinases, protein kinase C, and Ras protein, which is modulated by intracellular cyclic AMP. Biochimica et Biophysica Acta (BBA) - Molecular Cell Research. 1996;1310(2):223-32.

341. Chatila T, Silverman L, Miller R, Geha R. Mechanisms of T cell activation by the calcium ionophore ionomycin. 1989;143(4):1283-9.

342. Macintyre AN, Gerriets VA, Nichols AG, Michalek RD, Rudolph MC, Deoliveira D, et al. The glucose transporter Glut1 is selectively essential for CD4 T cell activation and effector function. Cell metabolism. 2014;20(1):61-72.

343. Devenish RJ, Prescott M, Boyle GM, Nagley P. The Oligomycin Axis of Mitochondrial ATP Synthase: OSCP and the Proton Channel. Journal of Bioenergetics and Biomembranes. 2000;32(5):507-15.

344. XF_Glycolysis_Stress_Test_Kit_User_Guide. 2017. Wilmington, USA: Agilent Technologies Inc.

345. Zhang S-L, Hu X, Zhang W, Yao H, Tam KY. Development of pyruvate dehydrogenase kinase inhibitors in medicinal chemistry with particular emphasis as anticancer agents. Drug Discovery Today. 2015;20(9):1112-9.

346. TeSlaa T, Teitell MA. Chapter Five - Techniques to Monitor Glycolysis. In: Galluzzi L, Kroemer G, editors. Methods in Enzymology. 542: Academic Press; 2014. p. 91-114.

347. Plitzko B, Loesgen S. Measurement of Oxygen Consumption Rate (OCR) and Extracellular Acidification Rate (ECAR) in Culture Cells for Assessment of the Energy Metabolism. Bio-protocol. 2018;8(10):e2850.

348. Tan H, Yang K, Li Y, Shaw TI, Wang Y, Blanco DB, et al. Integrative Proteomics and Phosphoproteomics Profiling Reveals Dynamic Signaling Networks and Bioenergetics Pathways Underlying T Cell Activation. Immunity. 2017;46(3):488-503.

349. Gubser PM, Bantug GR, Razik L, Fischer M, Dimeloe S, Hoenger G, et al. Rapid effector function of memory CD8+ T cells requires an immediate-early glycolytic switch. Nature immunology. 2013;14(10):1064-72.

350. Fox CJ, Hammerman PS, Thompson CB. Fuel feeds function: energy metabolism and the T-cell response. Nature Reviews Immunology. 2005;5(11):844-52.

351. Mookerjee SA, Goncalves RLS, Gerencser AA, Nicholls DG, Brand MD. The contributions of respiration and glycolysis to extracellular acid production. Biochimica et Biophysica Acta (BBA) - Bioenergetics. 2015;1847(2):171-81.

352. Yang C, Ko B, Hensley Christopher T, Jiang L, Wasti Ajla T, Kim J, et al. Glutamine Oxidation Maintains the TCA Cycle and Cell Survival during Impaired Mitochondrial Pyruvate Transport. Molecular Cell. 2014;56(3):414-24.

353. Gorentla BK, Wan C-K, Zhong X-P. Negative regulation of mTOR activation by diacylglycerol kinases. Blood. 2011;117(15):4022-31.

354. Jones N, Vincent EE, Cronin JG, Panetti S, Chambers M, Holm SR, et al. Akt and STAT5 mediate naïve human CD4+ T-cell early metabolic response to TCR stimulation. Nature communications. 2019;10(1):2042.

355. Bost F, Decoux-Poullot AG, Tanti JF, Clavel S. Energy disruptors: rising stars in anticancer therapy? Oncogenesis. 2016;5:e188.

356. Huang J, Lo P-F, Żal T, Gascoigne NRJ, Smith BA, Levin SD, et al. CD28 plays a critical role in the segregation of PKCθ within the immunologic synapse. 2002;99(14):9369-73.

357. Kane LP, Weiss A. The PI-3 kinase/Akt pathway and T cell activation: pleiotropic pathways downstream of PIP3. 2003;192(1):7-20.

358. Salmond RJ. mTOR Regulation of Glycolytic Metabolism in T Cells. Front Cell Dev Biol. 2018;6:122-.

359. Laplante M, Sabatini DM. mTOR signaling at a glance. 2009;122(20):3589-94.

360. Lee K, Gudapati P, Dragovic S, Spencer C, Joyce S, Killeen N, et al. Mammalian Target of Rapamycin Protein Complex 2 Regulates Differentiation of Th1 and Th2 Cell Subsets via Distinct Signaling Pathways. Immunity. 2010;32(6):743-53.

361. Smeltz RB, Chen J, Ehrhardt R, Shevach EM. Role of IFN-gamma in Th1 differentiation: IFN-gamma regulates IL-18R alpha expression by preventing the negative effects of IL-4 and by inducing/maintaining IL-12 receptor beta 2 expression. Journal of immunology. 2002;168(12):6165-72.

362. Hsieh CS, Macatonia SE, Tripp CS, Wolf SF, O'Garra A, Murphy KM. Development of TH1 CD4+ T cells through IL-12 produced by Listeria-induced macrophages. Science. 1993;260(5107):547-9.

363. Kaplan MH, Sun YL, Hoey T, Grusby MJ. Impaired IL-12 responses and enhanced development of Th2 cells in Stat4-deficient mice. Nature. 1996;382(6587):174-7.

364. Liu W, Guo W, Shen L, Chen Z, Luo Q, Luo X, et al. T lymphocyte SHP2-deficiency triggers anti-tumor immunity to inhibit colitis-associated cancer in mice. Oncotarget. 2017;8(5):7586-97.

365. Riella LV, Paterson AM, Sharpe AH, Chandraker A. Role of the PD-1 Pathway in the Immune Response. 2012;12(10):2575-87.

366. Francisco LM, Salinas VH, Brown KE, Vanguri VK, Freeman GJ, Kuchroo VK, et al. PD-L1 regulates the development, maintenance, and function of induced regulatory T cells. 2009;206(13):3015-29.

367. Dulos J, Carven GJ, van Boxtel SJ, Evers S, Driessen-Engels LJA, Hobo W, et al. PD-1 blockade augments Th1 and Th17 and suppresses Th2 responses in peripheral blood from patients with prostate and advanced melanoma cancer. J Immunother. 2012;35(2):169-78.

368. Amarnath S, Mangus CW, Wang JC, Wei F, He A, Kapoor V, et al. The PDL1-PD1 axis converts human TH1 cells into regulatory T cells. Science translational medicine. 2011;3(111):111ra20.

369. Kimura A, Kishimoto T. IL-6: regulator of Treg/Th17 balance. European journal of immunology. 2010;40(7):1830-5.

370. Muller R, Herr C, Sukumaran SK, Omosigho NN, Plomann M, Riyahi TY, et al. The cytohesin paralog Sec7 of Dictyostelium discoideum is required for phagocytosis and cell motility. Cell communication and signaling : CCS. 2013;11:54.

371. Sendide K, Reiner NE, Lee JS, Bourgoin S, Talal A, Hmama Z. Cross-talk between CD14 and complement receptor 3 promotes phagocytosis of mycobacteria: regulation by phosphatidylinositol 3-kinase and cytohesin-1. Journal of immunology. 2005;174(7):4210-9.

372. El Azreq MA, Garceau V, Harbour D, Pivot-Pajot C, Bourgoin SG. Cytohesin-1 regulates the Arf6-phospholipase D signaling axis in human

neutrophils: impact on superoxide anion production and secretion. Journal of immunology. 2010;184(2):637-49.

373. Pearce EL, Walsh MC, Cejas PJ, Harms GM, Shen H, Wang L-S, et al. Enhancing CD8 T-cell memory by modulating fatty acid metabolism. 2009;460(7251):103.

374. Pan Y, Kupper TS. Metabolic Reprogramming and Longevity of Tissue-Resident Memory T Cells. 2018;9(1347).

375. Torii T, Miyamoto Y, Sanbe A, Nishimura K, Yamauchi J, Tanoue A. Cytohesin-2/ARNO, through its interaction with focal adhesion adaptor protein paxillin, regulates preadipocyte migration via the downstream activation of Arf6. Journal of Biological Chemistry. 2010;285(31):24270-81.

376. Zhu W, London NR, Gibson CC, Davis CT, Tong Z, Sorensen LK, et al. Interleukin receptor activates a MYD88-ARNO-ARF6 cascade to disrupt vascular stability. Nature. 2012;492(7428):252-5.

377. Diomede F, Zingariello M, Cavalcanti M, Merciaro I, Pizzicannella J, De Isla N, et al. MyD88/ERK/NFkB pathways and pro-inflammatory cytokines release in periodontal ligament stem cells stimulated by Porphyromonas gingivalis. European journal of histochemistry : EJH. 2017;61(2):2791.

378. Fife BT, Pauken KE. The role of the PD-1 pathway in autoimmunity and peripheral tolerance. Annals of the New York Academy of Sciences. 2011;1217:45-59.

379. Nagel W, Zeitlmann L, Schilcher P, Geiger C, Kolanus J, Kolanus W. Phosphoinositide 3-OH Kinase Activates the β2Integrin Adhesion Pathway and Induces Membrane Recruitment of Cytohesin-1. Journal of Biological Chemistry. 1998;273(24):14853-61.

380. Jackson TR, Kearns BG, Theibert AB. Cytohesins and centaurins: mediators of PI 3-kinase-regulated Arf signaling. Trends Biochem Sci. 2000;25(10):489-95.

381. DiNitto JP, Delprato A, Gabe Lee M-T, Cronin TC, Huang S, Guilherme A, et al. Structural Basis and Mechanism of Autoregulation in 3-Phosphoinositide-Dependent Grp1 Family Arf GTPase Exchange Factors. Molecular Cell. 2007;28(4):569-83.

382. Dierks H, Kolanus J, Kolanus W. Actin cytoskeletal association of cytohesin-1 is regulated by specific phosphorylation of its carboxyl-terminal polybasic domain. J Biol Chem. 2001;276(40):37472-81.

383. Stephanou A, Latchman DS. Opposing actions of STAT-1 and STAT-3. Growth factors (Chur, Switzerland). 2005;23(3):177-82.

384. Schweitzer JK, Sedgwick AE, D'Souza-Schorey C. ARF6-mediated endocytic recycling impacts cell movement, cell division and lipid homeostasis. Seminars in cell & developmental biology. 2011;22(1):39-47.

385. Moreau K, Ravikumar B, Puri C, Rubinsztein DC. Arf6 promotes autophagosome formation via effects on phosphatidylinositol 4,5-bisphosphate and phospholipase D. 2012;196(4):483-96.

386. Tanguy E, Tran Nguyen AP, Kassas N, Bader M-F, Grant NJ, Vitale N. Regulation of Phospholipase D by Arf6 during FcγR-Mediated Phagocytosis. 2019:ji1801019.

387. Van Acker T, Eyckerman S, Walle LV, Gerlo S, Goethals M, Lamkanfi M, et al. The small GTPase Arf6 is essential for the Tram/Trif pathway in TLR4 signaling. 2014;289(3):1364-76.

388. Macek B, Mann M, Olsen JV. Global and site-specific quantitative phosphoproteomics: principles and applications. Annual review of pharmacology and toxicology. 2009;49:199-221.